

Advances in Biochemical Engineering/Biotechnology 146  
Series Editor: T. Scheper

Kai Muffler  
Roland Ulber *Editors*

# Productive Biofilms

 Springer

**146**

**Advances in Biochemical  
Engineering/Biotechnology**

**Series editor**

T. Scheper, Hannover, Germany

**Editorial Board**

S. Belkin, Jerusalem, Israel

P. M. Doran, Hawthorn, Australia

I. Endo, Saitama, Japan

M. B. Gu, Seoul, Korea

W. S. Hu, Minneapolis, MN, USA

B. Mattiasson, Lund, Sweden

J. Nielsen, Gothenburg, Sweden

H. Seitz, Potsdam, Germany

G. N. Stephanopoulos, Cambridge, MA, USA

R. Ulber, Kaiserslautern, Germany

A.-P. Zeng, Hamburg-Harburg, Germany

J.-J. Zhong, Shanghai, China

W. Zhou, Framingham, MA, USA

## **Aims and Scope**

This book series reviews current trends in modern biotechnology and biochemical engineering. Its aim is to cover all aspects of these interdisciplinary disciplines, where knowledge, methods and expertise are required from chemistry, biochemistry, microbiology, molecular biology, chemical engineering and computer science.

Volumes are organized topically and provide a comprehensive discussion of developments in the field over the past 3–5 years. The series also discusses new discoveries and applications. Special volumes are dedicated to selected topics which focus on new biotechnological products and new processes for their synthesis and purification.

In general, volumes are edited by well-known guest editors. The series editor and publisher will, however, always be pleased to receive suggestions and supplementary information. Manuscripts are accepted in English.

In references, *Advances in Biochemical Engineering/Biotechnology* is abbreviated as *Adv. Biochem. Engin./Biotechnol.* and cited as a journal.

More information about this series at <http://www.springer.com/series/10>

Kai Muffler · Roland Ulber  
Editors

# Productive Biofilms

With contributions by

J. C. Aurich · Jerome Babauta · Haluk Beyenal · S. Buhl  
N. Davoudi · Harald Horn · S. Kuhne · Susanne Lackner  
M. Lakatos · John R. Lawrence · Gerard H. Markx  
Sayani Mitra · K. Muffler · Joydeep Mukherjee  
C. Müller-Renno · Thomas R. Neu · Stephen Payne  
S. Ripperger · Barindra Sana · C. Schlegel  
Jochen J. Schuster · D. Strieth · R. Ulber  
Lingchong You · Ch. Ziegler

 Springer

*Editors*

Kai Muffler  
Department of Life Sciences  
and Engineering  
University of Applied Sciences Bingen  
Bingen  
Germany

Roland Ulber  
Institute of Bioprocess Engineering  
University of Kaiserslautern  
Kaiserslautern  
Germany

ISSN 0724-6145

ISBN 978-3-319-09694-0

DOI 10.1007/978-3-319-09695-7

ISSN 1616-8542 (electronic)

ISBN 978-3-319-09695-7 (eBook)

Library of Congress Control Number: 2014950394

Springer Cham Heidelberg New York Dordrecht London

© Springer International Publishing Switzerland 2014

This work is subject to copyright. All rights are reserved by the Publisher, whether the whole or part of the material is concerned, specifically the rights of translation, reprinting, reuse of illustrations, recitation, broadcasting, reproduction on microfilms or in any other physical way, and transmission or information storage and retrieval, electronic adaptation, computer software, or by similar or dissimilar methodology now known or hereafter developed. Exempted from this legal reservation are brief excerpts in connection with reviews or scholarly analysis or material supplied specifically for the purpose of being entered and executed on a computer system, for exclusive use by the purchaser of the work. Duplication of this publication or parts thereof is permitted only under the provisions of the Copyright Law of the Publisher's location, in its current version, and permission for use must always be obtained from Springer. Permissions for use may be obtained through RightsLink at the Copyright Clearance Center. Violations are liable to prosecution under the respective Copyright Law.

The use of general descriptive names, registered names, trademarks, service marks, etc. in this publication does not imply, even in the absence of a specific statement, that such names are exempt from the relevant protective laws and regulations and therefore free for general use.

While the advice and information in this book are believed to be true and accurate at the date of publication, neither the authors nor the editors nor the publisher can accept any legal responsibility for any errors or omissions that may be made. The publisher makes no warranty, express or implied, with respect to the material contained herein.

Printed on acid-free paper

Springer is part of Springer Science+Business Media ([www.springer.com](http://www.springer.com))

# Preface

The application of immobilized cells as well as enzymes is a common technique in contemporary biotechnological production processes. Usually, the biocatalysts are encapsulated in an artificial matrix and/or bound to a (particle) surface. A reduction of the catalyst's activity is widely accepted considering the higher lifetime and a simplified recirculation of the immobilized catalyst. One of the broad varieties of parameters affecting the activity is the utilization of chemical agents that modify the chemical surrounding as well as the physiological state in comparison to the native suspended cell. However, biofilms representing encapsulated cells in a matrix produced by their own combine the mentioned beneficial attributes and can be considered as a natural way of immobilized (whole cell) biocatalysts. Even though biofilms are predominantly associated in terms of process engineering with fouling processes resulting in a reduced process as well as product quality, their application for the production of valuables might be an interesting option which is up to now markedly underestimated. From an ecological point of view the biofilm state of a microorganism commonly represents the native growth state rather than the planktonic mode which is preferred for most bioprocesses, in particular with respect to mixing and supply of nutrients, respectively. But one has to consider that some characteristic traits of a microbial cell or a consortium of microorganisms appear solely if the organism grows attached to a surface, i.e., many prospective strains found in nature and featuring interesting product spectra often do not show this profile after transfer of the strain and its (suspended) handling in a lab. Besides a cell's expression pattern the robustness of a biofilm toward non-physiological conditions and its long-term stability is emphasized if biofilms are discussed as tools for the production of biotechnological valuable compounds. However, such utilization requires a sophisticated knowledge of several realms of basic sciences as well as engineering aspects. Some of them which are considered of tremendous importance to fulfill the broader application of biofilms within biotechnology are addressed within this issue of the "Advances in Biochemical Engineering/Biotechnology" series.

Elucidation of biofilm structure is a prerequisite to understand and to model the mass transfer and growth of cells within the extracellular matrix sheltering the cells.

Since biofilms are used for a long time in bioremediation and sewage treatment, mathematical models were developed to characterize the processes of such applications; however, state-of-the-art techniques for structure elucidation and models are presented, which might be useful to describe the corresponding processes occurring in “Productive Biofilms”. A transfer of the biofilm concept for production of valuables requires so-called synthetic biofilms, whereas the composition and architecture of the biofilm is controlled by the experimenter. How biofilm function and architecture could be controlled by artificial and/or natural means is another topic of this issue as well as the engineering of cell-to-cell communication. Communication circuits such as quorum sensing can be modified to equip the cells with specific traits or to tune the sensitivity of the communication system. Since the technical application of biofilms require a different cultivation strategy in comparison to suspended cells, an overview of biofilm reactors and materials that are currently in use or are developed is given. The selected processes can be considered as prime examples, whereby the production of a broad range of bulk and fine chemicals is presented. Moreover, the ecological role of marine and intertidal biofilms of microorganisms is addressed, including the application of such kind of biofilms and analytical techniques are presented enabling the investigation of physicochemical processes in biofilms.

This special issue bringing together the work of basic scientists and engineers which we consider as a prerequisite to facilitate the application of biofilms as biological tools for the production of valuables. We are very thankful to the authors for their valuable contributions.

Bingen  
Kaiserslautern  
September 2014

Kai Muffler  
Roland Ulber

# Contents

<b>Investigation of Microbial Biofilm Structure by Laser Scanning Microscopy</b> . . . . .	1
Thomas R. Neu and John R. Lawrence	
<b>Modeling of Biofilm Systems: A Review</b> . . . . .	53
Harald Horn and Susanne Lackner	
<b>Biofilm Architecture</b> . . . . .	77
Jochen J. Schuster and Gerard H. Markx	
<b>Engineered Cell–Cell Communication and Its Applications</b> . . . . .	97
Stephen Payne and Lingchong You	
<b>Application of Biofilm Bioreactors in White Biotechnology</b> . . . . .	123
K. Muffler, M. Lakatos, C. Schlegel, D. Strieth, S. Kuhne and R. Ulber	
<b>Ecological Roles and Biotechnological Applications of Marine and Intertidal Microbial Biofilms</b> . . . . .	163
Sayani Mitra, Barindra Sana and Joydeep Mukherjee	
<b>Novel Materials for Biofilm Reactors and their Characterization</b> . . . . .	207
C. Müller-Renno, S. Buhl, N. Davoudi, J. C. Aurich, S. Ripperger, R. Ulber, K. Muffler and Ch. Ziegler	
<b>Microsensors and Microscale Gradients in Biofilms</b> . . . . .	235
Haluk Beyenal and Jerome Babauta	
<b>Index</b> . . . . .	257



# Investigation of Microbial Biofilm Structure by Laser Scanning Microscopy

Thomas R. Neu and John R. Lawrence

**Abstract** Microbial bioaggregates and biofilms are hydrated three-dimensional structures of cells and extracellular polymeric substances (EPS). Microbial communities associated with interfaces and the samples thereof may come from natural, technical, and medical habitats. For imaging such complex microbial communities confocal laser scanning microscopy (CLSM) is the method of choice. CLSM allows flexible mounting and noninvasive three-dimensional sectioning of hydrated, living, as well as fixed samples. For this purpose a broad range of objective lenses is available having different working distance and resolution. By means of CLSM the signals detected may originate from reflection, autofluorescence, reporter genes/fluorescence proteins, fluorochromes binding to specific targets, or other probes conjugated with fluorochromes. Recorded datasets can be used not only for visualization but also for semiquantitative analysis. As a result CLSM represents a very useful tool for imaging of microbiological samples in combination with other analytical techniques.

**Keywords** 1-photon excitation · 2-photon excitation · Bioaggregates · Biofilms · Confocal laser scanning microscopy · Fluorescence

## Abbreviations

CARD-FISH	CAlyzed Reported Deposition—Fluorescence In Situ Hybridization
CLSM	Confocal Laser Scanning Microscopy
eDNA	Extracellular DNA
EPS	Extracellular Polymeric Substances
FISH	Fluorescence In Situ Hybridisation
FITC	Fluorescein IsoThioCyanate
FISH-MAR	Fluorescence In Situ Hybridisation—Micro Auto Radiography
FLBA	Fluorescence Lectin-Binding Analysis
GFP	Green Fluorescent Protein

---

T. R. Neu (✉)

Department of River Ecology, Helmholtz Centre for Environmental Research—UFZ,  
Brueckstrasse 3a, 39114 Magdeburg, Germany  
e-mail: thomas.neu@ufz.de

J. R. Lawrence

Environment Canada, Saskatoon SK, Canada

GSD	Ground State Depletion microscopy with individual molecule return (GSDIM)
LSM	Laser Scanning Microscopy
MIP	Maximum Intensity Projection
MRI	Magnetic Resonance Imaging
nanoSIMS	Nano Secondary Ion Mass Spectrometry
OCT	Optical Coherence Tomography
PALM	PhotoActivated Localization Microscopy
SIM	Structured Illumination Microscopy
SPIM	Selected Plane Illumination Microscopy
STED	Stimulated Emission Depletion microscopy
STXM	Scanning Transmission X-ray Microscopy
TRITC	Tetramethyl Rhodamine IsoThioCyanate

## Contents

1	Introduction.....	3
2	Laser Scanning Microscopy.....	4
2.1	Confocal Laser Scanning Microscopy.....	4
2.2	Two-Photon Laser Scanning Microscopy.....	5
2.3	Sample Preparation.....	5
2.4	Digital Image Analysis.....	6
3	Probes and Approaches for Analyzing Biofilms and Bioaggregates.....	6
3.1	Fluorochromes.....	6
3.2	Fluorescence In Situ Hybridization.....	8
3.3	EPS Analysis.....	8
3.4	Viability.....	11
3.5	Activity Measurements.....	13
3.6	Antibodies.....	13
3.7	FISH-MAR.....	14
3.8	GFP.....	14
4	Applications of CLSM and Fluorescence Techniques.....	15
4.1	Biofilms.....	15
4.2	River and Phototrophic Biofilms.....	19
4.3	Flocs, Aggregates.....	19
4.4	Grazing.....	19
4.5	Fungi, Lichens.....	23
4.6	Bacteria on Plant Surfaces.....	23
4.7	Granules.....	24
4.8	Viruses, Phages.....	26
4.9	Technical and Model Systems.....	26
5	Future Prospects.....	27
	References.....	30

## 1 Introduction

In microbiology the light microscope has been a basic instrument from the very beginning. Initially the application was for suspended bacterial cells usually mounted in between the slide and cover slip. Subsequent examination by different light microscopy techniques provided acceptable results as long as the sample was thin enough, meaning a few micrometers. However, a change in paradigms revealed that natural microbial communities are complex mixed cultures found in the form of three-dimensional structures such as bioaggregates or biofilms [215]. In parallel the invention of confocal laser scanning microscopy (CLSM) opened the way for three-dimensional optical sectioning of biological samples. As is often the case, this technique was first applied in medical and cell biology research. A key publication by Lawrence and coworkers was the beginning of CLSM as a standard technique in different fields of microbiology [166]. Throughout the 1990s CLSM was available in only a few microbiological laboratories. Currently, CLSM is present in most laboratories, although not always used in a highly sophisticated way. This comprises a number of issues: (1) the general approach of how to take advantage of CLSM, for example, just for a taking a “photo” or recording scientific images; (2) the actual fluorescence techniques used, for example, showing just some green or red-green points on a black background as compared to structured image data with a specific meaning allowing interpretation of effects and processes; (3) the way of doing digital image analysis, for example, just by using a quick 3D tool not showing anything convincing or by applying a specific projection showing data with respect to the actual image/object content and the method of recording it; (4) the question of CLSM performance, for example, just using the instrument without questioning the result as compared to using a number of tests allowing assessment of the CLSM performance.

In this review we focus on laser scanning microscopy (LSM) and its variations as a tool for structure elucidation of microbial bioaggregates and biofilms. Comparing the various hardware options and fluorescence techniques, traditional CLSM is still the workhorse in microbiological imaging. For this purpose the key publications are discussed. After explaining the basic principles, the main part of the review comprises the many options available for staining and imaging of structural features in microbial communities. The various approaches are compiled in extended tables in order to provide as much information as possible. We then show the many diverse applications of LSM in the wide area of microbiology. Nevertheless we cannot cover the entire field of laser microscopy and its use in biofilm research. A quick Internet search for only two keywords, “biofilm” and “confocal,” revealed about 15,000 references in a general search and more than 90,000 references in a popular microbiological journal search. As a consequence we have to focus on selected references we think are relevant for studying microorganisms associated with interfaces.

**Table 1** Reviews on laser scanning microscopy with applications in microbiology and biofilm research

Focus of article	Reference
First overview on CLSM applications	Caldwell et al. [37]
Medical biofilms	Gorman et al. [99]
Medical biofilms	Manning [210]
Environmental applications	Lawrence et al. [167]
Comprehensive review of CLSM	Lawrence et al. [180]
CLSM methodology	Lawrence and Neu [170]
Short CLSM overview	Palmer and Sternberg [282]
Medical biofilms	Adair et al. [1]
Structured CLSM approach	Neu and Lawrence [250]
Environmental applications	Lawrence et al. [168]
CLSM in soil microbiology	Li et al. [190]
Spatiotemporal approaches	Palmer et al. [281]
Environmental applications	Lawrence et al. [165]
CLSM techniques and protocols	Lawrence and Neu [172]
CLSM of aggregates	Lawrence and Neu [173]
CLSM—MRI—STXM	Neu et al. [253]

## 2 Laser Scanning Microscopy

### 2.1 Confocal Laser Scanning Microscopy

In CLSM an object is sectioned optically resulting in crisp images without a blurred signal from other optical planes. Single sections, or in most cases series of sections, are recorded as two-dimensional images that finally will allow three-dimensional reconstruction. For this purpose the sample has to be stained with fluorochromes that are specific for certain compounds. In addition, the autofluorescence and the reflection signals may be recorded. Modern multichannel instruments have several photomultipliers that allow separation of up to five different emission signals. Recently, improved detectors with increased sensitivity have been offered. The instrument is available in different configurations, as a point scanner (for high resolution) or as a disk scanner (for motile objects). In addition, hybrid systems are offered with a compromise of both features. A major characteristic of a CLSM set-up is the laser lines available for excitation of fluorochromes. The laser options include traditional gas lasers (e.g. Ar, He/Ne), laser diodes, two-photon lasers, and more recently white lasers. The possible wavelengths range from UV (ultraviolet) to IR (infrared), although most instruments are equipped with visible lasers only. Usually three laser lines are available, for example, at 488, 561, and 633 nm. These three lines are sufficient for most samples and cover many of the popular fluorochromes. For more information a list of reviews on the topic of CLSM and its application in microbiology is supplied (see Table 1). This will allow further reading in terms of CLSM technique, sample

preparation, data recording, and digital image analysis. The flexibility of CLSM for examination of multiple parameters in microbiological samples established this particular microscopy technique as a routine tool in many laboratories.

## ***2.2 Two-Photon Laser Scanning Microscopy***

In two-photon LSM a fluorochrome is excited by two photons of the double wavelength as compared to one-photon (confocal) excitation. The laser source necessary to achieve two-photon excitation is a pulsed infrared laser. The two-photon effect occurs in the focal plane only and as a result no pinhole is needed. In general most of the fluorochromes used for confocal imaging can be applied on a two-photon instrument. In addition, UV fluorochromes such as 4,6-diamidino-2-phenylindole (DAPI) can be excited. A further advantage is the higher penetration of IR light into the sample resulting in a better resolution in deep locations. Two-photon LSM was first proven to be useful in biology in 1990 [67]. So far only few reports in microbiology have been published. The first application was on oral biofilms [92, 357]. Later two-photon LSM was suggested as a tool in biofilm research in a methodological report [34]. The suitability of common fluorochromes was tested on different types of biofilms [247]. Later the usefulness of the technique for examination of phototrophic biofilms was reported [256]. A general overview of two-photon LSM as a technique for biofilm studies was published by the same group [251]. The advantage of two-photon excitation as a replacement for UV was employed in a study on Zn distribution in microbial biofilms [130]. However, it seems that the two-photon technique is available in only a few microbiology research groups. Although two-photon LSM overcomes some drawbacks of conventional CLSM two reasons may hinder a wider application. These include the additional costs for investment and on the other hand two-photon effects that are sometimes not readily explainable. Furthermore, axial elongation of signals remains an issue for both systems. Overall conventional confocal LSM remains the method of choice in most biofilm applications.

## ***2.3 Sample Preparation***

Sample mounting will be determined by the type of microscope attached to the CLSM. In many clinical and cell biological laboratories the inverted microscope is preferred. Usually the samples are in sterile dishes or plates with a bottom window suitable for microscopic observation. However, the experience with many different types of samples from various habitats has shown that the upright microscope may be more suitable for environmental samples, especially with water-immersible (dipping) lenses that allow imaging of any specimen mounted in a Petri dish [252]. Most critical is the issue of high resolution versus working distance. In samples

that are spatially structured often the high numerical aperture (NA) lenses, having a short working distance, cannot be used. Consequently water-immersible lenses with a free working distance in the mm range perfectly match the needs for imaging deep areas of the sample. Smaller specimens can be mounted in coverwell chambers (e.g., from Grace Biolabs) having spacers of various heights (0.5–2 mm). If the specimen matches the chamber perfectly and the free working distance allows, high NA (high-resolution) objective lenses can be used.

## ***2.4 Digital Image Analysis***

Analysis of datasets recorded by CLSM can be done in two ways, by visualization and by quantification. First of all the image series can be visualized using commercial software or freeware. Therefore a wide choice of tools is available to project the raw data, which are a series of two-dimensional images recorded at a certain stepsize ( $XZ$  direction), in a meaningful way. Visualization may comprise maximum intensity-, transparent-, isosurface-, shadow-,  $XYZ$ -, and ortho slice-projections. Second, the image series can be quantified by counting pixels (2D) or voxels (3D) after thresholding the raw dataset. In fact thresholding is the most critical step in quantification. As a consequence several publications exist in which different approaches for thresholding were tested [333, 412, 415, 416]. In certain applications deconvolution may be used to achieve a higher resolution [332]. This might be necessary for three reasons: if the dataset contains noise, in order to improve resolution, and due to the unequal  $XY$  (superior) to  $XZ$  resolution in light/laser microscopy. However deconvolution may also lead to artifacts if it is not done properly. This may comprise the need to record the point spread function of fluorescent beads within the sample which is rarely done or the actual algorithm used for deconvolution. Although it might be easy to assess deconvolution of a bead with known geometry, this is not the case for unknown objects. In addition, the need to record the data at high resolution in the  $XY$  as well as in the  $Z$  direction leads to dramatic bleaching of the fluorochromes. So far there are very few publications in microbiology taking advantage of deconvolution for image improvement in microbiological datasets [182, 211, 231, 292, 302].

## **3 Probes and Approaches for Analyzing Biofilms and Bioaggregates**

### ***3.1 Fluorochromes***

The fluorochromes available at the beginning of LSM were the traditional ones already used for epifluorescence microscopy. Well-known examples are acridine orange and DAPI for nucleic acid staining or FITC, TRITC, CY3, and CY5 as a

**Table 2** Application of new nucleic acid specific fluorochromes for examination of microbiological samples

Fluorochrome	Sample	Reference
TOTO-1, TO-PRO-1	Planktonic bacteria	Li et al. [189]
Syto-13	Marine plankton	del Giorgio et al. [64]
YOYO-1, YO-PRO-1, PicoGreen	Suspended bacteria from pure cultures	Marie et al. [214]
Syto-13, TOTO-1, YOYO-1	Pure cultures, marine plankton	Guindulain et al. [108]
Syto-16	<i>Mycobacterium</i> cells	Ibrahim et al. [133]
PicoGreen	Plankton	Tranvik [368]
SybrGreen-1	Picoplankton	Marie et al. [213]
Syto-9, Syto-11, Syto-13, Syto-16, SybrGreen-1, SybrGreen-2	Freshwater, saline water	Lebaron et al. [184]
SybrGreen-1	Marine viruses, bacteria	Noble and Fuhrman [267]
SybrGreen-2	Soil and sediment bacteria	Weinbauer et al. [392]
Syto-13	Plankton	Troussellier et al. [369]
Propidium iodide, POPO-3	Geological samples	Tobin et al. [365]
SybrGold	Marine viruses	Chen et al. [41]
Coriphosphine O, YOYO-1, YOPRO-1	Groundwater bacteria	Stopa and Mastromanolis [350]
PicoGreen	Plankton	Cotner et al. [50]
SybrGreen-2	Sediment bacteria	Sunamura et al. [355]
Syto-60	Pure culture biofilm	Nancharaiah et al. [241]
SybrGreen-1	Sediment bacteria	Lunau et al. [201]
PicoGreen, SybrGreen-1, SybrGreen-2	Laboratory cultures	Martens-Habbena and Sass [216]

label conjugated to other probes, for example, antibodies. However, with the wider availability of multichannel CLSM instruments new fluorochromes were developed and became commercially available (e.g., from Molecular Probes). The possibility of using the CLSM in multichannel mode allowed the combination of two, three, or even four markers that could be recorded in separate channels. A list of publications testing new nucleic acid specific fluorochromes for their suitability in CLSM and flow cytometry is given in Table 2. In the meantime a whole range of fluorochromes specific for nucleic acids can be selected for matching possible autofluorescence and combinations of fluorescent stains. Apart from cell biomass and distribution other features can be measured (Table 3). These fluorochromes are specific for certain cell structures and properties. These stains may target external protein structures, cell surface properties, bacterial cell wall types, membranes, vesicles, and cell internal storage compounds.

**Table 3** Evaluation of other fluorochromes suitable for microbiological samples

Fluorochrome	Application	Reference
Hexidium iodide, Syto-13	Gram-stain	Mason et al. [220]
SYPRO	Total protein, bacteria	Zubkov et al. [425]
NanoOrange	Bacterial fine structures	Grossart et al. [103]
Hexidium iodide, CFDA	Gram-stain, activity	Forster et al. [84]
BCECF/AM	Oral bacteria	Gaines et al. [89]
Alexa-594, Dil C <sub>18</sub> (5)	Cell surface properties	Stoderegger and Herndl [349]
DAPI	Polyphosphate	Diaz and Ingall [68], Kulakova et al. [155]
Nile red	Neutral lipids	Bertozzini et al. [22], Pick and Rachutin-Zalugin [294], Sitepu et al. [337]
FM4-64	Bacterial membrane	Sharp and Pogliano [330]

### 3.2 Fluorescence In Situ Hybridization

In addition to general nucleic-acid—specific fluorochromes staining all bacteria, more specific probes were needed in order to identify groups of bacteria and individual bacterial species. In early reviews the potential of these molecular probes was discussed and different approaches were suggested [66, 117, 319, 391]. After several years of methodological development the technique of fluorescence in situ hybridization (FISH) became established [4, 132]. To date numerous applications of FISH in various environmental habitats have been reported (Table 4). The suitability of FISH in wastewater treatment was published recently in a handbook describing the major probes useful for detection of common microbial groups found in activated sludge samples [264]. In the meantime there are several variations of the original FISH technique. Very recently the principles of these variations were summarized in a special issue of *Systematic and Applied Microbiology* (2012, Volume 35, Issue 8). The most popular technique, CARD-FISH, dramatically improves the sensitivity due to signal amplification [324, 327]. This technique was applied for identification of cyanobacteria [323], picoplankton [271], marine bacteria [291], soil bacteria [80], epiphytic microorganisms [373], and freshwater biofilms [202]. A general disadvantage of FISH is the need for fixation and dehydration of the sample. Especially, dehydration using an ethanol series will destroy the original structure of bioaggregates and biofilms. By using ethanol, the polymer matrix of biofilm systems is essentially precipitated.

### 3.3 EPS Analysis

Due to the highly variable biochemical components of EPS, the analysis of EPS remains a dilemma. Chemical approaches require extraction of EPS constituents from the remains of the biofilm which is hampered by possible cell lyses. On top of



**Table 4** Fluorescence in situ hybridization in combination with confocal laser scanning microscopy applied to different microbial samples

Focus of article	Reference
Microbial consortia, activated sludge	Wagner et al. [386]
General methodology	Amann et al. [4]
Ammonia-oxidizing bacteria	Wagner et al. [388]
Activated sludge	Amann et al. [5]
Toluene degrading <i>Pseudomonas</i>	Möller et al. [235]
Nitrifying biofilm	Schramm et al. [325]
Methanol-fed biofilm	Neef et al. [244]
Bacteria associated with roots	Macnaughton et al. [206]
Multispecies biofilms	Möller et al. [235]
Aureobasidium on leaf surfaces	Li et al. [188]
River biofilms	Manz et al. [212]
Waste gas biofilms	Pedersen et al. [285]
Sulphate reducing bacteria, wastewater	Okabe et al. [274]
<i>Magnospira bakii</i>	Snaird et al. [339]
Cyanobacteria	Schönhuber et al. [323]
Anoxic niches, activated sludge	Schramm et al. [326]
Nitrifying reactor	Bouchez et al. [29]
Poly-P-accumulating bacteria	Crocetti et al. [55]
FISH methodology	Moter and Göbel [239]
Imaging methodology	Daims et al. [59]
Nitrifying bacteria	Gieseke et al. [94]
Anaerobic granules	Lanthier et al. [157]
Nitrifying biofilm	Gieseke et al. [93]
Sulphur-oxidizing bacteria, wastewater	Ito et al. [135]
FISH methodology	Pernthaler and Amann [290]
Oral bacterial biofilm	Thurnheer et al. [363]
Sulphur-oxidizing bacteria	Okabe et al. [273]
Low pH nitrifying biofilms	Gieseke et al. [95]
Nitrifying trickling filter	Lydmark et al. [203]
Ammonium-oxidizing bacteria, wastewater	Kindaichi et al. [148], Tsushima et al. [372]
CLASI FISH	Valm et al. [378]
See also	Special issue <i>Systematic and Applied Microbiology</i> 2012, 15 (8)

that, extraction might be straightforward in pure cultures, but in real-world biofilms the complexity of EPS constituents makes it nearly impossible to analyze individual polymer fractions. As a result lectins have been suggested as in situ probes for glycoconjugates [228, 249, 255]. Lectins were initially used for cell surface characterization in electron microscopy. Now fluorescently labeled lectins are employed for glycoconjugate detection in biofilms and bioaggregates. The usefulness of lectins is demonstrated by listing the major reports using the lectin approach in biofilms and bioaggregates in combination with epifluorescence or laser microscopy (Table 5). In many cases the procedure was employed with the standard lectin ConA, being one of

**Table 5** Application of lectins for in situ detection of glycoconjugates in biofilms and bioaggregates by means of light or laser microscopy

Lectin	Application	Reference
ConA, HPA, LPA	Marine biofilms	Michael and Smith [228]
WGA	<i>Staphylococcus</i> biofilm	Sanford et al. [316]
ConA, ECA, PNA, UEA	River biofilms	Neu and Lawrence [248]
WGA	River biofilms	Lawrence et al. [174]
APA, ConA, GS-I, LcH, Lotus, LPA, PNA, RCA, UEA, WGA	River aggregates (snow)	Neu [246]
ConA, PHA, PNA, UEA, WGA	<i>Sphingomonas</i> biofilms	Johnsen et al. [140]
ConA	Reactor biofilms	Wijeyekoon et al. [404]
ConA, Lotus, LPA, PNA, UEA, WGA	Evaluation of method in river biofilms	Neu et al. [255]
ConA	<i>Sphingomonas</i> biofilms	Kuehn et al. [154]
ConA, WGA	<i>Pseudomonas</i> biofilms	Strathmann et al. [352]
Screening with all commercially available lectins	Reactor biofilms	Staudt et al. [343]
ConA, UEA	Marine aggregate	Ciglenecki et al. [46]
AAL	Reactor biofilms	Staudt et al. [344]
WGA	<i>Streptococcus</i> biofilm	Donlan et al. [73]
ConA	<i>Sphingomonas</i> biofilms	Venugopalan et al. [381]
ConA, GS-I, Lotus, PHA, PNA	Marine biofilms	Wigglesworth-Cooksey and Cooksey [402]
ConA	Wastewater sludge	McSwain et al. [227]
Screening with all commercially available lectins	<i>Pseudomonas</i> biofilms	Laue et al. [161]
ACA, ECA, LBA, PNA	<i>Deinococcus</i> biofilms	Saarima et al. [313]
Con A	<i>Shewanella</i> aggregation	McLean et al. [226]
Screening with all commercially available lectins	<i>Deinococcus</i> biofilms	Peltola et al. [286]
ConA	<i>Rhizobium</i> biofilms	Santaella et al. [317]
ConA	Cold seep mats	Wrede et al. [411]
AAL	River aggregates	Luef et al. [198, 199]
ConA	Pure culture biofilms	Truong et al. [370]
ConA	Composting biofilms	Yu et al. [419]
Screening with all commercially available lectins	Tufa biofilms	Zippel and Neu [422]

the cheapest and having specificity for  $\alpha$  D-glucose and  $\alpha$  D-mannose. This technique is now known as fluorescence lectin-binding analysis (FLBA; [422]). With new sample types, the ideal first step involves a screening with all the commercially available lectins (see Table 5 for several references). This usually allows one to select lectins suitable for glycoconjugates present in a particular sample.

Proteins are present in the EPS in the form of enzymes that allow bacteria degradation and access to polymeric substrates. For enzyme activity measurements several fluorescent substrates are available. One of the compounds is particularly suited for CLSM as the product of activity is precipitated and can be easily located

**Table 6** Studies showing eDNA imaging in microbial communities

Focus of article	Reference
<i>P. aeruginosa</i> biofilms, mutants	Allesen-Holm et al. [3]
<i>H. influenzae</i> biofilms, pili	Jurcisek and Bakaletz [143]
<i>P. aeruginosa</i> biofilms, effect of iron	Yang et al. [413]
<i>P. aeruginosa</i> biofilms, resistance	Mulcahy et al. [240]
<i>E. faecalis</i> biofilms, autolysis	Thomas et al. [362]
<i>S. aureus</i> biofilms, maturation	Mann et al. [209]
<i>B. cereus</i> biofilms, adhesin	Vilain et al. [383]
<i>P. aeruginosa</i> biofilms, EPS matrix	Ma et al. [205]
<i>E. faecalis</i> biofilms, autolysis	Guiton et al. [109]
<i>N. meningitis</i> biofilms, dual role	Lappmann et al. [158]
Caulobacter biofilm, progeny	Berne et al. [20]
Mixed biofilms	Dominiak et al. [71]
<i>V. cholerae</i> biofilms, nucleases	Seper et al. [328]

via its fluorescence [151]. Very recently amyloids have been identified as an important EPS component in microbial biofilms [160]. Functional amyloids were also found in Gram-positive bacteria and form part of the cell envelope [141]. Due to their characteristic structure amyloids can be visualized using different fluorescence techniques. In a detailed study with *Bacillus subtilis*, amyloids were reported as responsible for binding cells together in biofilms [309].

Another EPS compound is extracellular DNA (eDNA) which was known for some time to be present in microbial communities. However, only the publication by Whitchurch and coworkers triggered a series of studies establishing eDNA as a very common EPS compound involved in biofilm dynamics [398]. Several of the studies on eDNA and the approaches applied for imaging eDNA are listed in Table 6.

### 3.4 Viability

Viability represents a characteristic of bacteria that is of great interest in various habitats. As a consequence numerous combinations of fluorescent stains have been suggested to assess viability. Life and death appear to be a critical issue in microbiology and the many protocols reported may be found in several short reviews [31, 61, 145, 193, 353]. Some of the titles used in these reviews question the status of bacterial viability in between life and death. There are even conference titles such as “How dead is dead?” A compilation and comparison of protocols is given in Table 7. All of the fluorochromes tested are employed in order to assess the permeability of the cell wall and cell membrane as a measure for viability. The applications using a popular commercial kit are listed in Table 8. Again this test is the subject of some controversy although some groups use it without questioning. Other research groups seem to be more critical of the results

**Table 7** Fluorochromes and combinations suggested for assessment of viability in microbiological samples

Fluorochromes	Application	Reference
Different membrane potential dyes	Pure cultures	Mason et al. [219]
Rhodamine 123, propidium iodide, oxonol	Starvation survival of pure cultures in seawater	Vives-Rego et al. [385]
Ethidium bromide, propidium iodide, CFA, CCFAS, rhodamine 123, bis-oxonol	Pure cultures	Nebe-von Caron and Badley [242]
DiBAC <sub>4</sub> (3) in comparison to others	Gram-positive/negative pure cultures	Jepras et al. [139]
SytoxGreen	Pure cultures	Roth et al. [310]
	Starved pure cultures	Lebaron et al. [183]
CFDA, Chemchrome B, BCECF-AM, Rhodamine 123, BacLight	<i>Listeria</i>	Jacobsen et al. [136]
Ethidium bromide, bis-oxonol, propidium iodide	<i>Salmonella</i>	Nebe-von Caron et al. [243]
DAPI, propidium iodide	Bacterioplankton	Williams et al. [405]
CSE dye, ChemChrome V6	Freshwater bacteria	Catala et al. [38]
SybrGreen, propidium iodide	Freshwater/marine bacteria	Gregori et al. [102]
	Marine sediment	Luna et al. [200]
CFDA, CFDA/SE	Pure cultures	[125]
ViaGram Red, FISH	Bacteroides	[318]
Ethidium monoazide, PCR	Pure cultures	Rudi et al. [311]
Ethidium homodimer-2, SybrGreen-1	Sediment bacteria	Manini and Danovaro [208]
Carboxy-DFFDA SE, propidium iodide	<i>Comamonas</i>	Shimomura et al. [331]
Alexa fluor 633 hydrazide, DIOC <sub>2</sub> (3)	<i>Escherichia</i>	Saint-Ruf et al. [315]
Propidium iodide, thiazole orange	<i>Lactobacillus</i>	Doherty et al. [70]
TO-PRO-1 iodide, 5-CFDA-AM	Planktonic algae	Gorokhova et al. [100]
TO-PRO-3 iodide	<i>Candida</i>	Kerstens et al. [146]

obtained [21, 60, 61, 208, 348]. In any case, the test may be used for pure culture studies and has to be evaluated by using the appropriate positive and negative controls. Nevertheless, the test should be used with caution if environmental samples are examined. The many types of bacterial species having different cell wall structures may respond differentially towards the staining procedure making it difficult to discern live from dead.

**Table 8** Application of the BacLight—live/dead kit to different microbiological samples

Sample type	Reference
<i>Salmonella</i>	Korber et al. [153]
Gram-positive/negative	Virta et al. [384]
Drinking water bacteria	Boulos et al. [30]
Oral biofilms	Guggenheim et al. [107]
<i>Streptomyces</i>	Fernandez and Sanchez [79]
Oral biofilm	Hope and Wilson [128]
<i>Pseudomonas</i>	Finelli et al. [82]
Heavy metal resistance	Teitzel and Parsek [360]
<i>Extremophilic archaea</i>	Leuko et al. [186]
Evaluation	Stocks [348]
<i>Shewanella</i>	Teal et al. [359]
Evaluation	Berney et al. [21]
Dental biofilms	Filoche et al. [81]
Soil bacteria	Pascaud et al. [284]
<i>Saccharomyces</i>	Davey and Hexley [60]
Stressed bacteria	Czechowska and van der Meer [56]

### 3.5 Activity Measurements

Bacterial activity is typically measured by using radioactive compounds such as  $^3\text{H}$ -thymidine or  $^3\text{H}$ -leucine [304, 342]. Another approach uses tetrazolium salts that are reduced by active microorganisms resulting in the formation of insoluble formazan crystals. This particular test again is controversial and there are several publications indicating issues regarding the results [54, 260, 278, 329, 374].

The activity of bacteria may also be determined indirectly by using fluorescent compounds. The technique uses bromodeoxyuridine (BrdU) as a thymidine analogue for incorporation into DNA. BrdU is then detected by an immunoassay. Initially the assay was used in cell biology, but in the meantime this test was adapted and varied in microbiology. The BrdU labeled DNA can be analyzed by antibodies either in situ or after extraction and may be combined with other molecular techniques [9, 10, 112, 346, 358, 376, 390]. The BrdU technique can be also coupled to a substrate utilization assay in order to study the bacterial response to a specific amendment [417]. More recently new nontoxic thymidine analogues were synthesized and tested as replacements for BrdU [245].

### 3.6 Antibodies

Labeled antibodies specific to cell surface features have been used in many studies. Usually samples with suspended bacteria or aggregates were examined by electron or epifluorescence microscopy. Only a few groups have intensively employed

specific antibodies to investigate microbial biofilm samples. For example, the bacteria of the oral cavity have been assessed by using antibodies in order to follow their location in bioaggregates and biofilms [106]. In a methodological study, antibodies labeled with quantum dots were tested to demonstrate single-cell resolution of planktonic and biofilm bacteria of oral origin [40]. A similar approach was used in order to follow individual species in mixed culture biofilms of oral bacteria. However, in these cases the antibodies were labeled with organic fluorochromes [287, 289]. Another group used immunofluorescence to analyze bacteria associated with plant roots (see section below).

### 3.7 FISH-MAR

The combination of FISH and microautoradiography (MAR) allows simultaneously probing for identity and activity of bacteria [185, 259]. Basically the FISH protocol was extended by feeding a radioactive substrate with subsequent exposure to an autoradiographic gel. Signal detection of FISH fluorescence (fluorescent label of probe) and MAR reflection (silver grains) is done by using CLSM. The advantages of this combined approach were applied in *Achromatium* communities [101], Thiotrix [265], *Nitrospira* [58], iron reducers [261], sulphate-reducing bacteria [134], microbial biofilms [263], nitrifying bacteria [276], bacterioplankton [336], and *Chloroflexi* [232]. Although the technique has been applied in different habitats and appears to be a standard approach [262, 275], FISH-MAR is employed by only a few research groups.

### 3.8 GFP

Fluorescence signals recorded by CLSM are usually based on autofluorescence or staining with specific fluorochromes. In many cases fluorochromes are regarded as toxic for microorganisms. This represents an issue if the same sample has to be examined frequently over time. The discovery and incorporation of GFP and its variants into the genome of bacteria opened a whole new range of options for imaging. Thereby staining with potentially toxic fluorochromes became obsolete at least for many pure culture studies that can be genetically manipulated and express GFP. The publications taking advantage of fluorescent proteins for studying biofilms are compiled in Table 9. In the meantime, two spectrally different fluorescent proteins are often employed, one which is permanently expressed to localize the bacteria and one to “see,” for example, a specific gene activity such as in Klausen et al. [150] and Haagenen et al. [111].

**Table 9** Studies with fluorescent proteins as marker for microbial biofilms with subsequent analysis by confocal laser scanning microscopy

Focus of article	Reference
Activated sludge	Eberl et al. [77]
<i>Pseudomonas</i> biofilm	Christensen et al. [45]
Mixed culture biofilm	Möller et al. [236]
Marine microcolonies	Stretton et al. [354]
Activated sludge	Olofsson et al. [277]
Pure culture biofilms	Sternberg et al. [345]
Bacteria on leaves	Li et al. [187]
Flow-chamber biofilms	Heydorn et al. [123]
<i>Pseudomonas</i> biofilms GFP/RFP	Tolker-Nielsen et al. [366]
Dual species biofilms	Tolker-Nielsen and Molin [367]
Rhizosphere biofilms	Ramos et al. [301]
Dual species biofilms	Nielsen et al. [258]
Methodology	Cowan et al. [51]
Quorum sensing in flow chambers	Andersen et al. [6]
Wheat colonization	Unge and Jansson [375]
Gene transfer in flow chambers	Haagensen et al. [110]
<i>Pseudomonas</i> biofilms	Heydorn et al. [122]
Dual species biofilms	Christensen et al. [44]
<i>Streptococcus</i> biofilms	Yoshida and Kuramitsu [418]
<i>Pseudomonas</i> CFP/YFP mutants	Klausen et al. [150]
Drinking water model biofilms	Martiny et al. [218]
<i>Pseudomonas</i> biofilms	Werner et al. [395]
Methodology	Jansson [137]
Starved biofilms	Gjermansen et al. [97]
Review	Larrainzar et al. [159]
Evolution and species interactions in biofilms	Kirkelund Hansen et al. [149]
<i>Pseudomonas</i> biofilms	Haagensen et al. [111]
Mixed species biofilm	Hansen et al. [114]
<i>Staphylococcus</i> eDNA in biofilms	Qin et al. [299]
<i>Shewanella</i> CFP/YFP biofilms	McLean et al. [225]
EPS in <i>Pseudomonas</i> biofilms	Yang et al. [414]
<i>Sulfolobus</i> biofilms	Henche et al. [118]

## 4 Applications of CLSM and Fluorescence Techniques

### 4.1 Biofilms

Due to the three-dimensional features and immobilization of cells within microbial biofilms CLSM is ideally suited for examination of a broad range of very different biofilm samples. Some of the many applications are compiled in Table 10 and sorted according to different habitats and topics such as biofilms, river biofilms, mats, sediments/soil, rocks, oil/hydrocarbon, medical/oral, and so on. Samples for CLSM may come directly from the environment, for example, in the form of river

**Table 10** Applications of confocal laser scanning microscopy in various fields of microbiology

Focus of article	Reference
<i>Biofilms</i>	
Channel structure	Massol-Deya et al. [221]
Microbial-influenced corrosion	White et al. [399]
Escherichia coli biofilm	Swope and Flickinger [356]
Dual culture biofilm	Stewart et al. [347]
Corrosion inhibition by biofilms	Jayaraman et al. [138]
Marine biofilms on steel	Kolari et al. [152]
Marine biofilms	Norton et al. [270]
Alginate in <i>Pseudomonas</i> biofilms	Nivens et al. [266]
<i>Roseobacter</i> biofilms	Bruhn et al. [32]
Calgary biofilm device	Harrison et al. [115]
<i>Legionella</i> biofilm	Piao et al. [293]
Mycoplasma biofilms	McAuliffe et al. [224]
Gravity effect on biofilms	Lynch et al. [204]
<i>Salmonella</i> biofilms	Mangalappalli-Illathu et al. [207]
Coaggregation biofilms	Min and Rickard [230]
Cold saline spring streamers	Niederberger et al. [257]
Agarose stabilization	Pittman et al. [297]
Proteus biofilms	Schlapp et al. [320]
<i>River biofilms</i>	
Three-channel imaging	Lawrence et al. [174]
Phosphorous limitation	Mohamed et al. [233]
Effect of nickel	Lawrence and Neu [171], Lawrence et al. [162]
Effect of CNP	Neu et al. [254]
Biophysical control	Besemer et al. [24]
<i>Microbial mats</i>	
Algal mat	Lawrence et al. [176]
Alpine mats	Wiggli et al. [149]
Hot spring mats	Pierson and Parenteau [295]
Stromatolites	Sabater [314]
Cyanobacterial mats	de los Rios et al. [62]
Cyanobacterial mats	Sole et al. [340]
<i>Sediment/soil</i>	
Bacteria in geological media, sand, minerals	Lawrence and Hendry [163], Hendry et al. [119], Lawrence et al. [169]
<i>Cryptosporidium oocysts</i>	Anguish and Ghiorse [7]
Aquifer microcosm	DeLeo et al. [65]
Peat microbial ecology	Lloyd et al. [194]
Contaminated soil	Karimi-Lotfabad and Gray [144]
Fresh marine sediments	Waite et al. [389]
Porous media clogging	Kim et al. [147]
<i>Rocks</i>	
Antarctic lithobionts	Ascaso and Wierzchos [11]
Antarctic lithobionts	de los Rios et al. [63]

(continued)



**Table 10** (continued)

Focus of article	Reference
Hypogean biofilms	Hernandez-Marine et al. [121]
Hypogean biofilms	Roldan et al. [306]
Antarctic lithobionts	Wierzchos et al. [401]
<i>Degradation</i>	
Diclofop	Wolfaardt et al. [407–409]
Effect of herbicides	Lawrence et al. [164]
Effect of pharmaceuticals	Winkler et al. [406], Lawrence et al. [178, 179]
Effect of chlorhexidine	Lawrence et al. [181]
<i>Oil /hydrocarbons</i>	
Acinetobacter on diesel droplets	Baldi et al. [14]
Alkane assimilation at low temperature	Whyte et al. [400]
Organic compound degradation	Cowan et al. [52]
Hexadecane degradation	Holden et al. [126]
Hydrocarbon degradation	Stach and Burns [341]
Growth on crystals and emulsions	Baldi et al. [15]
Stabilization of oil–water emulsions	Dorobantu et al. [76]
<i>Mycobacterium</i> biofilms	Wouters et al. [410]
<i>Medical/oral</i>	
Mass transport in plaque	Thurnheer et al. [364]
Coaggregation, oral bacteria	Palmer et al. [280]
Coaggregation, oral bacteria	Periasamy and Kolenbrander [288]
Coaggregation, oral bacteria	Periasamy and Kolenbrander [289]
<i>Actinomyces</i> biofilm	Dige et al. [69]
<i>Reactors</i>	
Glycoconjugate distribution	Staudt et al. [343]
Fluidized bed reactor	Boessmann et al. [27]
Bacterial and EPS biomass	Staudt et al. [344]
Biofilm strength	Möhle et al. [234]
Development and detachment	Garny et al. [90]
Sloughing and detachment	Garny et al. [91]
Online monitoring	Wagner et al. [387]
<i>Miscellaneous</i>	
Spore germination	Coote et al. [49]
Conjugation in biofilms	Hausner and Wuertz [116]
Mine tailings	Podda et al. [298]
Adhesion to apples	Burnett et al. [36]
Bacteria attached to nematode cyst	Nour et al. [272]
Phototrophic pigments	Roldan et al. [308]
Bacterial single-cell adhesion	Lower et al. [195]
Phototrophic biofilms	Roldan et al. [307]
Assessment of carrier material	Biggerstaff et al. [25]
Yeast colony shape	Vachova et al. [377]
<i>Pseudomonas</i> swarming	Morris et al. [238]
<i>Synechococcus</i> single-cell study	Ruffing and Jones [312]

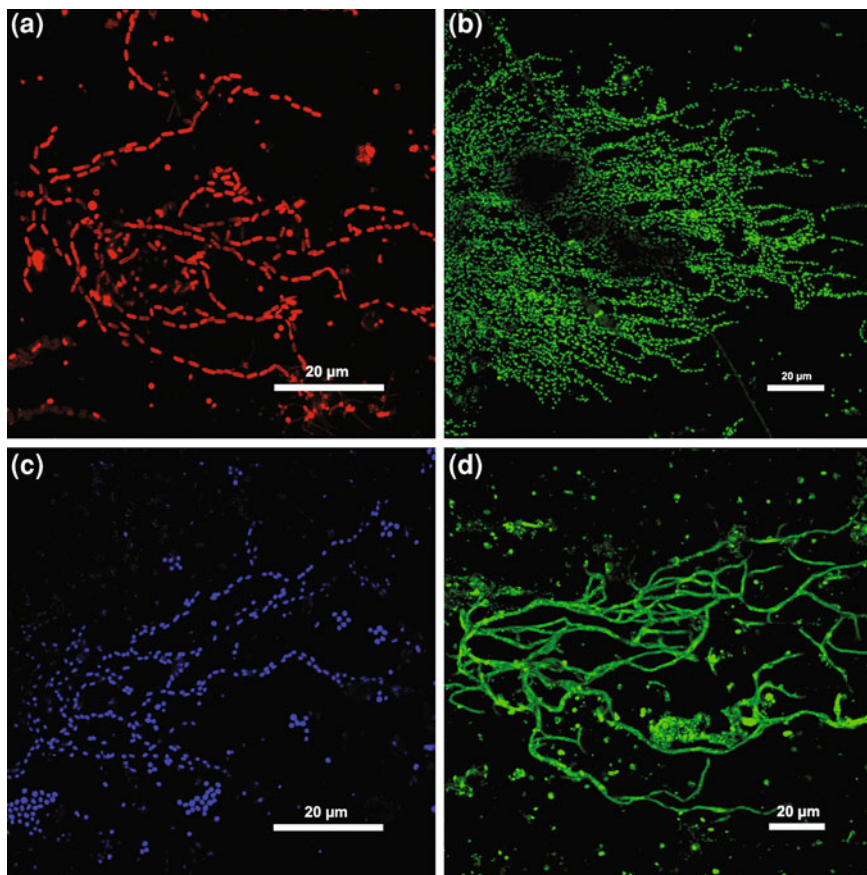


**Fig. 1** CLSM dataset shown as *MIP* maximum intensity projection showing rotating annular reactor biofilms developing in flow direction (*right*). Samples were stained with SyproRed (a). Acridine orange (b). DAPI (c). WGA-FITC lectin (d)

pebbles, aquifer material, roots, leaf litter, and the like. They can be used preferably by putting samples into small Petri dishes and imaged by water-immersible lenses. In addition, laboratory microcosms were developed for growing biofilms under seminatural conditions [23, 177, 335, 423]. The advantage of microcosms lies of course in the precisely determinable substratum size and properties. The wide range of biofilm types that can be examined by CLSM imaging resulted in the enormous success of CLSM which in many laboratories replaced widefield and epifluorescence microscopy. Some examples demonstrating CLSM on thin biofilms stained with different fluorochromes are presented in Fig. 1. Biofilms are also used in studies with a focus on biotechnology, structure function dynamics, degradation and sorption of organic and inorganic compounds, as well as in corrosion (Table 10). CLSM of laboratory reactor biofilms, biofouling, and other technical samples are discussed in Sect. 4.9.

## 4.2 River and Phototrophic Biofilms

One of the first applications of CLSM on river biofilms was reported in 1997. The biofilms developed in a model system showed a ridged structure in the flow direction and a predominance of EPS-embedded bacteria in the outer regions of the biofilm [248]. This initial paper resulted in a series of reports looking at different aspects of river biofilms (see Table 10 for references). Some of the results were presented in a review on river biofilms and the applicability of CLSM [171]. Phototrophic biofilms were also the focus of several studies including the EC project PHOBIA [423]. Some of the investigations took advantage of imaging autofluorescence of phototrophs that can be easily separated in different channels [174, 256].

More recently Battin's group picked up the topic "river biofilms" and produced a series of excellent publications. They used CLSM to study ecosystem processes in a streamside flume [17]. Another part of their work focused on the physical, chemical, and biotic control of stream biofilm development [24]. As a consequence structure–function coupling with respect to carbohydrate uptake was investigated [334]. One outcome of the research was a novel concept for biofilm research that looks at biofilms as a form of landscape [18]. An example of the complex composition of lotic biofilms is shown in Fig. 2.

## 4.3 Flocs, Aggregates

The suitability of CLSM for studying the fragile structure of marine aggregates was demonstrated by using a variety of staining approaches. It was shown that marine snow aggregates are structurally very diverse with areas of different density [53, 127]. A similar approach was employed to investigate river snow (Fig. 3) in order to assess cell and glycoconjugate distribution [246]. Later this was extended by combining fluorescence lectin-binding analysis and FISH [26]. The combination of FLBA and CARD-FISH was reported recently for marine aggregates from the North Sea [19]. Both approaches, FISH and FLBA, may be used as an indicator for community diversity. The various approaches for imaging microbial flocs, aggregates, and granules were compiled in a comprehensive review [173].

## 4.4 Grazing

There are numerous studies of protist grazing on planktonic microorganisms as well as on microbial biofilms that were summarized in a review with a focus on freshwater biofilms [283]. The issue with protists in combination with point scanning CLSMs is their motility. Although instruments with fast scanners are now available, the best choice might be using a spinning disk CLSM. The suitability of CLSM for

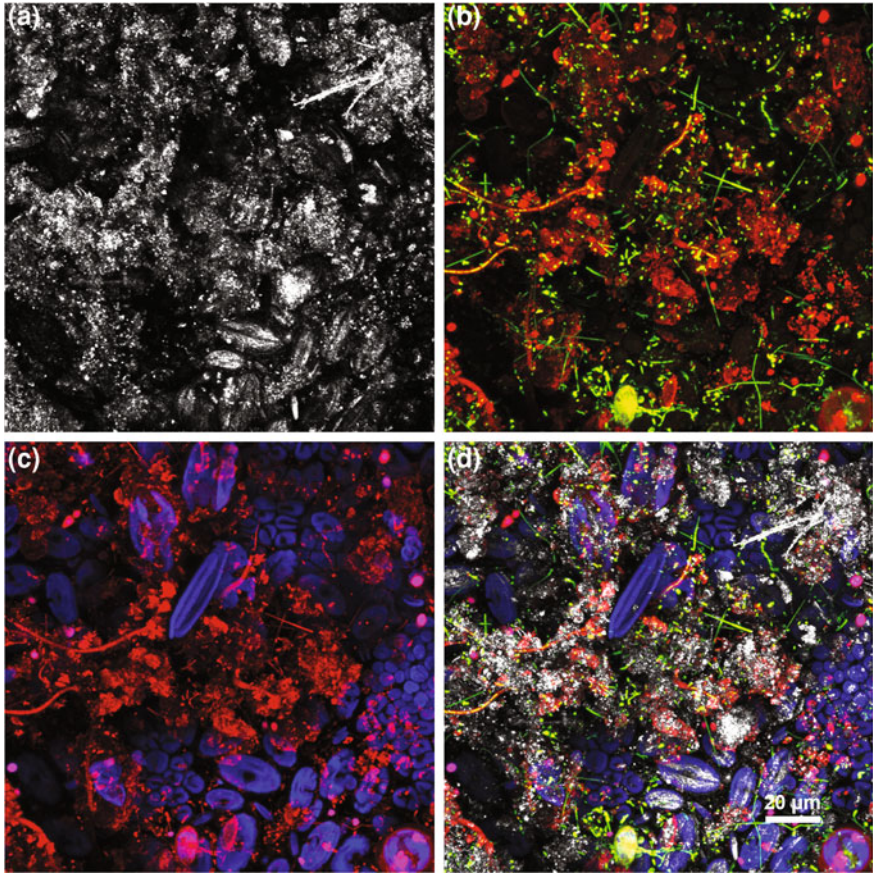


**Fig. 2** CLSM dataset as maximum intensity projection showing a river biofilm with complex environmental features. The same dataset is presented as reflection (a), nucleic acid and lectin staining (b), lectin staining and autofluorescence (c), all four channels (d). Color allocation: reflection = *white*, nucleic acid staining = *green*, lectin staining = *red*, autofluorescence of chlorophyll A = *blue*

imaging protozoa was confirmed in a taxonomic study of testate amoebae [35]. The various reports on the effects of protist grazing on microbial biofilms examined by CLSM are compiled in Table 11. Most of the studies used CLSM not for visualization of protists but for measuring the effect of grazing on the resulting biofilm structure. Other studies focused on biofilm grazing by invertebrates and examined the changes in biofilm architecture and composition by CLSM [175]. Different aspects of grazing are presented in Fig. 4.

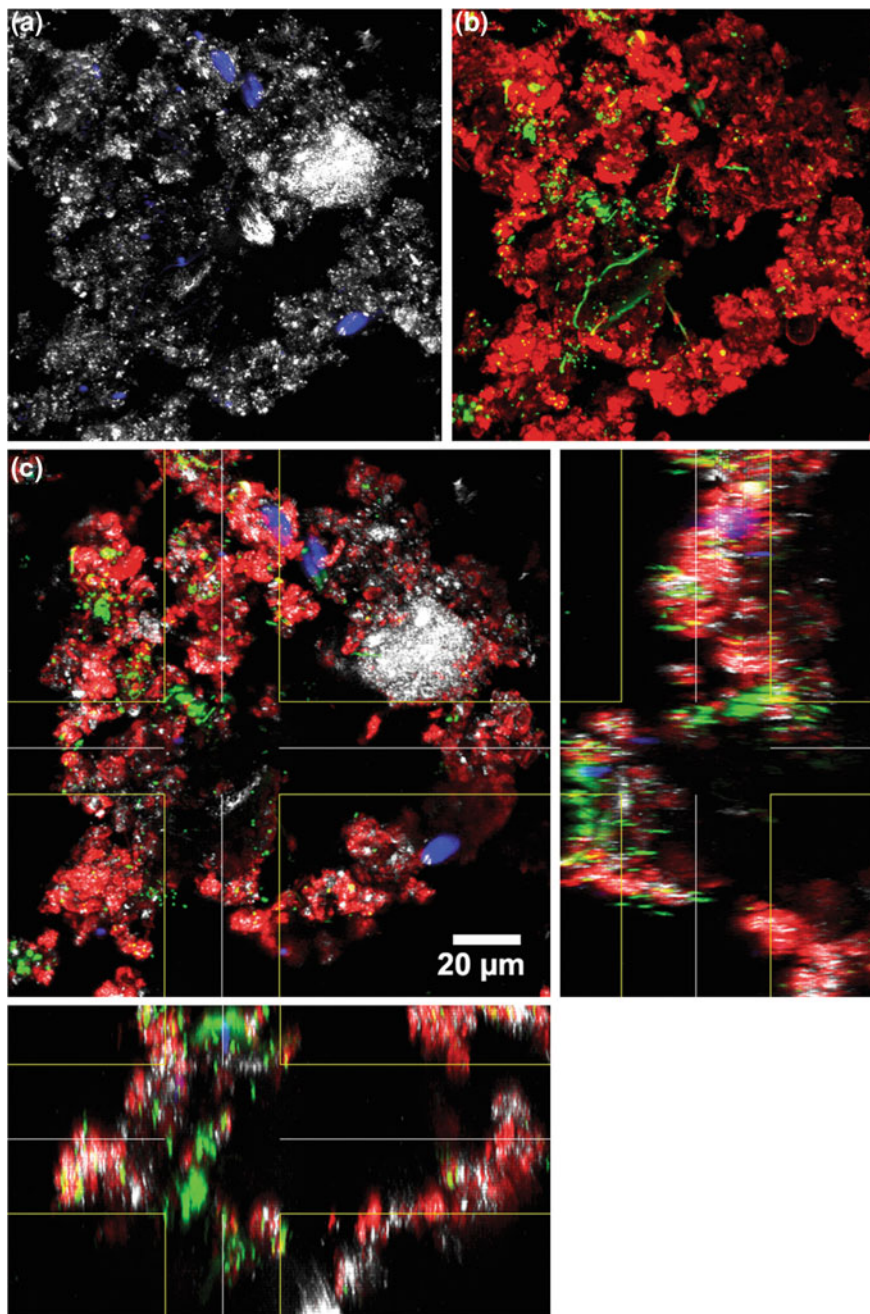


**Fig. 3** CLSM dataset showing a mobile biofilm in form of a river aggregate with complex environmental features. The same dataset is presented as MIP showing reflection and autofluorescence **(a)**, nucleic acid and lectin staining **(b)**, all four channels projected in XYZ with side views **(c)**. Color allocation: reflection = *white*, nucleic acid staining = *green*, lectin staining = *red*, autofluorescence of chlorophyll A = *blue*

**Table 11** Grazing of protists on microbial biofilms studied by means of confocal laser scanning microscopy

Focus of article	Reference
Wastewater biofilm	Eisenmann et al. [78]
Rotating contactor biofilm	Martin-Cereceda et al. [217]
Methodology	Packroff et al. [279]
<i>Pseudomonas</i> biofilm	Matz et al. [222]
<i>Pseudomonas</i> biofilm	Weitere et al. [394]
<i>Serratia</i> biofilms	Queck et al. [300]
Flow cell biofilms	Böhme et al. [28]
River biofilms	Wey et al. [396]
Evaluation of methods	Burdikova et al. [35]
River biofilms	Wey et al. [397]
Flow cell biofilms	Dopheide et al. [75]

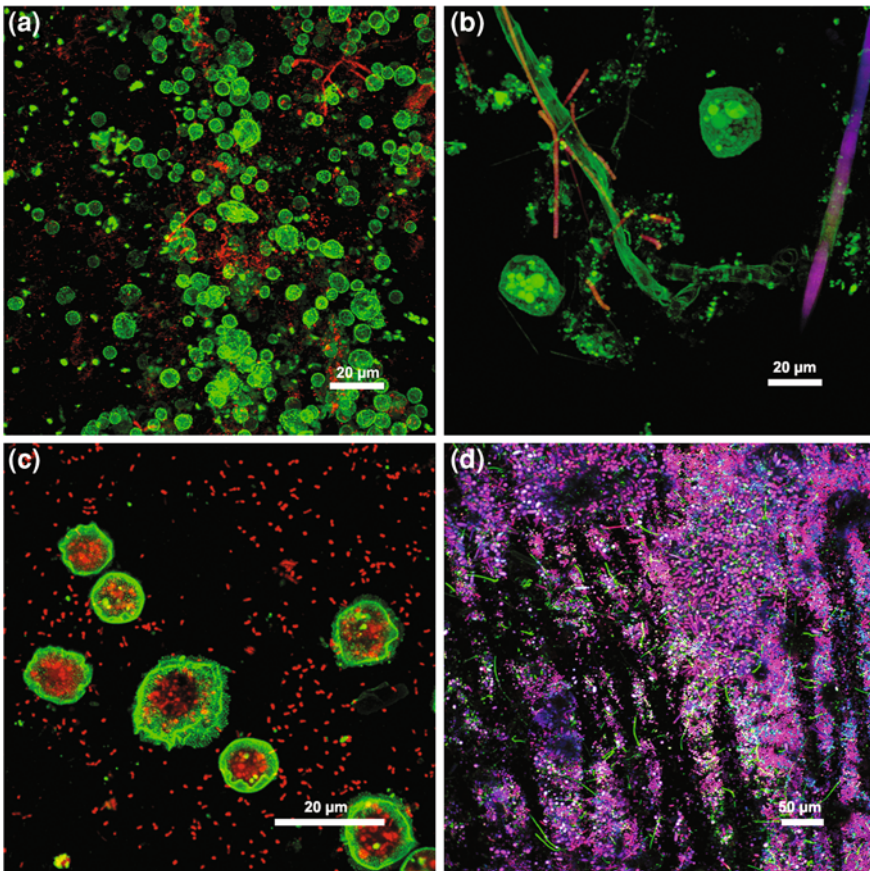


**Fig. 4** CLSM dataset as MIP showing grazing of biofilms by protists (a–c) and snails (d). Please take notice of the grazing pattern caused by the snail in (d). The samples were stained with AAL-Alexa488 lectin and Syto60 (a). ConA-OregonGreen lectin (b). AAL-Alexa488 lectin and Syto60 (c). Syto9 and autofluorescence (d). Color allocation: reflection = white, nucleic acid staining = red (a, c), autofluorescence of phycobilins = pink

## 4.5 *Fungi, Lichens*

The applicability of CLSM in mycology was recognized very early [57]. Several reports describe fluorochromes suitable for staining fungi. For example, FUN-1 was developed especially for yeast cells to assess distribution and viability [120, 229]. Additional fluorochromes were suggested for filamentous fungi to study cell wall porosity and viability [33]. Other lipophilic probes were employed to follow endocytosis and vesicle transport in fungal hyphae [83]. Fungi as eukaryotic microorganisms can also be stained using fluorochromes specific for cell organelles [47]. Overall CLSM has been employed in mycology to assess cellular status and also to follow the spatial development of fungal hyphae [268, 269]. An overview showing current state-of-the-art CLSMs of fungi was published by Reid and coworkers in Edinburgh [124]. Related studies focused on the interaction of fungi with other organisms. For example, CLSM was used to investigate the interaction of bacteria and fungi with sugar beet roots [420]. It was found that bacteria may take the fungal “highway” in order to access their substrate in soil. These bacterial–fungal interactions can be followed directly by CLSM imaging [87, 88]. Similarly CLSM may be used to study the symbiosis between phototrophic microorganisms and fungi in lichens [104, 105]. Examples of fungal biofilm systems examined by CLSM are shown in Fig. 5.

## 4.6 *Bacteria on Plant Surfaces*

Hartman’s group used CLSM together with different techniques for specific detection of bacteria associated with plant roots. They used antibodies [321, 322] as well as rRNA-targeted oligonucleotide probes [12] for localization of rhizosphere bacteria. Both techniques have been combined for improved tracking of bacteria in the rhizosphere of wheat [13] and rice plants [96]. The same combined approach was used for detection of *Pseudomonas* on sugar beet roots [197]. Another study looked at colonization of barley roots by *Pseudomonas* using immunofluorescence techniques [113]. Examples of the association of bacteria with root surfaces are shown in Fig. 6. CLSM was also applied to observe microorganisms on leaf surfaces. The authors compared epifluorescence, scanning electron, and CLSM as an imaging tool on a range of different leaf types [237]. Adhesion of pathogens to leaves also represents an issue in food microbiology. This was studied using *Arabidopsis* and potentially critical bacterial strains [48]. Bacteria on leaves may also contribute to growth as shown for cyanobacteria on rice leaves [8]. Nitrogen-fixation in *Rhizobium*–legume symbiosis was studied using inert surfaces as well as different host plants. Thereby the factors important for colonization were established [86].

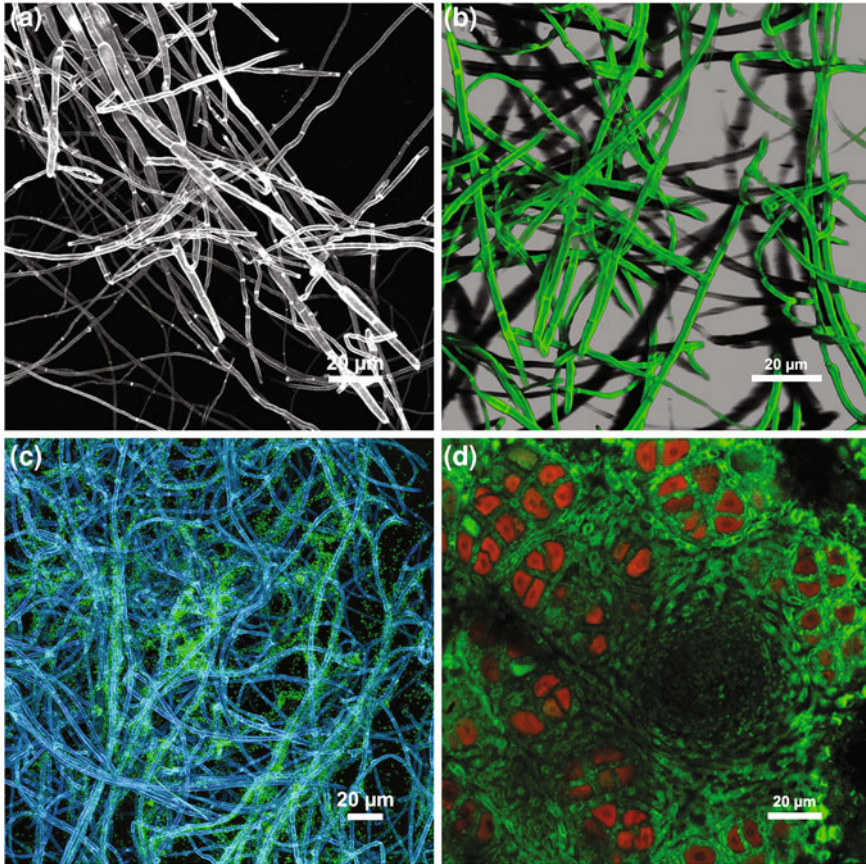


**Fig. 5** CLSM datasets of fungi as pure culture biofilm (**a** as MIP, **b** as shadow projection) and in association with other organisms (**b** with bacteria, **c** with phototrophs). All fungal filaments were stained with CalcoFluor white shown in different colors. Bacteria were stained with Syto9 (**c**) and autofluorescence is shown in red (**d**)

#### 4.7 Granules

Microbial granules are important in wastewater treatment. Initially reactors were run with anaerobic granules but more recently granules have been developed under aerobic conditions. Due to their solid appearance they are dense and often impenetrable by laser beam, but they are amenable to sectioning and subsequent CLSM examination. More recently several publications on aerobic granules were published in order to understand their development and dynamics (Table 12). Nevertheless there might be a limitation if multiple stains are applied to one sample. Application of six different fluorochromes specific for different biochemical features indicated issues due to fluorochrome specificity, fluorochrome



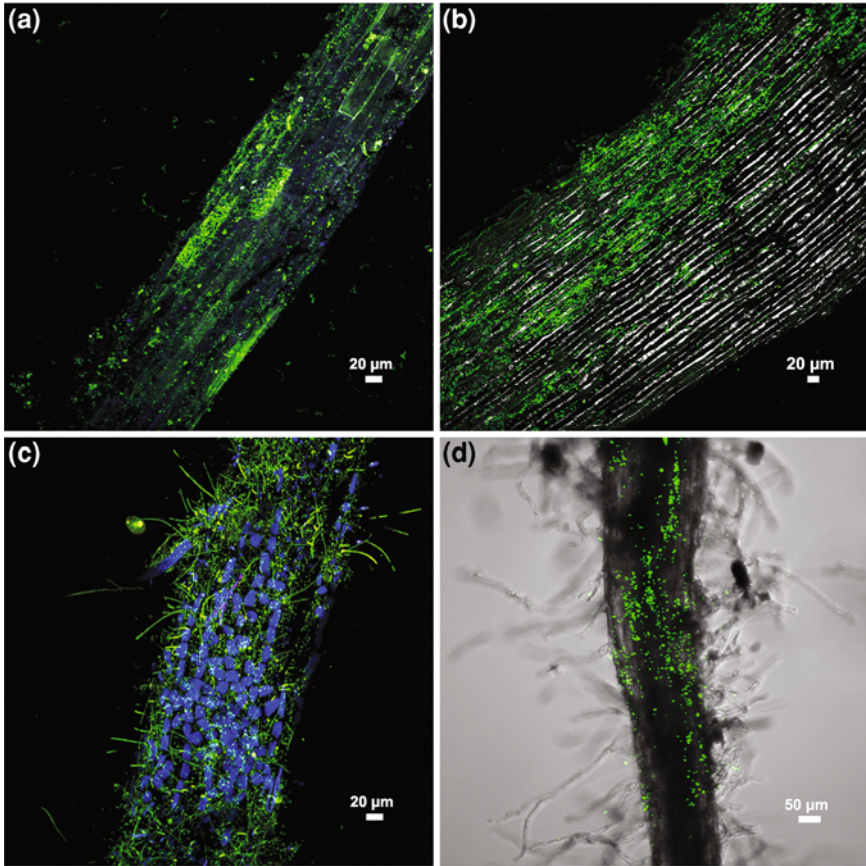


**Fig. 6** CLSM datasets of root biofilms shown as MIP. Samples originate from sand filters (a), laboratory experiments (b, d), water plant (c). Bacteria on roots were stained with: Syto9 (a, b, c) and were labeled with GFP (d). Color allocations Syto 9 and GFP = *green*, autofluorescence of chlorophyll A = *blue*, reflection = *white*. The confocal image of GFP was combined with the nonconfocal transmission image (d)

interactions, fluoro-chrome penetration, fluoro-chrome excitation, and crosstalk between emission signals. Although some of the issues can be solved with state-of-the-art hardware (e.g., white laser) and software (e.g., unmixing) as well as improved sample preparation (e.g., staining after sectioning), multiple staining remains a challenge in complex microbial communities. Very recently a detailed study of granules developed in different reactors presented a variety of staining approaches for assessment of granule structure and composition [393].

**Table 12** Reports on granules examined by confocal laser scanning microscopy

Focus of article	Reference
Anaerobic granule	Rocheleau et al. [305]
Staining procedures	Chen et al. [42]
EPS distribution	Chen et al. [43]
Fluorochrome diffusion	Tsai et al. [371]
Granule stability	Adav et al. [2]
Hydrogen-producing granules	Zhang et al. [421]
Granule-formation mechanism	Barr et al. [16]
Internal growth	Juang et al. [142]
Mass transfer	Liu et al. [192]
Development of granules	Verawaty et al. [382]
Granule formation and structure	Weissbrodt et al. [393]

## 4.8 Viruses, Phages

Studying the interaction of viruses and phages with microbial communities is not just based on pure scientific interest. In fact there are very practical issues in terms of the stability of pure and mixed cultures or the potential control of infections and biofilms by means of phage treatment [72, 196]. Viruses and phages are below the resolution of the light and laser microscope (Fig. 7). Nevertheless, viruslike particles can be stained and visualized by means of epifluorescence and laser microscopy as shown in an early report [74]. Viruses were also investigated in association with river aggregates. One study has critically discussed the challenges when viruses are analyzed by light or laser microscopy [198]. Electron and laser microscopy were also applied in order to examine marine bacteria and viruses and their association with black carbon particles. A comparison with molecular techniques showed the limitation of quantitative imaging with both SEM and CLSM [39]. In a very recent article an issue regarding fake virus particles has been raised [85]. Apart from true viruses and phages there might be membrane-derived vesicles, gene transfer elements, and cell debris all of which can contain nucleic acids and result in staining if nucleic-acid—specific fluorochromes are applied. In most studies the effect of bacteriophages on biofilm development has been indirectly assessed in order to avoid high-resolution imaging [98, 223, 303].

## 4.9 Technical and Model Systems

Frequently CLSM is applied to study reactor biofilms in order to assess the growth and performance of the system especially in terms of wastewater treatment or contaminant degradation (Fig. 8). Unwanted biofilms in the form of biofouling represent another sample type often examined by means of CLSM in order to estimate the degree of fouling (Fig. 9a, c, d). CLSM as an imaging technique can not only be used on medical and (micro)biological samples but also in technical systems with no biological objects present. For example, the porosity of samples can be

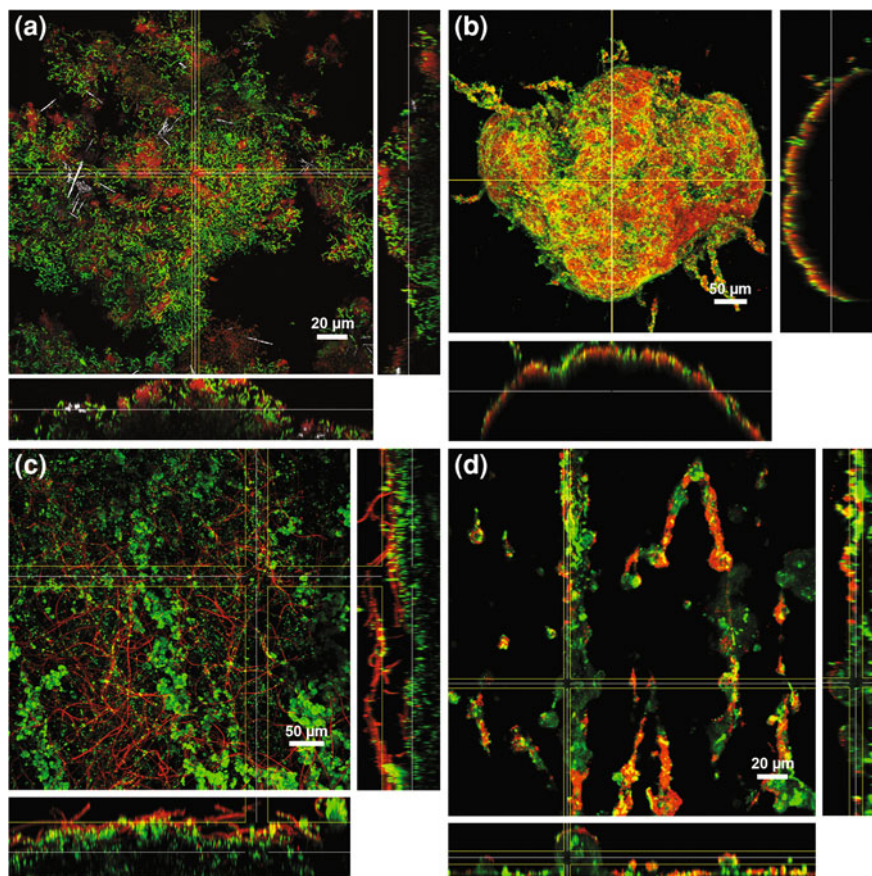


**Fig. 7** CLSM dataset in XYZ projection showing reactor biofilms with different structural features. Substratum exposed in a stirred tank reactor **(a)**, fluidized bed reactor biofilm on carrier **(b)**, tube reactor with filamentous bacteria on biofilm surface **(c)**, tube reactor with biofilm ridges in flow direction **(d)**. Color allocation: nucleic acid staining = *green*, lectin staining = *red*, reflection = *white*

measured. Similarly emulsions of different types may be characterized by CLSM. Furthermore, the flow pattern and diffusion of compounds in porous media such as chromatography column material can be studied by using fluorochromes as tracers. For this reason some of the applications that might be of interest in biotechnology are compiled in Table 13. An example of this type of application is given in Fig. 8.

## 5 Future Prospects

The development of LSM changed the way light/laser microscopy is done today. Nevertheless new techniques are becoming available for the imaging of microbiological samples. These exciting techniques are following two paths. First, they

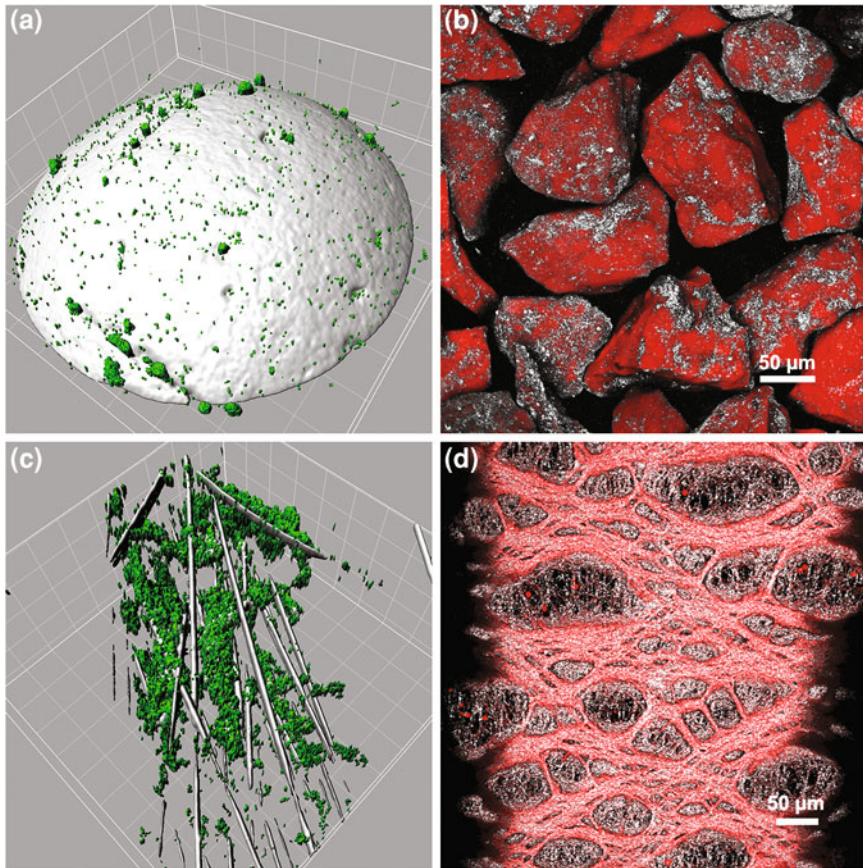


**Fig. 8** CLSM datasets of biofilms from technical habitats shown as isosurface projection (**a, c**) and MIP (**b, d**). Bacteria attached to a bead and to fibers from a water purification set-up (**a, c**) were stained with Syto9. Coating of particles with silicone and stained using NileRed (**b**). Fouling of a membrane was visualized by staining with SyproOrange (**d**)

are aimed at enhancing the resolution beyond the diffraction limit. With normal light or laser microscopes this limit is in the range of 300–200 nm depending on the wavelength and sample type. The new microscopy techniques that are now available have a resolution of 120 nm in structured illumination microscopy (SIM), 70 nm in stimulated emission depletion microscopy (STED), and 30 nm in localization/stochastic/blink microscopy (PALM/STORM/GSD). The drawback of these techniques lies in the fact that the sample somehow has to match the technical requirements of the instrument. As a result they cannot be used with the same flexibility as, for example, CLSM. Second, other new techniques are aiming at macroscale imaging. For example, optical coherence tomography (OCT) can be used to image biofilms at the mm scale in a top-down fashion. Another technique,

**Fig. 9** CLSM data showing an example of viruses from a multiple-filtered river water sample stained by SybrGreen. The large objects are bacteria and the tiny signals are viruslike particles

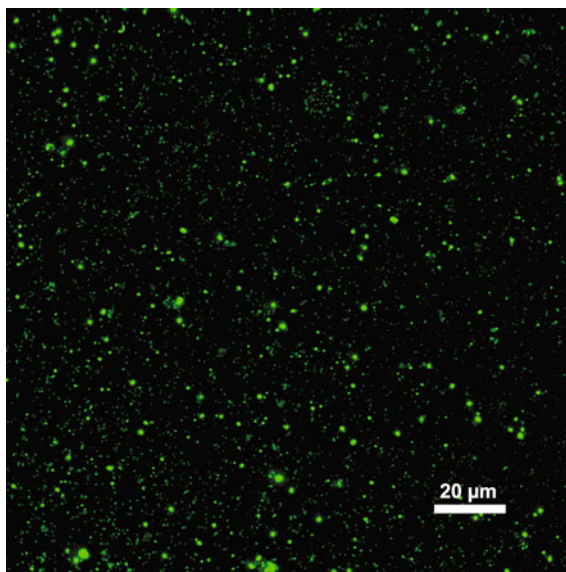


**Table 13** Technical systems studied by confocal laser scanning microscopy

Focus of article	Reference
Oil inclusions	Pironon et al. [296]
Aggregation of latex particles	Thill et al. [361]
Protein diffusion in beads	Laca et al. [156]
Protein diffusion in porous media	Linden et al. [191]
Droplets size water/fat	Van Dalen [379]
Biopolymer mixtures	van de Velde et al. [380]
Alginate capsules	Strand et al. [351]
Chromatography matrix	Siu et al. [338]
Chromatography applications	Hubbuch and Kula [131]
Sandstone porosity	Zoghiami et al. [424]
Material science	Hovis and Heuer [129]

selected plane illumination microscopy (SPIM) can be used for imaging larger objects from different angles, thereby getting improved resolution in thick specimens. As a consequence the imaging approach will finally comprise correlative microscopy in order to take advantage of the individual techniques. This may include macroscale techniques, confocal microscopy, and high-resolution microscopy. In addition, chemical imaging that could not be covered in this review is becoming more and more available. The techniques available in this category among others include Raman microscopy, nanoSIMS, and synchrotron imaging.

## References

1. Adair CG, Gorman SP, Byers LB, Jones DS, Gardiner TA (2000) Confocal laser scanning microscopy for examination of microbial biofilms. In: An YH, Friedman RJ (eds) Handbook of bacterial adhesion. Humana Press, Totowa, pp 249–256
2. Adav SS, Lee D-J, Tay J-H (2008) Extracellular polymeric substances and structural stability of aerobic granule. *Water Res* 42:1644–1650
3. Allesen-Holm M, Bundvik Barken K, Yang L, Klausen M, Webb JS, Kjelleberg S, Molin S, Givskov M, Tolker-Nielsen T (2006) A characterisation of DNA release in *Pseudomonas aeruginosa* cultures and biofilms. *Mol Microbiol* 59:1114–1128
4. Amann R, Ludwig W, Schleifer K (1995) Phylogenetic identification and in situ detection of individual microbial cells without cultivation. *Microbiol Rev* 59:143–169
5. Amann R, Snaird J, Wagner M, Ludwig W, Schleifer K-H (1996) In situ visualization of high genetic diversity in a natural microbial community. *J Bacteriol* 178:3496–3500
6. Andersen JBO, Heydorn A, Hentzer M, Eberl L, Geisenberger O, Christensen BB, Molin S, Givskov M (2001) *gfp*-based *N*-acyl homoserine-lactone sensor systems for detection of bacterial communication. *Appl Environ Microbiol* 67:575–585
7. Anguish LJ, Ghiorse WC (1997) Computer-assisted laser scanning and video microscopy for analysis of *Cryptosporidium parvum* oocysts in soil, sediment, and feces. *Appl Environ Microbiol* 63:724–733
8. Ariosa Y, Quesada A, Aburto J, Carrasco D, Carreres R, Leganes F, Valiente EF (2004) Epiphytic cyanobacteria on *Chara vulgaris* are the main contributors to N<sub>2</sub> fixation in rice fields. *Appl Environ Microbiol* 70:5391–5397
9. Artursson V, Finlay RD, Jansson JK (2005) Combined bromodeoxyuridine immunocapture and terminal-restriction fragment length polymorphism analysis highlights differences in the active soil bacterial metagenome due to *Glomus mosseae* inoculation or plant species. *Environ Microbiol* 7:1952–1966
10. Artursson V, Jansson JK (2003) Use of bromodeoxyuridine immunocapture to identify active bacteria associated with arbuscular mycorrhizal hyphae. *Appl Environ Microbiol* 69:6208–6215
11. Ascaso C, Wierchos J (2003) New approaches to the study of Antarctic lithobiontic microorganisms and their inorganic traces, and their application in the detection of life in Martian rocks. *Int Microbiol* 5:215–222
12. Assmus B, Hutzler P, Kirchhof G, Amann R, Lawrence JR, Hartmann A (1995) In situ localization of *Azospirillum brasilense* in the rhizosphere of wheat with fluorescently labeled rRNA-targeted oligonucleotide probes and scanning confocal laser microscopy. *Appl Environ Microbiol* 61:1013–1019
13. Assmus B, Schloter M, Kirchhof G, Hutzler P, Hartmann A (1997) Improved in situ tracking of rhizosphere bacteria using dual staining with fluorescence-labeled antibodies and rRNA-targeted oligonucleotides. *Microb Ecol* 33:32–40
14. Baldi F, Ivosevic N, Minacci A, Pepi M, Fani R, Svetlicic V, Zutic V (1999) Adhesion of *Acinetobacter venetianus* to diesel fuel droplets studied with in situ electrochemical and molecular probes. *Appl Environ Microbiol* 65:2041–2048
15. Baldi F, Pepi M, Fava F (2003) Growth of *Rhodospirium toruloides* strain DBVPG 6662 on dibenzothiophene crystals and orimulsion. *Appl Environ Microbiol* 69:4689–4696
16. Barr JJ, Cook AE, Bond PL (2010) Granule formation mechanisms within an aerobic wastewater system for phosphorus removal. *Appl Environ Microbiol* 76:7588–7597
17. Battin TJ, Kaplan LA, Newbold JD, Hansen CME (2003) Contributions of microbial biofilms to ecosystem processes in stream mesocosms. *Nature* 426:439–442
18. Battin TJ, Sloan WT, Kjelleberg S, Daims H, Head IM, Curtis TP, Eberl L (2007) Microbial landscapes: new paths to biofilm research. *Nature* 5:76–81
19. Bennke CM, Neu TR, Fuchs BM, Amann R (2013) Mapping glycoconjugate-mediated interactions of marine Bacteroidetes with diatoms. *Systematic Appl Microbiol* 36:417–425

20. Berne C, Kysela DT, Brun YV (2010) A bacterial extracellular DNA inhibits settling of motile progeny cells within a biofilm. *Mol Microbiol* 77:815–829
21. Berney M, Hammes F, Bosshard F, Weilenmann H-U, Egli T (2007) Assessment and interpretation of bacterial viability by using the LIVE/DEAD baclight kit in combination with flow cytometry. *Appl Environ Microbiol* 73:3283–3290
22. Bertozzini E, Galluzzi L, Penna A, Magnani M (2011) Application of the standard addition method for the absolute quantification of neutral lipids in microalgae using Nile red. *J Microbiol Methods* 87:17–23
23. Besemer K, Singer G, Hödl I, Battin TJ (2009) Bacterial community composition of stream biofilms in spatially variable-flow environments. *Appl Environ Microbiol* 75:7189–7195
24. Besemer K, Singer G, Limberger R, Chlup A-K, Hochedlinger G, Hödl I, Baranyi C, Battin TJ (2007) Biophysical controls on community succession in stream biofilms. *Appl Environ Microbiol* 73:4966–4974
25. Biggerstaff JP, Le Puil M, Weidow BL, Leblanc-Gridley J, Jennings E, Busch-Harris J, Sublette KL, White DC, Alberte RS (2007) A novel and in situ technique for the quantitative detection of MTBE and benzene degrading bacteria in contaminated matrices. *J Microbiol Methods* 68:437–441
26. Böckelmann U, Manz W, Neu TR, Szewzyk U (2002) A new combined technique of fluorescent in situ hybridization and lectin-binding-analysis (FISH-LBA) for the investigation of lotic microbial aggregates. *J Microbiol Methods* 49:75–87
27. Boessmann M, Neu TR, Horn H, Hempel DC (2004) Growth, structure and oxygen penetration in particle supported autotrophic biofilms. *Water Sci Technol* 49:371–377
28. Böhme A, Risse-Buhl U, Küsel K (2009) Protists with different feeding modes change biofilm morphology. *FEMS Microbiol Ecol* 69:158–169
29. Bouchez T, Patureau D, Dabert P, Juretschko S, Dore J, Delgenes P, Moletta R, Wagner M (2000) Ecological study of a bioaugmentation failure. *Environ Microbiol* 2:179–190
30. Boulos L, Prevost M, Barbeau B, Coallier J, Desjardins R (1999) LIVE/DEAD<sup>®</sup> BacLight<sup>™</sup>: application of a new rapid staining method for direct enumeration of viable and total bacteria in drinking water. *J Microbiol Methods* 37:77–86
31. Breeuwer P, Abee T (2000) Assessment of viability of microorganisms employing fluorescence techniques. *Int J Food Microbiol* 55:193–200
32. Bruhn JB, Haagensen JAJ, Bagge-Ravn D, Gram L (2006) Culture conditions of *Roseobacter* strain 27-4 affect its attachment and biofilm formation as quantified by real-time PCR. *Appl Environ Microbiol* 72:3011–3015
33. Brul S, Nussbaum J, Dielbandhoesing SK (1997) Fluorescent probes for wall porosity and membrane integrity in filamentous fungi. *J Microbiol Methods* 28:169–178
34. Bryers JD (2001) Two-photon excitation microscopy for analyses of biofilm processes. *Methods Enzymol* 337:259–269
35. Burdikova Z, Capek M, Ostasov P, Machac J, Pelc R, Mitchell EAD, Kubinova L (2010) Testate amoebae examined by confocal and two-photon microscopy: Implications for taxonomy and ecophysiology. *Microsc Anal* 16:735–746
36. Burnett SL, Chen J, Beuchat LR (2000) Attachment of *Escherichia coli* O157:H7 to the surfaces and internal structures of apples as detected by confocal scanning laser microscopy. *Appl Environ Microbiol* 66:4679–4687
37. Caldwell DE, Korber DR, Lawrence JR (1992) Confocal laser scanning microscopy and digital image analysis in microbial ecology. *Adv Microb Ecol* 12:1–67
38. Catala P, Parthuisot N, Bernard L, Baudart J, Lemarchand K, Lebaron P (1999) Effectiveness of CSE to counterstain particles and dead bacterial cells with permeabilised membranes: application to viability assessment in waters. *FEMS Microbiol Lett* 178:219–226
39. Cattaneo R, Rouviere C, Rassoulzadegan F, Weinbauer MG (2010) Association of marine viral and bacterial communities with reference black carbon particles under experimental conditions: an analysis with scanning electron, epifluorescence and confocal laser scanning microscopy. *FEMS Microbiol Ecol* 74:382–396

40. Chalmers NI, Palmer RJ Jr, Du-Thumm L, Sullivan R, Shi W, Kolenbrander PE (2007) Use of quantum dot luminescent probes to achieve single-cell resolution of human oral bacteria in biofilms. *Appl Environ Microbiol* 73:630–636
41. Chen F, Lu JR, Binder BJ, Liu YC, Hodson RE (2001) Application of digital image analysis and flow cytometry to enumerate marine viruses stained with SYBR gold. *Appl Environ Microbiol* 67:539–545
42. Chen MY, Lee DJ, Tay JH (2007) Distribution of extracellular polymeric substances in aerobic granules. *Appl Microbiol Biotechnol* 73:1463–1469
43. Chen M-Y, Lee D-J, Tay J-H, Show K-Y (2007) Staining of extracellular polymeric substances and cells in bioaggregates. *Appl Microbiol Biotechnol* 75:467–474
44. Christensen BB, Haagensen JAJ, Heydorn A, Molin S (2002) Metabolic commensalism and competition in a two-species microbial consortium. *Appl Environ Microbiol* 68:2495–2502
45. Christensen BB, Sternberg C, Andersen JB, Eberl L, Möller S, Givskov M, Molin S (1998) Establishment of new genetic traits in a microbial biofilm community. *Appl Environ Microbiol* 64:2247–2255
46. Ciglenecki I, Plavsic M, Vojvodic V, Cosovic B, Pepi M, Baldi F (2003) Mucopolysaccharide transformation by sulfide in diatom cultures and natural mucilage. *Mar Ecol Prog Ser* 263:17–23
47. Cole L, Davies D, Hyde GJ, Ashford AE (2000) ER-tracker dye and BODIPY-breveldin A differentiate the endoplasmic reticulum and golgi bodies from the tubularvacuole system in living hyphae of *Pisolithus tinctorius*. *J Microsc* 197:239–248
48. Cooley MB, Miller WG, Mandrell RE (2003) Colonization of *Arabidopsis thaliana* with *Salmonella enterica* and enterohemorrhagic *Escherichia coli* O157:H7 and competition by *Enterobacter asburiae*. *Appl Environ Microbiol* 69:4915–4926
49. Coote PJ, Billon CMP, Pennell S, McClure PJ, Ferdinando DP, Cole MB (1995) The use of confocal scanning laser microscopy (CSLM) to study the germination of individual spores of *Bacillus cereus*. *J Microbiol Methods* 21:193–208
50. Cotner JB, Ogdahl ML, Biddanda BA (2001) Double-stranded DNA measurement in lakes with the fluorescent stain PicoGreen and the application to bacterial assays. *Aquat Microb Ecol* 25:65–74
51. Cowan SE, Gilbert E, Khlebnikov A, Keasling JD (2000) Dual labeling with green fluorescent proteins for confocal microscopy. *Appl Environ Microbiol* 66:413–418
52. Cowan SE, Gilbert E, Liepmann D, Keasling JD (2000) Commensal interactions in a dual-species biofilm exposed to mixed organic compounds. *Appl Environ Microbiol* 66:4481–4485
53. Cowen JP, Holloway CF (1996) Structural and chemical analysis of marine aggregates: in situ macrophotography and laser confocal and electron microscopy. *Mar Biol* 126:163–174
54. Creach V, Baudoux A-C, Bertru G, Rouzic BL (2003) Direct estimate of active bacteria: CTC use and limitations. *J Microbiol Methods* 52:19–28
55. Crocetti GR, Hugenholtz P, Bond PL, Schuler A, Keller J, Jenkins D, Blackall LL (2000) Identification of polyphosphate-accumulating organisms and design of 16S rRNA-directed probes for their detection and quantification. *Appl Environ Microbiol* 66:1175–1182
56. Czechowska K, van der Meer JR (2011) Reversible and irreversible pollutant-induced bacterial cellular stress effects measured by ethidium bromide uptake and efflux. *Environ Sci Technol* 46:1201–1208
57. Czynnemek KJ, Whallon JH, Klomparens KL (1994) Confocal microscopy in mycological research. *Exp Mycol* 18:275–293
58. Daims H, Nielsen JL, Nielsen PH, Schleifer K-H, Wagner M (2001) In situ characterization of *Nitrospira*-like nitrite-oxidizing bacteria active in waste water treatments plants. *Appl Environ Microbiol* 67:5273–5284
59. Daims H, Ramsing NB, Schleifer K-H, Wagner M (2001) Cultivation-independent, semiautomatic determination of absolute bacterial cell numbers in environmental samples by fluorescence in situ hybridization. *Appl Environ Microbiol* 67:5810–5818
60. Davey HM, Hexley P (2011) Red but not dead? Membranes of stressed *Saccharomyces cerevisiae* are permeable to propidium iodide. *Environ Microbiol* 13:163–171



61. Davey HM (2011) Life, death, and in-between: meanings and methods in microbiology. *Appl Environ Microbiol* 77:5571–5576
62. de los Rios A, Ascaso C, Wierzechos J, Fernandez-Valiente E, Quesada A (2004) Microstructural characterization of cyanobacterial mats from the McMurdo ice shelf, Antarctica. *Appl Environ Microbiol* 70:569–580
63. de los Rios A, Wierzechos J, Sancho LG, Ascaso C (2003) Acid microenvironments in microbial biofilms of antarctic endolithic microecosystems. *Environ Microbiol* 5:231–237
64. del Giorgio PA, Bird DF, Prairie YT, Planas D (1996) Flow cytometric determination of bacterial abundance in lake plankton with the green nucleic acid stain SYTO 13. *Limnol Oceanogr* 41:783–789
65. DeLeo PC, Baveye P, Ghiorse WC (1997) Use of confocal laser scanning microscopy on soil thin-sections for improved characterization of microbial growth in unconsolidated soils and aquifer materials. *J Microbiol Methods* 30:193–203
66. DeLong EF, Wickham GS, Pace NR (1989) Phylogenetic stains: ribosomal RNA-based probes for the identification of single cells. *Science* 243:1360–1363
67. Denk W, Strickler JH, Webb WW (1990) Two-photon laser scanning fluorescence microscopy. *Science* 248:73–76
68. Diaz JM, Ingall ED (2010) Fluorometric quantification of natural inorganic polyphosphate. *Environ Sci Technol* 44:4665–4671
69. Dige I, Raarup MK, Nyengaard JR, Kilian M, Nyvad B (2009) *Actinomyces naeslundii* in initial dental biofilm formation. *Microbiology* 155:2116–2126
70. Doherty SB, Wang L, Ross RP, Stanton C, Fitzgerald GF, Brodkorb A (2010) Use of viability staining in combination with flow cytometry for rapid viability assessment of *Lactobacillus rhamnosus* GG in complex protein matrices. *J Microbiol Methods* 82:301–310
71. Dominiak DM, Nielsen JL, Nielsen PH (2011) Extracellular DNA is abundant and important for microcolony strength in mixed microbial biofilms. *Environ Microbiol* 13:710–721
72. Donlan RM (2009) Preventing biofilms of clinically relevant organisms using bacteriophage. *Trends Microbiol* 17:66–72
73. Donlan RM, Piede JA, Heyes CD, Sani L, Edmonds P, El-Sayed I, El-Sayed MA (2004) Model system for growing and quantifying *Streptococcus pneumoniae* biofilms in situ and in real time. *Appl Environ Microbiol* 70:4980–4988
74. Doolittle MM, Cooney JJ, Caldwell DE (1996) Tracing the interaction of bacteriophage with bacterial biofilms using fluorescent and chromogenetic probes. *J Ind Microbiol* 16:331–341
75. Dopheide A, Lear G, Stott R, Lewis G (2011) Preferential feeding by the ciliates *Chilodonella* and *Tetrahymena* spp. and effects of these protozoa on bacterial biofilm structure and composition. *Appl Environ Microbiol* 77:4564–4572
76. Dorobantu LS, Yeung AKC, Foght JM, Gray MR (2004) Stabilization of oil–water emulsions by hydrophobic bacteria. *Appl Environ Microbiol* 70:6333–6336
77. Eberl L, Schulze R, Ammendola A, Geisenberger O, Erhart R, Sternberg C, Molin S, Amann R (1997) Use of green fluorescent protein as a marker for ecological studies of activated sludge communities. *FEMS Microbiol Lett* 149:77–83
78. Eisenmann H, Letsiou J, Feuchtinger A, Beisker W, Mannweiler E, Hutzler P, Amz P (2001) Interception of small particles by flocculent structures, sessile ciliates, and the basic layer of a wastewater biofilm. *Appl Environ Microbiol* 67:4286–4292
79. Fernandez M, Sanchez J (2002) Nuclease activities and cell death processes associated with the development of surface cultures of *Streptomyces antibioticus* ETH 7451. *Microbiology* 148:405–412
80. Ferrari BC, Tujula N, Stoner K, Kjelleberg S (2006) Catalyzed reporter deposition—fluorescence in situ hybridization allows for enrichment-independent detection of microcolony—forming soil bacteria. *Appl Environ Microbiol* 72:918–922
81. Filoche SK, Coleman MJ, Angker L, Sissons CH (2007) A fluorescence assay to determine the viable biomass of microcosm dental plaque biofilms. *J Microbiol Methods* 69:489–496

82. Finelli A, Gallant CV, Jarvi K, Burrows LL (2003) Use of in-biofilm expression technology to identify genes involved in *Pseudomonas aeruginosa* biofilm development. *Appl Environ Microbiol* 69:2700–2710
83. Fischer-Parton S, Parton RM, Hickey PC, Dijksterhuis J, Atkinson HA, Read ND (2000) Confocal microscopy of FM4-64 as a tool for analysing endocytosis and vesicle trafficking in living fungal hyphae. *J Microsc* 198:246–259
84. Forster S, Snape JR, Lappin-Scott HM, Porter J (2002) Simultaneous fluorescent gram staining and activity assesment of activated sludge bacteria. *Appl Environ Microbiol* 68:4772–4779
85. Forterre P, Soler N, Krupovic M, Marguet E, Ackermann HW (2013) Fake virus particles generated by fluorescence microscopy. *Trends Microbiol* 21:1–5
86. Fujishige NA, Kapadia NN, De Hoff PL, Hirsch AM (2006) Investigations of *Rhizobium* biofilm formation. *FEMS Microbiol Ecol* 56:195–206
87. Furuno S, Pätzolt K, Rabe C, Neu TR, Harms H, Wick LY (2010) Fungal mycelia allow chemotactic dispersal of polycyclic aromatic hydrocarbon-degrading bacteria in water-unsaturated systems. *Environ Microbiol* 12:1391–1398
88. Furuno S, Foss S, Wild E, Jones KC, Semple KT, Harms H, Wick LY (2012) Mycelia promote active transport and spatial dispersion of polycyclic aromatic hydrocarbons. *Environ Sci Technol* 46:5463–5470
89. Gaines S, James TC, Folan M, Baird AW, O'Farrelly C (2003) A novel spectrofluorometric microassay for *Streptococcus mutans* adherence to hydroxylapatite. *J Microbiol Methods* 54:315–323
90. Garny K, Horn H, Neu TR (2008) Interaction between biofilm development, structure and detachment in rotating annular reactors. *Bioprocess Biosyst Eng* 31:619–629
91. Garny K, Neu TR, Horn H (2009) Sloughing and limited substrate conditions trigger filamentous growth in heterotrophic biofilms—measurements in flow-through tube reactor. *Chem Eng Sci* 64:2723–2732
92. Gerritsen HC, Grauw dCJ (1999) Imaging of optically thick specimen using two-photon excitation microscopy. *Microsc Res Tech* 47:206–209
93. Gieseke A, Bjerrum L, Wagner M, Amann R (2003) Structure and acitivity of multiple nitrifying bacterial populations co-existing in a biofilm. *Environ Microbiol* 5:355–369
94. Gieseke A, Purkhold U, Wagner M, Amann R, Schramm A (2001) Community structure and activity dynamics of nitrifying bacteria in a phosphate-removing biofilm. *Appl Environ Microbiol* 67:1351–1362
95. Gieseke A, Tarre S, Green M, de Beer D (2006) Nitrification in a biofilm at low pH values: role of in situ microenvironments and acid tolerance. *Appl Environ Microbiol* 72:4283–4292
96. Gilbert B, Assmus B, Hartmann A, Frenzel P (1998) In situ localization of two methanotrophic strains in the rhizosphere of rice plants. *FEMS Microbiol Ecol* 25:117–128
97. Gjermansen M, Ragas P, Sternberg C, Molin S, Tolker-Nielsen T (2005) Characterization of starvation-induced dispersion in *Pseudomonas putida* biofilms. *Environ Microbiol* 7:894–904
98. Godeke J, Paul K, Lassak J, Thormann KM (2011) Phage-induced lysis enhances biofilm formation in *Shewanella oneidensis* MR-1. *ISME J* 5:613–626
99. Gorman SP, Mawhinney WM, Adair CG (1993) Confocal laser scanning microscopy of adherent microorganisms, biofilms and surfaces. In: Denyer SP, Gorman SP, Sussman M (eds) *Microbial biofilms: formation and control*. Blackwell, London, pp 95–107
100. Gorokhova E, Mattsson L, Sundström AM (2012) A comparison of TO-PRO-1 iodide and 5-CFDA-AM staining methods for assessing viability of planktonic algae with epifluorescence microscopy. *J Microbiol Methods* 89:216–221
101. Gray ND, Howarth R, Pickup RW, Jones JG, Head IM (2000) Use of combined microautoradiography and fluorescence in situ hybridization to determine carbon metabolism in mixed natural communities of uncultured from the genus *Achromatium*. *Appl Environ Microbiol* 66:4518–4522
102. Gregori G, Citterio S, Ghiani A, Labra M, Sgorbati S, Brown S, Denis M (2001) Resolution of vial and membrane-compromised bacteria in freshwater and marine waters based on

- analytical flow cytometry and nucleic acid double staining. *Appl Environ Microbiol* 67:4662–4670
103. Grossart H-P, Steward GF, Martinez J, Azam J (2000) A simple, rapid method for demonstrating bacterial flagella. *Appl Environ Microbiol* 66:3632–3636
  104. Grube M, Cardinale M, de Castro JV Jr, Müller H, Berg G (2009) Species-specific structural and functional diversity of bacterial communities in lichen symbiosis. *ISME J* 3:1105–1115
  105. Grube M, Berg G (2009) Microbial consortia of bacteria and fungi with focus on the lichen symbiosis. *Fungal Biol Rev* 23:72–85
  106. Gu F, Lux R, Du-Thumm L, Stokes I, Kreth J, Anderson MH, Wong DT, Wolinsky L, Sullivan R, Shi W (2005) In situ and non-invasive detection of specific bacterial species in oral biofilms using fluorescently labelled monoclonal antibodies. *J Microbiol Methods* 62:145–160
  107. Guggenheim M, Shapiro S, Gmür R, Guggenheim B (2001) Spatial arrangements and associative behavior of species in an in vitro oral biofilm model. *Appl Environ Microbiol* 67:1343–1350
  108. Guindulain T, Comas J, Vives-Rego J (1997) Use of nucleic acid dyes SYTO-13, TOTO-1, and YOYO-1 in the study of *Escherichia coli* and marine prokaryotic populations by flow cytometry. *Appl Environ Microbiol* 63:4608–4611
  109. Guiton PS, Hung CS, Kline KA, Roth R, Kau AL, Hayes E, Heuser J, Dodson KW, Caparon MG, Hultgren SJ (2009) Contribution of autolysin and sortase A during *Enterococcus faecalis* DNA-dependent biofilm development. *Infect Immun* 77:3626–3638
  110. Haagensen JAJ, Hansen SK, Johansen T, Molin S (2002) In situ detection of horizontal transfer of mobile genetic elements. *FEMS Microbiol Ecol* 42:261–268
  111. Haagensen JAJ, Klausen M, Ernst RK, Miller SI, Folkesson A, Tolker-Nielsen T, Molin S (2007) Differentiation and distribution of colistin—and sodium dodecyl sulfate—tolerant cells in *Pseudomonas aeruginosa* biofilms. *J Bacteriol* 189:28–37
  112. Hamasaki K, Long RA, Azam F (2004) Individual cell growth rates of marine bacteria, measured by bromodeoxyuridine incorporation. *Aquat Microb Ecol* 35:217–227
  113. Hansen M, Kragelund L, Nybroe O, Sørensen J (1997) Early colonization of barley roots by *Pseudomonas fluorescens* studied by immunofluorescence technique and confocal laser scanning microscopy. *FEMS Microbiol Ecol* 23:353–360
  114. Hansen SK, Haagensen JAJ, Gjermansen M, Jørgensen TM, Tolker-Nielsen T, Molin S (2007) Characterization of a *Pseudomonas putida* rough variant evolved in a mixed-species biofilm with *Acinetobacter* sp. strain C6. *J Bacteriol* 189:4932–4943
  115. Harrison JJ, Ceri H, Yerly J, Stremick CA, Hu Y, Martinuzzi RJ, Turner RJ (2006) The use of microscopy and three-dimensional visualisation to evaluate the structure of microbial biofilms cultivated in the Calgary biofilm device. *Biol Proced* 8:194–215
  116. Hausner M, Wuertz S (1999) High rates of conjugation in bacterial biofilms as determined by quantitative in situ analysis. *Appl Environ Microbiol* 65:3710
  117. Hazen TC, Jiménez L (1988) Enumeration and identification of bacteria from environmental samples using nucleic acid probes. *Microbiol Sci* 5:340–343
  118. Henche AL, Koerdt A, Ghosh A, Albers SV (2012) Influence of cell surface structures on crenarchaeal biofilm formation using a thermostable green fluorescent protein. *Environ Microbiol* 14:779–793
  119. Hendry MJ, Lawrence JR, Maloszewski P (1997) The role of sorption in the transport of *Klebsiella oxytoca* through saturated silica sand. *Ground Water* 35:574–583
  120. Henry-Stanley MJ, Garni RM, Wells CL (2004) Adaptation of FUN-1 and Calcofluor white stains to assess the ability of viable and non-viable yeast to adhere to and be internalized by cultured mammalian cells. *J Microbiol Methods* 59:289–292
  121. Hernandez-Marine M, Clavero E, Roldan M (2003) Why there is such luxurious growth in the hypogean environments. *Archiv für Hydrobiologie Supplement* 148:229–239
  122. Heydorn A, Ersboll B, Kato J, Hentzer M, Parsek MR, Tolker-Nielsen T, Givskov M, Molin S (2002) Statistical analysis of *Pseudomonas aeruginosa* biofilm development: impact of

- mutations in genes involved in twitching motility, cell-to-cell signaling, and stationary-phase sigma factor expression. *Appl Environ Microbiol* 68:2008–2017
123. Heydorn A, Ersböll BK, Hentzer M, Parsek MR, Givskov M, Molin S (2000) Experimental reproducibility in flow-chamber biofilms. *Microbiology* 146:2409–2415
  124. Hickey PC, Swift SR, Roca MG, Read ND (2004) Live-cell imaging of filamentous fungi using vital fluorescent dyes and confocal microscopy. *Methods Microbiol* 34:63–87
  125. Hoefel D, Grooby WL, Monis PT, Andrews S, Saint CP (2003) A comparative study of carboxyfluorescein diacetate and carboxyfluorescein diacetate succinimidyl ester as indicators of bacterial activity. *J Microbiol Methods* 52:379–388
  126. Holden PA, LaMontagne MG, Bruce AK, Miller WG, Lindow SE (2002) Assessing the role of *Pseudomonas aeruginosa* surface-active gene expression in hexadecane biodegradation in sand. *Appl Environ Microbiol* 68:2509–2518
  127. Holloway CF, Cowen JP (1997) Development of a scanning confocal laser microscopic technique to examine the structure and composition of marine snow. *Limnol Oceanogr* 42:1340–1352
  128. Hope CK, Wilson M (2003) Measuring the thickness of an outer layer of viable bacteria in an oral biofilm by viability mapping. *J Microbiol Methods* 54:403–410
  129. Hovis DB, Heuer AH (2010) The use of laser scanning confocal microscopy (LSCM) in materials science. *J Microsc* 240:173–180
  130. Hu Z, Hidalgo G, Houston PL, Hay AG, Shuler ML, Abruna HD, Ghiorse WC, Lion LW (2005) Determination of spatial distribution of zinc and active biomass in microbial biofilms by two-photon laser scanning microscopy. *Appl Environ Microbiol* 71:4014–4021
  131. Hubbuch J, Kula M-R (2008) Confocal laser scanning microscopy as an analytical tool in chromatographic research. *Bioprocess Biosyst Eng* 31:241–259
  132. Hugenholtz P, Pace NR (1996) Identifying microbial diversity in the natural environment: a molecular phylogenetic approach. *Trends Biotechnol* 14:190–197
  133. Ibrahim P, Whiteley AS, Barer MR (1997) SYTO 16 labelling and flow cytometry of *Mycobacterium avium*. *Lett Appl Microbiol* 25:437–441
  134. Ito T, Nielsen JL, Okabe S, Watanabe Y, Nielsen PH (2002) Phylogenetic identification and substrate uptake patterns of sulfate-reducing bacteria inhabiting anoxic-anoxic sewer biofilm fluorescent in situ hybridization. *Appl Environ Microbiol* 68:356–364
  135. Ito T, Sugita K, Okabe S (2004) Isolation, characterization, and in situ detection of a novel chemolithoautotrophic sulfur-oxidizing bacterium in wastewater biofilms growing under microaerophilic conditions. *Appl Environ Microbiol* 70:3122–3129
  136. Jacobsen CN, Rasmussen J, Jakobsen M (1997) Viability staining and flow cytometric detection of *Listeria monocytogenes*. *J Microbiol Methods* 28:35–43
  137. Jansson JK (2003) Marker and reporter genes: illuminating tools for environmental microbiologists. *Curr Opin Microbiol* 6:310–316
  138. Jayaraman A, Earthman JC, Wood TK (1997) Corrosion inhibition by aerobic biofilms on SAE 1018 steel. *Appl Microbiol Biotechnol* 47:62–68
  139. Jepras RI, Carter J, Pearson SC, Paul FE, Wilkinson MJ (1995) Development of a robust flow cytometric assay for determining numbers of viable bacteria. *Appl Environ Microbiol* 61:2696–2701
  140. Johnsen AR, Hausner M, Schnell A, Wuertz S (2000) Evaluation of fluorescently labeled lectins for noninvasive localization of extracellular polymeric substances in *Sphingomonas* biofilms. *Appl Environ Microbiol* 66:3487–3491
  141. Jordal PB, Dueholm MS, Larsen P, Petersen SV, Enghild JJ, Christiansen G, Hojrup P, Nielsen PH, Otzen DE (2009) Widespread abundance of functional bacterial amyloid mycolata and other gram-positive bacteria. *Appl Environ Microbiol* 75:4101–4110
  142. Juang Y-C, Adav SS, Lee D-J, Lai J-Y (2010) Influence of internal biofilm growth on residual permeability loss in aerobic granular membrane reactors. *Environ Sci Technol* 44:1267–1273

143. Jurcisek JA, Bakaletz LO (2007) Biofilms formed by nontypeable *Haemophilus influenzae* in vivo contain both double-stranded DNA and type IV pilin protein. *J Bacteriol* 189:3868–3875
144. Karimi-Lotfabad S, Gray MR (2000) Characterization of contaminated soils using confocal laser scanning microscopy and cryogenic-scanning electron microscopy. *Environ Sci Technol* 34:3408–3414
145. Keer JT, Birch L (2003) Molecular methods for the assessment of bacterial viability. *J Microbiol Methods* 53:175–183
146. Kerstens M, Gl Boulet, Pintelon I, Hellings M, Voeten L, Delputte P, Maes L, Cos P (2013) Quantification of *Candida albicans* by flow cytometry using TO-PRO<sup>®</sup>-3 iodide as a single-stain viability dye. *J Microbiol Methods* 92:189–191
147. Kim J-W, Choi H, Pachepsky YA (2010) Biofilm morphology as related to the porous media clogging. *Water Res* 44:1193–1201
148. Kindaichi T, Tushima I, Ogasawara Y, Shimokawa M, Ozaki N, Satoh H, Okabe S (2007) In situ activity and spatial organization of anaerobic ammonium-oxidizing (anammox) bacteria in biofilms. *Appl Environ Microbiol* 73:4931–4939
149. Kirkelund Hansen S, Rainey P, Haagensen JAJ, Molin S (2007) Evolution of species interactions in a biofilm community. *Nature* 445:533–536
150. Klausen M, Aaes-Jørgensen A, Molin S, Tolker-Nielsen T (2003) Involvement of bacterial migration in the development of complex multicellular structures in *Pseudomonas aeruginosa* biofilms. *Mol Microbiol* 50:61–68
151. Van Ommen Kloecke F, Geesey GG (1999) Localization and identification of populations of phosphatase—active bacterial cells associated with activated sludge flocs. *Microbiol Ecol* 38:201–214
152. Kolari M, Mattila K, Mikkola R, Salkinoja-Salonen MS (1998) Community structure of biofilms on ennobled stainless steel in Baltic Sea water. *J Ind Microbiol Biotechnol* 21:261–274
153. Korber DR, Choi A, Wolfaardt GM, Ingham SC, Caldwell DE (1997) Substratum topography influences susceptibility of *Salmonella enteritidis* biofilms to trisodium phosphate. *Appl Environ Microbiol* 63:3352–3358
154. Kuehn M, Mehl M, Hausner M, Bungartz H-J, Wuertz S (2001) Time-resolved study of biofilm architecture and transport processes using experimental and simulation techniques: the role of EPS. *Water Sci Technol* 43:143–151
155. Kulakova AN, Hobbs D, Smithen M, Pavlov E, Gilbert JA, Quinn JP, McGrath JW (2011) Direct quantification of inorganic polyphosphate in microbial cells using 4'-6-diamidino-2-phenylindole (DAPI). *Environ Sci Technol* 45:7799–7803
156. Laca A, Garcia LA, Argüeso F, Diaz M (1999) Protein diffusion in alginate beads monitored by confocal microscopy. The application of wavelets for data reconstruction and analysis. *J Ind Microbiol Biotechnol* 23:155–165
157. Lanthier M, Tartakovsky B, Villemur R, DeLuca G, Guiot SR (2002) Microstructure of anaerobic granules bioaugmented with *Desulfitobacterium frappieri* PCP-1. *Appl Environ Microbiol* 68:4035–4043
158. Lappmann M, Claus H, van Alen T, Harmsen M, Elias J, Molin S, Vogel U (2010) A dual role of extracellular DNA during biofilm formation of *Neisseria meningitidis*. *Mol Microbiol* 75:1355–1371
159. Larrainzar E, O'Gara F, Morrissey JP (2005) Applications of autofluorescent proteins for in situ studies in microbial ecology. *Annu Rev Microbiol* 59:257–277
160. Larsen P, Nielsen JL, Dueholm MS, Wetzel R, Otzen D, Nielsen PH (2007) Amyloid adhesins are abundant in natural biofilms. *Environ Microbiol* 9:3077–3090
161. Laue H, Schenk A, Hongqiao L, Lambertsen L, Neu TR, Molin S, Ullrich MS (2006) Contribution of alginate and levan to biofilm formation by *Pseudomonas syringae*. *Microbiology* 152:2909–2918
162. Lawrence JR, Chenier MR, Roy R, Beaumier D, Swerhone GDW, Neu TR, Greer CW (2004) Microscale and molecular assessment of the impacts of nickel, nutrients, and oxygen

- level on the structure and function of river biofilm communities. *Appl Environ Microbiol* 70:4326–4339
163. Lawrence JR, Hendry MJ (1996) Transport of bacteria through geologic media. *Can J Microbiol* 42:410–422
  164. Lawrence JR, Kopf G, Headley JV, Neu TR (2001) Sorption and metabolism of selected herbicides in river biofilm communities. *Can J Microbiol* 47:634–641
  165. Lawrence JR, Korber D, Neu TR (2007) Analytical imaging and microscopy techniques. In: Hurst CJ, Crawford RL, Garland JL, Lipson DA, Mills AL, Stetzenbach LD (eds) *Manual of environmental microbiology*. ASM Press, Washington D.C., pp 40–68
  166. Lawrence JR, Korber DR, Hoyle BD, Costerton JW, Caldwell DE (1991) Optical sectioning of microbial biofilms. *J Bacteriol* 173:6558–6567
  167. Lawrence JR, Korber DR, Wolfaardt GM, Caldwell DE (1996) Analytical imaging and microscopy techniques. In: Hurst CJ, Knudsen GR, McInerney MJ, Stetzenbach LD, Walter MV (eds) *Manual of environmental microbiology*. ASM, Washington, pp 29–51
  168. Lawrence JR, Korber DR, Wolfaardt GM, Caldwell DE, Neu TR (2002) Analytical imaging and microscopy techniques. In: Hurst CJ, Crawford RL, Knudsen GR, McInerney MJ, Stetzenbach LD (eds) *Manual of environmental microbiology*. ASM, Washington, pp 39–61
  169. Lawrence JR, Kwong YTJ, Swerhone GDW (1997) Colonization and weathering of natural sulfide mineral assemblages by *Thiobacillus ferrooxidans*. *Can J Microbiol* 43:178–188
  170. Lawrence JR, Neu TR (1999) Confocal laser scanning microscopy for analysis of microbial biofilms. *Methods Enzymol* 310:131–144
  171. Lawrence JR, Neu TR (2003) Microscale analyses of the formation and nature of microbial biofilm communities in river systems. *Rev Environ Sci Bio/Technol* 2:85–97
  172. Lawrence JR, Neu TR (2007) Laser scanning microscopy. In: Reddy CA, Beveridge TJ, Breznak JA, Marzluf GA, Schmidt TM, Snyder LR (eds) *Methods for general and molecular microbiology*. ASM, Washington DC, pp 34–53
  173. Lawrence JR, Neu TR (2007) Laser scanning microscopy for microbial flocs and particles. In: Wilkinson KJ, Lead JR (eds) *Environmental colloids: behavior, structure and characterisation*. Wiley, Chichester, pp 469–505
  174. Lawrence JR, Neu TR, Swerhone GDW (1998) Application of multiple parameter imaging for the quantification of algal, bacterial and exopolymer components of microbial biofilms. *J Microbiol Methods* 32:253–261
  175. Lawrence JR, Scharf B, Packroff G, Neu TR (2002) Microscale evaluation of the effects of grazing by invertebrates with contrasting feeding modes on river biofilm architecture and composition. *Microb Ecol* 43:199–207
  176. Lawrence JR, Swerhone GDW, Kwong YTJ (1998) Natural attenuation of aqueous metal contamination by an algal mat. *Can J Microbiol* 44:825–832
  177. Lawrence JR, Swerhone GDW, Neu TR (2000) A simple rotating annular reactor for replicated biofilm studies. *J Microbiol Methods* 42:215–224
  178. Lawrence JR, Swerhone GDW, Topp E, Korber D, Neu TR, Wassenaar LI (2007) Structural and functional responses of river biofilms communities to the non-steroidal anti-inflammatory diclofenac. *Environ Toxicol Chem* 26:573–582
  179. Lawrence JR, Swerhone GDW, Wassenaar LI, Neu TR (2005) Effects of selected pharmaceuticals on riverine biofilm communities. *Can J Microbiol* 51:655–669
  180. Lawrence JR, Wolfaardt G, Neu TR (1998) The study of microbial biofilms by confocal laser scanning microscopy. In: Wilkinson MHF, Shut F (eds) *Digital image analysis of microbes*. Wiley, Chichester, pp 431–465
  181. Lawrence JR, Zhu B, Swerhone GDW, Topp E, Roy J, Wassenaar LI, Rema T, Korber DR (2008) Community-level assessment of the effects of the broad-spectrum antimicrobial chlorhexidine on the outcome of river microbial biofilm development. *Appl Environ Microbiol* 74:3541–3550
  182. Le Puil M, Biggerstaff JP, Weidow BL, Price JR, Naser SA, White DC, Alberte RS (2006) A novel fluorescence imaging technique combining deconvolution microscopy and spectral

- analysis for quantitative detection of opportunistic pathogens. *J Microbiol Methods* 67:597–602
183. Lebaron P, Catala P, Parthuisot N (1998) Effectiveness of SYTOX green stain for bacterial viability assessment. *Appl Environ Microbiol* 64:2697–2700
  184. Lebaron P, Parthuisot N, Catala P (1998) Comparison of blue nucleic acid dyes for flow cytometric enumeration of bacteria in aquatic systems. *Appl Environ Microbiol* 64:1725–1730
  185. Lee N, Nielsen PH, Andreassen KH, Juretschko S, Nielsen JL, Schleifer K, Wagner M (1999) Combination of fluorescent in situ hybridisation and microautoradiography—a new tool for structure-function analyses in microbial ecology. *Appl Environ Microbiol* 65:1289–1297
  186. Leuko S, Legat A, Fendrihan S, Stan-Lotter H (2004) Evaluation of the LIVE/DEAD BacLight kit for detection of *Extremophilic archaea* and visualisation of microorganisms in environmental hypersaline samples. *Appl Environ Microbiol* 70:6884–6886
  187. Li L, Li Y, Lim TM, Pan SQ (1999) GFP-aided confocal laser scanning microscopy can monitor *Agrobacterium tumefaciens* cell morphology and gene expression associated with infection. *FEMS Microbiol Lett* 179:141–146
  188. Li S, Spear N, Andrews JH (1997) Quantitative fluorescence in situ hybridization of *Aureobasidium pullulans* on microscope slides and leaf surfaces. *Appl Environ Microbiol* 63:3261–3267
  189. Li WKW, Jellett JF, Dickie PM (1995) DNA distributions in planktonic bacteria stained with TOTO or TO-PRO. *Limnol Oceanogr* 40:1485–1495
  190. Li Y, Dick WA, Tuovinen OH (2004) Fluorescence microscopy for visualisation of soil microorganisms—a review. *Biol Fertil Soils* 39:301–311
  191. Linden T, Ljunglöf A, Kula M-R, Thömmes J (1999) Visualizing two-component protein diffusion in porous adsorbents by confocal scanning laser microscopy. *Biotechnol Bioeng* 65:622–630
  192. Liu L, Li WW, Sheng GP, Liu ZF, Zeng RJ, Liu JX, Yu HQ, Lee DJ (2010) Microscale hydrodynamic analysis of aerobic granules in the mass transfer process. *Environ Sci Technol* 44:7555–7560
  193. Lloyd D, Hayes AJ (1995) Vigour, vitality and viability of microorganisms. *FEMS Microbiol Lett* 133:1–7
  194. Lloyd D, Thomas KL, Hayes A, Hill B, Hales BA, Edwards C, Saunders JR, Ritchie DA, Upton M (1998) Micro-ecology of peat: minimally invasive analysis using confocal laser scanning microscopy, membrane inlet mass spectrometry and PCR amplification of methanogen-specific gene sequences. *FEMS Microbiol Ecol* 25:179–188
  195. Lower BH, Yongsunthon R, Vellano FP III, Lower SK (2005) Simultaneous force and fluorescence measurements of a protein that forms a bond between a living bacterium and a solid surface. *J Bacteriol* 187:2127–2137
  196. Lu TK, Collins JJ (2007) Dispersing biofilms with engineered enzymatic bacteriophage. *Proc Nat Acad Sci USA* 104:11197–11202
  197. Lübeck PS, Hansen M, Sørensen J (2000) Simultaneous detection of the establishment of seed-inoculated *Pseudomonas fluorescens* strain DR54 and native soil bacteria on sugar beet root surfaces using fluorescence antibody and in situ hybridization techniques. *FEMS Microbiol Ecol* 33:11–19
  198. Luef B, Neu TR, Peduzzi P (2009) Imaging and quantifying virus fluorescence signals on aquatic aggregates: a new method and its implication for aquatic microbial ecology. *FEMS Microbiol Ecol* 68:372–380
  199. Luef B, Neu TR, Zweimüller I, Peduzzi P (2009) Structure and composition of aggregates in two large European rivers, based on confocal laser scanning microscopy and image and statistical analysis. *Appl Environ Microbiol* 75:5952–5962
  200. Luna GM, Manini E, Danovaro R (2002) Large fraction of dead and inactive bacteria in coastal marine sediments: comparison of protocols for determination and ecological significance. *Appl Environ Microbiol* 68:3509–3513

201. Lunau M, Lemke A, Walther K, Martens-Habbena W, Simon M (2005) An improved method for counting bacteria from sediments and turbid environments by epifluorescence microscopy. *Environ Microbiol* 7:961–968
202. Lupini G, Proia L, Di Maio M, Amalfitano S, Fazi S (2011) CARD-FISH and confocal laser scanner microscopy to assess successional changes of the bacterial community in freshwater biofilms. *J Microbiol Methods* 86:248–251
203. Lydmark P, Lind M, Sörensson F, Hermansson M (2006) Vertical distribution of nitrifying populations in bacterial biofilms from a full—scale nitrifying trickling filter. *Environ Microbiol* 8:2036–2049
204. Lynch SV, Mukundakrishnan K, Benoit MR, Ayyaswamy PS, Matin A (2006) *Escherichia coli* biofilms formed under low—shear modeled microgravity in a ground-based system. *Appl Environ Microbiol* 72:7701–7710
205. Ma L, Conover M, Lu H, Parsek MR, Bayles K, Wozniak DJ (2009) Assembly and development of the *Pseudomonas aeruginosa* biofilm matrix. *PLoS Pathogens* 5(3):e1000354
206. Macnaughton SJ, Booth T, Embley TM, O'Donnell AG (1996) Physical stabilization and confocal microscopy of bacteria on roots using 16S rRNA targeted, fluorescent-labeled oligonucleotide probes. *J Microbiol Methods* 26:279–285
207. Mangalappalli-Illathu AK, Lawrence JR, Swerhone GDW, Korber DR (2008) Architectural adaptation and protein expression patterns of *Salmonella enterica* serovar enteritidis biofilms under laminar flow conditions. *Int J Food Microbiol* 123:109–120
208. Manini E, Danovaro R (2006) Synoptic determination of living/dead and active/dormant bacterial fractions in marine sediments. *FEMS Microbiol Ecol* 55:416–423
209. Mann EE, Rice KC, Boles BR, Endres JL, Ranjit D, Chandramohan L, Tsang LH, Smeltzer MS, Horswill AR, Bayles KW (2009) Modulation of eDNA release and degradation affects *Staphylococcus aureus* biofilm maturation. *PLoS ONE* 4:e5822
210. Manning PA (1995) Use of confocal microscopy in studying bacterial adhesion and invasion. *Methods Enzymol* 253:159–167
211. Manz W, Arp G, Schumann-Kindel G, Szewzyk U, Reitner J (2000) Widefield deconvolution epifluorescence microscopy combined with fluorescence in situ hybridization reveals the spatial arrangement of bacteria in sponge tissue. *J Microbiol Methods* 40:125–134
212. Manz W, Wendt-Potthoff K, Neu TR, Szewzyk U, Lawrence JR (1999) Phylogenetic composition, spatial structure, and dynamics of lotic bacterial biofilms investigated by fluorescent in situ hybridization and confocal laser scanning microscopy. *Microb Ecol* 37:225–237
213. Marie D, Partensky F, Jacquet S, Vaulot D (1997) Enumeration and cell cycle analysis of natural populations of marine picoplankton by flow cytometry using the nucleic acid stain SYBR Green I. *Appl Environ Microbiol* 63:186–193
214. Marie D, Vaulot D, Partensky F (1996) Application of the novel nucleic acid dyes YOYO-1, Yo-Pro-1, and PicoGreen for flow cytometric analysis of marine prokaryotes. *Appl Environ Microbiol* 62:1649–1655
215. Marshall KC (1976) Interfaces in microbial ecology. Harvard University Press, Cambridge
216. Martens-Habbena W, Sass H (2006) Sensitive determination of microbial growth by nucleic acid staining in aqueous suspension. *Appl Environ Microbiol* 72:87–95
217. Martin-Cereceda M, Alvarez AM, Serrano S, Guinea A (2001) Confocal and light microscope examination of protozoa and other microorganisms in the biofilms from a rotating biological contactor wastewater treatment plant. *Acta Protozoologica* 40:263–272
218. Martiny AC, Jorgensen TM, Albrechtsen H-J, Arvin E, Molin S (2003) Long-term succession of structure and diversity of a biofilm formed in a model drinking water distribution system. *Appl Environ Microbiol* 69:6899–6907
219. Mason DJ, Lopez-Amoros R, Allman R, Stark JM, Lloyd D (1995) The ability of membrane potential dyes and calcofluor white to distinguish between viable and non-viable bacteria. *J Appl Bacteriol* 78:309–315
220. Mason DJ, Shanmuganathan S, Mortimer FC, Gant VA (1998) A fluorescent gram stain for flow cytometry and epifluorescence microscopy. *Appl Environ Microbiol* 64:2681–2685



221. Massol-Deya AA, Whallon J, Hickey RF, Tiedje JM (1995) Channel structures in aerobic biofilms on fixed-film reactors treating contaminated groundwater. *Appl Environ Microbiol* 61:769–777
222. Matz C, Bergfeld T, Rice SA, Kjelleberg S (2004) Microcolonies, quorum sensing and cytotoxicity determine the survival of *Pseudomonas aeruginosa* biofilms exposed to protozoan grazing. *Environ Microbiol* 6:218–226
223. May T, Tsuruta K, Okabe S (2011) Exposure of conjugative plasmid carrying *Escherichia coli* biofilms to male-specific bacteriophages. *ISME J* 5:771–775
224. McAuliffe L, Ellis RJ, Miles K, Ayling RD, Nicholas RAJ (2006) Biofilm formation by mycoplasma species and its role in environmental persistence and survival. *Microbiology* 152:913–922
225. McLean JS, Majors PD, Reardon CL, Bilskis CL, Reed SB, Romine MF, Fredrickson JK (2008) Investigations of structure and metabolism within *Shewanella oneidensis* MR-1 biofilms. *J Microbiol Methods* 74:47–56
226. McLean JS, Pinchuk GE, Geydebekht OV, Bilskis CL, Zakrajsek BA, Hill EA, Saffarini DA, Romine MF, Gorby YA, Frederickson JK, Beliaev AS (2008) Oxygen-dependent autoaggregation in *Shewanella oneidensis* MR-1. *Environ Microbiol* 10:1861–1876
227. McSwain BS, Irvine RL, Hausner M, Wilderer PA (2005) Composition and distribution of extracellular polymeric substances in aerobic flocs and granular sludge. *Appl Environ Microbiol* 71:1051–1057
228. Michael T, Smith CM (1995) Lectins probe molecular films in biofouling: characterization of early films on non-living and living surfaces. *Mar Ecol Prog Ser* 119:229–236
229. Millard PJ, Roth BL, Thi HT, Yue ST, Haugland RP (1997) Development of the FUN-1 family of fluorescent probes for vacuole labeling and viability testing of yeasts. *Appl Environ Microbiol* 63:2897–2905
230. Min KR, Rickard AH (2009) Coaggregation by the freshwater bacterium *Sphingomonas natatoria* alters dual-species biofilm formation. *Appl Environ Microbiol* 75:3987–3997
231. Mir M, Babacan SD, Bednarz M, Do MN, Golding I, Popescu G (2012) Visualizing *Escherichia coli* sub-cellular structure using sparse deconvolution spatial light interference tomography. *PLoS ONE* 7:e39816
232. Miura Y, Okabe S (2008) Quantification of cell specific uptake activity of microbial products by uncultured *Chloroflexi* by microautoradiography combined with fluorescence in situ hybridization. *Environ Sci Technol* 42:7380–7386
233. Mohamed MN, Lawrence JR, Robarts RD (1998) Phosphorus limitation of heterotrophic biofilms from the Fraser River, British Columbia, and the effect of pulp mill effluent. *Microb Ecol* 36:121–130
234. Möhle RB, Langemann T, Haesner M, Augustin W, Scholl S, Neu TR, Hempel DC, Horn H (2007) Structure and shear strength of microbial biofilms as determined with confocal laser scanning microscopy and fluid dynamic gauging using a novel rotating disc biofilm reactor. *Biotechnol Bioeng* 98:747–755
235. Möller S, Pedersen AR, Poulsen LK, Arvin E, Molin S (1996) Activity and three-dimensional distribution of toluene-degrading *Pseudomonas putida* in a multispecies biofilm assessed by quantitative in situ hybridization and scanning confocal laser microscopy. *Appl Environ Microbiol* 62:4632–4640
236. Möller S, Sternberg C, Andersen JB, Christensen BB, Ramos JL, Givskov M, Molin S (1998) In situ gene expression in mixed-culture biofilms: evidence of metabolic interactions between community members. *Appl Environ Microbiol* 64:721–732
237. Morris C, Monier J-M, Jacques M-A (1997) Methods for observing microbial biofilms directly on leaf surfaces and recovering them for isolation of culturable microorganisms. *Appl Environ Microbiol* 63:1570–1576
238. Morris JD, Hewitt JL, Wolfe LG, Kamatkar NG, Chapman SM, Diener JM, Courtney AJ, Leevy WM, Shrout JD (2011) Imaging and analysis of *Pseudomonas aeruginosa* swarming and rhamnolipid production. *Appl Environ Microbiol* 77:8310–8317

239. Moter A, Göbel UB (2000) Fluorescence in situ hybridization (FISH) for direct visualization of microorganisms. *J Microbiol Methods* 41:85–112
240. Mulcahy H, Charron-Mazenod L, Lewenza S (2009) Extracellular DNA chelates cations and induces antibiotic resistance in *Pseudomonas aeruginosa* biofilms. *PLoS Pathogens* 4(11):e1000213
241. Nancharaiyah YV, Venugopalan VP, Wuertz S, Wilderer PA, Hausner M (2005) Compatibility of the green fluorescent protein and a general nucleic acid stain for quantitative description of a *Pseudomonas putida* biofilm. *J Microbiol Methods* 60:179–187
242. Nebe-von Caron G, Badley RA (1995) Viability assessment of bacteria in mixed populations using flow cytometry. *J Microsc* 179:55–66
243. Nebe-von Caron G, Stephens P, Badley RA (1998) Assessment of bacterial viability status by flow cytometry and single cell sorting. *J Appl Microbiol* 84:988–998
244. Neef A, Zaglauer A, Meier H, Amann R, Lemmer H, Schleifer K-H (1996) Population analysis in a denitrifying sand filter: conventional and in situ identification of *Paracoccus* spp. in methanol-fed biofilms. *Appl Environ Microbiol* 62:4329–4339
245. Neef AB, Luedtke NW (2011) Dynamic metabolic labeling of DNA in vivo with arabinosyl nucleosides. *Proc Natl Acad Sci* 108:20404–20409
246. Neu TR (2000) In situ cell and glycoconjugate distribution in river snow studied by confocal laser scanning microscopy. *Aquat Microb Ecol* 21:85–95
247. Neu TR, Kuhlicke U, Lawrence JR (2002) Assessment of fluorochromes for two-photon laser scanning microscopy biofilms. *Appl Environ Microbiol* 68:901–909
248. Neu TR, Lawrence JR (1997) Development and structure of microbial biofilms in river water studied by confocal laser scanning microscopy. *FEMS Microbiol Ecol* 24:11–25
249. Neu TR, Lawrence JR (1999) Lectin-binding-analysis in biofilm systems. *Methods Enzymol* 310:145–152
250. Neu TR, Lawrence JR (2002) Laser scanning microscopy in combination with fluorescence techniques for biofilm study. In: Bitton G (ed) *The encyclopedia of environmental microbiology*, vol 4. Wiley, New York, pp 1772–1788
251. Neu TR, Lawrence JR (2005) One-photon versus two-photon laser scanning microscopy and digital image analysis of microbial biofilms. *Methods Microbiol* 34:87–134
252. Neu TR, Lawrence JR (2010) Examination of microbial communities on hydrocarbons by means of laser scanning microscopy. In: Timmis KN (ed) *Microbiology of hydrocarbons, oils, lipids and derived compounds*. Springer, Heidelberg, pp 4073–4084
253. Neu TR, Manz B, Volke F, Dynes JJ, Hitchcock AP, Lawrence JR (2010) Advanced imaging techniques for assessment of structure, composition and function in biofilm systems. *FEMS Microbiol Ecol* 72:1–21
254. Neu TR, Swerhone GDW, Böckelmann U, Lawrence JR (2005) Effect of CNP on composition and structure of lotic biofilms as detected with lectin-specific glycoconjugates. *Aquat Microb Ecol* 38:283–294
255. Neu TR, Swerhone GDW, Lawrence JR (2001) Assessment of lectin-binding analysis for in situ detection of glycoconjugates in biofilm systems. *Microbiology* 147:299–313
256. Neu TR, Woelfl S, Lawrence JR (2004) Three-dimensional differentiation of photoautotrophic biofilm constituents by multi-channel laser scanning microscopy (single-photon and two-photon excitation). *J Microbiol Methods* 56:161–172
257. Niederberger TD, Perreault NN, Lawrence JR, Nadeau JL, Mielke RE, Greer CW, Anderson AB, Whyte LG (2009) Novel sulfur-oxidizing streamers thriving in perennial cold saline springs of the Canadian high Arctic. *Environ Microbiol* 11:616–629
258. Nielsen AT, Tolker-Nielsen T, Barken KB, Molin S (2000) Role of commensal relationships on the spatial structure of a surface—attached microbial consortium. *Environ Microbiol* 2:59–68
259. Nielsen JL, Christensen D, Kloppenborg M, Nielsen PH (2003) Quantification of cell-specific substrate uptake by probe-defined bacteria under in situ conditions by microautoradiography and fluorescence in situ hybridization. *Environ Microbiol* 5:202–211

260. Nielsen JL, de Muro MA, Nielsen PH (2003) Evaluation of the redox dye 5-cyano-2,3-tolyl-tetrazolium chloride for activity studies by simultaneous use of microautoradiography and fluorescence in situ hybridization. *Appl Environ Microbiol* 69:641–643
261. Nielsen JL, Juretschko S, Wagner M, Nielsen PH (2002) Abundance and phylogenetic affiliation of iron reducers in activated sludge as assessed by fluorescence in situ hybridization and microautoradiography. *Appl Environ Microbiol* 68:4629–4636
262. Nielsen JL, Nielsen PH (2005) Advances in microscopy: Microautoradiography of single cells. *Methods Enzymol* 397:237–256
263. Nielsen JL, Wagner M, Nielsen PH (2003) Use of microautoradiography to study in situ physiology of bacteria in biofilms. *Rev Environ Sci Bio/Technol* 2:261–268
264. Nielsen PH, Daims H, Lemmer H (2009) *FISH Handbook for biological wastewater treatment*. IWA Publishing, London
265. Nielsen PH, de Muro MA, Nielsen JL (2000) Studies on the in situ physiology of *Thiothrix* spp. present in activated sludge. *Environ Microbiol* 2:389–398
266. Nivens DE, Ohman DE, Williams J, Franklin MJ (2001) Role of alginate and its O acetylation in formation of *Pseudomonas aeruginosa* microcolonies and biofilms. *J Bacteriol* 183:1047–1057
267. Noble RT, Fuhrman JA (1998) Use of SYBR Green I for rapid epifluorescence counts of marine viruses and bacteria. *Aquat Microb Ecol* 14:113–118
268. Nopharatana M, Mitchell DA, Howes T (2003) Use of confocal scanning laser microscopy to measure the concentrations of aerial and penetrative hyphae during growth of *Rhizopus oligosporus* on a solid surface. *Biotechnol Bioeng* 84:71–77
269. Nopharatana M, Mitchell DA, Howes T (2003) Use of confocal microscopy to follow the development of penetrative hyphae during growth of *Rhizopus oligosporus* in an artificial solid-state fermentation system. *Biotechnol Bioeng* 81:438–447
270. Norton TA, Thompson RC, Pope J, Veltkamp CJ, Banks B, Howard CV, Hawkins SJ (1999) Using confocal laser scanning microscopy, scanning electron microscopy and phase contrast light microscopy to examine marine biofilms. *Aquat Microb Ecol* 16:199–204
271. Not F, Simon N, Biegala IC, Vaultot D (2002) Application of fluorescent in situ hybridization coupled with tyramide signal amplification (FISH-TSA) to assess eucaryotic picoplankton composition. *Aquat Microb Ecol* 28:157–166
272. Nour SM, Lawrence JR, Zhu H, Swerhone GDW, Welsh M, Welacky TW, Topp E (2003) Bacteria associated with cysts of the soybean cyst nematode (*Heterodera glycines*). *Appl Environ Microbiol* 69:607–615
273. Okabe S, Ito T, Sugita K, Satoh H (2005) Succession of internal sulfur cycles and sulfur-oxidizing bacterial communities in microaerophilic wastewater biofilms. *Appl Environ Microbiol* 71:2520–2529
274. Okabe S, Itoh T, Satoh H, Watanabe Y (1999) Analysis of spatial distributions of sulfate-reducing bacteria and their activity in aerobic wastewater biofilms. *Appl Environ Microbiol* 65:5107–5116
275. Okabe S, Kindaichi T, Ito T (2004) MAR-FISH - An ecophysiological approach to link phylogenetic affiliation and in situ metabolic activity of microorganisms at a single-cell resolution. *Microbes Environ* 19:83–98
276. Okabe S, Kindaichi T, Ito T (2005) Fate of C-labeled microbial products derived from nitrifying bacteria in autotrophic nitrifying biofilms. *Appl Environ Microbiol* 71:3987–3994
277. Olofsson AC, Zita A, Hermansson M (1998) Floc stability and adhesion of green-fluorescent-protein-marked bacteria to flocs in activated sludge. *Microbiology* 144:519–528
278. Oren A (1987) On the use of tetrazolium salts for the measurement of microbial activity in sediments. *FEMS Microbiol Ecol* 45:127–133
279. Packroff G, Lawrence JR, Neu TR (2002) In situ confocal laser scanning microscopy of protozoans in culture and complex biofilm communities. *Acta Protozoologica* 41:245–253
280. Palmer RJ Jr, Gordon SM, Cisar JO, Kolenbrander PE (2003) Coaggregation-mediated interactions of Streptococci and *Actinomyces* detected in initial human dental plaque. *J Bacteriol* 185:3400–3409

281. Palmer RJ Jr, Haagenen J, Neu TR, Sternberg C (2006) Confocal microscopy of biofilms—spatiotemporal approaches. In: Pawley JB (ed) Handbook of biological confocal microscopy. Springer, New York, pp 882–900
282. Palmer RJ Jr, Sternberg C (1999) Modern microscopy in biofilm research: confocal microscopy and other approaches. *Curr Opin Biotechnol* 10:263–268
283. Parry JD (2004) Protozoan grazing of freshwater biofilms. *Adv Appl Microbiol* 54:167–196
284. Pascaud A, Amellal S, Soulas M-L, Soulas G (2009) A fluorescence-based assay for measuring the viable cell concentration of mixed microbial communities in soil. *J Microbiol Methods* 76:81–87
285. Pedersen AR, Möller S, Molin S, Arvin E (1997) Activity of toluene-degrading *Pseudomonas putida* in the early growth phase of a biofilm for waste gas treatment. *Biotechnol Bioeng* 54:131–141
286. Peltola M, Neu TR, Kanto-Oqvist L, Raulio M, Kolari M, Salkinoja-Salonen MS (2008) Architecture of *Deinococcus geothermalis* biofilms on glass and steel: a lectin study. *Environ Microbiol* 10:1752–1759
287. Periasamy S, Kolenbrander PE (2009) Mutualistic biofilm communities develop with *Porphyromonas gingivalis* and initial, early and late colonizers of enamel. *J Bacteriol* 191: 6804–6811
288. Periasamy S, Kolenbrander PE (2009) *Aggregatibacter actinomycetemcomitans* builds mutualistic biofilm communities with *Fusobacterium nucleatum* and *Veillonella* species in saliva. *Infect Immun* 77:3542–3551
289. Periasamy S, Kolenbrander PE (2010) Central role of the early colonizer *Veillonella* sp. in establishing multispecies biofilm communities with initial, middle, and late colonizers of enamel. *J Bacteriol* 192:2965–2972
290. Pernthaler A, Amann R (2004) Simultaneous fluorescence in situ hybridisation of mRNA and rRNA in environmental bacteria. *Appl Environ Microbiol* 70:5426–5433
291. Pernthaler A, Pernthaler J, Amann R (2002) Fluorescence in situ hybridisation and catalyzed reporter deposition for the identification of marine bacteria. *Appl Environ Microbiol* 68:3094–3101
292. Phipps D, Rodriguez G, Ridgway H (1999) Deconvolution fluorescence microscopy for observation and analysis of membrane biofilm architecture. *Methods Enzymol* 310:178–194
293. Piao Z, Sze CC, Barysheva O, Iida K-I, Yoshida S-I (2006) Temperature-regulated formation of mycelial mat-like biofilms by *Legionella pneumophila*. *Appl Environ Microbiol* 72:1613–1622
294. Pick U, Rachutin-Zalagin T (2012) Kinetic anomalies in the interactions of Nile red with microalgae. *J Microbiol Methods* 88:189–196
295. Pierson BK, Parenteau MN (2000) Phototrophs in high iron microbial mats: microstructure of mats in iron-depositing hot springs. *FEMS Microbiol Ecol* 32:181–196
296. Pironon J, Canals M, Dubessy J, Walgenwitz F, Laplace-Builhe C (1998) Volumetric reconstruction of individual oil inclusions by confocal scanning laser microscopy. *Eur J Mineral* 10:1143–1150
297. Pittman KJ, Robbins CM, Osborn JL, Stubblefield BA, Gilbert ES (2010) Agarose stabilization of fragile biofilms for quantitative structure analysis. *J Microbiol Methods* 81:101–107
298. Podda F, Zuddas P, Minacci A, Pepi M, Baldi F (2000) Heavy metal coprecipitation with hydrozincite [ $Zn_5(CO_3)_2(OH)_6$ ] from mine waters caused by photosynthetic microorganisms. *Appl Environ Microbiol* 66:5092–5098
299. Qin Z, Ou Y, Yang L, Zhu Y, Tolker-Nielsen T, Molin S, Qu D (2007) Role of autolysin-mediated DNA release in biofilm formation of *Staphylococcus epidermidis*. *Microbiology* 153:2083–2092
300. Queck SY, Weitere M, Moreno AM, Rice SA, Kjelleberg S (2006) The role of quorum sensing mediated developmental traits in the resistance of *Serratia marcescens* biofilms against protozoan grazing. *Environ Microbiol* 8:1017–1025

301. Ramos C, Mölbak L, Molin S (2000) Bacterial activity in the rhizosphere analyzed at the single-cell level by monitoring ribosome contents and synthesis rates. *Appl Environ Microbiol* 66:801–809
302. Reiche M, Lu S, Cibiota V, Neu TR, Nietzsche S, Rösch P, Popp J, Küsel K (2013) Pelagic boundary conditions affect the biological formation of iron-rich particles (iron snow) and their microbial communities. *Limnol Oceanogr* 56:1386–1398
303. Rice SA, Tan CH, Mikkelsen PJ, Kung V, Woo J, Tay M, Hauser A, McDougald D, Webb JS, Kjelleberg S (2009) The biofilm life cycle and virulence of *Pseudomonas aeruginosa* are dependent on a filamentous prophage. *ISME J* 3:271–282
304. Robarts RD, Zohary T (1993) Fact or fiction—bacterial growth rates and production as determined by [methyl-3H]-thymidine. *Adv Microb Ecol* 13:371–425
305. Rocheleau S, Greer CW, Lawrence JR, Cantin Ch, Laramee L, Guiot SR (1999) Differentiation of *Methanosaeta concilii* and *Methanosarcina barkeri* in anaerobic mesophilic granular sludge by fluorescent in situ hybridization and confocal scanning laser microscopy. *Appl Environ Microbiol* 65:2222–2229
306. Roldan M, Clavero E, Castel S, Hernandez-Marine M (2004) Biofilms fluorescence and image analysis in hypogean monuments research. *Archiv für Hydrobiologie Supplement* 150:127–143
307. Roldan M, Oliva F, Gonzalez del Valle MA, Saiz-Jimenez C, Hernandez-Marine M (2006) Does green light influence the fluorescence properties and structure of phototrophic biofilms? *Appl Environ Microbiol* 72:3026–3031
308. Roldan M, Thomas F, Castel S, Quesada A, Hernandez-Marine M (2004) Noninvasive pigment identification in single cells from living phototrophic biofilms by confocal imaging spectrofluorometry. *Appl Environ Microbiol* 70:3745–3750
309. Romero D, Aguilar C, Losick R, Kolter R (2010) Amyloid fibers provide structural integrity to *Bacillus subtilis* biofilms. *Proc Natl Acad Sci* 107:2230–2234
310. Roth BL, Poot M, Yue ST, Millard PJ (1997) Bacterial viability and antibiotic susceptibility testing with SYTOX green nucleic acid stain. *Appl Environ Microbiol* 63:2421–2431
311. Rudi K, Moen B, Dromtorp SM, Holck AL (2005) Use of ethidium monoazide and PCR in combination for quantification of viable and dead cells in complex samples. *Appl Environ Microbiol* 71:1018–1024
312. Ruffing AM, Jones HDT (2012) Physiological effects of free fatty acid production in genetically engineered *Synechococcus elongatus* PCC 7942. *Biotechnol Bioeng* 109: 2190–2199
313. Saarima C, Peltola M, Raulio M, Neu TR, Salkinoja-Salonen MS, Neubauer P (2006) Characterisation of adhesion threads of *Deinococcus geothermalis* as type IV pili. *J Bacteriol* 188:7016–7021
314. Sabater S (2000) Structure and architecture of a stromatolite from a mediterranean stream. *Aquat Microb Ecol* 21:161–168
315. Saint-Ruf C, Cordier C, Megret J, Matic I (2010) Reliable detection of dead microbial cells by using fluorescent hydrazides. *Appl Environ Microbiol* 76:1674–1678
316. Sanford BA, de Feijter AW, Wade MH, Thomas VL (1996) A dual fluorescence technique for visualization of *Staphylococcus epidermidis* biofilm using scanning confocal laser microscopy. *J Ind Microbiol* 16:48–56
317. Santaella C, Schue M, Berge O, Heulin T, Achouak W (2008) The exopolysaccharide of *Rhizobium* sp. YAS34 is not necessary for biofilm formation on *Arabidopsis thaliana* and *Brassica napus* roots but contributes to root colonization. *Environ Microbiol* 10:2150–2163
318. Savichtcheva O, Okayama N, Ito T, Okabe S (2005) Application of a direct fluorescence-based live/dead staining combined with fluorescence in situ hybridization for assessment of survival rate of *Bacteriodes* spp. in drinking water. *Biotechnol Bioeng* 92:356–363
319. Saylor GS, Layton AC (1990) Environmental application of nucleic acid hybridization. *Annu Rev Microbiol* 44:625–648

320. Schlapp G, Scavone P, Zunino P, H + Härtel S (2011) Development of 3D architecture of uropathogenic *Proteus mirabilis* batch culture biofilms - a quantitative confocal microscopy approach. *J Microbiol Methods* 87:234–240
321. Schloter M, Borlinghaus R, Bode W, Hartmann A (1993) Direct identification, and localization of Azospirillum in the rhizosphere of wheat using fluorescence-labelled monoclonal antibodies and confocal scanning laser microscopy. *J Microsc* 171:173–177
322. Schloter M, Wiehe W, Assmus B, Steindl H, Becke H, Höflich G, Hartmann A (1997) Root colonization of different plants by plant-growth-promoting *Rhizobium leguminosarum* bv. trifolii R39 studied with monospecific polyclonal antisera. *Appl Environ Microbiol* 63:2038–2046
323. Schönhuber M, Zarda B, Eix S, Rippka R, Herdmann M, Ludwig W, Amann R (1999) In situ identification of cyanobacteria with horseradish peroxidase-labeled, rRNA-targeted oligonucleotide probes. *Appl Environ Microbiol* 65:1259–1267
324. Schönhuber W, Fuchs B, Juretschko S, Amann R (1997) Improved sensitivity of whole-cell hybridization by the combination of horseradish peroxidase-labeled oligonucleotides and tyramide signal amplification. *Appl Environ Microbiol* 63:3268–3273
325. Schramm A, Larsen LH, Revsbech NP, Ramsing NB, Amann R, Schleifer K-H (1996) Structure and function of a nitrifying biofilm as determined by in situ hybridization and the use of microelectrodes. *Appl Environ Microbiol* 62:4641–4647
326. Schramm A, Santegoeds C, Nielsen H, Plouf H, Wagner M, Pribyl M, Wanner J, Amann R, DeBeer D (1999) On the occurrence of anoxic microniches, denitrification, and sulfate reduction in aerated activated sludge. *Appl Environ Microbiol* 65:4189–4196
327. Sekar R, Pernthaler A, Warnecke F, Posch T, Amann R (2003) An improved protocol for quantification of freshwater *Actinobacteria* by fluorescence in situ hybridization. *Appl Environ Microbiol* 69:2928–2935
328. Seper A, Fengler VHI, Roier S, Wolinski H, Kohlwein SD, Bishop AL, Camilli A, Reidl J, Schild S (2011) Extracellular nucleases and extracellular DNA play important roles in *Vibrio cholerae* biofilm formation. *Mol Microbiol* 82:1015–1037
329. Servais P, Agogue H, Courties C, Joux F, Lebaron P (2001) Are the actively respiring cells (CTC+) those responsible for bacterial production in aquatic environments? *FEMS Microbiol Ecol* 35:171–179
330. Sharp MD, Pogliano K (1999) An in vivo membrane fusion assay implicates SpoIIIE in the final stages of engulfment during *Bacillus subtilis* sporulation. *Proc Natl Acad Sci* 96:14553–14558
331. Shimomura Y, Ohno R, Kawai F, Kimbara K (2006) Method for assessment of viability and morphological changes of bacteria in the early stage of colony formation on a simulated natural environment. *Appl Environ Microbiol* 72:5037–5042
332. Sibarita J-B (2005) Deconvolution microscopy. *Adv Biochem Eng Biotechnol* 85:201–243
333. Sieracki ME, Reichenbach SE, Webb KL (1989) Evaluation of automated threshold selection methods for accurately sizing microscopic fluorescent cells by image analysis. *Appl Environ Microbiol* 55:2762–2772
334. Singer G, Besemer K, Hochedlinger G, Chlup AK, Battin TJ (2011) Monomeric carbohydrate uptake and structure-function coupling in stream biofilms. *Aquat Microb Ecol* 62:71–83
335. Singer G, Besemer K, Hödl I, Chlup A-K, Hochedlinger G, Stadler P, Battin T (2006) Microcosm design and evaluation to study stream microbial biofilms. *Limnol Oceanogr Methods* 4:436–447
336. Sintes E, Herndl GJ (2006) Quantifying substrate uptake by individual cells of marine bacterioplankton by catalyzed reporter deposition fluorescence in situ hybridization combined with microautoradiography. *Appl Environ Microbiol* 72:7022–7028
337. Sitepu IR, Ignatia L, Franz AK, Wong DM, Faulina SA, Tsui M, Kanti A, Boundy-Mills K (2012) An improved high-throughput Nile red fluorescence assay for estimating intracellular lipids in a variety of yeast species. *J Microbiol Methods* 91:321–328

338. Siu SC, Boushaba R, Topoyassakul V, Graham A, Choudhury S, Moss G, Titchener-Hooker NJ (2006) Visualising fouling of a chromatographic matrix using confocal scanning laser microscopy. *Biotechnol Bioeng* 95:714–723
339. Snaird J, Fuchs B, Wallner G, Wagner M, Schleifer K-H, Amann R (1999) Phylogeny and in situ identification of a morphologically conspicuous bacterium, *Candidatus Magnospira bakii*, present at very low frequency in activated sludge. *Environ Microbiol* 1:125–135
340. Sole A, Diestra E, Esteve I (2009) Confocal laser scanning microscopy image analysis for cyanobacterial biomass determined at microscale level in different microbial mats. *Microb Ecol* 57:649–656
341. Stach JEM, Burns RG (2002) Enrichment versus biofilm culture: a functional and phylogenetic comparison of polycyclic aromatic hydrocarbon-degrading microbial communities. *Environ Microbiol* 4:169–182
342. Staley JT, Konopka A (1985) Measurement of in situ activities of nonphotosynthetic microorganisms in aquatic and terrestrial habitats. *Annu Rev Microbiol* 39:321–346
343. Staudt C, Horn H, Hempel DC, Neu TR (2003) Screening of lectins for staining lectin-specific glycoconjugates in the EPS of biofilms. In: Lens P, Moran AP, Mahony T, Stoodley P, O’Flaherty V (eds) *Biofilms in medicine, industry and environmental technology*. IWA Publishing, UK, pp 308–327
344. Staudt C, Horn H, Hempel DC, Neu TR (2004) Volumetric measurements of bacterial cells and extracellular polymeric substance glycoconjugates in biofilms. *Biotechnol Bioeng* 88:585–592
345. Sternberg C, Christensen BB, Johansen T, Toftgaard Nielsen A, Andersen JB, Givskov M, Molin S (1999) Distribution of bacterial growth activity in flow-chamber biofilms. *Appl Environ Microbiol* 65:4108–4117
346. Steward GF, Azam F (1999) Bromodeoxyuridine as an alternative to <sup>3</sup>H-thymidine for measuring bacterial productivity in aquatic samples. *Aquat Microb Ecol* 19:57–66
347. Stewart PS, Camper AK, Handran SD, Huang C-T, Warnecke M (1997) Spatial distribution and coexistence of *Klebsiella pneumoniae* and *Pseudomonas aeruginosa* in biofilms. *Microb Ecol* 33:2–10
348. Stocks SM (2004) Mechanism and use of the commercially available viability stain BacLight. *Cytometry Part A* 61A:189–195
349. Stoderegger KE, Herndl GJ (2004) Dynamics in bacterial cell surface properties assessed by fluorescent stains and confocal laser scanning microscopy. *Aquat Microb Ecol* 36:29–40
350. Stopa PJ, Mastromanolis SA (2001) The use of blue-excitable nucleic-acid dyes for the detection of bacteria in well water using a simple field fluorometer and a flow cytometer. *J Microbiol Methods* 45:143–153
351. Strand BL, Mörch YA, Espevik T, Skjak-Brak G (2003) Visualization of alginate-poly-L-lysine-alginate microcapsules by confocal laser scanning microscopy. *Biotechnol Bioeng* 82:386–394
352. Strathmann M, Wingender J, Flemming H-C (2002) Application of fluorescently labelled lectins for the visualization and biochemical characterization of polysaccharides in biofilms of *Pseudomonas aeruginosa*. *J Microbiol Methods* 50:237–248
353. Sträuber H, Müller S (2010) Viability states of bacteria—specific mechanisms of selected probes. *Cytometry Part A* 77A:623–634
354. Stretton S, Techkarnjanaruk S, McLennan AM, Goodman AE (1998) Use of green fluorescent protein to tag and investigate gene expression in marine bacteria. *Appl Environ Microbiol* 64:2554–2559
355. Sunamura M, Maruyama A, Tsuji T, Kurane R (2003) Spectral imaging detection and counting of microbial cells in marine sediment. *J Microbiol Methods* 53:57–65
356. Swope KL, Flickinger MC (1996) The use of confocal scanning microscopy and other tools to characterize *Escherichia coli* in a high-cell-density synthetic biofilm. *Biotechnol Bioeng* 52:340–356
357. Sytsma J, Vroom JM, Grauw dCJ, Gerritsen HC (1998) Time-gated fluorescence lifetime imaging and microvolume spectroscopy using two-photon excitation. *J Microsc* 191:39–51

358. Tada Y, Taniguchi A, Hamasaki K (2010) Phylotype-specific growth rates of marine bacteria measured by bromodeoxyuridine immunocytochemistry and fluorescence in situ hybridisation. *Aquat Microb Ecol* 59:229–238
359. Teal TK, Lies DP, Wold BJ, Newman DK (2006) Spatiometabolic stratification of *Shewanella oneidensis* biofilms. *Appl Environ Microbiol* 72:7324–7330
360. Teitzel GM, Parsek MR (2003) Heavy metal resistance of biofilm and planktonic *Pseudomonas aeruginosa*. *Appl Environ Microbiol* 69:2313–2320
361. Thill A, Wagner M, Bottero JY (1999) Confocal scanning laser microscopy as a tool for the determination of 3D floc structure. *J Colloid Interface Sci* 220:465–467
362. Thomas VC, Thurlow LR, Boyle D, Hancock LE (2008) Regulation of autolysis-dependent extracellular DNA release by *Enterococcus faecalis* extracellular proteases influences biofilm development. *Appl Environ Microbiol* 190:5690–5698
363. Thurnheer T, Gmür R, Guggenheim B (2004) Multiplex FISH analysis of a six-species bacterial biofilm. *J Microbiol Methods* 56:37–47
364. Thurnheer T, Gmür R, Shapiro S, Guggenheim B (2003) Mass transport of macromolecules within an invitro model of supragingival plaque. *Appl Environ Microbiol* 69:1702–1709
365. Tobin JM, Onstott TC, DeFlaun MF, Colwell FS, Fredricksen J (1999) In situ imaging of microorganisms in geologic material. *J Microbiol Methods* 37:201–213
366. Tolker-Nielsen T, Brinch UC, Ragas PC, Andersen JB, Jacobsen CS, Molin S (2000) Development and dynamics of *Pseudomonas* sp. biofilms. *J Bacteriol* 182:6482–6489
367. Tolker-Nielsen T, Molin S (2000) Spatial organization of microbial biofilm communities. *Microb Ecol* 40:75–84
368. Tranvik LJ (1997) Rapid fluorometric assay of bacterial density in lake water and seawater. *Limnol Oceanogr* 42:1629–1634
369. Troussellier M, Courties C, Lebaron P, Servais P (1999) Flow cytometric discrimination of bacterial populations in seawater based on SYTO 13 staining of nucleic acid. *FEMS Microbiol Ecol* 29:319–330
370. Truong VK, Rundell S, Lapovok R, Estrin Y, Wang JY, Berndt CC, Barnes DG, Fluke CJ, Crawford RJ, Ivanova EP (2009) Effect of ultrafine-grained titanium surfaces on adhesion of bacteria. *Appl Microbiol Biotechnol* 83:925–937
371. Tsai M-W, Lee D-J, Lai J-Y (2008) Mass transfer limit of fluorescent dyes during multicolor staining of aerobic granules. *Appl Microbiol Biotechnol* 78:907–913
372. Tsushima I, Ogasawara Y, Kindaichi T, Satoh H, Okabe S (2007) Development of high-rate anaerobic ammonium-oxidizing (anammox) biofilm reactors. *Water Res* 41:1623–1634
373. Tujula NA, Holmström C, Mußmann M, Amann R, Kjelleberg S, Crocetti GR (2006) A CARD—FISH protocol for the identification and enumeration of epiphytic bacteria on marine algae. *J Microbiol Methods* 65:604–607
374. Ullrich S, Karrasch B, Hoppe H-G, Jeksulke K, Mehrens M (1996) Toxic effects on bacterial metabolism of the redox dye 5-cyano-2,3-ditolyl tetrazolium chloride. *Appl Environ Microbiol* 62:4587–4593
375. Unge A, Jansson J (2001) Monitoring population size, activity, and distribution of gfp-luxAB-tagged *Pseudomonas fluorescens* SBW25 during colonization of wheat. *Microb Ecol* 41:290–300
376. Urbach E, Vergin KL, Giovannoni SJ (1999) Immunochemical detection and isolation of DNA from metabolically active bacteria. *Appl Environ Microbiol* 65:1207–1213
377. Vachova L, Chernyavskiy O, Strachotova D, Bianchini P, Burdikova Z, Fercikova I, Kubinova L, Palkova Z (2009) Architecture of developing multicellular yeast colony: spatio-temporal expression of Ato1p ammonium exporter. *Environ Microbiol* 11:1866–1877
378. Valm AM, Welch JLM, Rieken CW, Hasegawa Y, Sogin ML, Oldenbourg R, Dewhirst FE, Borisy GG (2011) Systems-level analysis of microbial community organization through combinatorial labeling and spectral imaging. *Proc Natl Acad Sci* 108:4152–4157
379. Van Dalen G (2002) Determination of the water droplet size distribution of fats spreads using confocal scanning laser microscopy. *J Microsc* 208:116–133



380. van de Velde F, Weinbreck F, Edelman MW, van der Linden E, Tromp RH (2003) Visualisation of biopolymer mixtures using confocal scanning laser microscopy (CSLM) and covalent labelling techniques. *Colloids Surf, B* 31:159–168
381. Venugopalan VP, Kuehn M, Hausner M, Springael D, Wilderer PA, Wuertz S (2005) Architecture of a nascent *Sphingomonas* sp. biofilm under varied hydrodynamic conditions. *Appl Environ Microbiol* 71:2677–2686
382. Verawaty M, Pijuan M, Yuan Z, Bond PL (2012) Determining the mechanisms for aerobic granulation from mixed seed of floccular and crushed granules in activated sludge wastewater treatment. *Water Res* 46:761–771
383. Vilain S, Pretorius JM, Theron J, Brözel VS (2009) DNA as an adhesin: *Bacillus cereus* requires extracellular DNA to form biofilms. *Appl Environ Microbiol* 75:2861–2868
384. Virta M, Lineri S, Kankaanpää P, Karp M, Peltonen K, Nuutila J, Lilius EM (1998) Determination of complement-mediated killing of bacteria by viability staining and bioluminescence. *Appl Environ Microbiol* 64:515–519
385. Vives-Rego J, Lopez-Amoros R, Comas J (1994) Flow cytometric narrow-angle light scatter and cell size during starvation of *Escherichia coli* in artificial seawater. *Lett Appl Microbiol* 19:374–376
386. Wagner M, Assmus B, Hartmann A, Hutzler P, Amann R (1994) In situ analysis of microbial consortia in activated sludge using fluorescently labelled, rRNA-targeted oligonucleotide probes and confocal laser scanning microscopy. *J Microsc* 176:181–187
387. Wagner M, Manz B, Volke F, Neu TR, Horn H (2010) Online monitoring of biofilm development, sloughing and forced detachment in tube reactor by means of magnetic resonance microscopy. *Biotechnol Bioeng* 107:172–181
388. Wagner M, Rath G, Amann R, Koops H-P, Schleifer K-H (1995) In situ identification of ammonia-oxidizing bacteria. *Syst Appl Microbiol* 18:251–264
389. Waite AM, Safi KA, Hall JA, Nodder SD (2000) Mass sedimentation of picoplankton embedded in organic aggregates. *Limnol Oceanogr* 45:87–97
390. Walters SP, Field KG (2006) Persistence and growth of fecal *Bacteroidales* assessed by bromodeoxyuridine immunocapture. *Appl Environ Microbiol* 72:4532–4539
391. Ward DM (1989) Molecular probes for analysis of microbial communities. In: Characklis WG, Wilderer P (eds) *Structure and function of biofilms*. Wiley, New York, pp 145–163
392. Weinbauer MG, Beckmann C, Höfle MG (1998) Utility of green fluorescent nucleic acid dyes and aluminum oxide membrane filters for rapid epifluorescence enumeration of soil and sediment bacteria. *Appl Environ Microbiol* 64:5000–5003
393. Weissbrodt DG, Neu TR, Kuhlicke U, Rappaz Y, Holliger C (2013) Assessment of bacterial and structural dynamics in aerobic granular biofilms. *Front Microbiol* 4:175
394. Weitere M, Bergfeld T, Rice SA, Matz C, Kjelleberg S (2005) Grazing resistance of *Pseudomonas aeruginosa* biofilms depends on type of protective mechanism, developmental stage and protozoan feeding mode. *Environ Microbiol* 7:1593–1601
395. Werner E, Roe F, Bugnicourt A, Franklin MJ, Heydorn A, Molin S, Pitts B, Stewart PS (2004) Stratified growth in *Pseudomonas aeruginosa* biofilms. *Appl Environ Microbiol* 70:6184–6188
396. Wey JK, Scherwass A, Norf H, Arndt H, Weitere M (2008) Effects of protozoan grazing within river biofilms under semi-natural conditions. *Aquat Microb Ecol* 52:283–296
397. Wey JK, Jürgens K, Weitere M (2012) Seasonal and successional influences on bacterial community composition exceed that of protozoan grazing in river biofilms. *Appl Environ Microbiol* 78:2013–2024
398. Whitchurch CB, Tolker-Nielsen T, Ragas P, Mattick JS (2002) Extracellular DNA required for bacterial biofilm formation. *Science* 295:1487
399. White DC, Arrage AA, Nivens DE, Palmer RJ Jr, Rice JF, Saylor GS (1996) Biofilm ecology: on-line methods bring new insights into mic and microbial biofouling. *Biofouling* 10:3–16

400. Whyte LG, Slagman SJ, Pietrantonio F, Bourbonniere L, Koval SF, Lawrence JR, Inniss WE, Greer CW (1999) Physiological adaptations involved in alkane assimilation at a low temperature by *Rhodococcus* sp. strain Q15. *Appl Environ Microbiol* 65:2961–2968
401. Wierzechos J, de los Rios A, Sancho LG, Ascaso C (2004) Viability of endolithic microorganisms in rocks from the McMurdo Dry Valley of Antarctica established by confocal and fluorescence microscopy. *J Microsc* 216:57–61
402. Wigglesworth-Cooksey B, Cooksey KE (2005) Use of fluorophore-conjugated lectins to study cell–cell interactions in model marine biofilms. *Appl Environ Microbiol* 71:428–435
403. Wiggli M, Smallcombe A, Bachofen R (1999) Reflectance spectroscopy and laser confocal microscopy as tools in an ecophysiological study of microbial mats in an alpine bog pond. *J Microbiol Methods* 34:173–182
404. Wijeyekoon S, Mino T, Satoh H, Matsuo T (2000) Growth and novel structural features of tubular biofilms produced under different hydrodynamic conditions. *Water Sci Technol* 41:129–138
405. Williams SC, Hong Y, Danavall DCA, Howard-Jones MH, Gibson D, Frischer ME, Verity PG (1998) Distinguishing between living and nonliving bacteria: evaluation of the vital stain propidium iodide and its combined use with molecular probes in aquatic samples. *J Microbiol Methods* 32:225–236
406. Winkler M, Lawrence JR, Neu TR (2001) Selective degradation of ibuprofen and clofibrate acid in two model river biofilm systems. *Water Res* 35:3197–3205
407. Wolfaardt GM, Lawrence JR, Robarts RD, Caldwell DE (1995) Bioaccumulation of the herbicide diclofop in extracellular polymers and its utilisation by a biofilm community during starvation. *Appl Environ Microbiol* 61:152–158
408. Wolfaardt GM, Lawrence JR, Robarts RD, Caldwell DE (1998) In situ characterization of biofilm exopolymers involved in the accumulation of chlorinated organics. *Microb Ecol* 35:213–223
409. Wolfaardt GM, Lawrence JR, Robarts RD, Caldwell SJ, Caldwell DE (1994) Multicellular organization in a degradative biofilm community. *Appl Environ Microbiol* 60:434–446
410. Wouters K, Maes E, Spitz JA, Roeffaers MJB, Wattiau P, Hofkens J, Springael D (2010) A non-invasive fluorescent staining procedure allows Confocal laser scanning microscopy based imaging of *Mycobacterium* in multispecies biofilms colonizing and degrading polycyclic aromatic hydrocarbons. *J Microbiol Methods* 83:317–325
411. Wrede C, Heller C, Reitner J, Hoppert M (2008) Correlative light/electron microscopy for the investigation of microbial mats from Black Sea cold seeps. *J Microbiol Methods* 73:85–91
412. Xavier JB, Schnell A, Wuertz S, Palmer R, White DC, Almeida JS (2001) Objective threshold selection procedure (OTS) for segmentation of scanning laser confocal microscope images. *J Microbiol Methods* 47:169–180
413. Yang L, Barken KB, Skindersoe ME, Christensen AB, Givskov M, Tolker-Nielsen T (2007) Effects of iron on DNA release and biofilm development by *Pseudomonas aeruginosa*. *Microbiology* 153:1318–1328
414. Yang L, Hu Y, Liu Y, Zhang J, Ulstrup J, Molin S (2011) Distinct roles of extracellular polymeric substances in *Pseudomonas aeruginosa* biofilm development. *Environ Microbiol* 13:1705–1717
415. Yang X, Beyenal H, Harkin G, Lewandowski Z (2001) Evaluation of biofilm image thresholding methods. *Water Res* 35:1149–1158
416. Yerly J, Hu Y, Jones SM, Martinuzzi RJ (2007) A two-step procedure for automatic and accurate segmentation of volumetric CLSM biofilm images. *J Microbiol Methods* 70:424–433
417. Yin B, Scupham AJ, Bent E, Borneman J (2007) BrdU substrate utilisation assay. In: Kowalchuk GA, Bruijn FJd, Head IM, Akkermans ADL, Elsas JDv (eds) *Molecular microbial ecology manual*, vol 2. Kluwer Academic Publisher, Dordrecht, pp 1651–1660
418. Yoshida A, Kuramitsu HK (2002) *Streptococcus mutans* biofilm formation: utilization of a gtfB promoter-green fluorescent protein (PgtfB: GFP) construct to monitor development. *Microbiology* 148:3385–3394

419. Yu GH, Tang Z, Xu YC, Shen QR (2011) Multiple fluorescence labeling and two dimensional ftir-<sup>13</sup>C NMR heterospectral correlation spectroscopy to characterize extracellular polymeric substances in biofilms produced during composting. *Environ Sci Technol* 45:9224–9231
420. Zachow C, Fatehi J, Cardinale M, Tilcher R, Berg G (2010) Strain-specific colonization pattern of *Rhizoctonia* antagonists in the root system of sugar beet. *FEMS Microbiol Ecol* 74:124–135
421. Zhang Z-P, Adav SS, Show K-Y, Tay J-H, Liang DT, Lee D-J, Su A (2008) Characteristics of rapidly formed hydrogen-producing granules and biofilms. *Biotechnol Bioeng* 101:926–936
422. Zippel B, Neu TR (2012) Characterization of glycoconjugates of extracellular polymeric substances in tufa-associated biofilms by using fluorescence lectin-binding analysis. *Appl Environ Microbiol* 77:505–516
423. Zippel B, Rijstenbil J, Neu TR (2007) A flow-lane incubator for studying freshwater and marine phototrophic biofilms. *J Microbiol Methods* 70:336–345
424. Zoghلامي K, Gomez-Gras D, Corbella M, Darragi F (2008) Laser scanning confocal microscopy characterization of water repellent distribution in a sandstone pore network. *Microsc Res Tech* 71:816–821
425. Zubkov MV, Fuchs BM, Eilers H, Burkill PH, Amann R (1999) Determination of total protein content of bacterial cells by SYPRO staining and flow cytometry. *Appl Environ Microbiol* 65:3251–3257

# Modeling of Biofilm Systems: A Review

Harald Horn and Susanne Lackner

**Abstract** The modeling of biochemical processes in biofilms is more complex compared to those in suspended biomass due to the existence of substrate gradients. The diffusion and reaction of substrates within the biofilms were simulated in 1D models in the 1970s. The quality of these simulation results was later improved by consideration of mass transfer at the bulk/biofilm interface and detachment of biomass from the surface. Furthermore, modeling of species distribution along the axis perpendicular to the substratum helped to simulate productivity and long-term behavior in multispecies biofilms. Multidimensional models that were able to give a realistic prediction of the surface structure of biofilms were published in the 1990s. The 2D or 3D representation of the distribution of the species in a matrix of extracellular polymeric substances (EPS) helped predict the behavior of multispecies biofilm systems. The influence of shear forces on such 2D or 3D biofilm structures was included by solving the Navier–Stokes equation for the liquid phase above the biofilm. More recently, the interaction between the fluid and biofilm structures was addressed more seriously by no longer considering the biofilm structures as being rigid. The latter approach opened a new door, enabling one to describe biofilms as viscoelastic systems that are not only able to grow and produce but also be deformed or even dislodged if external forces are applied.

**Keywords** Biofilm model · Detachment · Fluid structure interaction · Mass transfer · Multidimensional

## Abbreviations

AOB	Ammonium oxidizing bacteria
BbM	Biomass-based model
C	Constant in Eq. (14)
<i>c</i>	Concentration (g/m <sup>3</sup> )

---

H. Horn (✉) · S. Lackner  
Engler-Bunte-Institute, Karlsruhe Institute of Technology, Karlsruhe, Germany  
e-mail: horn@kit.edu

S. Lackner  
e-mail: susanne.lackner@kit.edu

CA	Cellular automata
$c_{Fi}$	Concentration of dissolved substance $i$ at the biofilm surface ( $\text{g}/\text{m}^3$ )
$c_{Bi}$	Concentration of dissolved substance $i$ in the completely mixed liquid phase (bulk phase) ( $\text{g}/\text{m}^3$ )
CBL	Concentration boundary layer
$D$	Diffusion coefficient ( $\text{m}^2/\text{s}$ )
$d$	Diameter (m)
IbM	Individual-based model
$j$	Mass flux ( $\text{g}/\text{m}^2 \text{ d}$ )
$k_d$	Detachment coefficient ( $1/d$ )
$k_{d,\text{random}}$	Detachment coefficient for random detachment events ( $1/d$ )
$k_L$	Mass transfer coefficient (m/s)
$K_S$	Monod constant ( $\text{g}/\text{m}^3$ )
$L$	Number of grid cells in height/Length (m)
$L_C$	Thickness of the concentration boundary layer (m)
$L_F$	Biofilm thickness (m)
$L_{F,\text{base}}$	Base biofilm thickness (m)
$m_X$	Mass of biomass (g)
$N$	Number grid cells in length
NOB	Nitrite oxidizing bacteria
$Pe$	Peclet number
$p$	Pressure ( $\text{N}/\text{m}^2$ )
$Re$	Reynolds number
RS	High rate strategist
$r$	Conversion rate ( $\text{g}/\text{m}^3 \text{ d}$ )
$Sc$	Schmidt number
$Sh$	Sherwood number
$t$	Time (d)
$u$	Flow velocity (m/s)
$u_F$	Relative velocity of a particulate component in the biofilm perpendicular to the substratum (m/d)
$V$	Volume ( $\text{m}^3$ )
$X$	Biomass concentration ( $\text{g}/\text{m}^3$ )
$Y$	Yield coefficient (g/g)
YS	High yield strategist
$Z_f$	Position of an occupied grid cell above the substratum within the grid (N,L)
$Z_{f\text{max}}$	Highest occupied grid cell above the substratum within the grid (N,L)
$z$	Space coordinate perpendicular to the substratum

### Greek Letters

$\alpha$	Biofilm surface enlargement
$\varepsilon$	Porosity
$\varepsilon_S$	Fraction of the solid phase in the biofilm volume

$\varepsilon_{Fl}$	Fraction of the liquid phase in the biofilm volume
$\kappa$	Parameter in Eq. (9)
$\delta$	Parameter in Eq. (9)
$\mu$	Growth rate (1/d)
$\mu_{max}$	Maximum growth rate (1/d)
$\Omega$	Parameter in Eq. (12)
$\sigma$	Biofilm surface roughness
$\nu$	Kinematic viscosity (m <sup>2</sup> /s)
$\rho$	Biofilm density (gX/m <sup>3</sup> ) or
.	Density of fluid (kg/m <sup>3</sup> )
$\tau$	Shear stress (N/m <sup>2</sup> )

**Subscripts**

EPS	Extracellular polymeric substances
<i>F</i>	Biofilm
<i>i</i>	Component i
O <sub>2</sub>	Oxygen
<i>P</i>	Particle
<i>S</i>	Substrate
<i>X</i>	Biomass

**Contents**

1	Introduction .....	55
2	1D Biofilm Models.....	57
	2.1 Mass Transfer at the Bulk/Biofilm Interface.....	57
	2.2 Reaction/Diffusion Models .....	59
	2.3 Detachment.....	63
3	Advanced Multidimensional Biofilm Models: Biofilm Structure .....	64
	3.1 Cellular Automata (CA).....	64
	3.2 Individual-Based and Particle-Based Biofilm Models .....	66
4	Coupling Fluid Dynamics with Biofilm Structure.....	68
5	Conclusions and Future Perspectives .....	69
	References .....	70

**1 Introduction**

The wish for a better understanding of the organization and function of microorganisms in biofilms has led to the development of a variety of models that capture the knowledge of biofilm systems which has accumulated over the last three decades. Such models are more than just an assembly of the biochemical processes that occur in biofilm systems. To represent a biofilm system adequately by mathematical

simulations, physical aspects such as transport mechanisms, shear forces, and mechanical strength have to be addressed in addition to the microbiological and/or ecological aspects of the “micro” organisms involved in biofilms. The modeling of biofilm systems thus quickly becomes a multidisciplinary effort combining microbiology, biogeochemistry, and fluid mechanics. Although biofilms do not yet play an important role in chemical production, the interest in modeling biofilm systems has been steadily increasing within the last 30 years [1]. One main reason has been an increasing acceptance that microorganisms in the real world like to organize themselves in biofilms and not as suspended individuals [2]. By opening this door a broad research field has emerged, and dozens of research groups worldwide have taken on the challenge of identifying the main factors influencing the structure and function of biofilms [3]. In recent years, specific aspects such as communication or quorum sensing between bacteria [4] have been implemented into a mathematical framework for biofilm modeling [5].

Very often the published manuscripts on biofilm models picked up new insights that have been generated with new experimental tools. The first significant contributions that led to a better understanding of mass transfer and mass transport in biofilm systems have been made with microelectrode studies [6–9] (see contribution of Beyenal in this volume). In the 1990s imaging of biofilm structures with confocal laser scanning microscopy (CLSM) became popular [10] and was then a driving force for multidimensional biofilm models [11] (see contribution of Neu and Lawrence in this volume). In the same decade molecular methods including DGGE, FISH, and PCR increased knowledge of microbiological composition and spatial distribution of biofilms [12]. Such methods are capable of showing the high diversity of microorganisms in mixed cultures. Nevertheless, the contribution of every single strain to the structure and function of mixed culture biofilm systems has seldom been addressed in biofilm models [13, 14].

In general, two main aspects can be found in the literature that led to the development and/or application of biofilm models.

*Biofilm reactor models* The first wave of model concepts for biofilms were all presented around the same time and were mainly designed to describe phenomena in fixed-bed reactors for wastewater treatment. All of these authors recognized that established mathematical models for suspended biomass were inadequate for fixed-bed reactors as they did not take the limiting diffusion in the biofilm matrix into account, and tried to remedy this by including reaction–diffusion mass balances. In the following three decades many models were developed and published that described mass transport and substrate conversion in biofilm reactors for wastewater treatment or other technical systems [15–18]. Most of these models can typically be linked to environmental engineering. A very good review on this topic was published in Ref. [19]. The authors provide an excellent overview of the existing tools for modeling biofilm reactors in wastewater treatment. Models aimed at consultants and engineers specific for the design of biofilm reactors are still scarce compared to those of activated sludges, although more and more commercially available software packages also include sections for the modeling of biofilms.

*General biofilm models* The second group of models was developed to describe processes and structures in biofilms, and was not aimed at specific applications. These models addressed issues such as detachment and attachment of particles at the biofilm surface, incorporation of EPS within the biofilm structure, population dynamics, and biofilm structure development. The latter can only be done with 2D or 3D models. These models form the majority of the publications in the last two decades [11, 20–26]. Recent developments deal with incorporation of physical biofilm properties into biofilm modeling [27, 28].

The number of reviews dealing with modeling of biofilm systems is limited. Reference [29] presented an early review of biofilm models. In 2006 an IWA task group produced a publication describing the state of the art of the mathematical modeling of biofilms [30]. In several benchmark problems the capability and limitations of both analytical and numerical solutions were discussed. The main focus of this report was on the comparison of 1D and 2D, respectively, 3D models. Advances in biofilm modeling with special focus on multidimensional aspects are presented in Ref. [31]. Klapper and Dockery [32] presented another review linking modeling and microbial ecology. A special focus in that review is on antimicrobial tolerance of microorganisms, biofilm mechanics, and quorum sensing. Medical biofilms and their tolerance against antibiotics has been a popular topic in biofilm research in the last decade. The review in Ref. [33] presents the main topics in this research area.

The review presented here discusses traditional biofilm models, coupling reaction/diffusion with population dynamics and biofilm structure. Both one-dimensional and multidimensional approaches are discussed. The focus is on the coupling of structure and function of biofilms. The often underestimated effect of mass transfer is also discussed as well as the impact of detachment. These processes form part of most one- and multidimensional biofilm models. Finally, the latest developments incorporating biofilm mechanics are shown.

## 2 1D Biofilm Models

### 2.1 Mass Transfer at the Bulk/Biofilm Interface

In many existing biofilm models the bulk/biofilm interface is not handled properly. Mass transfer at this interface is decisive for the supply of the active biomass with all types of soluble substrates. Assuming that the biofilm surface is separated from the bulk by a laminar layer, classical film theory can be applied. In several models the thickness of this layer has been set to values around 100  $\mu\text{m}$  [34–37]. In film theory the mass transport within this layer is assumed to be diffusive. Therefore the layer is often called the diffusion boundary layer (DBL) [38, 39]. The mass transfer coefficient  $k_L$  can then be calculated by dividing the diffusion coefficient  $D_i$  by the thickness of the boundary layer  $L_C$ :



$$k_L \cong \frac{D_i}{L_C} \quad (1)$$

Nevertheless, numerous microelectrode measurements indicate that both diffusive and advective transport drive the transport within the boundary layer [40–44]. Therefore, a linear approach as shown in Eq. (1) is not close to reality, as, for example, can be seen in Fig. 2 for an oxygen profile measured with a microelectrode in a hetero-/autotrophic biofilm. Consequently, the boundary layer should be addressed as the concentration boundary layer (CBL). The mass transfer at the bulk/biofilm interface is a result of flow conditions in the bulk phase and can be calculated if an empirically derived relation between flow and mass transfer is available. The Sherwood number  $Sh$  is the dimensionless number for mass transfer. It is used to determine the ratio of the total mass transfer flux to the diffusion flux:

$$Sh = \frac{k_L \cdot d}{D_i} \quad (2)$$

The characteristic length  $d$  depends on reactor geometry; in the case of a tube it is the tube diameter. The Sherwood number can be expressed as a function of the Reynolds number  $Re$  and the Schmidt number  $Sc$ :

$$Sh = f(Re, Sc) \quad \text{with} \quad Sc = \frac{\nu}{D_i}, \quad Re = \frac{u \cdot d}{\nu} \quad \text{and} \quad Pe = Re \cdot Sc \quad (3)$$

where  $u$  is the average flow velocity,  $\nu$  the kinematic viscosity, and  $Pe$  is the Peclet number as the product of  $Re$  and  $Sc$ . An overview of variations of the Sherwood number in biofilm systems is given in Table 1. Only a few of these equations were adapted specifically to biofilm systems by the authors. In fact, most of the equations were taken from process engineering where they were mainly used in connection with biofilm-free surfaces.

Equation (11) is based on microelectrode measurements [52]. The steepness of the oxygen concentration profiles has been combined with the measured mass flux  $j_{O_2}$ . Thereby, averaged mass transfer coefficients  $k_L$  could be calculated based on the Neumann boundary condition at the bulk/biofilm interface:

$$j_i = k_L \cdot (c_{Bi} - c_{Fi}) \quad (4)$$

Picioreanu et al. [54] extended the equation for the Sherwood number for biofilms by including the enlargement of the surface area  $\alpha$  [Eq. (14)]. A comparable approach was published in Ref. [53] both for laminar and turbulent flow in tubes [Eqs. (12) and (13)]. The structure factor  $\mathcal{Q}$  is a function of growth rate  $\mu$  and flow conditions during growth. Such approaches attempting to incorporate the effect of biofilm structure into 1D models have not been fully successful. The possibility of generating the required “real” surface structures is better provided with 2D or 3D models (see Chap. 3).

**Table 1** Equations for the Sherwood number in biofilm systems (adapted from Ref. [45])

Sherwood number Sh	Reactor type	References	Equation
Laminar: $88 + (1.11 \times 10^{-11}/d_p) Re^{4.33} \times Sc^{1/3}$	Gravel in a flow channel	[46]	(5)
$2 + f_K (Re Sc)^{1.7}/(1 + (Re Sc)^{1.2*})$ with $f_K = 0.66/[1 + (0.84 Sc^{1.6})^3]^{1/3}$	Immobilized biocatalyst	[47, 48]	(6)
Laminar: $1.615 (Re d/L)^{1/3} Sc^{0.27*}$	Membrane tube reactor	[49]	(7)
Turbulent: $0.037 (Re^{0.75} - 180) Sc^{0.27} [1 + (d/L)]^{2/3*}$			(8)
Turbulent: $0.0153 Re^{0.833} Sc^{0.32*}$	Open flow channel	[50]	(9)
Laminar: $2 + 0.51 (\kappa Re_p \delta)^{0.6} Sc^{1/3*}$ ( $\kappa, \delta = f(Re_p)$ with $Re_p \equiv u d_p/\nu$ )	Biofilter with particle-fixed biofilms	[51]	(10)
Laminar: $2 Re^{1/2} Sc^{1/2} (d/L)^{1/2} (1 + 0.0021 Re)$	Biofilm tube reactor	[52, 53]	(11)
$2 Re^{1/2} Sc^{1/2} (d/L)^{1/2} (0.24 \Omega)^{-1}$			(12)
Turbulent: $0.037 Re^{0.75} Sc^{1/2} (0.24 \Omega)^{-1}$			(13)
Laminar: $C \alpha^{-n} Re^{1/3} Sc^{1/3}$	Particle-fixed biofilms	[54]	(14)

\*Not specifically adapted to biofilms

## 2.2 Reaction/Diffusion Models

Knowledge of the substrate concentration at the biofilm surface [Eq. (14)] is essential for solving models of reaction/diffusion processes in the biofilm. As mentioned above, the first model approaches were published around 1976 [55–58]. The authors tried to describe mass transport and conversion in fixed-bed reactors used for wastewater treatment. Substrate conversion in the biofilm was coupled to diffusion and a steady-state approach ( $dc/dt = 0$ ) based on Fick's second law was used:

$$D_S \frac{\partial^2 c_S}{\partial z^2} = r_S \quad (15)$$

with

$$r_S = \mu_{\max} * \frac{1}{Y_{X/S}} \frac{c_S}{(c_S + K_S)} X$$

This reaction/diffusion model is still used. The biggest challenge is still how to describe the distribution of biomass along the axis perpendicular to the substratum. As long as one species or one group of microorganisms (i.e., biomass  $X$ ) has to be modeled, the biomass can be handled easily and more or less evenly distributed

based on the availability of substrate  $S$ . As soon as two or more species with different growth rates  $\mu$  and yield coefficients  $Y$  are involved, the outcome of the model strongly depends on where the different species can be found at which concentration along the  $z$ -axis.

Kissel et al. [20] made one of the first significant contributions to overcome this problem. The biofilm was divided into segments. Both the biomass growth and the proportion of the involved species as well as their distribution in the biofilm were then calculated. Another approach [22] discretized both biofilm and water layer perpendicular to the substratum. The authors identified the important influence of biofilm density  $\rho_X$ , which is formulated as follows:

$$\rho_X = m_X/V_F \quad (16)$$

$\rho_X$  determines the amount of biomass  $X$  of a certain species that is available in a volume element. Depending on cultivation conditions and specific growth rate of the species  $\rho_X$  can vary between 10,000 g/m<sup>3</sup> [53] and 110,000 g/m<sup>3</sup> [59]. The general assumption is that the lower the growth rate, the higher the density, and the lower the flow velocity (or shear rate) above the biofilm the lower the density [60, 61].

One of the most used 1D models was published in 1986 by Wanner and Gujer with further developments over the following 10 years [23, 62]. The particulate components (i.e., biomass and particulate inert material) were treated in a continuum approach. Wanner and Gujer used a differential equation to describe the mass balance of particulate components in biofilms:

$$\frac{\partial X_i}{\partial t} = -\frac{u_F}{\partial z} \frac{\partial X_i}{\partial z} + r_{X_i} \quad (17)$$

Inclusion of this made it possible to synchronize substrate transport and utilization [Eq. (15)] along the  $z$ -axis with the change of particulate component concentration  $X_i$ . In Eq. (15)  $r_S$  describes the substrate conversion whereas the rate for conversion of particulate components  $X_i$  is symbolized in Eq. (17) by  $r_{X_i}$ .

The key parameter  $u_F$  represents the velocity of particulate components  $i$  moving perpendicular to the sub-stratum (see Fig. 1). The velocity can be positive if the component  $X_i$  is produced by growth and can be negative if the component undergoes, for example, lysis.

$$u_F = u_{F(z=0)} + \int_0^{L_F} \sum_{i=1}^n \frac{r_{X_i}}{\rho_i} dz \quad (18)$$

The value of  $\rho_i$  will have a strong impact. If the biofilm density  $\rho_i$  is set to a low value the biofilm thickness  $L_F$  will grow with a higher velocity. Most published 1D simulation studies do not try to predict the biofilm density but rely on experience or measured values [63–66]. An advanced approach of the model shown above, which

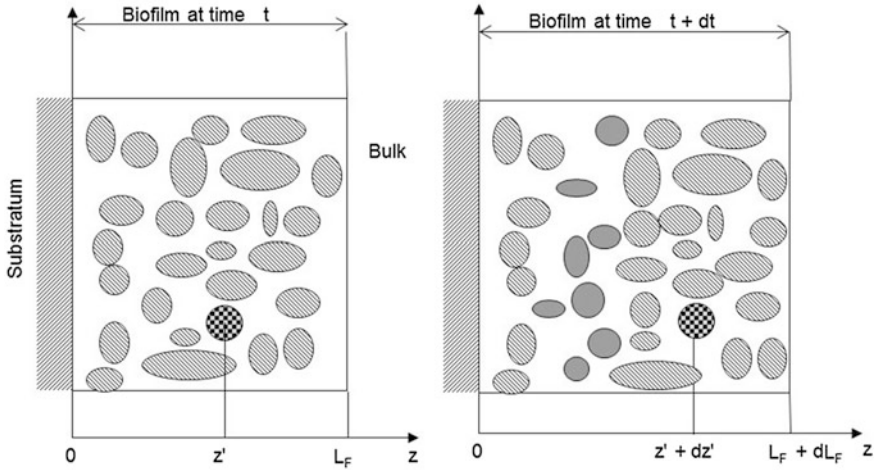


**Fig. 1** Transport of a particulate component (*crossed sphere*) after growth of new components (*dark grey*) in the underlying layer (adapted from Ref. [62])

was published in 1989 by Gujer and Wanner, separated the biofilm into a liquid phase  $\epsilon_{FI}$  and a solid phase  $\epsilon_S$  [62]. Microorganisms and other particulate material are part of the solid phase and the dissolved components such as substrate and oxygen are transported in the liquid phase.

$$\epsilon_{FI} + \sum \epsilon_{Si} = 1 \tag{19}$$

Figure 2 shows a typical example for an application of the Wanner–Gujer model, a competition between ammonium oxidizing autotrophic bacteria and organic carbon utilizing heterotrophic bacteria, which is often used as the classic case for 1D biofilm models [34, 67, 68] in wastewater treatment. In the latter case micro-electrode measurements are used to optimize the kinetic parameters. Similar simulation studies have been conducted for biofilms growing on permeable membranes [69]. In this case the biofilm is membrane bound and supplied with oxygen from the membrane side. The setup allows for simultaneous nitrification and denitrification in one biofilm. Membrane bound biofilm reactors also offer different selection mechanisms, for example, to select for ammonium or nitrite oxidizing bacteria (AOB and NOB) [70, 71].

The outcome of such simulation studies is mainly driven by the underlying kinetics of the involved species. In this case ammonium oxidizing bacteria AOB, nitrite oxidizing bacteria NOB, heterotrophic bacteria HB, and inert material are competing for space and oxygen. For wastewater treatment the activated sludge model ASM is typically applied to describe the kinetics [72]. Nevertheless, as the competition of AOB and NOB is not explicitly described in the ASM, most modelers use the kinetic parameters accumulated for these two types of organisms by [65] from different sources.

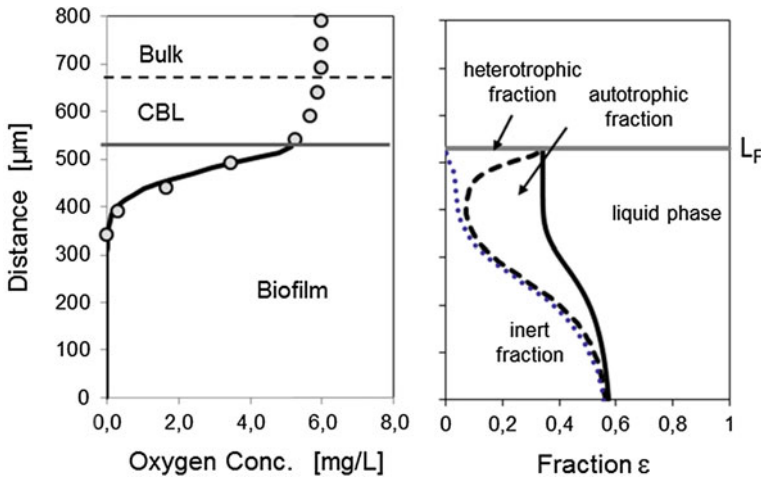


**Fig. 2** Simulation results for a heterotrophic/autotrophic biofilm system. *Right graph* species distribution; *left image* measured (grey circle) oxygen profile with concentration boundary layer (CBL) and the simulated profile within the biofilm for the same day (data and permission from Ref. [68])

If there are large differences between the growth rates  $\mu$  of the bacteria involved, the species will be stratified as shown in Fig. 2. Physical parameters, such as the mass transfer coefficient  $k_L$  and diffusion coefficient  $D$ , will not have a high impact, as the diffusion coefficients of the different substrate molecules involved are rather similar [73–75].

A successful tool for the above-described 1D simulations of biofilm systems is AQUASIM, which has been available for 20 years and is still widely used [76] (<http://www.eawag.ch/forschung/siam/software/aquasim/index>). Various types of active or inactive particulate biological or inorganic components within the biofilm can be included in the simulations including:

- Bacteria (AOB, NOB, AnAOB, heterotrophic bacteria) [69, 70, 77–81]
- Extracellular polymeric substances (EPS) produced by bacteria [82, 83]
- Phototrophic microorganisms [84–86]
- Fungi [87, 88]
- Inorganic materials [89]

The results of such simulation studies might be partly predictable, as most of the dynamic processes behave quite linearly. More or less unexpected results are achieved if instationary detachment processes are applied to allow slower growing microorganisms to appear at the biofilm surface because of detachment of the faster ones [90].

### 2.3 Detachment

The prediction of detachment is still an unsolved problem. Like transport processes, it is driven more by physics and less so by the microbiology. Already in the 1980s simple models were proposed on how the process of biomass detachment should be described. Several approaches have been published aiming to model the loss of biomass by detachment. These biofilm models mainly focus on erosion and sloughing. Erosion is characterized by the detachment of smaller particles in the range of 10  $\mu\text{m}$ , whereas sloughing involves the removal of large parts up to several mm from the biofilm. Two other mechanisms that may also cause biofilm to be removed have not really been addressed by modelers, that is, abrasion and grazing by higher organisms.

Detachment occurs when external forces (e.g., through shear) are larger than the internal strength of the biofilm matrix. In principle there are two mechanisms that can lead to detachment: (i) increase of the external shear forces (e.g., during backwashing), or (ii) decrease of the internal strength (e.g., through hydrolysis of the polymeric biofilm matrix) [91]. Generally the detachment process can be formulated as

$$\frac{dL_F}{dt} = f(\rho_F, L_F, \mu, \tau, \dots) \quad (20)$$

Detachment is caused by a combination of biological, chemical, and physical processes [92] and detachment has been linked to different parameters [see Eq. (20)]. Little is known about the biological mechanisms of the bacterial species involved. As a result detachment is often incorporated into biofilm models on the basis of simplified assumptions [68, 93]. Sometimes a constant biofilm thickness is assumed to focus on the microbial processes inside the biofilm [21, 94]. Table 2 provides several approaches by which detachment can be incorporated into biofilm modeling. Typically a detachment coefficient  $k_d$  is used as the lumped parameter. Early models often used biofilm thickness [34, 95–98]. A more physical approach is the use of shear stress  $\tau$  [26, 99, 100] or the change of shear stress  $\tau$  [101]. The rate of increase of shear stress delivers an especially significant contribution to detachment [91].

Other authors identified the influence of growth rate  $\mu$  of the microorganisms as a significant factor in the detachment process [101, 103, 105, 106, 107]. Detachment processes can be a function of time, for example, during back washing [64, 108]. A dimensionless analysis of the detachment rate is provided by Nicolella [109]. One-dimensional models with shear and nonshear detachment are compared in Ref. [110].

**Table 2** Detachment models for one-dimensional biofilm models (adapted from Ref. [102])

Biofilm growth under constant substrate load	Formulation of the detachment rate (g/m <sup>2</sup> d)	References	Equation
Constant	Constant biofilm thickness	[21]	
Constant	$k_d X_f^2$	[98, 95]	(21)
Constant	$k_d \rho_F L_F \tau^{0.58}$	[100]	(22)
Constant	$k_d \rho_F L_F^2$	[34]	(23)
Constant	$L_F (k_d' + k_d'' \mu)$	[103]	(24)
Constant	$k_d \rho_F L_F$	[96, 97, 104]	(25)
Constant	$k_d \rho_F \tau$	[99]	(26)
Constant	$k_d \rho_F u_F$	[23]	(27)
Time dependent detachment differentiating between normal operation and backwashing*	No detachment ... In operation $k_d (L_F - L_{F,base})$ ... During backwash	[102]	(28)
Random	$k_{d,random} (L_F - L_{F,base})$	[91]	(29)

The dimensions of  $k_d$ ,  $k_d'$  and  $k_d''$  are different for different models

\*Model of a sequencing batch reactor (SBR)

## 3 Advanced Multidimensional Biofilm Models: Biofilm Structure

### 3.1 Cellular Automata (CA)

At the end of the 1990s the first multidimensional biofilm models were published on cellular automata (CA). The authors used a discrete formulation, which was able to describe the spatial heterogeneity of biofilms produced by growth and decay of microorganisms [24, 111, 112]. Two-dimensional approaches used a uniform rectangular grid, whereas 3D models used cubical elements. The available squares (2D) or cuboids (3D) were filled with biomass based on growth driven by the turnover of available substrate. The state of a system was determined based on the substrate concentration  $S$  and biomass density  $C$  (in dimensionless form). A third matrix element described whether a space was filled with bacteria, inert material, or liquid [113].

Figure 3 shows an example for a 2D grid. The substrate concentration is calculated based on the reaction diffusion Eq. (5). The biomass density is a key parameter as it drives the turnover of the reaction/diffusion model. The modeler has to decide how much biomass is allowed for one square. If the biomass density reaches its maximum level the excess biomass will be transferred to one of the

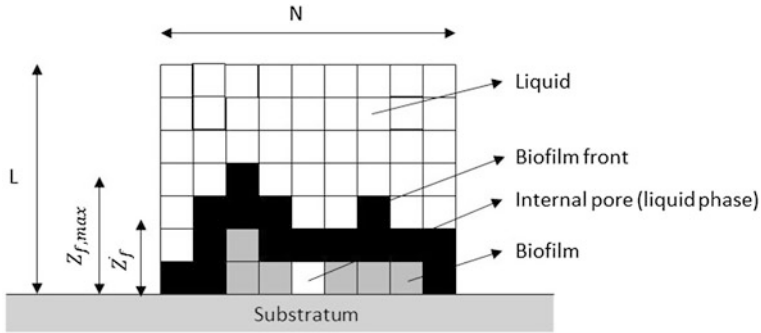


**Fig. 3** Grid (N,L) for CA with cells filled with biomass or liquid phase (adapted from Ref. [11])

adjacent cells. If all adjacent cells are occupied one randomly chosen cell is displaced following the same rule.

When run, these 2D or 3D structures develop a structural heterogeneity of biofilms similar to those seen with CLSM techniques in the 1990s (see review on imaging by Neu and Lawrence in this volume). Picioreanu et al. further specified the CA approach with respect to the different states of the cells within their model [11]. Figure 3 shows the different states of the cells within a grid that are defined as with liquid phase, biomass at the biofilm front, biomass within the biofilm, and internal pores. The work shows how biofilm roughness  $\sigma$  developed based on substrate availability. The roughness was calculated based on the state of matrix  $c$  and the deviation of the local biofilm thickness  $Z_f$  (see Fig. 3).

Figure 4 shows a biofilm structure generated with the CA approach [11]. The example is based on slow-growing bacteria with a growth rate  $\mu_{max}$  of  $1.2 \text{ d}^{-1}$ . Different biofilm structures can develop based on inoculation strategy, substrate availability, and flow field [24, 114]. In general the surface roughness  $\sigma$  increases with decreasing substrate availability. Fingerlike structures as can be seen in Fig. 4 have also been generated with continuum approaches using pressure (generated within the biofilm by growth) as the driver for biofilm growth [115]. Other continuum approaches tried to describe the spreading of biomass with diffusion [116].

Detachment has been included in biofilm models based on CA. For example, in Ref. [117] detachment of biomass was assumed to be caused by the internal stress generated by a liquid phase moving above the biofilm. The biofilm was assumed to be a homogeneous and isotropic elastic material. The biofilm would detach if the external forces driven by the flow field exceeded the internal strength. A more conservative CA approach for describing detachment that included detachment coefficients and maximum biofilm height was presented by Chambless and Stewart [118].



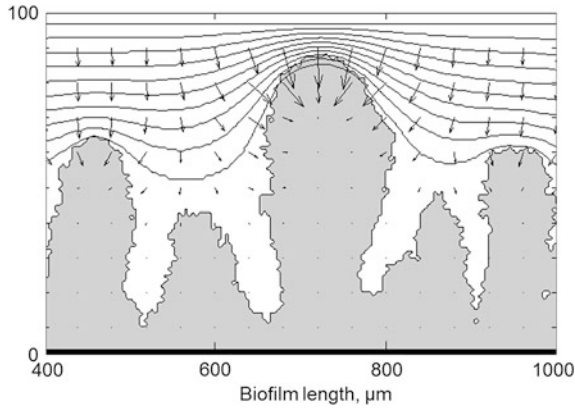


**Fig. 4** Application of the CA-based biofilm model, shown with permission from Ref. [11]. The model shows a biofilm structure after 31 days at an average substrate concentration. The lines above the biofilm structure show the substrate concentration field; the *arrows* indicate the flux

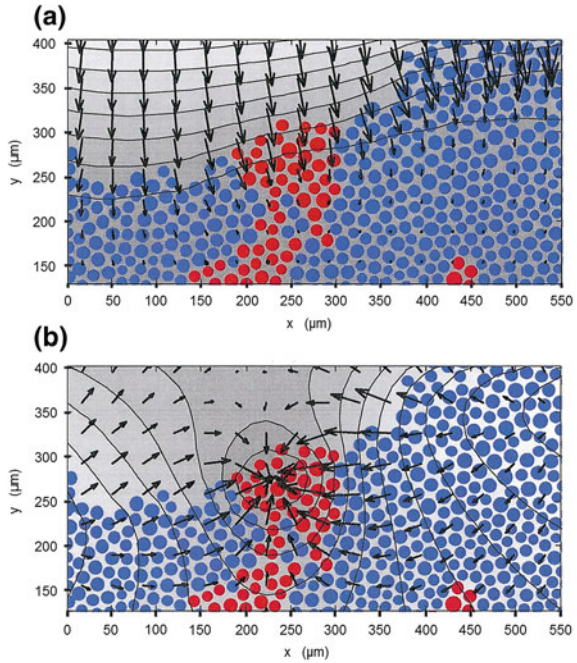
### 3.2 Individual-Based and Particle-Based Biofilm Models

A main trigger for the development of 3D model approaches other than CA was the question of how single cells really behave in terms of spreading. Kreft et al. were the first to develop an individual-based model that focused on single cells as individual particulate units [93]. The idea was to generate biofilm structures that give a more realistic distribution of bacteria in a biofilm matrix. The model, BacSim, was organized similar to the CA models described above. Cells were represented by shapes, typically spheres. A minimum distance was maintained between the neighboring cells [119]. Growth was again based on the reaction/diffusion equation for the soluble substrates [see Eq. (5)] The biomass accumulation was simulated by the insertion of new cells. After insertion the new position of cells within the matrix was determined based on the calculated overlap with neighboring cells.

In general CA biomass-based models (BbM) and individual-based models (IbM) show no major differences except in biofilm shape and distribution of so-called minority species [119]. The behavior of competing egoistic and altruistic bacteria has been studied with IbM [120]. The author compared two bacteria with different strategies but growing on the same substrate: a high yield (YS) and a high rate strategist (RS). Compared to suspended cultures, where the RS are better off, YS can dominate biofilms. YS do have a chance to maintain within the system if they form clusters, which have to be broken up in single cells occasionally to colonize new surfaces. The simulation shows a possible benefit of multidimensional models compared to the 1D approach. The behavior of different strategies or species in terms of dispersal can be studied easily.

To reduce the resources needed for computing an extension of the IbM has been proposed in which the particles are clumped together to form units with a larger diameter (up to 20  $\mu\text{m}$  compared to 1  $\mu\text{m}$  in the standard IbM) [121]. The particles

**Fig. 5** Particle-based biofilm model with AOB (*blue*) and NOB (*red*). Particle size is around 20  $\mu\text{m}$ . Fluxes of oxygen (**a**) and nitrite (**b**) indicated by the length of the *arrows*. The two images nicely show the concentration fields for the two substrates of which one (nitrite) is produced within the biofilm and the other (oxygen) comes with the liquid phase from outside the biofilm (reproduced with permission from Ref. [121])



consist of one type of bacteria and inert biomass. Redistribution of the clumps is organized in the same way as in the standard IbM. The spread of biomass is again the result of biomass growth, and occurs by spheres pushing each other out of the way when they get too close to each other [121].

Figure 5 shows one advantage of 2D models over the traditional 1D simulation. A cluster of NOB is embedded in AOBs, receiving their substrates from different sources (nitrite from AOB activity and oxygen from the bulk). The necessary resolution of AOB and NOB in two dimensions to demonstrate the impact on local substrate distribution is not possible with 1D models.

Most of the early individual-based models did not address hydrodynamics. The main problem was the time scale. There were several magnitudes of difference in the time scales between processes such as advective flow and the growth of new bacteria:

- Advection ( $10^{-2}$  –  $10^{-1}$  s)
- Biochemical substrate conversion ( $10^{-1}$  –  $10^2$  s)
- Diffusion ( $10^3$  s)
- Biomass growth ( $10^5$  s)
- Detachment, erosion (10 s), and sloughing ( $10^5$  s)

Xavier et al. published a particle-based model that included a realistic liquid flow above the biofilm structure [122] by calculating the laminar flow field above the biofilm structure using the Navier–Stokes equation:

$$\frac{\partial u}{\partial t} = \nu \nabla^2 u - u \cdot \nabla u - \frac{1}{\rho} \nabla p \quad \nabla \cdot u = 0 \quad (30)$$

By solving this equation the mass transfer at the bulk/biofilm interface could be solved in parallel and the Sherwood number no longer had to be calculated based on empirical equations (see Table 1). Furthermore, the detachment was addressed in the particle-based biofilm models by the use of a level-set method to identify the bulk/biofilm interface [123]. The model incorporates the production of heterotrophic biomass, EPS, and inert material. Detachment processes including erosion and sloughing are coupled, with higher erosion less sloughing can be observed.

In the last decade multidimensional biofilm models have been used to simulate processes in technical aquatic systems mainly by the biofilm modeling group at TU Delft:

- Anaerobic ammonium oxidation [121]
- Microbial fuel cells [124]
- Porous media [125]
- Biofouling in membrane technology [126]

Recently Lardon et al. formulated a general IbM (IDYNOMICS) with an open-source code [127]. The biofilm pressure field introduced by Alpkvist and Klapper [27] was also implemented. These approaches directly lead to the fluid–structure interaction, which is discussed in the next chapter.

## 4 Coupling Fluid Dynamics with Biofilm Structure

Although the multidimensional structure and function of biofilms can be simulated with the models described before, the incorporation of physical processes such as deformation by shear forces is not addressed by these models. This can be difficult. The problem begins with the identification of required parameters [128]. Methods to measure physical biofilm characteristics are challenging and do not easily provide the necessary parameters (Young’s modulus, shear modulus, adhesive or tensile strength) that are needed to feed such models [129, 130]. It is, however, worthwhile. Biofilms typically behave as viscoelastic structures if shear forces are applied. The deformation that follows the application of shear will have an impact on mass transfer, compactness of biomass, and detachment. A moving structure will also back-couple on the flow field.

A ball-spring model for biofilms was proposed by Alpkvist and Klapper (2007), which applied an immersed boundary method to describe the mechanical response and in the end detachment of biomass from biofilms in a flow field [27]. This contribution was a significant step forward in biofilm modeling because the biofilm structure was no longer assumed to be rigid. The role of biofilm cohesion with respect to growth-induced pressure stress within the biofilm was described by Dockery and Klapper [131]. Another example of a two-dimensional biofilm

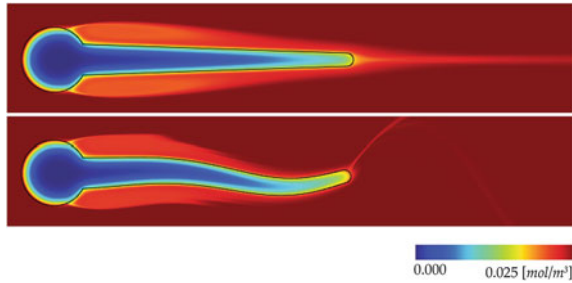


**Fig. 6** Substrate concentration around a rigid (*upper image*) and an oscillating (*lower image*) biofilm streamer (reproduced with permission from Ref. [137])

structure deformed due to applied shear forces was presented by Cogan (2008). The author assumed the biofilm as viscoelastic fluid surrounded by another fluid with a lower viscosity [132].

Recently, finite element methods (FEM) or extended finite element methods (XFEM) found their way into the modeling of fluid–structure interaction in biofilm systems [133]. One example is provided by Duddu et al. [134], who presented a model that included mass transfer, growth, and detachment of biomass based on XFEM and a level-set interface tracking method. Another development is the use of images from CLSM to study detachment of biomass in combination with FEM [28]. Real biofilm structures are used to simulate the detachment. Such a combination of imaging with CLSM and simulation with FEM was also applied for a surgical suture covered with colonies of *Staphylococcus aureus* [135]. The aim was to predict the detachment of bacterial cells as a result of the deformation of the suture.

The influence of flow velocity on the oscillation of a biofilm streamer and the back coupling on the surrounding flow field was studied by Taherzadeh et al. [136]. The formation of a Kármán vortex street behind the biofilm streamer was shown to create eddies that influenced the streamers growing downstream. The oscillation of the streamer reduced the forces that were induced by the moving fluid. Furthermore, the movement clearly led to improved mass transfer at the tip of the streamer. Comparison of a rigid structure and an oscillating streamer (Fig. 6) showed a significantly better substrate supply for the latter [137].

## 5 Conclusions and Future Perspectives

The last three decades have seen huge developments in biofilm modeling. Simple reaction/diffusion models for biofilms have been further developed into multidimensional, multispecies models that are used in biofilm research today. However, compared to the activated sludge models (ASM) [72] that are intensively used for the design and operation of wastewater treatment plants, the available biofilm models have not had much success [30, 138–140]. It seems that isolated questions

about mass transfer, species distribution, and detachment can be answered with the available modeling tools but the entire situation in a full-scale biofilm reactor cannot easily be predicted. This is because, on top of the biofilm, the geometry of the reactor and carrier material has to be considered. This makes it difficult to make accurate predictions as the necessary data for the reactor model are seldom available.

It is evident that the dilemma described above cannot be solved by more complex multidimensional or multiphysics biofilm models. The development of multidimensional biofilm models (CA, IBM, and particle-based models) has, however, a positive impact on the understanding of the underlying processes in biofilms. One good example is the development of biofouling in reverse osmosis (RO) spiral-wound modules. As this is a very local problem the simulation results of 2D studies with a fully resolved flow field provide a very good insight into the development of biofilms on the feed spacer material in RO [141].

The perspective of having more models that are able to couple the above-described biochemical part (substrate transport/consumption and biomass growth/distribution) with mechanical characteristics and behavior is very promising. Computing time remains an issue; however, it has become a minor one. Measurement of the necessary parameters continues to be challenging and needs further improvement. Forty years ago microelectrode studies pushed the first reaction/diffusion models [40]. Twenty years ago the multidimensional models were inspired by imaging techniques such as CLSM [10]. Perhaps current biofilm models can take a step forward by the characterization of mechanical properties of biofilms [129, 130].

**Acknowledgment** Many thanks to Roland Möhle and Danial Taherzadeh. Both did their PhDs on modeling of biofilm systems and thereby contributed significantly to the understanding of structure and function of mixed culture biofilm systems.

## References

1. Halan B, Buehler K, Schmid A (2012) Biofilms as living catalysts in continuous chemical syntheses. *Trends Biotechnol* 30:453–465
2. Costerton JW, Lewandowski Z, Caldwell DE, Korber DR, Lapin-Scott HM (1995) Microbial biofilms. *Annu Rev Microbiol* 49:711–745
3. Wilderer PA, Characklis WG (1989) Structure and function of biofilms. Wiley, New York
4. Miller MB, Bassler BL (2001) Quorum sensing in bacteria. *Annu Rev Microbiol* 55:165–199
5. Dockery J, Keener J (2001) A mathematical model for quorum sensing in *Pseudomonas aeruginosa*. *Bull Math Biol* 63:95–116
6. Kuenen JG, Jørgensen BB, Revsbech NP (1986) Oxygen microprofiles of trickling filter biofilm. *Water Res* 20:1589–1598
7. Revsbech NP, Christensen PB, Nielsen LP, Sørensen J (1989) Denitrification in a trickling filter biofilm studied by a microsensor for oxygen and nitrous oxide. *Water Res* 23:867–871
8. Lewandowski Z, Walser G, Characklis W (1991) Reaction Kinetics in Biofilms. *Biotechnol Bioeng* 38:877–882

9. Cronenberg CCH, den Heuvel JCv (1991) Determination of glucose diffusion coefficient in biofilms with microelectrodes. *Biosens Bioelectron* 6:255–262
10. Lawrence JR, Korber DR, Hoyle BD, Costerton JW, Caldwell DE (1991) Optical sectioning of microbial biofilms. *J Bacteriol* 173:6558–6567
11. Picioreanu C, van Loosdrecht MCM, Heijnen JJ (1998) Mathematical modeling of biofilm structure with a hybrid differential-discrete cellular automaton approach. *Biotechnol Bioeng* 58:101–116
12. Muyzer G, Ramsing NB (1995) Molecular methods to study the organization of microbial communities. *Water Sci Technol* 32:1–10
13. Vogelsang C, Schramm A, Picioreanu C, Loosdrecht MCM, Ostgaard K (2002) Microbial community analysis by FISH for mathematical modelling of selective enrichment of gel-entrapped nitrifiers obtained from domestic wastewater. *Hydrobiologia* 469:165–178
14. Oehmen A, Lopez-Vazquez CM, Carvalho G, Reis MAM, van Loosdrecht MCM (2010) Modelling the population dynamics and metabolic diversity of organisms relevant in anaerobic/anoxic/aerobic enhanced biological phosphorus removal processes. *Water Res* 44:4473–4486
15. Gonenc E, Harremoës P (1985) Nitrification in rotating disc systems-1: criteria for transition from oxygen to ammonia rate limitation. *Water Res* 19:1119–1127
16. Arvin E, Harremoës P (1990) Concepts and models for biofilm reactor performance. *Water Sci Technol* 22:171–192
17. Muslu Y (1992) Developments in modelling biofilm reactors. *J Biotechnol* 23:183–191
18. Picioreanu C, van Loosdrecht MCM, Heijnen JJ (1997) Modelling the effect of oxygen concentration on nitrite accumulation in a biofilm airlift suspension reactor. *Water Sci Technol* 36:147–156
19. Boltz JP, Morgenroth E, Sen D (2010) Mathematical modelling of biofilms and biofilm reactors for engineering design. *Water Sci Technol* 62:1821–1836
20. Kissel JC, McCarty PL, Street R (1984) Numerical simulation of mixed-culture biofilm. *J Environ Eng* 110:393–411
21. Wanner O, Gujer W (1984) Competition in biofilms. *Water Sci Technol* 17:27–44
22. Benefield L, Molz F (1985) Mathematical simulation of a biofilm process. *Biotechnol Bioeng* 27:921–931
23. Wanner O, Reichert P (1996) Mathematical Modeling of Mixed-Culture Biofilms. *Biotechnol Bioeng* 49:172–184
24. Picioreanu C, van Loosdrecht MCM, Heijnen JJ (1998) A new combined differential-discrete cellular automaton approach for biofilm modeling: application for growth in gel beads. *Biotechnol Bioeng* 57:718–731
25. Alpkvist E, Picioreanu C, van Loosdrecht MCM, Heyden A (2006) Three-dimensional biofilm model with individual cells and continuum eps matrix. *Biotechnol Bioeng* 94:961–979
26. Wang GTY, Bryers JD (1997) A dynamic model for receptor mediated specific adhesion of bacteria under uniform shear flow. *Biofouling* 11:227–252
27. Alpkvist E, Klapper I (2007) Description of Mechanical Response Including Detachment Using a novel Particle Model of Biofilm/Flow Interaction. *Water Sci Technol* 55:265–273
28. Böhl M, Möhle RB, Haesner M, Neu TR, Horn H, Krull R (2009) 3D finite element model of biofilm detachment using real biofilm structures from CLSM data. *Biotechnol Bioeng* 103:177–186
29. Chaudhry MAS, Beg SA (1998) A Review on the mathematical modeling of biofilm processes: advances in fundamentals of biofilm modeling. *Chem Eng Technol* 21:701–710
30. Wanner O, Eberl HJ, Morgenroth E, Noguera DR, Picioreanu C, Rittmann BE, van Loosdrecht MCM (2008) *Mathematical modeling of biofilms*, IWA Publishing
31. Picioreanu C, Xavier JB, van Loosdrecht MCM (2004) *Advances in mathematical modeling of biofilm structure*. *Biofilms* 1:1–12
32. Klapper I, Dockery J (2010) Mathematical description of microbial biofilms. *SIAM Rev* 52:221–265

33. Hall-Stoodley L, Costerton JW, Stoodley P (2004) Bacterial biofilms: from the Natural environment to infectious diseases. *Nat Rev Micro* 2:95–108
34. Wanner O, Gujer W (1986) A Multispecies biofilm model. *Biotechnol Bioeng* 28:314–328
35. Chen GH, Ozaki H, Terashima Y (1989) Modelling of the simultaneous removal of organic substances and Nitrogen in a biofilm. *Water Sci Technol* 21:791–804
36. Liehr SK, Suidan MT, Eheart JW (1989) Effect of concentration boundary layer on carbon limited algal biofilms. *J Environ Eng* 115:320–335
37. Suidan MT, Flora RV, Biswas P, Sayles GD (1996) Optimization modelling of anaerobic biofilm reactors. *Water Sci Technol* 30:347–355
38. Elberling B, Damgaard LR (2001) Microscale Measurement of oxygen diffusion and consumption in subaqueous sulfide tailings. *Geochim Cosmochim Acta* 65:1897–1905
39. Lorke A, Müller B, Maerki M, Wüest A (2003) Breathing sediments: the control of diffusive transport across the sediment–waterinterface by periodic boundary-layer turbulence. *Limnol Oceanogr* 48:2077–2085
40. Bungay HR, Whalen WJ, Sanders WM (1969) Microprobe techniques for determining diffusivities and respiration rates in microbial slime systems. *Biotechnologie and Bioengineering* XI:765–772
41. Zhang TC, Bishop PL (1994) Experimental determination of the dissolved oxygen boundary layer and mass transfer resistance near the fluid-biofilm interface. *Water Sci Technol* 30:47–58
42. Kühl M, Cohen YDT, Jørgensen BB, Revsbech NP (1995) Microenvironment and photosynthesis of zooxanthellae in scleractinian corals studied with microsensors for O<sub>2</sub>, pH and light. *Mar Ecol Prog Ser* 117:159–172
43. Wäsche S, Horn H, Hempel DC (2000) Mass transfer phenomena in biofilm systems. *Water Sci Technol* 41:357–360
44. Beyenal H, Lewandowski Z (2000) Combined effect of substrate concentration and flow velocity on effective diffusivity in biofilms. *Water Res* 34:528–538
45. Horn H (2003) Modellierung von Stoffumsatz und Stofftransport in Biofilmsystemen. FIT-Verlag, Paderbron
46. Gantzer CJ, Rittman BE, Herricks EE (1988) Mass transfer to streambed biofilms. *Water Res* 22:709–722
47. Brauer H (1971) Stoffaustausch einschließlich chemischer Reaktoren, Verlag Sauerländer Aarau
48. Hooijmans CM (1990) Diffusion coupled with bioconversion in immobilized systems: use of an oxygen microsensor, Promotionsschrift an der Uni Delft
49. Debus O (1993) Aerober Abbau von flüchtigen Abwasserinhaltsstoffen in Reaktoren mit membrangebundenem Biofilm. GFEU an der TUHH, Hamburg
50. Li S, Chen GH (1994) Modelling the organic removal and oxygen consumption by biofilms in an open-channel flow. *Water Sci Technol* 30:53–61
51. Christiansen P, Hollesen L, Harremoes P (1995) Liquid film diffusion on reaction rate in submerged biofilters. *Water Res* 29:947–952
52. Horn H, Hempel DC (1995) Mass transfer coefficients for an autotrophic and a heterotrophic biofilm system. *Water Sci Technol* 32:199–204
53. Wäsche S, Horn H, Hempel DC (2002) Influence of growth conditions on biofilm development and mass transfer at the bulk/biofilm interface. *Water Res* 36:4775–4784
54. Picioreanu C, van Loosdrecht MCM, Heijnen JJ (2000) A theoretical study on the effect of surface roughness on mass transport and transformation in biofilms. *Biotechnol Bioeng* 68:355–369
55. Williamson K, McCarty PL (1976) A Model of substrate utilization by Bacterial Films. *J Water Pollut Control* 48:9–24
56. LaMotta EJ (1976) Internal diffusion and reaction in biological films. *Environ Sci Technol* 10:765–769
57. Harremoes P (1976) The significance of pore diffusion to filter denitrification. *J Water Pollut Control Fed* 48:377–388

58. Harris NP, Hansford GS (1976) A study of substrate removal in a microbial film reactor. *Water Res* 10:935–943
59. Timmermans P, Van Haute A (1984) Influence of the type of organisms on the biomass hold-up in a fluidized-bed reactor. *Appl Microbiol Biotechnol* 19:36–43
60. van Loosdrecht MCM, Eikelboom D, Gjaltema A, Mulder A, Tjihuis L, Heijnen JJ (1995) Biofilm structures. *Water Sci Technol* 32:35–44
61. Stoodley P, Dodds I, Boyle JD, Lappin-Scott HM (1999) Influence of hydrodynamics and nutrients on biofilm structure. *J Appl Microbiol Symp Suppl* 85:19S–28S
62. Gujer W, Wanner O (1989) Modeling mixed population biofilms, In: Characklis WG, Marshall KC (eds) *Biofilms*, John Wiley & Sons, New York pp 397–445
63. Sanderson SS, Stewart PS (1997) Evidence of bacterial adaptation to Monochloramine in *Pseudomonas aeruginosa* biofilms and evaluation of biocide action model. *Biotechnol Bioeng* 56:201–209
64. Rittmann BE, Stilwell D, Ohashi A (2002) The transient-state, multiple-species biofilm model for biofiltration processes. *Water Res* 36:2342–2356
65. Hao X, Heijnen JJ, Van Loosdrecht MCM (2002) Sensitivity analysis of a biofilm model describing a one-stage completely autotrophic nitrogen removal (CANON) process. *Biotechnol Bioeng* 77:266–277
66. Wichern M, Lindenblatt C, Lübken M, Horn H (2008) Experimental results and mathematical modelling of an autotrophic and heterotrophic biofilm in a sand filter treating landfill leachate and municipal wastewater. *Water Res* 42:3899–3909
67. Fruhen M, Christan E, Gujer W, Wanner O (1991) Significance of Spatial Distribution of Microbial Species in Mixed Culture Biofilms. *Water Sci Technol* 23:1365–1374
68. Horn H, Hempel DC (1997) Growth and decay in an auto-/heterotrophic biofilm. *Water Res* 31:2243–2252
69. Matsumoto S, Terada A, Tsuneda S (2007) Modeling of membrane-aerated biofilm: Effects of C/N ratio, biofilm thickness and surface loading of oxygen on feasibility of simultaneous nitrification and denitrification. *Biochem Eng J* 37:98–107
70. Lackner S, Smets BF (2012) Effect of the kinetics of ammonium and nitrite oxidation on nitrification success or failure for different biofilm reactor geometries. *Biochem Eng J* 69:2123–2129
71. Lackner S, Terada A, Horn H, Henze M, Smets BF (2010) Nitrification performance in membrane-aerated biofilm reactors differs from conventional biofilm systems. *Water Res* 44:6073–6084
72. Henze M, Gujer W, Mino T, van Loosdrecht M (2000) *Activated sludge models ASM1, ASM2, ASM2d and ASM3*, IWA Publishing, London
73. Siegrist H, Gujer W (1985) Mass transfer mechanisms in a heterotrophic biofilm. *Water Res* 19:1369–1378
74. Fan LS, Leyva-Ramos R, Wisecarver KD, Zehner BJ (1990) Diffusion of phenol through a biofilm grown on activated carbon particles in a draft-tube three-phase fluidized-bed bioreactor. *Biotechnol Bioeng* 35:279–286
75. Horn H, Morgenroth E (2006) Transport of oxygen, sodium chloride, and sodium nitrate in biofilms. *Chem Sci Eng* 61:1347–1356
76. Reichert P (1994) *AQUASIM—Computer program for simulation and data analysis of aquatic systems*. Schriftenreihe der EAWAG, Dübendorf
77. Bernet N, Sanchez O, Cesbron D, Steyer JP, Delgenès JP (2005) Modeling and control of nitrite accumulation in a nitrifying biofilm reactor. *Biochem Eng J* 24:173–183
78. Julio Pérez J, Costa E, Kreft JU (2009) Conditions for partial nitrification in biofilm reactors and a kinetic explanation. *Biotechnol Bioeng* 103:282–295
79. Rauch W, Vanhooren H, Vanrolleghem P (1999) A simplified mixed-culture biofilm model. *Water Res* 33:2148–2162
80. Ni BJ, Chen YP, Liu SY, Fang F, Xie WM, Yu HQ (2009) Modeling a Granule-Based Anaerobic Ammonium Oxidizing (ANAMMOX) Process. *Biotechnol Bioeng* 103:490–499



81. Brockmann D, Rosenwinkel K-H, Morgenroth E (2006) Modelling deammonification in biofilm systems: Sensitivity and identifiability analysis as a basis for the design of experiments for parameter estimation. In: Marquardt W, Pantelides C, (eds) Computer Aided Chemical Engineering, Elsevier pp 221–226
82. Horn H, Neu TR, Wulkow M (2001) Modelling the structure and function of extracellularpolymeric substances in biofilms with new numerical techniques. *Water Sci Technol* 43:121–127
83. Lapidou C, Rittmann BE (2002) A Unified Theory for Extracellular polymeric Substances, Soluble Microbial Products, and Active and Inert Biomass. *Wat. Res.* 36:2711–2720
84. Wolf G, Picioreanu C, van Loosdrecht MCM (2007) Kinetic model of phototrophic biofilms —the PHOBIA model. *Biotechnol Bioeng* 97:1064–1079
85. Flora JRV, Suidan MT, Biswas P, Sayles GD (1995) Modeling algal biofilms: role of carbon, light, cell surface charge, and ionic species. *Water Environ Res* 67:87–94
86. Rauch W, Vanrolleghem PA (1998) Modelling benthic activity in shallow eutrophic rivers. *Water Sci Technol* 37:129–137
87. Rinas U, El-Enshasy H, Emmeler M, Hille A, Hempel DC, Horn H (2005) Model-based prediction of substrate conversion and protein synthesis and excretion in recombinant *Aspergillus niger* biopellets. *Chem Sci Eng* 60:2729–2739
88. Sakurai A, Imai H, Sakakibara M (1999) Citric acid production using biofilm of *aspergillus niger*. *Recent Res Dev Biotechnol Bioeng* 2:1–13
89. Tekerlekopoulou AG, Tsiflikiotou M, Akritidou L, Viennas A, Tsiamis G, Pavlou S, Bourtzis K, Vayenas DV (2013) Modelling of biological Cr(VI) removal in draw-fill reactors using microorganisms in suspended and attached growth systems. *Water Res* 47:623–636
90. Morgenroth E, Wilderer PA (2000) Influence of detachment mechanisms on competition in biofilms. *Water Res* 34:417–426
91. Horn H, Reiff H, Morgenroth E (2003) Simulation of growth and detachment in biofilm systems under defined hydrodynamic conditions. *Biotechnol Bioeng* 81:607–617
92. Stewart PS, McFeters GA, Huang CT (2000) Biofilm formation and persistence. In: Bryers JD, (ed) *Biofilms II: process analysis and application*, Wiley-Liss, Inc
93. Kreft JU, Wimpenny JWT (2001) Effect of EPS on biofilm structure and function as revealed by an individual-based model of biofilm growth. *Water Sci Technol* 43:135–141
94. Eberl HJ, Picioreanu C, Heijnen JJ, van Loosdrecht MCM (2000) A three-dimensional numerical study on the correlation of spatial structure, hydrodynamic conditions, and mass transfer and conversion in biofilms. *Chem Eng Sci* 55:6209–6222
95. Bryers JD (1984) Biofilm formation and chemostat dynamics: Pure and mixed culture considerations. *Biotechnol Bioeng* 26:948–958
96. Chang HT, Rittmann BE (1987) Mathematical modeling of biofilm on activated carbon. *Environ Sci Technol* 21:273–280
97. Kreikenbohm R, Stephan W (1985) Application of a two-compartment model to the wall growth of *Pelobacter acidigallici* under continuous culture conditions. *Biotechnol Bioeng* 27:296–301
98. Trulear MG, Characklis WG (1982) Dynamics of biofilm processes. *J WPCF* 54:1288–1301
99. Bakke R, Trulear MG, Robinson JA, Characklis WG (1984) Activity of *pseudomonas aeruginosa* in biofilms: steady stat. *Biotechnol Bioeng* 26:1418–1424
100. Rittman BE (1982) The effect of shear stress on biofilm loss rate. *Biotechnol Bioeng* 24:501–506
101. Peyton BM, Characklis WG (1993) A Statistical-analysis of the effect of substrate utilization and shear-stress on the kinetics of biofilm detachment. *Biotechnol Bioeng* 41:728–735
102. Morgenroth E, Wilderer PA (1999) Controlled biomass removal—the key parameter to achieve enhanced biological phosphorus removal in biofilm systems. *Water Sci Technol* 39:33–40
103. Speitel GE, DiGiano FA (1987) Biofilm shearing under dynamic conditions. *J Environ Eng —ASCE* 113:464–475

104. Rittmann BE (1989) Detachment from Biofilms, In: Characklis WG, Marshall KC (eds) *Biofilms*, John Wiley & Sons, New York pp 49–58
105. Peyton BM, Characklis WG (1992) Kinetics of biofilm detachment. *Water Sci Technol* 26:1995–1998
106. Robinson JA, Trulear MG, Characklis WG (1984) Cellular reproduction and extracellular polymer formation by *Pseudomonas aeruginosa* in continuous culture. *Biotechnol Bioeng* 26:1409–1417
107. Stewart PS (1993) A model of biofilm detachment. *Biotechnol Bioeng* 41:111–117
108. Morgenroth E, Wilderer PA (1998) Modeling the enhanced biological phosphorus removal in a sequencing batch biofilm reactor. *Water Sci Technol* 37:583–587
109. Nicolella C, Di Felice R, Rovatti M (1996) An experimental model of biofilm detachment in liquid fluidized bed biological reactors. *Biotechnol Bioeng* 51:713–719
110. Abbas F, Sudarsan R, Eberl HJ (2012) Longtime behavior of one-dimensional biofilm models with shear dependent detachment rates. *Math Biosci Eng* 9:215–239
111. Wimpenny JWT, Colasanti R (1997) A unifying hypothesis for the structure of microbial biofilms based on cellular automaton models. *FEMS Microbiol Ecol* 22:1–16
112. Hermanowicz SW (1999) Two-dimensional simulations of biofilm development: effects of external environmental conditions. *Water Sci Technol* 39:107–114
113. Picioreanu C, van Loosdrecht MCM, Heijnen JJ (1999) Discret-differential modelling of biofilm structure. *Water Sci Technol* 39:115–123
114. Picioreanu C, van Loosdrecht MCM, Heijnen JJ (2000) Effect of diffusive and convective substrate transport on biofilm structure formation: a two-dimensional modeling study. *Biotechnol Bioeng* 69:504–515
115. Dockery J, Klapper I (2001) Finger formation in biofilm layers. *Siam J Appl Math* 62:853–869
116. Eberl H, Parker D, van Loosdrecht M (2001) A new deterministic spatio-temporal continuum model for biofilm development. *Journal of Theoretical Medicine* 3:161–175
117. Picioreanu C, van Loosdrecht MCM, Heijnen JJ (2001) Two-dimensional model of biofilm detachment caused by internal stress from liquid flow. *Biotechnol Bioeng* 72:205–218
118. Chambless JD, Stewart PS (2007) A three-dimensional computer model analysis of three hypothetical biofilm detachment mechanisms. *Biotechnol Bioeng* 97:1573–1584
119. Kreft J-U, Picioreanu C, Wimpenny JWT, van Loosdrecht MCM (2001) Individual-based modelling of biofilms. *Microbiology* 147:2897–2912
120. Kreft JU (2004) Biofilms promote altruism. *Microbiology* 150:2751–2760
121. Picioreanu C, Kreft JU, van Loosdrecht MCM (2004) Particle-Based multidimensional multispecies biofilm model. *Appl Environ Microbiol* 70:3024–3040
122. Xavier JB, Picioreanu C, Van Loosdrecht MCM (2005) A framework for multidimensional modelling of activity and structure of multispecies biofilms. *Environ Microbiol* 7:1085–1103
123. Xavier JB, Picioreanu C, van Loosdrecht MCM (2005) A general description of detachment for multidimensional modelling of biofilms. *Biotechnol Bioeng* 6:651–669
124. Picioreanu C, Head IM, Katuri KP, van Loosdrecht MCM, Scott K (2007) A computational model for biofilm-based microbial fuel cells. *Water Res* 41:2921–2940
125. von der Schulenburg DAG, Pintelon TRR, Picioreanu C, Van Loosdrecht MCM, Johns ML (2009) Three-dimensional simulations of biofilm growth in porous media. *AIChE J* 55:494–504
126. Radu AI, Picioreanu C, Vrouwenvelder JS, van Loosdrecht MCM (2010) Modeling the effect of biofilm formation on reverse osmosis performance: flux, feed channel pressure drop and solute passage. *J Membr Sci* 365:1–15
127. Lardon LA, Merkey BV, Martins S, Dötsch A, Picioreanu C, Kreft J-U, Smets BF (2011) iDynoMiCS: next-generation individual-based modelling of biofilms. *Environ Microbiol* 13:2416–2434
128. Möhle R (2008) An Analytic-synthetic approach combining mathematical modeling and experiments—towards an understanding of biofilm systems. Institute of Biochemical Engineering Technische Universität Braunschweig, Braunschweig

129. Böl M, Ehret AE, Albero AB, Hellriegel J, Rainer Krull R (2013) Recent advances in mechanical characterisation of biofilm and their significance for material modelling. *Crit Rev Biotechnol* 33:145–171
130. Guelon T, Mathias JD, Stoodley P (2011) *Advances in Biofilm Mechanics*. Springer, Berlin
131. Klapper I, Dockery J (2006) Role of cohesion in the material description of biofilms. *Phys Rev E* 74:031902
132. Cogan NG (2008) Two-fluid model of biofilm disinfection. *Bull Math Biol* 70:800–819
133. Taherzadeh D (2011) *Mechanics and Substrate Transport of Moving Biofilm Structures*. Technische Universität München, Munich, Institute of Water Quality Control
134. Duddu R, Chopp DL, Moran B (2009) A two-dimensional continuum model of biofilm growth incorporating fluid flow and shear stress based detachment. *Biotechnol Bioeng* 103:92–104
135. Limbert G, Bryan R, Cotton R, Young P, Hall-Stoodley L, Kathju S, Stoodley P (2013) On the mechanics of bacterial biofilms on non-dissolvable surgical sutures: a laser scanning confocal microscopy-based finite element study. *Acta Biomater* 9:6641–6652
136. Taherzadeh D, Picioreanu C, Küttler U, Simone A, Wall WA, Horn H (2010) Computational study of the drag and oscillatory movement of biofilm streamers in fast flows. *Biotechnol Bioeng* 105:600–610
137. Taherzadeh D, Picioreanu C, Horn H (2012) Mass transfer enhancement in moving biofilm structures. *Biophys J* 102:1483–1492
138. Morgenroth E, van Loosdrecht MCM, Wanner O (2000) Biofilm models for the practitioner. *Water Sci Technol* 41:509–512
139. Brockmann D, Horn H, Alex J, Beier M, Morgenroth E, Ochmann C, Sørensen K, Wanner O, Wichern M (2008) Simulation of Nitrification in a Full-scale Biofilter—Comparison of Different Approaches. *IWA Biofilm Technologies*, pp 229–231, IWA, Singapore
140. Boltz JP, Morgenroth E, Brockmann D, Bott C, Gellner WJ, Vanrolleghem PA (2011) Systematic evaluation of biofilm models for engineering practice: components and critical assumptions. *Water Sci Technol* 64:930–944
141. Picioreanu C, Vrouwenvelder JS, Kruihof JC, van Loosdrecht MCM (2010) Biofouling in spiral wound membrane systems: Three-dimensional CFD model based evaluation of experimental data. *J Membr Sci* 346:71–85

# Biofilm Architecture

Jochen J. Schuster and Gerard H. Markx

**Abstract** Microbial biofilms are complex self-organized communities of microbial cells that provide protective environments for the cells that inhabit the biofilm, enabling them to respond efficiently to challenges. The enhanced resistance and altered metabolism of the cells in the biofilm makes biofilms potentially very useful in chemical production processes, including the production of pharmaceuticals and biofuels. Synthetic biofilms in which the composition and architecture of the biofilm is controlled by the designer could help in harnessing this potential. In this chapter we discuss biofilm architecture, how it can be created by natural or artificial means, and how it affects biofilm function.

**Keywords** Architecture · Biocatalysis · Biofilm · Microenvironment · Synthetic

## Contents

1	Introduction.....	78
2	Architecture of Naturally Formed Biofilms.....	79
	2.1 Biofilm Architecture and Resistance.....	82
	2.2 Biofilm Architecture and Metabolism.....	83
3	Artificial Biofilms.....	84
	3.1 Construction of Artificial Biofilms with Well-Defined Architectures.....	84
	3.2 What Happens with the Architecture of Synthetic Biofilms over Time?.....	89
4	Outlook.....	91
	References.....	92

---

J. J. Schuster · G. H. Markx (✉)

Microstructures and Microenvironments Research Group, Institute of Biological Chemistry,  
Biophysics and Bioengineering, Heriot-Watt University, Riccarton,

Edinburgh EH14 4AS, UK

e-mail: g.h.markx@hw.ac.uk

## 1 Introduction

It has been recognized for many years that microorganisms in natural ecosystems do not usually live as single suspended (planktonic) cells, but instead mainly live in communities attached to surfaces or each other. The interest in such communities—commonly referred to as biofilms (if associated with a phase boundary such as a liquid–solid surface) or flocs (if suspended) [1]—has increased exponentially over the last three decades, not only because of the relevance of such systems in nature, for example, in biomineralization processes, but also because such communities are also important in many man-made systems.

The presence of biofilms can lead to problems in areas where biofilms are not supposed to occur. For example, biofilms can cause large problems in the maintenance of human health. A good example is biofilm on teeth, known as dental plaque [2], which can lead to tooth decay. Another is biofilm that develops on medical devices such as intravascular and urinary catheters, or orthopedic implants that can lead to the infection of the patients [3]. Other examples of areas in which biofilms can lead to problems are food, chemical, or power plants or other pipeline networks. The growth of microorganisms inside pipelines or on other surfaces exposed to a flowing medium is generally known as biofouling, and decreases the process efficiency by lowering mass transfers, increasing friction, and reducing heat transfer [4]; also product quality can be adversely affected, for example, in food or pharmaceutical production. Biofilms also play a role in corrosion, and can be a source of pathogens in water supplies [5]. The presence of biofilms and the difficulty of removing them lead to increased running and maintenance costs.

On the other hand biofilms can also be useful. Biofilms are already extensively used in wastewater treatment [6] and play roles in the production of biofuels, such as methane production by methanogenesis [7–9]. Biofilms are used in food production (e.g., for the production of vinegar), and biofilms are also potentially useful in biocatalysis [10].

One of the reasons for the high scientific interest in these communities is the fact that when a biofilm is formed the microorganism assembly has different properties compared to planktonic cells. These include an enhanced persistence and resistance to environmental threats such as antimicrobial agents, toxic substances, thermal stress, predation, oxidative stress, UV light, and so on [5, 11]. Also the metabolic activities of microbial cells can show significant differences compared to suspension cultures of the same cells. Understanding what causes these differences can not only help one to combat biofilms where they pose a problem, but harnessing the ability of microbial cells in biofilm to withstand the often harsh and toxic environment in bioreactors [7, 12] and efficiently metabolize substrates within the biofilm environment could be of significant utility in biocatalysis [12–14].

Although small but significant differences have been found in the geno- and phenotype of the microbial cells that are in biofilms compared to planktonic cells, such differences are not sufficient to explain the apparently anomalous resistance

and metabolic activity in biofilms, and other factors are thought to play a role. A major factor is thought to be the architecture of the biofilm. In this chapter we explore biofilm architecture, how it is created, what roles it plays in biofilm activity, and how altering biofilm architecture by artificial means could potentially be used to advantage.

## 2 Architecture of Naturally Formed Biofilms

Early models of naturally occurring biofilms considered them to be relatively homogeneous structures consisting of a gel matrix of extracellular polymeric substances (EPS) with microbes evenly embedded within. The development of advanced imaging techniques such as confocal laser scanning microscopy (CLSM), which allows the 3-dimensional (3D) structure of biofilms to be imaged [15] have since shown that many biofilms are indeed relatively simple, and are relatively flat and compact structures that covered all the surface available [16, 17]. However, other biofilms have been shown to be more complex, with structures ranging from patchy clumps to elaborate morphological structures such as pillars or mushroom shapes with water channels in between for the exchange of materials within the biofilm and with the surroundings [16, 18, 19]. The developmental processes that lead to the formation of such structures have intrigued many scientists [20, 21] and as a result have been studied intensively, aided by advanced staining and tagging techniques that allow cells to be identified and followed during biofilm development, and changes in their physiology identified [14, 15, 22].

A five-stage process model has been suggested for the development of biofilms [23]. The stages involved were (i) the initial attachment of cells to the surface, (ii) irreversible attachment of the cells, (iii) early development of biofilm architecture, (iv) maturation of biofilm, and (v) the dispersion of single cells from the biofilm. Attachment of the cells to the surface during the first stages is thought to lead to physiological changes of the cells and be accompanied by the production of EPS which functions as a glue, fixing the cells to the surface. The EPS is a hydrogel that consists mainly of polysaccharides, proteins, and nucleic acids, and gives the biofilm most of its mechanical strength [24, 25]. After the initial attachment process the cells divide and form microcolonies. During the maturation process the cells continue dividing and produce more EPS. At this stage the biofilm can extend from the surface, building a 3D structure. After maturation, cells may leave the biofilm to colonize new regions [23].

The structure of the biofilm that is formed changes over time and is determined by many factors. They include the properties of the surface and the initial distribution of the cells over the surface, the organisms that form the biofilm, the transcription of their genes, and the interaction between the cells, as well as the physical and chemical properties of the external environment. Significant detachment of cells occurs, and also cells from the suspending medium attach

themselves to the biofilm. The interplay between all these factors is complex, and comparable to developmental processes seen in multicellular organisms [26, 27].

Comparison of different biofilms formed by different organisms and strains typically shows that many, if not the majority of, biofilms are very simple structures, either flat and featureless, or consisting of simple aggregates [17]. Such biofilms can be envisaged to have been formed by random growth processes or simple chaotic aggregation processes [1, 28]. However, even in such simple systems different microenvironments can be found. The presence of EPS limits convective mass transfer of nutrients from the medium to the cells or of metabolic substrates, products, and intermediates, so that diffusion is the only mechanism for transferring nutrients and chemicals in a biofilm [22, 29]. This leads to chemical gradients and niches in the biofilm that are rather more suitable for one cell type than for another. A typical example is the fact that cells at the surface of a biofilm have direct access to the fresh medium, whereas those deeper in the biofilm or aggregate do not. As a consequence, cells may grow better in one place or change position and move to that region where they can find better environmental conditions if given the opportunity. Because environment and cell metabolism are strongly linked to each other the cells will adapt to their new microenvironment by altering their metabolic activities, which in turn affects the chemical gradients [30]. These simple mechanisms will result in a heterogeneous distribution of cells and species, on top of the biological heterogeneity that already exists in the biofilm due to genetic variation and stochastic gene expression [22, 30].

More complex structures such as pillars and mushroom shapes can be formed by certain organisms only under certain environmental conditions. For example, *Pseudomonas aeruginosa* makes featureless biofilms when grown under low-flow conditions in succinate, but mushroom shapes when grown in 1 % tryptic soy broth [16]. To form such mushroom shapes and other complex structures the bacteria must cooperate to build the structure, and also differentiate to form the stalk and the head of the mushroom. The existence of social behavior in what are essentially individual units, and the decision processes involved in selfish versus altruistic behavior in itself is a fascinating area of research [31, 32]. One of the mechanisms by which microorganisms coordinate their action is the quorum sensing (QS) system [33–37]. Quorum sensing involves the production of extra-cellular chemical signals by the cells that act on the cells themselves and their neighbors if they have suitable receptors. If the local concentration of communication molecules reaches a critical concentration, gene expression in the cells is altered in the receptive cells, enabling all cells experiencing the same concentration to coordinate their gene expression and subsequent action.

A variety of QS systems has been found, but in *Pseudomonas aeruginosa* and other proteobacteria it has been found to involve mainly acylhomoserine lactones (AHL). Two AHL-based signaling systems are thought to be in *P. aeruginosa*, controlling 4–6 % of the *P. aeruginosa* genes. They in particular affect rhamnolipid production, which is involved in keeping the waterchannels between structures open, and EPS production [36]. What actually constitutes a “quorum” in the context of a biofilm and what its purpose is has been the subject of some debate

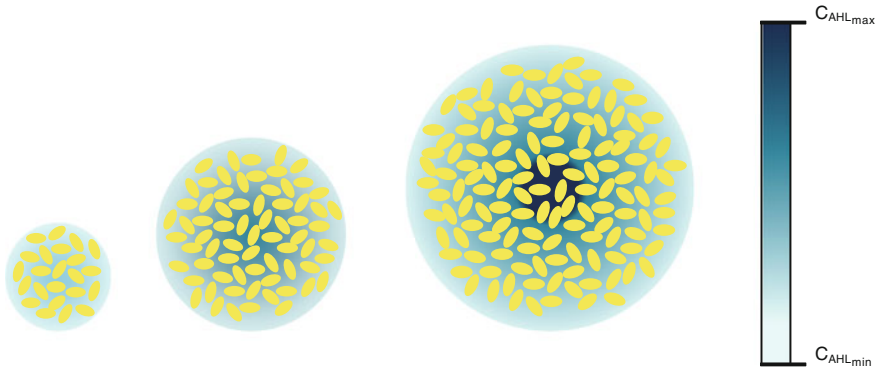


**Fig. 1** Accumulation of QS molecules in particles of different sizes. In larger structures higher QS molecule concentrations will be reached

[37, 38]. Because of the high cell density and the tendency for products to accumulate, biofilms are particularly suited for signaling through QS. Accumulation will depend on the thickness of the biofilm and the structures that form it (see also Fig. 1) in addition to any reactions or absorption processes that occur which may remove QS molecules from the pool, as well as the structures surrounding QS-producing cells [35].

The social behavior of *P. aeruginosa* and other biofilm-forming bacteria allows them to thrive in a variety of environmental conditions by changing the biofilm structure according to external conditions. Structure formation is highly affected by the carbon source and concentration [16, 39, 40]; structuring the biofilm can increase the surface area, making it easier for the exchange of nutrients and cells with the medium during carbon limitation [40].

Strong interactions have been demonstrated between surface motility, QS, and the formation of structures in biofilms [16]. For example, the mushroom structures in *P. aeruginosa* have been shown to be formed by nonmotile cells forming the stalks, and motile cells forming the head. Surface structures such as pili and flagella play an important role in cell surface motility. The interplay between motility and QS may arguably also explain why microorganisms that form complex structures through a coordinated QS response are so successful. Such microorganisms can not only more effectively respond to fluctuating environmental conditions by changing the biofilm structure, but they also would spread more easily and compete more effectively with other organisms by overwhelming competitors through coordinated actions and movements.

Hydrodynamic conditions in the system in which the biofilm is formed also strongly affect structure formation in biofilms [23, 41, 42]. Under dynamic flow conditions the biofilms formed are often flat and compact, without rising structures [43]. Too high a flow rate can lead to patchy biofilms. With the right balance, smooth and stable biofilms can be obtained. Kwon et al. [44] have argued that the balance of detachment forces and biofilm surface loading is needed. When



detachment forces are relatively high only a patchy biofilm will develop, whereas at low detachment forces the biofilm becomes highly heterogeneous with many pores and protuberances to increase the transfer of substrate (and removal of products). QS may play a role in this, as flow has been shown to affect mass transfer of the molecules involved in QS, influencing the onset of the QS response [45].

## ***2.1 Biofilm Architecture and Resistance***

Cells in biofilms are much more resistant than planktonic cells to challenges such as toxic chemicals and antibiotics. There are many reasons for this [46], and we only discuss a limited number. One of these reasons is that it may be more difficult for toxic chemicals to penetrate the biofilm. For example, large amounts of EPS are present in the biofilms. The presence of EPS in biofilms causes transport within the biofilms to be primarily through diffusion, which is a much slower transport process than convective transport. However, unless the molecules are very large and get enmeshed in the chains of macromolecules forming the gel, or actually bind to the macromolecules, the diffusion rates of compounds within the EPS will be similar in magnitude as in pure water. Cells can form a barrier, but only if present in very high densities. Thus, the formation of a biofilm by cells will retard the penetration of cytotoxic compounds, but not prevent it. Other mechanisms will have to play a role as well.

One mechanism by which biofilms may be more resistant is through the presence within the biofilm of persister cells [47]. One feature of biofilms is the large variety of the microenvironments that are available for the cells. Some of these will be better for the cells, and some worse. Adverse conditions will cause some of the cells to have lower activities. Also some may switch on defense mechanisms that enable them to survive adverse conditions. Often these involve dormant or similar states that again make the cells switch to a state of no or very low activity, and take on forms that are more resistant (thicker cell walls, etc.). If a biofilm is challenged by a toxic compound or an antibiotic, active cells will be killed, but the cells that have a more resistant physiology or are inactive will be able sit out the environmental challenge.

Another mechanism by which biofilms may be more resistant to environmental stresses is simply through strength in numbers. For example, a single planktonic cell may contain catalase to destroy hydrogen peroxide, but if challenged the degradation capability of the single cell will simply not be enough, and the cell will be overwhelmed [48]. If the cells, however, are assembled in a biofilm or aggregate then the amount of catalase available in an individual cell may be small, but the total amount may be sufficient to degrade the  $H_2O_2$  before it kills all the cells.

Many biofilms contain many different organisms with different metabolic activities. The metabolic activities of some of the cells in a consortium may help in protecting the others, such as the preceding example of cells with catalase; the

presence of catalase producers will protect noncatalase-producing cells from  $H_2O_2$ . Similar effects have been repeatedly reported, for example, protection of anaerobes by aerobes from oxygen [49], of strains sensitive to Hg ions by Hg-reducing strains [50], and of pentachlorophenol-sensitive cells by pentachlorophenol-degrading strains [51].

## 2.2 *Biofilm Architecture and Metabolism*

There are many advantages from a metabolic point of view of being in a biofilm. These include the proximity of the substrate if the substrate is a solid; proximity of other organisms, making it possible to obtain high concentrations of any enzymes that are used to dissolve the substrate; direct and fast exchange of metabolites between cells; the ability to use an extended range of concentrations of nutrients; the ability to destroy inhibitors, and the ability to keep the concentration of intermediate products at low concentrations, and thereby allow reactions to proceed despite unfavorable thermodynamic conditions.

The metabolic efficiency that is achieved in natural biofilms formed by microorganisms is the result of the cells employing physiological cooperation comparable to that in the tissues of multicellular organisms [26, 52]. Microorganisms, however, can grow under a larger range of environmental conditions (higher temperature, anoxic conditions etc.) than multicellular higher organisms. The metabolic potential of microorganisms is also much higher, being able to consume a much larger range of substrates.

Syntrophic degradation allows consortia to utilize a much larger range of nutrient sources than species on their own, including minerals and recalcitrant organic materials such as organochlorides and lignocellulosic substrates [53, 54]. The ability of natural consortia can be augmented by the addition of species introducing new metabolic capabilities. For example, anaerobic granules can be augmented by adding *Desulfitobacterium frappieri* that can degrade pentachlorophenol [51], thus protecting the biofilm against this toxic compound and expanding the metabolic capacity of the biofilm.

A typical example of a reaction that can proceed in biofilms that can proceed despite unfavorable thermodynamics can be found during methanogenesis [55]. During these processes biofilms and aggregates are formed with very well-defined structures, containing a specific organism in a specific location. Typical examples are shown in Fig. 2. The order in which the cells are layered is determined by the order in which the substrate is consumed, which ensures that the outermost cells have direct access to fresh nutrients from the medium, and the cells in the more inward layers have access to the products made by the more outward layers. During methanogenesis the layered structure helps to keep the hydrogen concentration low as the intermediate product  $H_2$  acts as an inhibitor. Channels are formed in the biofilms/aggregates to aid the removal of gaseous products. Layered structures are mainly formed at high nutrient concentrations; at lower

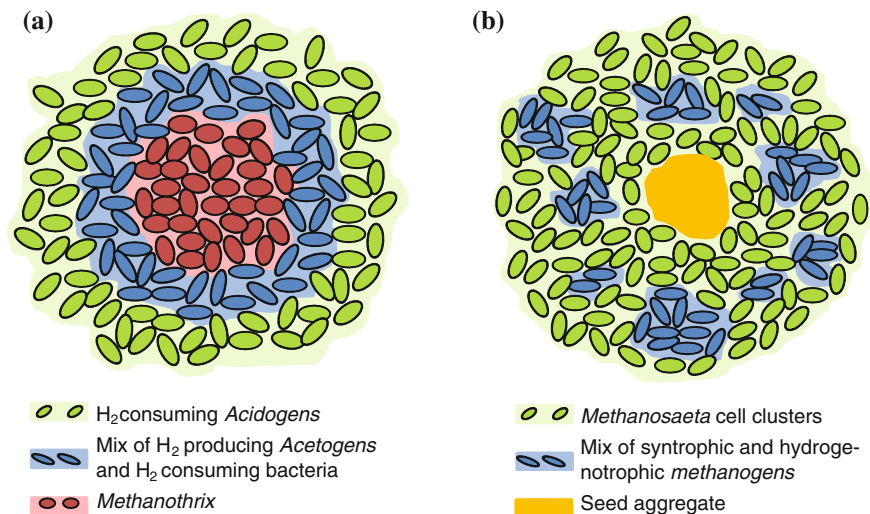


**Fig. 2** Structure of spontaneously formed consortia found in wastewater treatment plants. **a** Methanogenic aggregates formed at high concentrations of the carbon source. **b** Clustered aggregates formed at low concentrations [55, 58]. Spontaneous organization is also common in films and aggregates formed during (de)nitrification [59]

concentrations a clustered structure is more beneficial as the surface area for transfer to the clustered cells is increased. Similar effects have been found in synthetic biofilms. For example, Brenner and Arnold [56] showed a synthetic biofilm of two strains of *E. coli*, in which one was self-sufficient but the other was dependent on lysine or diaminopimelate produced by the other cells. Similarly (although complicated by the oxygen dependency of the cells) in biofilms of the syntrophic consortium of *Acinetobacter* and *Pseudomonas* fed on benzylalcohol, in which *Pseudomonas* fed on the benzoic acid produced by *Pseudomonas*, *Pseudomonas* formed clumps on *Acinetobacter* [57].

### 3 Artificial Biofilms

#### 3.1 Construction of Artificial Biofilms with Well-Defined Architectures

In recent years there has been an increasing interest in the construction of synthetic/artificial biofilms with well-defined architectures. Much of this has been driven by the emergence and increasing emphasis on synthetic biology, which aims to design and fabricate biological components and systems that do not already exist in the natural world, and redesign and fabricate existing biological systems. The assembly of multicellular systems (biofilms) from smaller

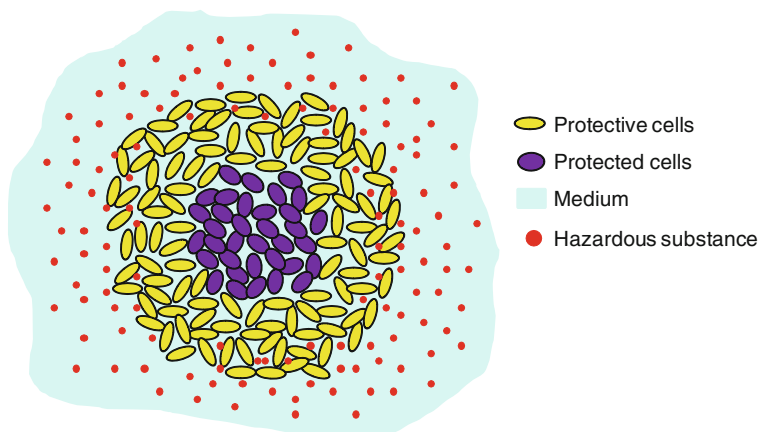


**Fig. 3** Example of a system with a well-defined architecture that could be built to enhance bioproduction. The cells in the outer layer have the ability to remove a chemical that is harmful to the cells in the core

components (microbial cells) falls under this topic. Proposed possible applications have been wide, ranging from bioprocessing, including biocatalysis for the production of biopharmaceuticals and fine chemicals and bioremediation [12, 14], biofuel production [54], mineral processing [53], and electricity generation [60] to information processing/biological computing [61]. Other proposed applications have included enhanced crop production [62], and the culture of currently unculturable microorganisms [63].

Most proposed applications of biofilms have been related to bioprocessing, and used consortia. However, the greatest majority of current bioprocesses are based on the use of a single clone, in submerged culture, and not consortia. Apart from the water industries, where extensive use is made of (ill-defined) consortia for water purification and wastewater treatment, the use of consortia is rare, and synthetic consortia even rarer, although some have been reported [13].

Figure 3 shows an example of a synthetic biofilm (floc) with an artificial architecture that could be built for enhanced bioproduction. The cells in the outer layer could, for example, be species that degrade toxins to which the cell in the center is sensitive. In a similar way, layered biofilms could be constructed with microbes in the periphery that remove oxygen before it reaches oxygen-sensitive obligate anaerobes in deeper layers. Also, syntrophic consortia could be built in which different microbes perform different steps in a production process. It is important to make sure that the cells in the biofilm consortia cooperate to mutual benefit, and do not compete. This will be difficult, as microbes tend not to cooperate, but instead to compete [64]. As discussed by Zuroff and Curtis [54], it is also important to minimize the number of steps in a process to the minimum, as additional steps become energetically more difficult to perform.

Various methods have or could be used to construct synthetic biofilms. Approaches for the construction of synthetic biofilms can arguably be divided into (a) self-assembly and (b) directed assembly.

Self-assembly of biofilms makes use of genetic algorithms already in the cells, or genetic algorithms introduced into the cells by genetic engineering. Examples of the use of already existing algorithms could include the self-organization of wild-type microorganisms into patterns under specific environmental conditions that do not occur in nature, or the formation of structured biofilms by microorganisms that do not normally occur together. Control over the architecture of such biofilms is currently very difficult because of the limited knowledge we have about the mechanisms that lead to pattern formation; also it will be very species- or even strain-specific. A number of recent papers have described the self-assembly of microorganisms in patterns after their genetic manipulation, often of QS systems [56, 61, 65–67] and their removal [68]. Currently these experiments are still mainly in the proof-of-principle stage and often aimed at the development and validation of models of biological computing, but the results are very promising.

In directed assembly the cells are directed to predefined locations. Immobilization of the cells is an essential part of the process, and the viability of the cells has to be maintained. The propelling force moving the cells can either be biological and come from the cells themselves, or be chemical or physical and be external.

Examples of biological forms of directed assembly include the use of chemo- or galvanotaxis to attract cells to certain regions. This method will be very species- or even strain-dependent, as not all cells will show this kind of behavior.

More generally applicable, as they can be used for most cell types, are physical or chemical methods of biofilm assembly. The simplest way to construct a biofilm involves directing a flow of cells at a membrane or a substrate surface [1, 14]. The biofilm thickness can be controlled by controlling the number of cells collected; the cells still need to be immobilized afterwards, either by the introduction of immobilizing agents or allowing the cells to produce EPS and attach themselves. For example, Stubblefield et al. [69] used a flow chamber in which the biofilm growth on a substrate was obtained by recirculating a well-defined cell suspension through this chamber until the biofilm was developed. By inserting sequentially additional types of microorganisms different horizontal layers could be achieved. The thickness and layering of biofilms can be controlled and the viability of cells is very high, but the secretion of the EPS and the biofilm development require a long time. To overcome this, Flickinger et al. [70] used nanoporous latex coatings to build artificial biofilms layer by layer. It was claimed the (initial) thickness of the biofilm and the composition of its layers could be well controlled. Tsoligkas et al. [71] described the use of spincoating to create engineered biofilms of *E. coli*. The adhesive strength of the engineered biofilm was reported to be much higher than that of naturally formed biofilms.

The previously described examples showed methods that can be used to obtain artificial biofilms, but apart from layering, the methods provide little control over the patterning at microscale. Other methods are needed to achieve this. One

approach to pattern microbes at microscale is to modify the substrate surface to facilitate cell attachment at specific areas [41, 72]. The cells can initially be distributed randomly but they will be able to fix only to certain positions on the surface. An example is the work by Zhao et al. [41] who demonstrated successful surface modification by the creation of adhesive and nonadhesive areas using scanning probe lithography and the soft lithography technique of microcontact printing patterns ( $\mu$ CP) of self-assembled monolayers. A disadvantage of this method is that once the available surface has been fully occupied by cells no further cells can be attached to that surface. The initial cell layer is therefore necessarily only one cell thick, and increased thickness can only be achieved by growing the cells or adding other cells through other methods.

Another approach is to suspend cells in a photosensitive gel precursor solution, and then confine light to specific areas/volumes in the gel, for example, through a mask [73]. Gel, and hence biofilm, will only be formed in those areas exposed to light. By repeatedly introducing different cell types and using different masks, or moving the existing mask, different cells can be immobilized in different areas.

A complementary approach to these techniques involves making sure there is a nonrandom distribution of cells, and then fixing them. Several approaches could be used, including the use of flow-based methods (e.g., microchannels, inkjets) and physical forces.

The use of inkjets for assembling synthetic biofilms is probably one of the best methods for constructing artificial biofilms with well-defined patterns of cells [72, 74, 75]. The method can achieve high-resolution patterns of different cell types in 3 dimensions while maintaining cell viability. A gel matrix is usually included to immobilize the cells.

Examples of other flow-based methods for constructing biofilms include the use of soft lithographic techniques to create PDMS rubber stamps to create microfluidic channels on a surface to introduce cells locally. Once the cells have been immobilized, for example, in a gel, the stamp can be removed and other cells introduced [76].

Another interesting method that has recently been described [77] for the construction of artificial biofilms with well-defined patterns of cells is based on the use of two aqueous phase systems. The method involves dispersing cells in one of the phases, and making a pattern of droplets on a surface that is submerged in the other phase using a pipette. Nutrients can still diffuse across the interface of the two phases, enabling the cells to self-immobilize and form a biofilm without the use of additional immobilizing agents.

A 7-barrelled micropipette was recently used to extrude a tubular synthetic biofilm with an outer layer containing a microorganism (*Ralstonia metallidurans*) that could reduce Hg(II), shielding a Hg(II)-sensitive species (*Sphingobium chlorophenicum*) that could degrade pentachlorophenol in the core. No chlorophenol degradation was obtained if the cells were simply mixed and there was no spatial structure, proving that the shell–core structure was essential for the protective effect to occur.

Physical forces that can be used to pattern cells and construct synthetic biofilms include ultrasound and optical and electrical forces [27].

Ultrasound can be used to trap single cells and manipulate their position on a surface [78] or many cells simultaneously [79–81] by producing patterns of interfering standing waves. Manipulation with ultrasound can be done directly in the growth medium. Ultrasound has a relatively long working distance. It could be used to make patterned biofilms, but its resolution is usually quite poor (typically tens of microns), small particles such as bacteria are difficult to handle, and only relatively simple patterns can be achieved (lines, spots in square or hexagonal patterns, etc.).

A broader range of manipulation options can be achieved with optical tweezers. Optical tweezers use the gradient in optical density near a focal point in a laser beam to induce a force in a particle (e.g., a cell) to trap it. The cell will follow movement of the focal point in any dimension. Typically near-infrared (NIR) beams are used to reduce heating of the particles. The method allows orientation of cells and works well in most growth media, and its resolution is very good (submicron). The magnitude of the force depends on laser power. The work of Haruff et al. [82], who could create multiple laser beams by splitting up one laser beam to create various constellations of the laser spots is interesting. Utilizing this, several cells can be handled simultaneously. This allows the user of the laser beam to place many cells simultaneously at defined points on a substrate.

Most interesting for the construction of biofilms with well-defined architectures, and relatively well-established, are techniques based on the use of electric fields. Both direct current (DC) [83] and alternating current (AC) techniques [35, 84–88] are proven technologies for the construction of artificial biofilms. Most advanced among the different ways to pattern cells with electric fields is an AC technique called dielectrophoresis (DEP). The term dielectrophoresis describes the movement of polarizable particles exposed to a nonuniform electric field. If the particle (e.g., a cell) is more polarizable than the surrounding medium, then a positive force is exerted on the particle and moves it to regions with higher field strengths; if the opposite is true it moves away from high field regions. Medium polarizability can be changed by the conductivity of the medium and therefore by removing or adding salt the dielectrophoretic behavior of the cells can be altered. This, however, leads to a need to keep the medium conductivity within certain limits, which are usually much lower than that in growth medium. The polarizability of cells is highly frequency-dependent, and the choice of the right frequency is important. For example, to attract cells to high electric field regions by positive DEP it is best not to stray too far from a frequency of 1 MHz.

Quite high electric field strengths on the order of  $2 \times 10^5$  V/m are needed to induce DEP, and for most experiments microelectrodes and voltages of 0–20 V peak-to-peak are used to generate the electric field strengths needed. This limits the range over which DEP forces can be generated to a few tens of microns, a few 100 microns max. The distribution of the areas of highest and lowest electric field strength in a given electrode geometry are easily predicted, and cells can be reliably deposited by DEP in well-defined areas in a microelectrode array. The

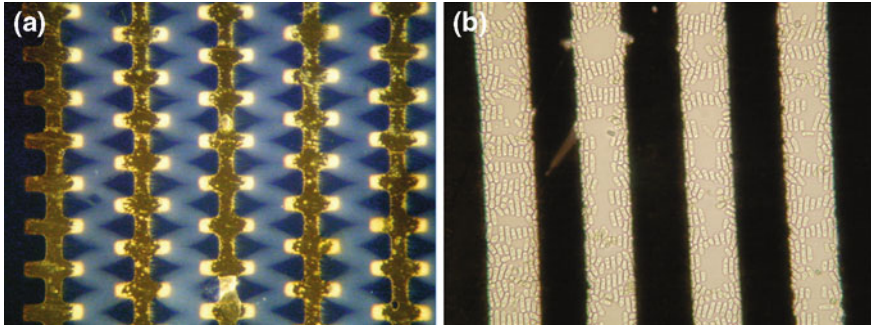


**Fig. 4** Synthetic biofilms made with AC electric fields. **a** Aggregates of *E. coli* cells formed with DEP at interdigitated alternately castellated electrodes giving a W-pattern between the microelectrodes. **b** *Schizosaccharomyces pombe* cells aligned by an electric field

electric field extends in three dimensions, and by changing the electrode size and shape, the size and shape of the aggregates can be changed. Also, by activating the electrodes in various sequences different cell types can be placed beside or in layers on top of each other [27, 35, 63, 84, 87]. By controlling the voltage, concentration, and timing it is possible to control the thickness of the cell deposition. The construction of biofilms over large areas is possible [88]. Orientation of the cells is possible [85]; also see Fig. 4.

### 3.2 What Happens with the Architecture of Synthetic Biofilms over Time?

After a synthetic biofilm has been created one has limited control over what happens with the architecture that has been built. The cells forming the biofilm are living organisms and thus will grow, replicate, and die; they may also move, and produce or degrade EPS [22]. All this will affect the architecture that was built. What actually happens depends on many factors, including the method by which it was formed and its composition.

In biofilms that self-assemble into a specific spatial structure this circumstance is less of an issue. However, even then biofilm architecture may change, and different architectures may be formed over time. For example, in the synthetic biofilm described by Brenner and Arnold [56] in which two interdependent yellow and blue *E. coli* strains together formed a biofilm, in the early stages of biofilm formation the yellow strain was dispersed inside the other (blue) strain. As the biofilm matured a layered structure was formed with the yellow strain covering the blue strain. Similar results have been seen in synthetic biofilms of *Acinetobacter* and *Pseudomonas* [57].

In biofilms in which the biofilm architecture has not been formed by self-organization of the cells, but instead has been assembled from component parts,



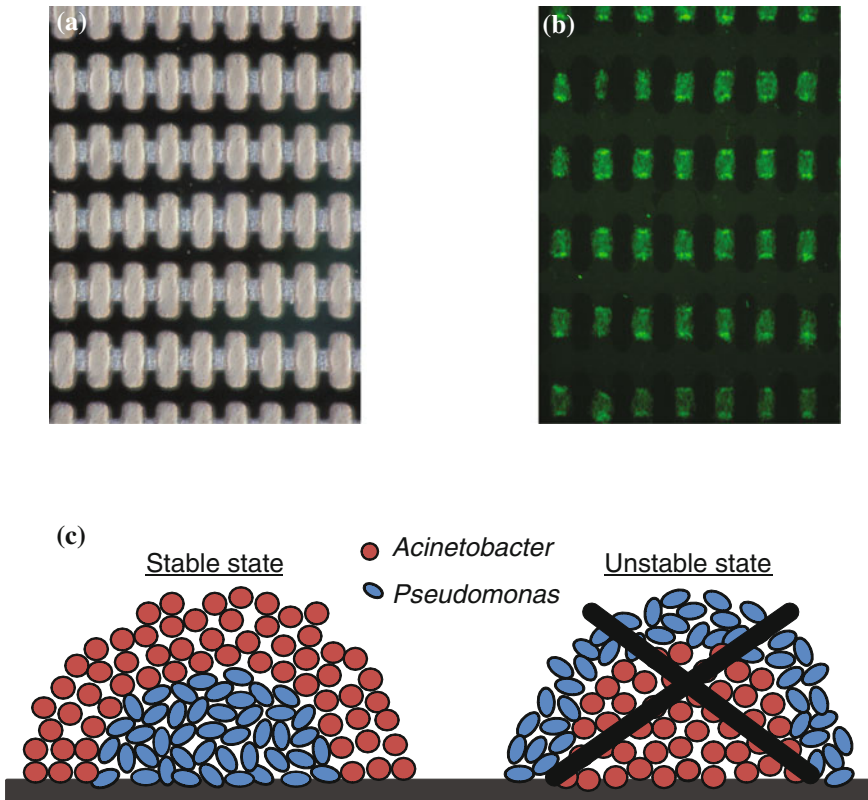


**Fig. 5** **a** Synthetic aggregates of *Pseudomonas putida* and *Acinetobacter* made with DEP (*Acinetobacter* on top of *Pseudomonas*). Aggregate size is approx  $30 \times 50$  microns. **b** Fluorescent image of the aggregates in a medium with benzylalcohol. *Pseudomonas* was genetically modified to produce GFP in the presence of benzoate, and the fluorescence observed therefore indicated that the cells interacted. **c** Effect of layering on aggregate stability. An aggregate with *Pseudomonas* on top of *Acinetobacter* as shown on the right was unstable, and the layering reversed to a structure as shown on the left [86, 89]

remodeling of the biofilm structure after it has been formed will most likely be common. It is also important to get the architecture right in the first place. For example, in synthetic syntrophic biofilms of *Acinetobacter* and *Pseudomonas* made with DEP, as shown in Fig. 5, if the cells are grown on benzylalcohol and *Acinetobacter* is deposited on top of *Pseudomonas*, then this layered structure remains unaltered. If *Pseudomonas* is deposited on top of *Acinetobacter*, then the bacteria swap places [86]. This swap occurs because *Acinetobacter* wants to be in the top layer near the medium, which is high in its carbon source benzylalcohol, whereas *Pseudomonas* wants to be in the lower layer where the benzoate produced by *Acinetobacter* accumulates [86, 89].

It has been suggested that making the bacteria dependent on each other can help in stabilizing a consortium [90, 91]. For example, by combining auxotrophs

symbiotic and beneficial interactions between species could be induced. However, making the bacteria interdependent does not necessarily guarantee they will not compete with and kill each other. A synthetic community of the soil bacteria *Azotobacter vinelandii*, *Bacillus licheniformis*, and *Paenobacillus curdlanolytica*, designed [92] to survive under nutrient-limited conditions by reciprocal syntrophy (i.e., unable to live without each other), was unable to live together if put together in the same culture well. If spatially separated in separate microwells, but still able to communicate and exchange nutrients and signals, the cells thrived. An optimum distance between the wells was found to be around 600 micron. The fact that spatially separating cells enables them to coexist may explain why in soil and other natural systems many bacteria live in spatially separated colonies. However, this is not only interesting from an academic point of view, but may also be of practical value, as it may be helpful to use the topography of surfaces [93] and the microstructure of (porous) materials to minimize competitive interaction to enable microbes in microbial communities to coexist. In fact, cooperation between microorganisms may well be quite rare, as competition and not cooperation dominates interaction between microbial species. Even within different but otherwise highly similar *E. coli* strains designed to cross-feed essential metabolites, cooperative effects were in the minority [91].

As changes in biofilm architecture are more likely to occur in biofilms made by directed assembly the question of why one would do it in the first place needs to be asked. The answer is that direct assembly of biofilms has many advantages. There is more control over the initial composition of the biofilm; its architecture and the strength of adhesion of the biofilm to the surface is often much higher than that of naturally formed biofilm, which often is very loose and suffers from sloughing. Another important reason is that the range of organisms that could be used in synthetic biofilms is very large. It would be infeasible to rely solely on self-assembly of biofilms, as these methods are often highly species- or even strain-specific, and are strongly influenced by external factors. Genetic modification of some species is currently not possible, and mutations and gene transfer can alter the genetic traits of the cells. Even if genetic modification is successful, fine-tuning the many interactions between multiple cell types will be difficult [56]. In contrast, most of the methods employed for directly assembling biofilms from their components are universal, and can be used with any cell type. Even if changes happen in the assembled biofilm the timescale of the changes may be long enough for the system to perform its designed function.

## 4 Outlook

Biofilm architecture is a fascinating subject on its own, of relevance in many systems, and the ability to control it could have many practical applications. Effectively controlling biofilm architecture will undoubtedly be difficult. The challenges presented by engineering biofilms from a synthetic biology point of

view have been discussed by Brenner et al. [65]. Halan et al. [14] and Rosche et al. [12] concentrate on the challenges related to bioprocessing. They argue that more effort is needed in the bioengineering and biotechnology of biofilms to develop feasible strategies for scale-up and bioprocess control. The proposal by Rosche et al. [12] to develop a series of well-characterized biofilm-forming strains as a toolbox for biocatalyst engineering is a sensible one.

As discussed previously [27], the multicellular behavior of the cells and the problems encountered during the (directed) assembly of synthetic biofilms are very similar to those in (human) tissue engineering, and cross-fertilization of the two subjects could be of considerable benefit [27, 94]. Synthetic biology is still in its infancy, and to some extent has different aims from the bioprocessing industries [95], focusing more on fundamental biological research facilitated by the use of synthetic DNA and genetic engineering. The difference between treating biological agents as units whose behavior is predictable on the basis of computation and electronic circuitry [61, 65, 66] and the messy world of biological manufacturing is still large. However, if one were to get it right, the potential rewards are large.

**Acknowledgments** We wish to thank the EC for funding under project “Macumba”.

## References

1. Wimpenny JWT (2003) Togetherness—not just a biofilm thing. In: McBain A, Allison D, Brading M, Rickard AH, Verran J, Walker J (eds) *Biofilm communities: order from chaos?* BioLine, Cardiff, pp 319–340
2. Marsh PD (2003) Plaque as a biofilm: pharmacological principles of drug delivery and action in the sub- and supragingival environment. *Oral Dis* 9:16–22
3. Francolini I, Donelli G (2010) Prevention and control of biofilm-based medical-device-related infections. *FEMS Immunol Med Microbiol* 59:227–238
4. Fayard EH (2008) Case studies: plant performance improvements through the use of innovative condenser cleaning technology and leak detection inspection. *Proceedings of the ASME Power Conference 2008*, New York
5. Huq A, Whitehouse CA, Grim CJ, Alam M, Colwell RR (2008) Biofilms in water, its role and impact in human disease transmission. *Curr Opin Biotechnol* 19:244–247
6. Winkler M (1981) Nitrogen and phosphor removal. In: *Biological treatment of wastewater*, Ellis Horwood Ltd, Chichester, pp 226–234
7. Junter GA, Jouenne T (2004) Immobilized viable microbial cells: from the process to the proteome em leader or the cart before the horse. *Biotechnol Adv* 22:633–658
8. Boone DR, Whitman WB, Rouviere P (1993) Diversity and taxonomy of methanogens, In: Ferry JG (ed) *Methanogenesis*, Chapman & Hall, London, p 35
9. Doelle HW (1975) Anaerobic respiration. In: *Bacterial metabolism*, 2nd edn. Academic Press, London, pp 157–158
10. Qureshi N, Annous BA, Ezeji TE, Karcher P, Maddox IS (2005) Biofilm reactors for industrial bioconversion processes: employing potential of enhanced reaction rates. *Microb Cell Fact* 4:24. doi:10.1186/1475-2859-4-24
11. Davies D (2003) Understanding biofilm resistance to antibacterial agents. *Nat Rev Drug Discov* 2:114–122
12. Rosche B, Li XZ, Hauer B, Schmid A, Buehler K (2009) Microbial biofilms: a concept for industrial catalysis? *Trends Biotechnol* 27:636–643

13. Shong J, Jimenez Diaz MR, Collins CH (2012) Towards synthetic microbial consortia for bioprocessing. *Curr Opin Biotechnol* 23:798–802
14. Halan B, Buehler K, Schmid A (2012) Biofilms as living catalysts in continuous chemical syntheses. *Trends Biotechnol* 30:453–465
15. Beyenal H, Lewandowski Z, Harkin G (2004) Quantifying biofilm structure: facts and fiction. *Biofouling* 20:1–23
16. Shrout JD, Tolker-Nielsen T, Givskov M, Parsek MR (2011) The contribution of cell–cell signaling and motility to bacterial biofilm formation. *MRS Bulletin* 36:367–373
17. Bridier A, Dubois-Brissonnet F, Boubetra A, Thomas V, Briandet R (2010) The biofilm architecture of sixty opportunistic pathogens deciphered using a high throughput CLSM Method. *J Microbiol Meth* 82:64–70
18. Halan B, Schmid A, Buehler K (2011) Real-time solvent tolerance analysis of *Pseudomonas* sp strain LB120 delta C catalytic biofilms. *Appl Environ Microb* 77:1563–1571
19. Klausen M, Heydorn A, Ragas P, Lambertsen L, Aaes-Jorgensen A, Molin S, Tolker-Nielsen T (2003) Biofilm formation by *Pseudomonas aeruginosa* wild type, flagella and type IV pili mutants. *Mol Microbiol* 48:1511–1524
20. Shapiro JA (1998) Thinking about bacterial populations as multicellular organisms. *Annu Rev Microbiol* 52:81–104
21. O’Toole G, Kaplan HB, Kolter R (2000) Biofilm formation as microbial development. *Annu Rev Microbiol* 54:49–79
22. Stewart PS, Franklin MJ (2008) Physiological heterogeneity in biofilms. *Nature Rev Microbiol* 6:199–210
23. Stoodley P, Sauer K, Davies DG, Costerton JW (2002) Biofilms as complex differentiated communities. *Ann Rev Microbiol* 56:187–209
24. Hall-Stoodley L, Stoodley P (2002) Developmental regulation of microbial biofilms. *Curr Opin Biotechnol* 13:228–233
25. Asally M, Kittisopikul M, Rue P, Du Y, Hu Z, Cagatay T, Robinson AB, Lu H, Garcia-Ojalvo J, Suel GM (2012) Localized cell death focuses mechanical forces during 3D patterning in a biofilm. *Proc Natl Acad Sci USA* 109:1–6
26. Rudge JT, Steiner PJ, Phillips A, Haselhof J (2012) Computational modeling of synthetic microbial biofilms. *ACS Synth Biol* 1:345–352
27. Markx GH, Andrews JS, Mason VP (2004) Towards microbial tissue engineering? *Trends Biotechnol* 22:417–422
28. Matsushita M, Fukijama H (1990) Diffusion-limited growth in bacterial colony formation. *Physica* 168:498–506
29. Stewart PS (2003) Diffusion in biofilms. *J Bacteriol* 185:1485–1491
30. Sauer K, Camper A, Ehrlich G, Costerton J, Davies D (2002) *Pseudomonas aeruginosa* displays multiple phenotypes during development as a biofilm. *J Bacteriol* 184:1140–1154
31. Kreft JU (2003) Cooperation and competition in biofilms: an evolutionary perspective. In: McBain A, Allison D, Brading M, Rickard AH, Verran J, Walker J (eds) *Biofilm communities: order from the chaos?*. BioLine, Cardiff, pp 371–380
32. Xavier JB (2011) Social interaction in synthetic and natural microbial communities. *Mol Sys Biol* 7:483
33. Ruiz LM, Valenzuela S, Castro M, Gonzalez A, Frezza M, Souler L, Rohwerder T, Queneau Y, Doutheau A, Sand W, Jerez CA, Guilian N (2008) AHL communication is a widespread phenomenon in biomining bacteria and seems to be involved in mineral-adhesion efficiency. *Hydrometallurgy* 94:133–137
34. Connell JL, Wessel AK, Parsek MR, Ellington AD, Whiteley M, Shear JB (2010) Probing prokaryotic social behaviors with bacterial “lobster traps”. *MBio* 1:1–8
35. Mason VP, Markx GH, Thompson IP, Andrews JS, Manefield M (2005) Colonial architecture in mixed species assemblages affects AHL mediated gene expression. *FEMS Microbiol Lett* 244:121–127

36. Schuster M, Lostroh CP, Ogi T, Greenber EP (2003) Identification, timing, and signal specificity of *Pseudomonas aeruginosa* quorum-controlled genes: a transcriptome analysis. *J Bacteriol* 185:2066–2079
37. Decho AW, Norman RS, Visscher PT (2010) Quorum sensing in natural environments: emerging views from microbial mats. *Trends Microbiol* 18:73–80
38. Platt TG, Fuqua C (2010) What's in a name? The semantics of quorum sensing. *Trends Microbiol* 18:383–387
39. Sanchez Z, Tani A, Suzuki N, Kariyama R, Kuman H, Kimbara K (2012) Assessment of change in biofilm architecture by nutrient concentration using a multichannel microdevice flow system. *J Biosci Bioeng* doi:10.1016/j.jbiosc.2012.09.018
40. Bester E, Kroukamp O, Hausner M, Edwards EA, Wolfaardt GM (2010) Biofilm form and function: carbon availability affects biofilm architecture, metabolic activity and planktonic cell yield. *J Appl Microbiol* 110:387–398
41. Zhao C, Burchardt M, Brinkhoff T, Beardsley C, Simon M, Wittstock G (2010) Microfabrication of patterns of adherent marine bacterium *Phaeobacter inhibens* using soft lithography and scanning probe lithography. *Langmuir* 26:8641–8647
42. Stoodley P, Boyle JD, DeBeer D, Lappin-Scott HM (1999) Evolving perspectives of biofilm structure. *Biofouling* 14:75–90
43. Bridier A, Le Coq D, Dubois-Brissonet F, Thomas V, Aymerich S, Briandet R (2011) The spatial architecture of *Bacillus subtilis* biofilms deciphered using a surface associated model and in situ imaging. *PLoS One* 6:e1677
44. Kwok WK, Picioareanu C, Ong SL, van Loosdrecht MCM, Ng WJ, Heijnen JJ (1998) Influence of biomass production and detachment forces on biofilm structures in a biofilm airlift suspension reactor. *Biotechnol Bioeng* 58:400–407
45. Kirisits MJ, Margolis JJ, Purevdorj-Gage BL, Vaughan B, Chopp DL, Stoodley P, Parsek MR (2007) Influence of the hydrodynamic environment on quorum sensing in *Pseudomonas aeruginosa* biofilms. *J Bacteriol* 189:8357–8360
46. Mah TFC, O'Toole GA (2001) Mechanisms of biofilm resistance to antimicrobial agents. *Trends Microbiol* 9:34–39
47. Lewis K (2008) Multidrug tolerance of biofilms and persister cells. *Curr Top Microbiol Immunol* 322:107–131
48. Stewart PS, Roe F, Rayner J, Eldins GJ, Lewandowski Z, Ochsner AU, Hassett JD (2000) Effect of catalase on hydrogen peroxide penetration into *Pseudomonas aeruginosa* biofilms. *Appl Environ Microb* 66:836–838
49. Field JA, Stams AJM, Kato M, Schraa G (1995) Enhanced biodegradation of aromatic pollutants in cocultures of anaerobic and aerobic bacterial consortia. *Antonie van Leeuwenhoek* 67:47–77
50. Kim HJ, Du W, Ismagilov RF (2011) Complex function by design using spatially pre-structured synthetic microbial communities: degradation of pentachlorophenol in the presence of Hg(II). *Integr Biol* 3:126–133
51. Lanthier M, Taratkovsky B, Villemur R, DeLuca G, Guiot SR (2002) Microstructure of anaerobic granules bioaugmented with *Desulfitobacterium frappieri* PCP-1. *Appl Environ Microb* 68:4035–4043
52. Cao B, Majors PD, Ahmed B, Renslow RS, Silvia CP, Shi L, Kjelleberg S, Fredrickson JK, Beyenal H (2012) Biofilm shows spatially stratified metabolic responses to contaminant exposure. *Environ Microbiol* 14:2901–2910
53. Brune KD, Bayer TS (2012) Engineering microbial consortia to enhance biomining and bioremediation. *Front Microbiol* 3:203
54. Zuroff TR, Curtis WR (2012) Developing symbiotic consortia for lignocellulosic biofuel production. *Appl Microbiol Biotechnol* 93:1423–1435
55. Gonzalez-Gil G, Lens PNL, van Aelst A, van As H, Versprille AI, Lettinga G (2001) Cluster structure of anaerobic aggregates of an expanded granular sludge bed reactor. *Appl Environ Microb* 67:3683–3692

56. Brenner K, Arnold FH (2011) Self-organization, layered structure, and aggregation enhance persistence of a synthetic biofilm consortium. *PLoS One* 6:e16791
57. Hansen SK, Rainey PB, Haagensen JAJ, Molin S (2007) Evolution of species interactions in a biofilm community. *Nature* 445:533–536. doi: [10.1038/nature05514](https://doi.org/10.1038/nature05514)
58. McLeod FA, Guiot SR, Costerton JW (1990) Layered structure of bacterial aggregates produced in an upflow anaerobic sludge bed and filter reactor. *Appl Environ Microb* 56:1598–1607
59. Woznica A, Karcz J, Nowak A, Gmur A, Bernas T (2010) Spatial architecture of nitrifying bacteria biofilm immobilized on polyurethane foam in an automatic bioreactor for water toxicity. *Microsc Microanal* 16:550–560
60. Summers ZM, Fogarty HE, Leang C, Franks AE, Malvankar NS, Lovley DR (2010) Direct exchange of electrons within aggregates of an evolved syntrophic coculture of anaerobic bacteria. *Science* 330:1413–1415
61. Tamsir A, Tabor JJ, Voigt CA (2011) Robust multicellular computing using genetically encoded NOR gates and chemical ‘wires’. *Nature* 469:212–215
62. Lakshmanan V, Kumar AS, Bais HP (2012) The ecological significance of plant-associated biofilms. In: Lear G, Lewis GD (eds) *Microbial biofilms: Current research and applications*. Caister Academic Press, Portland
63. Zhu K, Kaprelyants AS, Salina EG, Schuler M, Markx GH (2010) Construction by dielectrophoresis of microbial aggregates for the study of bacterial cell dormancy. *Biomicrofluidics* 4:022810-1–022810-13
64. Foster KR, Bell T (2012) Competition, not cooperation, dominates interactions among culturable microbial species. *Curr Biol* 22:1845–1850
65. Brenner K, You L, Arnold FH (2008) Engineering microbial consortia: a new frontier in synthetic biology. *Trends Biotechnol* 26:483–489
66. Chuang JS (2012) Engineering multicellular traits in synthetic microbial populations. *Curr Opin Chem Biol* 16:370–378
67. Agapakis CM, Boyle PM, Silver PA (2012) Natural strategies for the spatial optimization of metabolism in synthetic biology. *Nat Chem Biol* 8:527–535
68. Wood TK, Hong SH, Ma Q (2011) Engineering biofilm formation and dispersal. *Trends Biotechnol* 29:87–94
69. Stubblefield BA, Howery KE, Islam BN, Santiago AJ, Cardenas WE, Gilbert ES (2010) Constructing multispecies biofilms with defined compositions by sequential deposition of bacteria. *Appl Microbiol Biotechnol* 86:1941–1946
70. Flickinger MC, Schottel JL, Bond DR, Aksan A, Scriven LE (2007) Painting and printing living bacteria: engineering nanoporous biocatalytic coatings to preserve microbial viability and intensify reactivity. *Biotechnol Prog* 23:2–17
71. Tsoligkas AN, Bowen J, Winn M, Goss RJM, Overton TW, Simmons MJ (2012) Characterisation of spin coated engineered *Escherichia coli* biofilms using atomic force microscopy. *Coll Surf B: Biointerfaces* 89:152–160
72. Elad T, Lee JH, Gu MB, Belkin S (2010) Microbial cell arrays. *Adv Biochem Eng Biotechnol* 117:85–108
73. Albrecht DR, Liu Tsang V, Sah RL, Bhatia SN (2005) Photo-and electropatterning of live cellular arrays within hydrogels. *Lab Chip* 5:111–118
74. Choi WS, Ha D, Park S, Kim T (2010) Synthetic multicellular cell-to-cell communication in inkjet printed bacterial cell systems. *Biomaterials* 32:2500–2507
75. Xu T, Petridou S, Lee EH, Roth EA, Vyavahare NR, Hickman JJ, Boland T (2004) Construction of high-density bacterial colony arrays and patterns by the ink-jet method. *Biotechnol Bioeng* 85:29–33
76. Tan W, Desai TA (2004) Layer-by-layer microfluidics for biomimetic three-dimensional structures. *Biomaterials* 25:1355–1364
77. Yaguchi T, Lee S, Choi WS, Kim D, Kim T, Mitchell RJ, Takayama S (2010) Micropatterning bacterial suspensions using aqueous two phase systems. *Analyst* 135:2848–2852

78. Wiklund M, Onfelt B (2012) Ultrasonic manipulation of single cells. *Methods in Molecular Biology* 853:177–196
79. Spengler JF, Jekel M, Christensen KT, Adrian RJ, Hawkes JJ, Coakley WT (2000) Observation of yeast cell movement and aggregation in a small-scale MHz-ultrasonic standing wave field. *Bioseparation* 9:329–341
80. Evander M, Nilsson J (2012) Acoustofluidics 20: Applications in acoustic trapping. *Lab Chip* 12:4667–4676
81. Wiklund M, Radel S, Hawkes JJ (2013) Acoustofluidics 21: ultrasound-enhanced immunoassays and particle sensors. *Lab Chip* 13:25–39
82. Haruff HM, Munakata-Marr J, Marr DWM (2003) Directed bacterial surface attachment via optical trapping. *Coll Surf B: Biointerfaces* 27:189–195
83. Poortinga AT, Bos R, Busscher HJ (2000) Controlled electrophoretic deposition of bacteria to surfaces for the design of biofilms. *Biotechnol Bioeng* 67:117–120
84. Alp B, Stephens GM, Markx GH (2002) Formation of artificial, structured microbial consortia (ASMC) by dielectrophoresis. *Enz Microb Technol* 31:35–43
85. Markx GH, Alp B, McGilchrist A (2002) Electro-orientation of *Schizosaccharomyces pombe* in high conductivity media. *J Microbiol Meth* 50:55–62
86. Andrews JS, Mason VP, Thompson IP, Stephens GM, Markx GH (2006) Construction of artificially structured microbial consortia (ASMC) using dielectrophoresis: examining bacterial interactions via metabolic intermediates within environmental biofilms. *J Microbiol Meth* 64:96–106
87. Verdusco-Luque CE, Alp B, Stephens GM, Markx GH (2003) Construction of biofilms with defined internal architecture using dielectrophoresis and flocculation. *Biotechnol Bioeng* 83:39–44
88. Abidin ZZ, Downes L, Markx GH (2007) Large scale dielectrophoretic construction of biofilms using textile technology. *Biotechnol Bioeng* 96:1222–1225
89. Gonzalez-Ramirez CA, Andrews JS, Kookos I, Mason VP, Stephens GM, Thompson IP, Markx GH (2005) A study of metabolic interactions within artificial biofilms of consortia of *Acinetobacter* sp. C6 and *Pseudomonas putida* R1. In: McBain A, Allison D, Pratten J, Spratt D, Upton M, Verran J (eds) *Biofilms: persistence and ubiquity*. Biofilm Club, Manchester
90. Song H, Payne S, Gray M, You LC (2009) Spatiotemporal modulation of biodiversity in a synthetic chemical-mediated ecosystem. *Nat Chem Biol* 5:929–935
91. Wintermute EH, Silver PA (2010) Emergent cooperation in microbial metabolism. *Mol Sys Biol* 6:407
92. Kim HJ, Boedicker JQ, Choi JW, Ismagilov RF (2008) Defined spatial structure stabilizes a synthetic multispecies bacterial community. *Proc Natl Acad Sci USA* 105:18188–18193
93. Crawford RJ, Webb HK, Truong VK, Hasan J, Ivanova E (2012) Surface topographical factors influencing bacterial attachment. *Adv Coll Interf Sci* 179–182:142–149
94. Xu F, Sridharan B, Durmus NG, Wang S, Yavuz AS, Gurkan UA, Demirci U (2011) Living bacterial sacrificial porogens to engineer decellularized porous scaffolds. *Plos One* 6:1–12
95. Stephanopoulos G (2012) Synthetic biology and metabolic engineering. *ACS Synth Biol* 1:514–525

# Engineered Cell–Cell Communication and Its Applications

Stephen Payne and Lingchong You

**Abstract** Over the past several decades, biologists have become more appreciative of the fundamental role of intercellular communication in natural systems spanning prokaryotic biofilms to eukaryotic developmental systems and neurological networks. From an engineering perspective, the use of cell–cell communication provides an opportunity to engineer more complex and robust functions using cellular components. Indeed, this strategy has been adopted in synthetic biology in the creation of diverse gene circuits that program spatiotemporal dynamics in one or multiple populations. Gene circuits such as these may offer insights regarding basic biological questions and motifs or serve as a basis for novel applications.

## Contents

1	Introduction.....	98
2	Quorum Sensing .....	100
3	Using Engineered Cell–Cell Communication to Understand Natural Biological Phenomena.....	100
	3.1 Ecology .....	101
	3.2 Evolution .....	102
4	Applications of Cell–Cell Communication in Pattern Formation .....	103
5	Applications of Cell–Cell Communication in Biocomputation and Bioengineering .....	106
	5.1 Biocomputation.....	107
	5.2 Bioengineering .....	108

---

S. Payne · L. You

Department of Biomedical Engineering, Duke University, Durham, NC 27708, USA

L. You

Institute for Genome Sciences and Policy, Duke University, Durham, NC 27708, USA

L. You

Center for Systems Biology, Duke University, Durham, NC 27708, USA

L. You (✉)

CIEMAS 2355, 101 Science Drive, Box 3382 Durham, NC 27708, USA

e-mail: you@duke.edu



6	Disrupting Cell–Cell Communication for Potential Therapeutic Applications .....	111
7	Engineering Artificial Cell–Cell Communication Modules .....	113
7.1	Improvements to Existing Cell–Cell Communication Modules .....	113
7.2	Novel Microbial Cell–Cell Communication Modules.....	115
7.3	Engineered Mammalian Cell–Cell Communication Modules .....	116
7.4	Engineered Inter- and Intrakingdom Communication.....	117
8	Conclusion .....	117
	References.....	118

## 1 Introduction

One of the most defining achievements throughout evolutionary history was the advent of the ability of cells to communicate with one another. The obvious importance of this breakthrough was the ability of multicellular organisms to arise, with cells coordinating with one another to better survive in their respective environments [1]. Cell–cell communication then allowed for certain cells to become specialized, thus allowing for a division of labor within a multicellular organism [2]. Eventually, this specialization gave rise to different systems (i.e., respiratory, nervous, etc.), each with its own sophisticated cell–cell communication networks [3].

Until recently, most prokaryotic organisms were thought to exist alone as individuals. However, studies over the past four decades have increasingly recognized the importance of cell–cell communication among these species. This communication is responsible for coordinating integral population-level behaviors, including biofilm formation, competence development, expression of virulence factors, sporulation, and production of bioluminescence [4]. Each of these behaviors is inefficient when only a small number of cells are present, yet can be beneficial on the population level [4]. Therefore, cell–cell communication is not only integral to the proper functioning of multicellular organisms but also to unicellular organisms, which often perish or prosper as part of a larger population.

In synthetic biology, cell–cell communication has also been recognized as an effective strategy to achieve robust system dynamics in engineered cell populations. This recognition has led to a gradual shift from a cell-centric perspective to a population-centric perspective. In early work in the synthetic biology field, devices such as switches, oscillators, timers, and logic gates were mostly constructed to operate at the single-cell level [5–8]. Recently, increasing emphasis has been placed on the use of cell–cell communication modules to coordinate population-level behavior in synthetic biological systems [9–13]. There are two reasons for this shift from unicellular to multicellular programming. First, because of the broad-ranging importance of cell–cell communication in diverse natural biological systems, synthetic biologists can use engineered, communication-based systems to explore basic biological questions. By bypassing natural systems, which are often confounded with interconnected gene networks, complex environmental interactions, and interspecies relationships, engineered systems may serve as better-defined

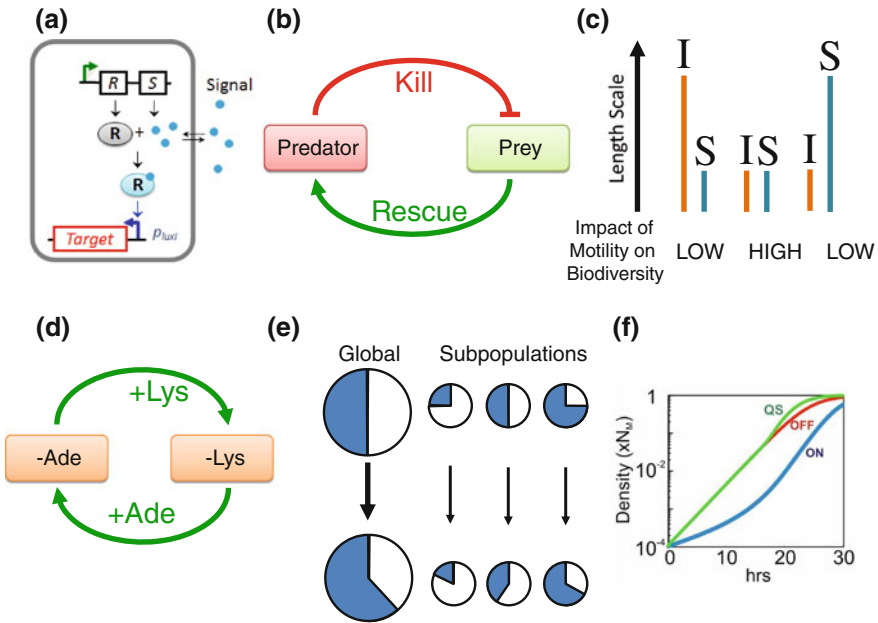


**Fig. 1** **a** Diagram of a generic QS system. A receptor gene ( $R$ ) and a synthase gene ( $S$ ) encode proteins  $R$  and  $S$ . Protein  $R$  is a receptor protein, which becomes activated upon binding the QS signal. The QS signal is synthesized by protein  $S$  (a synthase). Only when enough signal has accumulated in culture is enough  $R$  protein bound to the QS signal to activate the QS-regulated (blue) promoter sufficiently. When induced, this promoter activates transcription of a downstream target gene. **b** Logic of the synthetic predator–prey system. The predator kills the prey by inducing the toxin protein CcdB in the prey via the QS signal 3OC12HSL. The prey rescues the predator by inducing the antitoxin protein CcdA via the QS signal 3OC6HSL. CcdA rescues the predator from constitutively expressed CcdB [18]. **c** The interaction and segregation length scales ( $I$  and  $S$ , respectively) determine the impact of cell motility on biodiversity in the predator–prey system. If the length scale of the interaction (QS signaling) between predator and prey is large relative to the segregation distance (left) or vice versa (right), the impact of cell motility on biodiversity is low. However, if the length scales of the interaction and the segregation distance are comparable, the impact of cell motility on biodiversity is high (center) [19]. **d** Logic of the synthetic mutualism system. One strain lacks the ability to produce lysine (left), whereas the other lacks the ability to produce adenine but overproduces adenine (right). The populations survive best in coculture, thus mimicking a mutualistic relationship [20]. **e** Simpson’s Paradox. This phenomenon occurs when the proportion of producers (blue fraction) in the global population increases (left), while the proportion of producers decreases in each of the subpopulations (right). Chuang et al. were able to implement such a scenario in a synthetic, QS-based system and quantitatively characterize this evolutionary phenomenon [24]. **f** QS as a strategy for optimizing population growth. Pai et al. constructed a system whereby public goods were secreted throughout a population. Production and secretion of the public goods incurred a metabolic cost to producer cells. For certain conditions, QS-regulated production of public goods (green curve) was found to be the best growth strategy when compared to constitutive (blue curve) and no (red curve) production [25]

models to address certain biological questions regarding ecosystem interactions, evolutionary processes, and pattern formation. Second, programming cellular behavior on a population level can be more robust and efficient from an engineering perspective. To this end, the use of cell–cell communication may be critical in generating systems for robust pattern formation, biocomputing, and bioprocessing.

In this review, we first discuss a predominant method of cell–cell communication, quorum sensing (QS), which is the basis for numerous communication modules utilized in the field of synthetic biology. We then discuss recent synthetic biology studies that use engineered, communication-based circuits to address basic biological questions. This leads into a description of recent advances in engineering robust biological devices using cell–cell communication. Finally, we discuss examples of novel engineered cell–cell communication modules, which may be the basis for future synthetic biological systems.

## 2 Quorum Sensing

Quorum sensing has been identified in a large variety of both Gram-positive and Gram-negative bacteria [14–16]. In a QS system, bacteria synthesize a chemical signal that diffuses inside and outside the cell. As a bacterial population grows, the concentration of signal in the environment increases as more bacteria contribute to the synthesis of the chemical signal. At a sufficiently high bacterial density, or when the population reaches a “quorum”, the signal concentration reaches a threshold necessary to activate a signal cascade, leading to downstream gene expression. Fundamental to this process is that the threshold concentration is reached at the same time for all cells within a local population, and thus activation of downstream gene expression is coordinated across that local population (Fig. 1a).

A canonical QS system is the LuxR/LuxI system from *Vibrio fischeri* [17]. In this system, LuxI synthesizes a small molecule acyl-homoserine lactone (AHL), which acts as the diffusible signal discussed above. At a sufficiently high cell density, intracellular AHL can reach a high enough concentration that it binds to and activates the LuxR protein, which in turn activates downstream genes [17]. Many LuxR/LuxI-type QS systems have been identified in numerous bacterial species; they control a highly diverse set of genes, such as those critical for bioluminescence, biofilm formation, and virulence development [17].

## 3 Using Engineered Cell–Cell Communication to Understand Natural Biological Phenomena

Although most synthetic biological systems have been implemented as novel engineered devices, they have also been used to explore basic biological questions. Here, we focus on two major subjects explored using synthetic, communication-based systems: ecology and evolution.

### 3.1 Ecology

Ecologists have long been interested in the dynamics of predator–prey relationships. Balagadde et al. engineered a predator–prey gene circuit, which allows for two-way communication between two strains of *Escherichia coli* [18]. As shown in Fig. 1b, the system consists of a predator strain and a prey strain. Upon circuit induction, the predator expresses LasI, which synthesizes an AHL, 3OC12HSL; the prey expresses LuxI, which synthesizes another AHL, 3OC6HSL. Each strain produces the appropriate receptor protein (LasR and LuxR) corresponding to the AHL secreted from the other. 3OC12HSL from the predator induces downstream expression of a toxin protein, CcdB, in the prey, thereby killing it. 3OC6HSL from the prey induces downstream expression of an antitoxin protein, CcdA, in the predator, which rescues it from constitutively expressed CcdB [18]. Therefore, the prey is killed by the predator, and the predator is rescued by the prey (Fig. 1b), thus implementing the basic logic of the prototypical predator–prey relationship.

By studying the system in a microfluidic device, Balagadde et al. demonstrated complex predator–prey dynamics, including extinction, coexistence, and oscillations. Guided by modeling, the authors also examined how these dynamics would respond to experimental perturbations to specific system parameters [18]. Song et al. extended this study and used the engineered ecosystem as a model to examine the factors affecting biodiversity (as measured by relative abundance) in a solid-phase environment. The authors found that biodiversity would be sensitive to changes in cell motility if the segregation distance between the two populations were comparable to the length scale of AHL diffusion. In such a case, biodiversity would be inversely correlated with cell motility. If the AHL diffusion length scale is much greater than the segregation distance or vice versa, changes in cell motility do not significantly influence the system’s biodiversity (Fig. 1c) [19]. In both studies, the system represented a simple, well-defined, yet nontrivial model system by which investigators could confine their analyses of the predator–prey interaction to a few well-defined parameters, bypassing natural systems that are confounded by other species interactions, environmental variation, and the like. This approach allowed the authors to ask specific questions regarding the nature of a basic predator–prey relationship and answer those questions by precise experimentation guided by mathematical modeling.

In this manner, Shou et al. examined the dynamics of a synthetic ecosystem in which two strains of *Saccharomyces cerevisiae* mimic a mutualistic relationship through the cooperative production of two essential metabolites (lysine and adenine). One strain overproduces lysine and lacks the gene necessary to produce adenine, whereas the other strain overproduces adenine and lacks the gene necessary to produce lysine (Fig. 1d). Both strains in monoculture will die because they lack either adenine or lysine. When grown in coculture, however, the strains can grow well because each strain supplies the other with a missing essential metabolite. By combining modeling with an experimental approach, the

investigators demonstrated that the total initial cell number and the initial ratio between the two strains were critical determinants of viability in the system [20].

Using a similar strategy, Hu et al. created a mutualistic system consisting of two engineered *Escherichia coli* strains that use two-way QS communication systems to induce expression of antibiotic resistance genes in bacteria. In this system, the authors used an inducible promoter,  $P_{tetR}$ , to control the quorum-sensing genes LuxR, Rh1R, and Rh1I and another inducible promoter,  $P_{lac}$ , to control the other quorum-sensing gene LuxI. One strain (ER) expressed LuxI and Rh1R, and the other strain (EG) expressed LuxR and Rh1I. ER also contained the promoter Prh1 upstream of a kanamycin-resistance gene, whereas EG contained the promoter luxPR upstream of an ampicillin-resistance gene. When the system was induced, they, too, were able to model successfully the key factors influencing the ability of the coculture to survive under a variety of experimental conditions [21]. As with the previous study, this system was used to identify the driving forces of different dynamical behaviors possible in a mutualistic system.

Similar to the synthetic predator–prey system, the spatial population structure has been found to be an important determinant influencing the dynamics of engineered mutualistic ecosystems. By studying a synthetic community of three different bacterial species in a microfluidic device, Kim et al. demonstrated that spatial barriers between the bacterial species are necessary and sufficient for stable coexistence of the populations [22]. Similarly, Brenner and Arnold illustrated this same concept within a biofilm formed by a synthetic consortium of two engineered *E. coli* strains that communicate via QS. In the biofilm, the two populations formed defined layered structures of population aggregates, which enhanced the consortium’s ability to survive [23].

### 3.2 Evolution

Simpson’s paradox is an apparently paradoxical phenomenon by which two sub-populations evolve in many segmented cocultures. In these cocultures, one sub-population (the producers) produces a public good that benefits the entire population, and another subpopulation (the nonproducers) does not produce anything but reaps the benefits from the producers. Given the appropriate parameters, the proportion of producers in each segmented coculture can decrease over time, whereas the overall proportion of producers in the total population can increase (Fig. 1e).

To better understand this phenomenon, Chuang et al. built a system of two engineered *E. coli* strains, which both contain a gene encoding antibiotic resistance downstream of a promoter sensitive to QS signaling. One strain (the producer) expresses the QS signal, and the other (the nonproducer) does not. Thus, the producer alone bears the metabolic burden of producing the QS signal, yet both strains benefit from the producers’ QS signal, which allows them to resist the antibiotic in the medium [24]. Using this system, the investigators were able to

observe Simpson’s paradox in action. Furthermore, by studying this system in a well-controlled environment without conflicting interactions, they were able quantitatively to characterize the phenomenon with limited confounding factors.

A synthetic system has also been utilized to determine whether QS is an optimal strategy for regulating the production of public good exoproducts. Pai et al. recently constructed a gene circuit that produces a secreted form of beta-lactamase that confers resistance to 6-aminopenicillanic acid (6-APA) by degrading it in culture. The investigators studied the circuit under several conditions: (1) production of the exoproduct is regulated by the LuxR/LuxI QS module, (2) production is regulated by an inducible promoter, and (3) production does not occur. In this system, the production and secretion of the exoproduct incurs a metabolic cost to the host cell but, once secreted, the exoproduct benefits the entire population. Therefore, it serves as a public good. By quantitative analysis, the authors identified a set of conditions whereby QS regulation of the public good protein is the optimal strategy for maximizing cell growth (Fig. 1f). The authors conclude that the kinetic properties of the QS systems can be tuned to optimize bacterial survival [25], which confirms an earlier theoretic prediction [26]. This property may explain how QS systems can be utilized by bacteria to deal with stressful conditions (i.e., antibiotic exposure).

Waddington’s landscape has long been used as an analogy for phenotypic diversification within a cell lineage. The analogy invokes the image of a marble rolling down a landscape with different local minima where the marble will come to rest. In this analogy, the cell is the marble, and the different low states that the marble can settle into represent different cell fates. This analogy is often invoked to visualize how stem cells can differentiate into various tissue types depending on both intracellular gene expression and external signaling [27]. Using a synthetic circuit consisting of a QS-driven toggle switch, Sekine et al. demonstrated how cells diversify autonomously through cell–cell communication. Through experimentation and stochastic modeling, the group was able to confirm the QS-mediated bifurcation of switching from one state to another and found that this switching was critically dependent on initial cell number. The work’s importance lies in the fact that, although invoked in a variety of developmental systems, cells diversifying across Waddington’s landscape had never been directly confirmed experimentally. Therefore, the group’s synthetic system represents a direct demonstration of Waddington’s landscape in action [27].

## **4 Applications of Cell–Cell Communication in Pattern Formation**

Synthetic pattern-forming systems, as with synthetic cell–cell communication systems in general, serve a dual use. First, they reveal minimalistic strategies for achieving specific natural biological processes. Second, they represent a new method of engineering structures solely using biological components.

The importance of pattern formation in nature cannot be understated as it is ubiquitous throughout the biosphere, driving such varied biological processes as slime mold aggregation [28, 29], feather branching [30], and tissue stratification [31, 32]. By implementing pattern formation using synthetic gene circuits, investigators can extrapolate the key components necessary for pattern formation in natural systems. This exercise can provide insights as to how these processes occur in more complex systems. In addition, synthetic pattern-forming systems could become the basis of next-generation biomaterials, which self-organize into precise patterns of biological entities (i.e., proteins, metabolites, etc.).

Basu et al. [33] constructed the first synthetic pattern-forming system, which utilizes a population mixture of sender and receiver cells. Here, sender cells express LuxI, which synthesizes the AHL 3OC6HSL. Receiver cells express the receptor protein, LuxR. Upon binding 3OC6HSL from the sender cells, activated LuxR stimulates expression of a LacI mutant and cI, which inhibits expression of another LacI protein. LacI, in turn, inhibits GFP expression. Thus, the receiver cells contain a gene network constituting an incoherent feedforward loop (Fig. 2a), where too much or too little AHL results in repression of GFP expression. This lack of expression occurs at high AHL concentrations because the LacI mutant represses GFP expression, and expression is also blocked at low AHL concentrations inasmuch as there is not enough cI expressed to inhibit wild-type LacI from inhibiting GFP. Thus, the receiver cells constitute a band-detector, which only express GFP at intermediate AHL concentrations.

On a plate containing an undifferentiated lawn of receiver cells surrounding sender cells placed at the center, the receiver cells only express GFP in ring patterns at intermediate radii about the center. This pattern formation occurs because cells expressing GFP experience intermediate AHL concentrations, whereas cells closer to the center experience higher AHL concentrations and cells towards the edge of the plate experience lower AHL concentrations. By combining receiver gene circuits with varying sensitivities to AHL and different fluorescent proteins, Basu et al. were able to obtain multiple concentric rings, which constituted bulls-eye patterns (Fig. 2b). Furthermore, modifying the position(s) of the sender cells allowed the investigators to achieve more complex patterns. This system resembles the circuit underlying *D. melanogaster* blastoderm segmentation and can lead to the deduction of design principles in natural pattern-forming systems [33].

Another interesting synthetic system implementing pattern formation involves direct cell–cell interactions between mammalian cells using the Delta–Notch signaling pathway [34]. Instead of using QS, this system utilizes contact-based interactions mediated by surface proteins. Specifically, a gene encoding a Delta–GFP fusion protein is placed downstream of the Delta–Notch signaling pathway. The Delta–Notch signaling pathway is activated when a cell surface makes physical contact with another cell expressing Delta–Notch on the surface. In this manner, an effective positive-feedback loop driving Delta–GFP fusion protein expression operates when a cell comes into close physical contact with other cells in a field (Fig. 2c). When these engineered cells are placed around cells

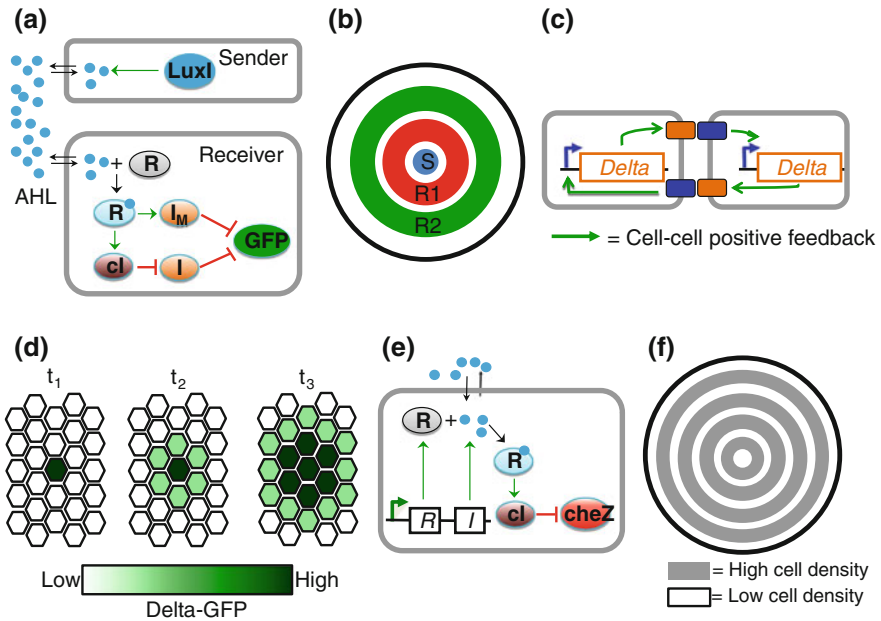


**Fig. 2** **a** Circuit diagram for a synthetic *sender–receiver* system. A sender cell constitutively expresses *LuxI*, which synthesizes the AHL 3OC6HSL. *Receiver* cells express *LuxR* (*R*), which binds AHL and activates *cI* and a mutant *LacI* (*I<sub>M</sub>*). *cI* inhibits another *LacI* (*I*). Both versions of *LacI* inhibit GFP. Thus, the *receiver* cell’s gene network can be viewed as an incoherent feedforward loop, where only midrange concentrations of AHL activate high levels of GFP [33]. **b** Spatial patterns generated via the circuits in (a). By constructing two versions of the *receiver* circuit in (a) with varying sensitivities and different fluorescent proteins (red and green), a lawn of cells containing two *receiver* circuits (*R1* and *R2*) can generate *concentric circles* about a small population of sender cells (*S*) at the center of an agar plate [33]. **c** Delta–Notch synthetic gene circuit. A Delta–GFP fusion protein is placed downstream of the Delta–Notch pathway. Upon cell–cell contact mediated by Delta–Notch, the gene circuits constitute a positive feedback loop [34]. **d** Circuit in (c) generates signal propagation in a field of cells. Cells containing the gene circuit are placed in a field surrounding a “trigger” cell (*center dark green cell*), which constitutively activates the Delta–Notch pathway. Activation of Delta–GFP is then propagated from the trigger cells to proximate cells and finally to distant cells over time [34]. **e** Synthetic circuit coupling cell density and motility. Activated *LuxR* induces expression of *cI* when a high cell density is detected. *cI* then inhibits *cheZ*, which in turn results in low cell motility [36]. **f** Alternating low and high cell density rings result in a field of expanding cells containing the circuit in (e). The oscillatory nature of the circuit in (e) gives rise to alternating ring patterns of low and high cell density [36]

constitutively expressing Delta (“trigger” cells), the system leads to signal propagation of GFP reporter expression in the spatial domain (Fig. 2d). The investigators in the study speculate that the system could be used to investigate the mechanistic bases for pattern formation in various mammalian developmental systems. Furthermore, such a system could be used to control differentiation pathways for tissue engineering applications [34].



However, a limitation of this mammalian system and Basu et al.'s system is that the patterns are determined by a predefined location that the trigger or sender cells occupy. This leads us to an important biological question that scientists have been pondering since Alan Turing first examined it in the 1950s [35]: how can biological patterns self-organize without any predetermined spatial configuration or external stimulus? Liu et al. addressed this question with their own synthetic circuit that programs self-organized pattern formation by regulating cell motility using the LuxR/LuxI QS module (Fig. 2e). At high cell densities, the QS module triggers expression of cI, which inhibits CheZ expression. Repression of CheZ reduces cell motility. When placed on a soft-agar plate, cells containing this circuit grew outward from a small initial population at the center and formed concentric rings of alternating high and low densities (Fig. 2f) [36]. This pattern was the direct result of an oscillatory dynamic between high and low population states being translated spatially in the radial direction. Interestingly, the synthetic system demonstrates how a spatially periodic pattern can be generated without an external clock, which is thought to be necessary in vertebrate development [36]. In addition, the system has potential for engineering spatially periodic biomaterials.

Another method for generating precise patterns is to combine synthetic gene networks with inkjet printing technology. Inkjet printing technology has been used in several previous studies to print precisely bacterial and mammalian cells onto surfaces at high resolution [37–39]. In addition, Choi et al. recently applied this technology to engineered *E. coli* cells containing synthetic QS components. Briefly, the investigators examined the spatiotemporal dynamics of precisely printed microcolonies of cells producing AHL (senders), cells expressing GFP in response to AHL (receivers), and cells that inhibit GFP expression in response to AHL (inverse receivers). Interestingly, neighboring microcolonies placed in large arrays communicated with one another efficiently, giving rise to synchronization of microcolonies within local spatial regions. Experiments indicated that this communication between cells could be tuned effectively with this framework by changing microcolony size, spacing distance, printing timing, and cell seeding number [40]. Thus, the system offers a high-throughput platform for analyzing cell–cell communication quantitatively. In addition, the precision of inkjet printing coupled with cell–cell communication could lead to a future generation of high-resolution spatial patterns.

## 5 Applications of Cell–Cell Communication in Biocomputation and Bioengineering

Cell–cell communication modules have also been adopted to construct biological systems, which perform computations or represent novel engineering feats. In biocomputing, scientists have long marveled at cells' capacities for informational storage and rapid processing. Likewise, many attributes of biological components

(a wide array of functions, the potential for adaptability and modularity, etc.) make synthetic biological systems attractive to engineers. For these reasons, there have been several recent advances in the areas of biocomputing and bioengineering using synthetic systems that contain cell–cell communication modules.

## 5.1 Biocomputation

Logic gates are fundamental components of modern computers, which have been utilized by computer scientists and electrical engineers for many decades. Thus, it is not surprising that synthetic biologists hoping to make cells compute have primarily concentrated on developing diverse biological logic gates. A large amount of progress in this area has occurred over the last several years, culminating in recent studies in which many logic gates have been integrated to achieve complex computational functions [41–44].

Many of these logic gates have utilized QS systems to synchronize logic signals across a cell population. For example, Brenner et al. developed a system in which two colocalized *E. coli* populations could converse with each other bidirectionally using two interlocked QS systems, the RhlR/RhlI and the LasR/LasI systems. Briefly, one cell population produces the RhlI signal, C4HSL, and the other population produces the LasI signal, 3OC12HSL. Each population only reads the QS signal from the other population by expressing the corresponding receptor protein. Once the complex between the receptor protein and the diffused QS signal (3OC12HSL or C4HSL) forms, it activates the promoter-driving production of the other QS signal (C4HSL or 3OC12HSL, respectively), along with a GFP reporter. Thus, the two populations constitute a logical AND gate in which GFP activation only occurs when both QS signals are present. The authors demonstrate that the AND gate is indeed activated when the populations are spatially colocalized in agar and in a biofilm consortium [45].

AND gates can also be utilized to perform complex biocomputing tasks. Tabor et al. accomplished such a task by executing a synthetic genetic edge detection program using a logical AND gate. The goal of the project was to shine a projected image onto a field of engineered *E. coli* cells and to have the *E. coli* release a black pigment at the boundaries where light and dark regions meet (the edges of the image). This task was accomplished using an engineered device, consisting of a dark sensor, an AND gate, a NOT gate, and a black pigment producer [41].

Briefly, the dark sensor is a modified version of a previously characterized switch [46], which contains a surface protein that activates a signaling cascade in the engineered bacteria when light is not present. When activated in the dark, this switch induces expression of LuxI, which produces the AHL 3OC6HSL, and cI. 3OC6HSL binds to and activates LuxR, which in turn activates a  $P_{\text{lux-}\lambda}$  promoter. Meanwhile, the  $P_{\text{lux-}\lambda}$  promoter is also repressed by cI. When the  $P_{\text{lux-}\lambda}$  promoter is activated, it triggers expression of  $\beta$ -galactosidase (the protein encoded by LacZ), which mediates production of a black pigment (Fig. 3a). Thus, in the presence of

abundant light, neither LuxI nor cI is activated, and black pigment is not produced. In the absence of light, both LuxI and cI are expressed abundantly, and cI effectively inhibits the production of black pigment. However, along the edges of the image, enough 3OC6HSL is produced from neighboring dark regions such that it activates  $P_{\text{lux-}\lambda}$ , whereas cI is not present in high enough concentrations to inhibit  $P_{\text{lux-}\lambda}$ . In this case, the engineered bacteria produce a black pigment. Therefore, the bacteria act as edge detectors due to the effective linking of AND and NOT gates, consisting of luxI, cI, luxR, and  $P_{\text{lux-}\lambda}$ , with the dark sensor and black pigment generator [41].

Another strategy to accomplish complex logic functions is to have separate *E. coli* strains perform different simple computations and link these logic functions using engineered communication between the different strains. By arranging these specialized cell colonies in different configurations and using QS molecules as virtual wires between the cells (Fig. 3b), Tamsir et al. constructed all 16 possible 2-input Boolean logic gates, including the very complex XOR and EQUALS functions. The group obtained five to >300-fold higher gene expression when transitioning from the OFF to the ON states for each of these logic networks [42]. Regot et al. used a similar strategy to perform complex logic functions in engineered yeast cells. In this study, two communication molecules ( $\alpha$ -factor from *S. cerevisiae* and  $\alpha$ -factor from *C. albicans*) were used to link single colonies, which performed simple logic functions. Using these elements, the authors implemented several basic logic gates, including AND, NOR, OR, NAND, XNOR, and XOR gates, as well as more complex devices, such as a multiplexer and a 1-bit adder with carry [43]. Obviously, the computational capacity of these devices is nowhere near that of their electronic counterparts. However, examples such as these represent the beginning of new methods in computation using biological substrates, which may improve with future advances in modularity, scalability, and reduction in cross-talk and noise.

## 5.2 Bioengineering

Cell-cell communication modules can also be used as critical components to aid in the engineering of circuits with practical applications. Along this line, an interesting problem that synthetic biologists encounter is that after their engineered cells perform a specific task, the cells are still present and capable of causing environmental harm or infections to human subjects. Furthermore, for specific tasks, it would be beneficial to control population size precisely if the task is sensitive to small fluctuations in gene expression. As a step towards addressing these issues, You et al. implemented a “population control” circuit, again using the LuxR/LuxI QS module. Upon circuit activation, LuxR and LuxI are both expressed. Once the population reaches a critical density, AHL can reach a high enough concentration to activate LuxR, thus inducing expression of a killer protein (CcdB) driven by a  $P_{\text{luxI}}$  promoter. An engineered cell population containing this

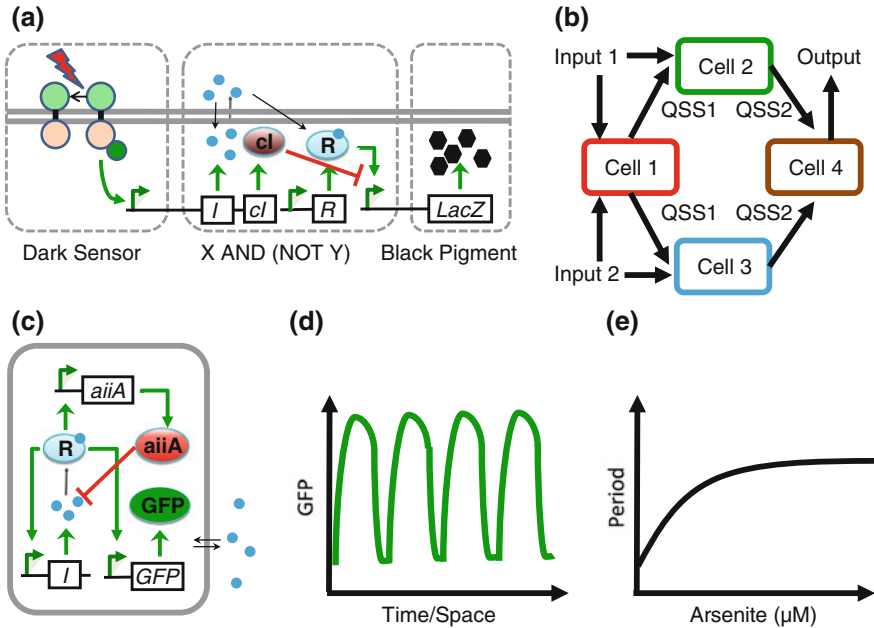


**Fig. 3** **a** Synthetic genetic edge detector. In the absence of light, a light-sensitive surface protein is phosphorylated and activates a promoter via a signal transduction pathway (*dark sensor*). This promoter drives the expression of LuxI (*I*) and *cI*. When enough AHL is synthesized in the vicinity, enough activated LuxR can induce the  $P_{lux-\lambda}$  promoter. Conversely, if enough *cI* is translated, it will repress the  $P_{lux-\lambda}$  promoter. This part of the gene network constitutes an X AND (NOT Y) logic gate. The  $P_{lux-\lambda}$  promoter then activates LacZ, which gives rise to a black pigment. The logic of the gene circuit dictates that black pigment will only be produced at the edges of a projected image, where cells are exposed to enough light such that *cI* levels are low and enough AHL from neighboring dark cells [41]. **b** QS systems as virtual wires linking logic gates. By growing isolated cell colonies containing single logic gates in a particular spatial configuration, complex computational functions can be carried out by linking colonies in close proximity via QS. For example, by adding *two inputs* (typically diffusible chemicals) to one side of a plate, one cell processor can connect with two other cell processors in parallel via a QS system. Then, these two cell processors can connect to a final cell processor in parallel via a second QS system. The final cell processor can then generate an output in the form of expression of a fluorescent protein [42]. **c** Synthetic gene circuit with interlocking positive and negative feedback loops. Genes encoding LuxI, AiiA, and *yemGFP* are all downstream of the  $P_{luxI}$  promoter, which is activated by the LuxR–AHL complex. LuxR is expressed constitutively. AiiA is an enzyme, which degrades intracellular AHL. Self-activation of LuxI constitutes a positive feedback loop, whereas inhibition via AiiA constitutes an interlocking negative feedback loop [51]. **d** Synchronized oscillations arise from the circuit in (c). The architecture of the circuit in (c) can synchronize oscillations of the GFP signal throughout a population harboring it in both the temporal and spatial domains. For a constant cell density in a microfluidic device, bulk fluorescence oscillations are observed over time. In addition, traveling waves emerge for growing colonies and densely packed monolayers [51]. **e** Modified version of the circuit in (c) can detect different arsenite concentrations. By further synchronizing the gene circuit in (c) through gaseous  $H_2O_2$  signaling and by putting LuxI downstream of an arsenite detecting pathway, Prindle et al. were able to detect statistically significant changes in oscillation period in response to varying arsenite concentrations [52]

circuit could maintain a constant population size well below carrying capacity for several days [47]. Depending on environmental conditions, the circuit could also generate robust, sustained population oscillations [48] (see below for further discussion on applications of QS in programming oscillatory dynamics).

Another application of QS-based communication modules is to coordinate the function of engineered tumor-killing bacteria [49, 50]. Several systems, constructed by Anderson et al., utilize sensor components in *E. coli* to target and kill cancer cell lines. Specifically, the systems consist of a sensor that is activated when programmed *E. coli* cells detect high cell density (QS is activated), hypoxia conditions, or arabinose in the environment. When this switch is turned ON, it activates expression of an invasion protein, derived from *Y. pseudotuberculosis*, that enables the bacteria to invade cancer cells and then release a cytotoxic agent. Interestingly, for the communication-based sensor, the group was able to demonstrate controlled invasion of cancer cells only at a high *E. coli* cell density. The authors speculate that by coupling this component with another sensor, which responds only in the presence of cancer cells (i.e., their hypoxia sensor), they can further improve specificity in targeting cancer cells [49]. This work is still ongoing and provides a useful and ambitious direction for synthetic biologists to pursue.

Cell–cell communication modules have also been used to coordinate more complex population-level dynamics, such as oscillations. Although a synthetic oscillator acting on the single-cell level was first developed over a decade ago [5], its oscillations were noisy and exhibited tremendous cell–cell variability within a population. Since then, cell–cell communication has been adopted to control such oscillations better in two ways. One approach is exemplified by the synthetic population control circuit mentioned above. In this circuit, the intracellular gene expression is directly integrated with population dynamics, leading to an integrated, population-level negative feedback. This circuit has been shown to generate robust sustained oscillations for up to several hundred hours in a microchemostat [48]. In this case, it is important to note that cell–cell variability is critical for the generation of oscillations; otherwise, the population would completely crash if all cells simultaneously commit suicide at a high enough cell density.

In contrast to the previous example, another approach is to use cell–cell communication to synchronize a population of cells, within which each cell contains its own oscillator [51]. Synthetic biologists familiar with physics and engineering are particularly excited about this development given the usefulness of the Huygens paradigm of coupled pendulum clocks, which has been applied in the development of lasers, superconductor junctions, and the global positioning system (GPS) [51]. In addition, the role of synchronized clocks in cardiac function as well as a wide variety of developmental processes makes the advance an interesting toy system for biologists. In Danino et al.'s system, *luxI*, *aiiA*, and *yemGFP* are all placed under the  $P_{luxI}$  promoter. Each component is activated when the cell density is sufficiently high, upon which the activated LuxR–AHL complex induces AiiA expression. AiiA then catalyzes AHL degradation. Thus, the system consists of interlocked positive-feedback (AHL-mediated activation of LuxI) and negative-

feedback (AiiA-mediated AHL degradation) loops (Fig. 3c). In a microfluidic device, the authors were able to demonstrate that this synthetic gene circuit produced spatiotemporal oscillations in GFP fluorescence. Importantly, the oscillatory signal was coordinated among a localized population of engineered cells via the cell–cell communication module utilized (Fig. 3d) [51].

Perhaps a population-level oscillator, by itself, does not constitute a practical application of synthetic biology. However, the same group took their system a step further by expanding on it to act as an arsenic detector. First, cells containing the modified gene circuit were arranged on a sensing array containing 500 “biopixels”. Each biopixel contained  $\sim 5,000$  *E. coli* cells. Within each biopixel, the oscillations were synchronized as described earlier via AHL signaling. In addition, the authors coordinated the oscillations among 500 biopixels using gas-phase redox signaling. The group then coupled this gene circuit to an arsenic sensor component by putting a supplementary *luxI* gene downstream of an arsenic-responsive promoter. Amazingly, when supplied with varying amounts of exogenously added arsenite, the device’s GFP oscillatory period was directly proportional to arsenite concentration (Fig. 3e). By reading the GFP oscillatory period among the many biopixels in their system, the investigators could effectively monitor arsenite concentration. They were able to quantify arsenite concentrations reliably down to  $0.2 \mu\text{M}$ , which is below the  $0.5 \mu\text{M}$  level recommended by the World Health Organization (WHO) for developing nations. Given this sensitivity, the authors put forth a design for integrating the system with a light-emitting diode (LED), photodetector, onboard processor, and graphic display in a handheld sensor to detect arsenite concentration effectively. They estimated that excluding the cost of biological components, the whole device would cost less than \$50 [52].

## 6 Disrupting Cell–Cell Communication for Potential Therapeutic Applications

Given the role of QS systems in virulence and in biofilm formation [4], efforts have been made to disrupt QS-mediated communication in pathogenic bacteria. Indeed, the development of QS inhibitors has been pursued aggressively in recent years, and various QS inhibitors have been the subject of clinical trials [53, 54]. In this section, we discuss some general strategies for inhibiting QS in pathogenic bacteria as well as a small sample of a few innovative applications of these strategies.

A common method for disrupting QS is the use of small molecules. Using this method, one can target three different steps of QS signal processing: (1) signal generation, (2) signal secretion, and (3) signal reception (Fig. 4a) [55]. Signal generation can be disrupted by inhibiting the synthase for the QS signal. Signal secretion can be interrupted by disrupting the membrane protein responsible for secretion (if it exists) or by increasing the degradation of the signal in extracellular

space. Finally, signal reception can be inhibited by introducing analog QS signals (competitive inhibition), by inactivating receptor proteins (noncompetitive inhibition), or by disrupting the signal transduction cascade leading to downstream gene activation.

One of the more common QS inhibition strategies to date is the disruption of signal reception and transduction using small molecules. As mentioned above, competitive inhibition and noncompetitive inhibition can be utilized to interfere with signal processing. Competitive inhibition is achieved through the use of analog small molecules that resemble the QS signal of interest. The goal is for the analog small molecules to saturate the receptor proteins such that the actual QS signal cannot effectively bind the receptor proteins and activate downstream gene expression. This type of competitive inhibition was introduced by Gamby et al., who synthesized a diverse set of analogs to the QS signal AI-2, which is utilized by over 70 bacterial species. Gamby et al. demonstrated that these analogs successfully disrupted AI-2 signaling in *E. coli*, *Salmonella typhimurium*, and *Pseudomonas aeruginosa* [56]. Another strategy for disrupting signal processing is noncompetitive inhibition in which a small molecule is designed to bind to the receptor protein, rendering it inactive. For example, Chen et al. engineered a small molecule that stabilized a closed conformation of the *Chromobacterium violaceum* LuxR-type protein CviR, which was unable to bind the QS signal C6-HSL [57].

Another strategy to inhibit QS involves the use of enzymatic modification of the QS signal such that it can no longer bind to its receptor protein. For example, Roy et al. introduced a protein kinase LsrK that phosphorylates and inactivates AI-2. This strategy was shown to be effective in inhibiting the QS response in *E. coli*, *S. typhimurium*, and *Vibrio harveyi* [58].

Inhibition of QS need not be restricted to the use of small molecules or proteins. Recently, investigators have developed some cell-based strategies where microbes are engineered to interfere with the QS capabilities of potentially harmful bacteria. For example, Saeidi et al. engineered *E. coli* to detect AHLs produced by pathogenic *P. aeruginosa* and then produce pyocin S5 and lysis E7 in response. The lysis protein lyses the engineered *E. coli* cells, thereby releasing pyocin S5, a bactericidal agent that kills the *P. aeruginosa* population. This method led to a 99 % reduction in viable *P. aeruginosa* cells as well as a 90 % reduction of *P. aeruginosa* biofilm formation [59]. In another example of cell-based QS inhibition, Hong et al. engineered an *E. coli* strain to produce the protein Hha13D6, which activates proteases that disperse biofilms, while communicating with other cell strains via QS. This cell strain was able to disperse an existing biofilm formed by another engineered *E. coli* strain via QS and then replace it with its own biofilm [60]. In the future, this strategy could perhaps be utilized to replace a biofilm of a pathogenic cell strain with a biofilm of a relatively innocuous strain, which could then be removed more easily.

Both studies discussed above were carried out in vitro and thus were not subject to the many complicating factors that are present physiologically. However, Duan and March provided a proof-of-concept demonstration of the efficacy of QS inhibition in vivo using an infant mouse model. Briefly, the *E. coli* Nissle 1917

strain was engineered to produce cholera autoinducer 1 (CAI-1), which was aimed at disrupting the proper timing of *Vibrio cholerae* virulence expression and colonization. Indeed, 8 h pretreatment with the *E. coli* strain increased the mouse's survival 92 % after ingestion of *V. cholerae*, whereas coingestion of the *E. coli* with *V. cholerae* increased survival 27 % [61]. Such a strategy may have implications for treating cholera and other infections that plague human health.

## 7 Engineering Artificial Cell–Cell Communication Modules

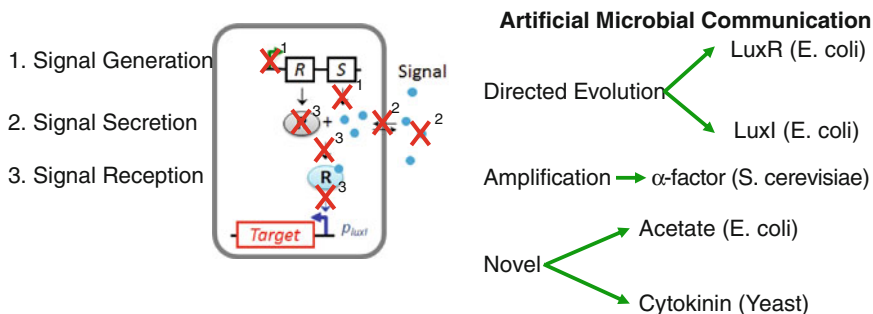
Most of the systems we have described previously rely on existing QS systems from closely related species to implement synthetic communication in bacteria and yeast pheromones to implement synthetic communication in yeast. However, improvements to these existing communication modules as well as the development of new communication modules are likely to expedite the advancement of synthetic systems that communicate on a population-level. Improvements to existing QS modules make components more malleable to mesh with other design specifications. Novel communication modules provide more options when constructing synthetic systems and alleviate various concerns regarding modularity, scalability, and cross-talk between closely related QS modules.

### 7.1 Improvements to Existing Cell–Cell Communication Modules

A common approach to improve naturally existing QS modules is to utilize directed evolution to evolve such modules towards desired functions (Fig. 4b). Briefly, the goal of directed evolution is to engineer a specific protein function through several rounds of mutation and selection. The process starts with a parent protein, which performs a task close to that desired for a specific component in the designed system. A large library of DNA encoding mutant versions of the parent protein can be generated via a number of methods, including error-prone PCR, recombination, and computer-guided mutagenesis. The library of mutants is then tested for functionality via a functional assay, which generally consists of a high-throughput screen or selection. After multiple rounds of mutation and selection, a mutant version of the parent protein is identified that best fits the design criteria of the engineered system [62].

This process of directed evolution has been applied to a number of QS components. For example, Collins et al. were able to change the signaling specificity of a version of LuxR using a dual selection assay. Specifically, they wanted to take an initial version of LuxR that responded to a broad range of acyl-HSLs, including straight-chain acyl-HSLs, and derive from it a mutant version which no longer responds to its native cognate signal 3OC6HSL, while retaining its response to straight-chain acyl-HSLs. The assay consists of two rounds of random mutagenesis





### Artificial Mammalian Communication

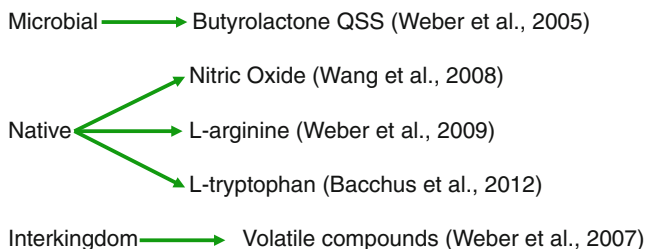


**Fig. 4** **a** Targets for disrupting QS. There are three targets for disrupting QSSs: (1) signal generation, (2) signal secretion, and (3) signal reception. Signal generation can be disrupted by inhibiting transcription or translation of the protein synthesizing the signal. Signal secretion can be disrupted by interfering with the secretion of the signal itself or by degrading the signal. Signal reception can be disrupted by interfering with the receptor protein or the ability of the receptor protein to activate downstream processes [55]. **b** Artificial microbial cell–cell communication channels. Directed evolution was utilized to change the responsiveness of LuxR to varying chemical signals and the synthesis rate of AHL by LuxI in *E. coli* [62]. Amplification of the  $\alpha$ -factor signal increased system responsiveness in *S. cerevisiae* [65]. Recent novel artificial communication systems include acetate in *E. coli* [66] and cytokinin in various yeast strains [67]. **c** Artificial mammalian cell–cell communication channels. These channels have three origins: microbial, native, and interkingdom. The QS system involving butyrolactone was ported from the microbe *S. coelicolor* and retrofitted to mammalian cells [68]. Native signals NO [69], L-arginine [70], and L-tryptophan [71] have all been used as communication signals in synthetic mammalian systems. Finally, various volatile compounds from many kingdoms have been used to mediate communication between synthetic mammalian cells and cells from other kingdoms [72]

and selection. For rounds of ON selection, a library of mutagenized *luxR* genes was cotransformed with a construct containing a chloramphenicol-resistance gene downstream of the  $P_{luxI}$  promoter. The colonies were exposed to alternate straight-chain acyl-HSLs in plates containing chloramphenicol. Thus, only those mutants that could effectively respond to the alternate acyl-HSLs were selected after several rounds. Similarly, for each round of OFF selection, the library of mutagenized *luxR* genes was cotransformed with a construct containing  $\beta$ -lactamase inhibitory protein (Bli) downstream of the  $P_{luxI}$  promoter along with constitutively expressed  $\beta$ -lactamase. Here,  $\beta$ -lactamase confers resistance to carbenicillin, and Bli can inhibit  $\beta$ -lactamase. In this manner, in the presence of 3OC6HSL and

carbenicillin, only the mutagenized LuxR proteins that do not respond to 3OC6HSL are selected. Multiple rounds of ON and OFF selection identified a LuxR mutant that responds to straight-chain acyl-HSLs but not 3OC6HSL [63]. This novel selection method can theoretically be applied to achieve LuxR specificity for any number of QS signals, while eliminating responses to other QS signals. Therefore, the method can be applied to eliminate or greatly reduce cross-talk in synthetic systems requiring multiple modes of communication.

Selection can also be applied to obtain mutants of LuxI, which synthesize more 3OC6HSL. Kambam et al. accomplished this by cotransforming a plasmid that constitutively expressed LuxR and LuxI mutants with a plasmid containing the  $P_{luxI}$  promoter driving expression of  $\beta$ -lactamase. By selecting for colonies that grew in the presence of very high concentrations of ampicillin (an analog of carbenicillin), the investigators obtained LuxI mutants that synthesize 80-fold more 3OC6HSL than the wild-type version [64]. From an engineering perspective, the ability to modulate 3OC6HSL synthesis capacity is useful as it may be necessary to tune such a parameter to fit the design of a given system.

Enhancement of the production of a communication signal can also be accomplished without the need for genetic selection. For example, using the *S. cerevisiae* pheromone  $\alpha$ -factor as a cell–cell communication module, Gross et al. introduced amplifier strains that would respond to environmental  $\alpha$ -factor by producing more  $\alpha$ -factor themselves. In this fashion, the group achieved a more sensitive response to  $\alpha$ -factor within a mixed population of yeast cells (Fig. 4b) [65]. Again, this strategy could be utilized by synthetic biologists constructing systems that require a highly sensitive response to cell–cell signaling.

## 7.2 Novel Microbial Cell–Cell Communication Modules

Bulter et al. engineered an artificial cell–cell communication system in *E. coli* by rewiring its metabolic pathway. The group knocked out the main production pathway of acetate from AcCoA to make acetate a function of cell growth, rather than a function of metabolic state or environmental conditions (Fig. 4b). Furthermore, by knocking out the histidine kinase NR<sub>II</sub>, the group simplified the intake process of acetate such that a signaling cascade initiated in proportion to acetate concentration induced the promoter *glnAp<sub>2</sub>* [66]. Similarly, Chen and Weiss effectively integrated a modified plant hormone communication system in yeast (Fig. 4b). In their system, the plant hormone cytokinin is synthesized in proportion to cell density and subsequently activates a phosphorylation pathway that induces an SSRE promoter [67]. Because both of these modules are synthetic, their signaling is highly specific and unlikely to initiate undesirable cross-talk. Furthermore, the modules provide synthetic biologists with more communication pathways to utilize when engineering systems that require many channels of communication.

### 7.3 *Engineered Mammalian Cell–Cell Communication Modules*

In general, engineering of mammalian cells has lagged behind engineering of bacteria or even yeast. This is primarily due to the mammalian cell's greater complexity and a poorer understanding of the cellular processes in the mammalian cell. However, the last several years have witnessed some rapid progress in the engineering of synthetic gene circuits in mammalian cells, including the creation of artificial cell–cell communication (Fig. 4c) [68–72].

One method of accomplishing artificial mammalian cell–cell communication is to port a well-studied communication module into mammalian cells. Weber et al. did precisely this by porting a QS module from the bacterium *Streptomyces coelicolor* into several mammalian (including human) cell lines. Briefly, this process was done in two steps: the QS receptor protein was fused to a human transsilencing domain; and the QS-inducible promoter was constructed using 8 tandem transsilencer-specific operator modules derived from a viral promoter. Thus, the QS module was “retrofitted” to be effective in mammalian cells. Weber et al. suggested several desirable features that this retrofitted system offers, including a high sensitivity to low doses of the QS signal butyrolactone and low basal expression in the absence of butyrolactone [68].

Another method for introducing artificial cell–cell communication in mammalian cells is to rely on natural cell–cell signaling molecules. For example, Wang et al. used nitric oxide (NO) as an effective QS signal in A549 human lung carcinoma cells. In their system, the QS signal NO was produced when NO synthase (NOS) catalyzed the conversion of L-arginine to L-citrulline, leaving behind NO, which is secreted outside the cell membrane. By inducing a signaling cascade, sufficient concentrations of NO activate the *c-fos* promoter. The authors suggest that this cell–cell communication module is advantageous to the previous portable QS network because NO is more compatible with mammalian cells. In addition, NO diffuses across cellular membranes without the need for specific membrane channels [69].

Another natural cell-signaling molecule utilized to enable mammalian cell–cell communication is L-arginine. Weber et al. synthesized this molecule using a human liver-type arginase in a human sender cell. Meanwhile, a Chinese hamster ovary (CHO) cell line, equipped with a transgene expression system, which converts L-arginine concentrations into transcription of GFP in a dose-dependent manner, constituted the receiver cell [70]. In this manner, Weber et al. successfully implemented a communication system in mammalian cells that was activated at high cell densities. Similarly, the same group recently implemented mammalian cell–cell communication with another amino acid, L-tryptophan [71]. However, for the L-tryptophan, L-arginine, and NO communication modules, given their widespread importance in mammalian cell signaling, those wishing to use these modules must be mindful of cross-talk with other natural gene networks.

## 7.4 *Engineered Inter- and Intrakingdom Communication*

Weber et al. also designed synthetic cell–cell communication among different species and kingdoms. Specifically, airborne communication was introduced between and within populations of mammalian cells, yeast, plants, and bacteria. The basis of this communication was volatile acetaldehyde. One potential advantage of airborne communication is that it affords the opportunity of communication between sender and receiver cells that do not occupy the same liquid-phase environment [72]. Furthermore, this mode of communication allows for synchronization of very different organisms with specific capabilities or specialties and therefore can aid in activating a consortium of varying organisms assigned to different tasks.

## 8 Conclusion

Here, we have discussed recent studies of synthetic biological systems that utilize cell–cell communication. These systems span a wide variety of implementations and applications. Although the number and quality of studies on such systems is impressive, it is important to remember that synthetic biology is still quite new. The field has started as more of an art form than an engineering discipline with many rounds of trial and error before a suitable system is identified that is sufficient to achieve the initial design goals. However, the field is now transitioning towards the engineering of well-defined components that behave as predicted. As the field reaches this transition point, synthetic biologists will likely be spared the frustrating trial-and-error process and be free to tackle new challenges better. These challenges will include biological challenges, such as the unintended consequences of host–circuit interactions [73, 74], the impact of stochastic gene expression [75–77], and the limits of the metabolic capacity of the cell [78, 79], as well as technical challenges, such as the realtime monitoring of gene circuit components [80, 81], the development of high-throughput functional assays to test new biological devices [82, 83], and the limits of high-fidelity DNA synthesis technologies [84, 85]. Although these problems may seem daunting, one can take comfort in the fact that incremental improvement in dealing with each of these challenges exponentially improves our capacity to generate useful biological parts faster, cheaper, and more predictably.

**Acknowledgments** Related research in the You lab is supported by NIH (1R01-GM098642), a DuPont Young Professorship (LY), a National Science Foundation CAREER award (LY), a David and Lucile Packard Fellowship (LY), North Carolina Biotechnology Center (2012-MRG-1102), and the Office of Naval Research (N00014-12-1-0631).

## References

1. Rokas A (2008) The origins of multicellularity and the early history of the genetic toolkit for animal development. *Annu Rev Genet* 42:235–251
2. Ispolatov I, Ackermann M, Doebeli M (2012) Division of labour and the evolution of multicellularity. *Proc Biol Sci* 279(1734):1768–1776
3. LeRoith D, Shemer J, Roberts CT Jr (1992) Evolutionary origins of intercellular communication systems: implications for mammalian biology. *Horm Res* 38(2):1–6
4. Choudhary S, Schmidt-Dannert C (2010) Applications of quorum sensing in biotechnology. *Appl Microbiol Biotechnol* 86(5):1267–1279
5. Elowitz MB, Leibler S (2000) A synthetic oscillatory network of transcriptional regulators. *Nature* 403(6767):335–338
6. Gardner TS, Cantor CR, Collins JJ (2000) Construction of a genetic toggle switch in *Escherichia coli*. *Nature* 403(6767):339–342
7. Yokobayashi Y, Weiss R, Arnold FH (2002) Directed evolution of a genetic circuit. *Proc Natl Acad Sci U S A* 99(26):16587–16591
8. Guet CC et al (2002) Combinatorial synthesis of genetic networks. *Science* 296(5572):1466–1470
9. Chuang JS (2012) Engineering multicellular traits in synthetic microbial populations. *Curr Opin Chem Biol* 16:370–378
10. Pai A et al (2009) Engineering multicellular systems by cell–cell communication. *Curr Opin Biotechnol* 20(4):461–470
11. Xavier JB (2011) Social interaction in synthetic and natural microbial communities. *Mol Syst Biol* 7:483
12. Tsao C-Y, Quan DN, Bentley WE (2012) Development of the quorum sensing biotechnological toolbox. *Curr Opin Chem Eng* 1(4):396–402
13. Shong J, Jimenez Diaz MR, Collins CH (2012) Towards synthetic microbial consortia for bioprocessing. *Curr Opin Biotechnol* 2:1–5
14. Waters CM, Bassler BL (2005) Quorum sensing: cell-to-cell communication in bacteria. *Annu Rev Cell Dev Biol* 21:319–346
15. Parsek MR, Greenberg EP (2000) Acyl-homoserine lactone quorum sensing in gram-negative bacteria: a signaling mechanism involved in associations with higher organisms. *Proc Natl Acad Sci U S A* 97(16):8789–8793
16. Schaefer AL et al (2008) A new class of homoserine lactone quorum-sensing signals. *Nature* 454(7204):595–599
17. Hooshangi S, Bentley WE (2008) From unicellular properties to multicellular behavior: bacteria quorum sensing circuitry and applications. *Curr Opin Biotechnol* 19(6):550–555
18. Balagadde FK et al (2008) A synthetic *Escherichia coli* predator-prey ecosystem. *Mol Syst Biol* 4:187
19. Song H et al (2009) Spatiotemporal modulation of biodiversity in a synthetic chemical-mediated ecosystem. *Nat Chem Biol* 5(12):929–935
20. Shou W, Ram S, Vilar JM (2007) Synthetic cooperation in engineered yeast populations. *Proc Natl Acad Sci U S A* 104(6):1877–1882
21. Hu B et al (2010) An environment-sensitive synthetic microbial ecosystem. *PLoS One* 5(5):e10619
22. Kim HJ et al (2008) Defined spatial structure stabilizes a synthetic multispecies bacterial community. *Proc Natl Acad Sci U S A* 105(47):18188–18193
23. Brenner K, Arnold FH (2011) Self-organization, layered structure, and aggregation enhance persistence of a synthetic biofilm consortium. *PLoS One* 6(2):e16791
24. Chuang JS, Rivoire O, Leibler S (2009) Simpson’s paradox in a synthetic microbial system. *Science* 323(5911):272–275

25. Pai A, Tanouchi Y, You L (2012) Optimality and robustness in quorum sensing (QS)-mediated regulation of a costly public good enzyme. *Proc Natl Acad Sci U S A* 109(48):19810–19815
26. Pai A, You L (2009) Optimal tuning of bacterial sensing potential. *Mol Syst Biol* 5:286
27. Sekine R et al (2011) Tunable synthetic phenotypic diversification on Waddington's landscape through autonomous signaling. *Proc Natl Acad Sci U S A* 108(44):17969–17973
28. Keller EF, Segel LA (1970) Initiation of slime mold aggregation viewed as an instability. *J Theor Biol* 26(3):399–415
29. Goldbeter A (2006) Oscillations and waves of cyclic AMP in *Dictyostelium*: a prototype for spatio-temporal organization and pulsatile intercellular communication. *Bull Math Biol* 68(5):1095–1109
30. Harris MP et al (2005) Molecular evidence for an activator-inhibitor mechanism in development of embryonic feather branching. *Proc Natl Acad Sci U S A* 102(33):11734–11739
31. Chou CS et al (2010) Spatial dynamics of multistage cell lineages in tissue stratification. *Biophys J* 99(10):3145–3154
32. Greco V et al (2009) A two-step mechanism for stem cell activation during hair regeneration. *Cell Stem Cell* 4(2):155–169
33. Basu S et al (2005) A synthetic multicellular system for programmed pattern formation. *Nature* 434(7037):1130–1134
34. Matsuda M et al (2012) Synthetic signal propagation through direct cell–cell interaction. *Sci Signal* 5(220):ra31
35. Turing AM (1990) The chemical basis of morphogenesis. 1953. *Bull Math Biol* 52(1–2):153–197 (discussion 119–152)
36. Liu C et al (2011) Sequential establishment of stripe patterns in an expanding cell population. *Science* 334(6053):238–241
37. Saunders RE, Gough JE, Derby B (2008) Delivery of human fibroblast cells by piezoelectric drop-on-demand inkjet printing. *Biomaterials* 29(2):193–203
38. Xu T et al (2005) Inkjet printing of viable mammalian cells. *Biomaterials* 26(1):93–99
39. Roth EA et al (2004) Inkjet printing for high-throughput cell patterning. *Biomaterials* 25(17):3707–3715
40. Choi WS et al (2011) Synthetic multicellular cell-to-cell communication in inkjet printed bacterial cell systems. *Biomaterials* 32(10):2500–2507
41. Tabor JJ et al (2009) A synthetic genetic edge detection program. *Cell* 137(7):1272–1281
42. Tamsir A, Tabor JJ, Voigt CA (2011) Robust multicellular computing using genetically encoded NOR gates and chemical 'wires'. *Nature* 469(7329):212–215
43. Regot S et al (2011) Distributed biological computation with multicellular engineered networks. *Nature* 469(7329):207–211
44. Moon TS et al (2012) Genetic programs constructed from layered logic gates in single cells. *Nature* 491(7423):249–253
45. Brenner K et al (2007) Engineered bidirectional communication mediates a consensus in a microbial biofilm consortium. *Proc Natl Acad Sci U S A* 104(44):17300–17304
46. Levskaaya A et al (2005) Synthetic biology: engineering *Escherichia coli* to see light. *Nature* 438(7067):441–442
47. You L et al (2004) Programmed population control by cell–cell communication and regulated killing. *Nature* 428(6985):868–871
48. Balagadde FK et al (2005) Long-term monitoring of bacteria undergoing programmed population control in a microchemostat. *Science* 309(5731):137–140
49. Anderson JC et al (2006) Environmentally controlled invasion of cancer cells by engineered bacteria. *J Mol Biol* 355(4):619–627
50. Xie Z et al (2011) Multi-input RNAi-based logic circuit for identification of specific cancer cells. *Science* 333(6047):1307–1311
51. Danino T et al (2010) A synchronized quorum of genetic clocks. *Nature* 463(7279):326–330

52. Prindle A et al (2012) A sensing array of radically coupled genetic ‘biopixels’. *Nature* 481(7379):39–44
53. Smyth AR et al (2010) Garlic as an inhibitor of *Pseudomonas aeruginosa* quorum sensing in cystic fibrosis—a pilot randomized controlled trial. *Pediatr Pulmonol* 45(4):356–362
54. Kohler T et al (2010) Quorum sensing inhibition selects for virulence and cooperation in *Pseudomonas aeruginosa*. *PLoS Pathog* 6(5):e1000883
55. Roy V, Adams BL, Bentley WE (2011) Developing next generation antimicrobials by intercepting AI-2 mediated quorum sensing. *Enzyme Microb Technol* 49(2):113–123
56. Gamby S et al (2012) Altering the communication networks of multispecies microbial systems using a diverse toolbox of AI-2 analogues. *ACS Chem Biol* 7:1023–1030
57. Chen G et al (2011) A strategy for antagonizing quorum sensing. *Mol Cell* 42(2):199–209
58. Roy V et al (2010) Cross species quorum quenching using a native AI-2 processing enzyme. *ACS Chem Biol* 5(2):223–232
59. Saeidi N et al (2011) Engineering microbes to sense and eradicate *Pseudomonas aeruginosa*, a human pathogen. *Mol Syst Biol* 7:521
60. Hong SH et al (2012) Synthetic quorum-sensing circuit to control consortial biofilm formation and dispersal in a microfluidic device. *Nat Commun* 3:613
61. Duan F, March JC (2010) Engineered bacterial communication prevents *Vibrio cholerae* virulence in an infant mouse model. *Proc Natl Acad Sci U S A* 107(25):11260–11264
62. Romero PA, Arnold FH (2009) Exploring protein fitness landscapes by directed evolution. *Nat Rev Mol Cell Biol* 10(12):866–876
63. Collins CH, Leadbetter JR, Arnold FH (2006) Dual selection enhances the signaling specificity of a variant of the quorum-sensing transcriptional activator LuxR. *Nat Biotechnol* 24(6):708–712
64. Kambam PK et al (2008) Directed evolution of LuxI for enhanced OHHL production. *Biotechnol Bioeng* 101(2):263–272
65. Gross A, Rodel G, Ostermann K (2011) Application of the yeast pheromone system for controlled cell–cell communication and signal amplification. *Lett Appl Microbiol* 52(5):521–526
66. Bulter T et al (2004) Design of artificial cell–cell communication using gene and metabolic networks. *Proc Natl Acad Sci U S A* 101(8):2299–2304
67. Chen MT, Weiss R (2005) Artificial cell–cell communication in yeast *Saccharomyces cerevisiae* using signaling elements from *Arabidopsis thaliana*. *Nat Biotechnol* 23(12):1551–1555
68. Weber W et al (2005) Engineered *Streptomyces* quorum-sensing components enable inducible siRNA-mediated translation control in mammalian cells and adjustable transcription control in mice. *J Gene Med* 7(4):518–525
69. Wang WD et al (2008) Construction of an artificial intercellular communication network using the nitric oxide signaling elements in mammalian cells. *Exp Cell Res* 314(4):699–706
70. Weber W et al (2009) A synthetic metabolite-based mammalian inter-cell signaling system. *Mol Biosyst* 5(7):757–763
71. Bacchus W et al (2012) Synthetic two-way communication between mammalian cells. *Nat Biotechnol* 30(10):991–996
72. Weber W, Daoud-El Baba M, Fussenegger M (2007) Synthetic ecosystems based on airborne inter- and intrakingdom communication. *Proc Natl Acad Sci U S A* 104(25):10435–10440
73. Tan C, Marguet P, You L (2009) Emergent bistability by a growth-modulating positive feedback circuit. *Nat Chem Biol* 5(11):842–848
74. Marguet P et al (2010) Oscillations by minimal bacterial suicide circuits reveal hidden facets of host-circuit physiology. *PLoS One* 5(7):e11909
75. Elowitz MB et al (2002) Stochastic gene expression in a single cell. *Science* 297(5584):1183–1186
76. Eldar A, Elowitz MB (2010) Functional roles for noise in genetic circuits. *Nature* 467(7312):167–173

77. Minsky B, Neuert G, van Oudenaarden A (2012) Using gene expression noise to understand gene regulation. *Science* 336(6078):183–187
78. Henry CS, Broadbelt LJ, Hatzimanikatis V (2007) Thermodynamics-based metabolic flux analysis. *Biophys J* 92(5):1792–1805
79. Varma A, Palsson BO (1993) Metabolic capabilities of *Escherichia-Coli*.1. Synthesis of biosynthetic precursors and cofactors. *J Theor Biol* 165(4):477–502
80. Young JW et al (2012) Measuring single-cell gene expression dynamics in bacteria using fluorescence time-lapse microscopy. *Nat Protoc* 7(1):80–88
81. Wyart M, Botstein D, Wingreen NS (2010) Evaluating gene expression dynamics using pairwise RNA FISH data. *PLoS Comput Biol* 6(11):e1000979
82. Khalil AS, Collins JJ (2010) Synthetic biology: applications come of age. *Nat Rev Genet* 11(5):367–379
83. Cheng AA, Lu TK (2012) Synthetic biology: an emerging engineering discipline. *Annu Rev Biomed Eng* 14:155–178
84. Kosuri S et al (2010) Scalable gene synthesis by selective amplification of DNA pools from high-fidelity microchips. *Nat Biotechnol* 28(12):1295–1299
85. Ma S, Tang N, Tian J (2012) DNA synthesis, assembly and applications in synthetic biology. *Curr Opin Chem Biol* 16(3–4):260–267



# Application of Biofilm Bioreactors in White Biotechnology

**K. Muffler, M. Lakatos, C. Schlegel, D. Strieth, S. Kuhne  
and R. Ulber**

**Abstract** The production of valuable compounds in industrial biotechnology is commonly done by cultivation of suspended cells or use of (immobilized) enzymes rather than using microorganisms in an immobilized state. Within the field of wastewater as well as odor treatment the application of immobilized cells is a proven technique. The cells are entrapped in a matrix of extracellular polymeric compounds produced by themselves. The surface-associated agglomerate of encapsulated cells is termed biofilm. In comparison to common immobilization techniques, toxic effects of compounds used for cell entrapment may be neglected. Although the economic impact of biofilm processes used for the production of valuable compounds is negligible, many prospective approaches were examined in the laboratory and on a pilot scale. This review gives an overview of biofilm reactors applied to the production of valuable compounds. Moreover, the characteristics of the utilized materials are discussed with respect to support of surface-attached microbial growth.

**Keywords** Biofilm · Biofilm engineering · Biofilm reactor · Bulk and fine chemicals · Catalysis · Industrial production · Productive biofilms

## Contents

1	Introduction.....	124
2	Biofilm Bioreactors and Applications .....	128
2.1	Substrates for Biofilm Support .....	130
2.2	Reactor Types for Biofilm Processes .....	136

---

K. Muffler · C. Schlegel · D. Strieth · S. Kuhne · R. Ulber (✉)  
Institute of Bioprocess Engineering, University of Kaiserslautern,  
Gottlieb-Daimler-Straße 49, 67663 Kaiserslautern, Germany  
e-mail: ulber@mv.uni-kl.de

M. Lakatos  
Experimental Ecology, University of Kaiserslautern, Erwin-Schrödinger-Straße 13,  
67663 Kaiserslautern, Germany

3	Potential of Biofilm Reactors within Biotechnological Production Processes .....	146
3.1	Applications of Biofilm Bioreactors for Production of Value-Added Bulk and Fine Chemicals .....	146
3.2	Prospective Applications of Biofilms in Biotechnological Production Processes .....	154
4	Summary and Outlook .....	155
	References .....	156

## 1 Introduction

Within industrial biotechnology production processes the term “biofilm” is mainly associated with strong negative impacts on process control and product quality related to adherent growing microorganisms. For example, they are able to block heat exchangers and thus process economy decreases. Applications of biofilms as well as microbial communities growing as flocs have a long history concerning the treatment of wastewater or flue gas, whereas the organisms reduce the organic load of the input streams. A high biomass concentration is required to allow the necessary degradation rates of the waste and to minimize the dimension of the plant. This chapter focuses on the production of value-added products by application of biofilms. However, discussion of the economics of biofilm processes may also consider these low-value high-scale applications for adherent growing organisms, as the general concept is quite the same for other processes: provide a maximum of (immobilized) biomass to establish a (semi-) continuous production process with an appropriate space–time yield.

One major argument to reject biofilm processes is the problem of controlling the adherent growth of microorganisms, even though many recombinant human proteins or monoclonal antibodies, for example, are produced on an industrial scale by adherent growing (mammalian) organisms [1]. However, there is commonly no alternative to produce the requested target compounds and thus “films” of organisms can be considered as well established within the field of red biotechnology, but up to now without using the expression “biofilm”. Harding et al. proposed some criteria that should be fulfilled to characterize adherent growing (fungal) cells as biofilms which can be summarized as [2]:

- Surface associated growth of cells
- Embedding of the cells in a self-produced and secreted matrix of extracellular polymeric substances
- Altered gene expression due to attached growth.

Even though Harding et al. focused on filamentous fungi and the debate about the ability of fungi to grow in a biofilm state, this set of traits can be considered as core criteria defining a biofilm. Thus, the definition can also be transferred to other prokaryotic and eukaryotic types of cells.

**Table 1** Properties of immobilized cells in biocatalysis (according to [3])

Advantages	Disadvantages
Application of a multistep enzyme reaction is possible	Catalysis of unwanted side-reactions due to occurrence of numerous catalytically active enzymes
High enzyme activity upon immobilization	Contamination of the suspension due to leakage of cells
Good operational stability	Mass transfer of the substrate and product through cell membrane and immobilizing matrix may be limited
Use of high cell densities	
Cell densities and enzyme activities can be expected over a long period of operation	
Products can easily be recovered from immobilized cells	
Immobilized cells appear to be less affected by microbial contamination	

Because the variety of products of white biotechnology operations range from low- to high-value commodities reflecting the production of bulk and fine chemicals, these operations have to compete with established processes that usually apply submerged growing organisms. An overview of the pros and cons concerning the application of immobilized cells, which can be transferred without further ado to the biofilm concept, is given in Table 1.

The relevance of the emerging field of biofilm research in biotechnology becomes particularly obvious if one considers the number of publications per year for the terms “biofilm” and “biotechnology” collected by Web of Knowledge (Thomson Reuters) in June 2013 (cf. Fig. 1). Even though only a small fraction of the number of papers is directly focused on productive biofilms, this diagram illustrates the prosperous field of this research area.

The immobilization of the target organism can be achieved by active or passive methods. Active methods are characterized by application of external compounds to link the cells together (*cross-linking*) or to a surface (*covalent bonding*) as well as entrapment in a matrix, whereas passive immobilization approaches use adsorption or colonization of a substratum by microbial cells [3]. Thus, the generation of biofilms falls in this latter category, but it is worth mentioning that a biofilm approach might also be used in a broader way than the common immobilization techniques. Usually, immobilized cells are used for biocatalytic processes that can be categorized into fermentation and biotransformation processes. Whereas, during fermentation, the target compound directly results from the carbon source used for cell growth, within biotransformation the product is formed from an additional supplied compound [4]. An accumulation of intracellular products as well as an accumulation of biomass is not addressed because the isolation of products from encapsulated cells is disfavored; furthermore, biomass accumulation may result in disruption of the matrix and release from the support.

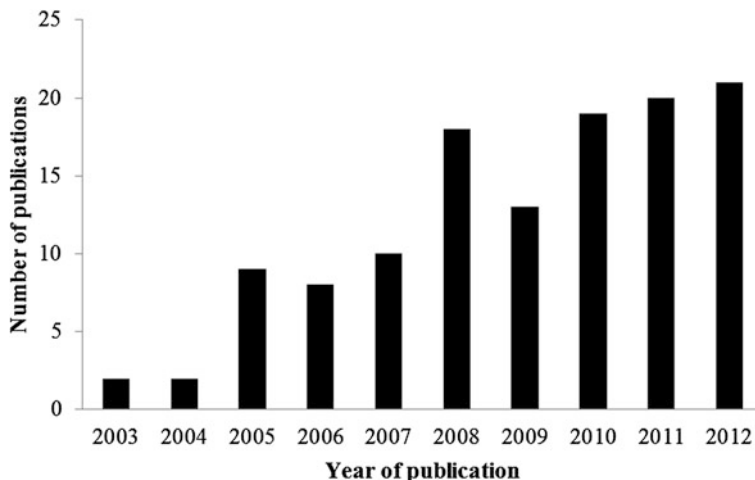


**Fig. 1** Number of publications per year for the terms “biofilm” and “biotechnology” collected by Web of Knowledge (Thomson Reuters) in June 2013

However, some approaches are reported whereas biofilms are used for production of intracellular compounds (see Sect. 3). This might be an interesting approach, inasmuch as the matrix is extended by the “productive” cells in the required manner, but a release of cells cannot be neglected. Of course, the production of intracellular compounds using immobilized microorganisms is a challenging task, in particular with respect to process engineering as well as the economics of the process. Thus, an application might be beneficial solely for high-value fine chemicals.

One of the first processes that used immobilized whole cells (*Rhodococcus* sp.) to produce a commodity was the production of acrylamide by Nitto Chemical Co. (now Mitsubishi Rayon), which was established in 1991 and produces more than 30,000 tons per year [5]. Unlike the standard copper-catalyzed hydration of acrylonitrile, carried out at 100 °C, the biotransformation approach can be performed below 10 °C. A tremendous advantage of this process is the reduced generation of by-products in comparison to the chemical route. However, for this industrial process, no self-immobilization is applied. *Rhodococcus rhodochrous* J1 is immobilized in a cationic acrylamide polymer gel lattice, by mixing cells suspended in a buffer (potassium phosphate) with a solution of monomers (acrylamide/dimethylaminoethyl methacrylate/*N,N'*-methylenebisacrylamide). Via addition of  $\beta$ -dimethylaminopropionitrile and ammonium persulfate the polymerization is initiated [6]. Indeed, the cells are immobilized in an artificial matrix, thus the definition of a biofilm is not fulfilled. But this process demonstrates that immobilized cells are already in use even for industrial-scale biocatalytic processes.

The most often cited application of biofilms in terms of industrial biotechnology is the production of acetic acid. The process is established on a 60-m<sup>3</sup> scale and is used for manufacturing vinegar rather than production of acetic acid as a

**Table 2** Major pros and cons of biofilm processes

Pros	Cons
Self-immobilization of the organism without additional (harmful) agents	Mass transfer is limited by the extracellular matrix
Robustness of the immobilized cells towards fluctuating process conditions	Process control of the adherent growing microorganisms is restricted
Long-term stability of processes; continuous process can be established	Generation and maintaining of biofilms currently not possible as required for production processes
Expression of target genes often increased in the biofilm state	No standard procedures for degradation of biofilms available (e.g., for cleaning processes)

bulk chemical [7]. This is due to process economics that is much more favorable for the Monsanto process, whereas acetic acid is produced from methanol by catalytic carbonylation. The biotechnological surface process—also termed *quick process*—uses immobilized acetic acid bacteria (Gram-negative, acid-tolerant strains such as *Acetobacter* sp. or *Gluconobacter* sp.) which grow on beechwood shavings in a trickle-bed reactor [8]. As substrates, ethanol or, for example, mashes from wine or cider production can be used. The oxidation of ethanol to acetic acid via acetaldehyde is coupled with the availability of oxygen, particularly due to the fact that the bacteria perish if the aeration is interrupted, even for short interruption cycles [7]. However, this example illustrates that actually strictly aerobic operations can be tackled on an industrial scale by use of biofilm reactors. With regard to scale and use for industrial manufacturing processes, the number of applications is very limited. Some prospective applications of biofilm reactors for the production of value-added products are outlined within the following sections. Some of the major pros and cons of biofilm processes are illustrated in Table 2.

In order to investigate the capability of widely used industrial and lab strains to grow in a biofilm state, Li et al. screened 68 strains, wherein 66 species featured biofilm formation and more than 50 % were classified as strong biofilm formers [9]. Moreover, the biofilm-forming capacity of a model organism (*Zymomonas mobilis*) was investigated in packed-bed reactors. Raschig rings of several construction materials (glass, polypropylene (PP), silastic, stainless steel) were tested for biofilm growth and stainless steel meshes have shown the highest accumulation of biomass. These data indicate that most of the commonly applied microorganisms in biotechnology feature the attached growth state. Thus, providing the right biofilm bioreactor set-up, such organisms might be cultivated and used as productive “work horses” even in industrial applications. However, the capability of a strain to adhere on a substratum (a prerequisite of biofilm generation) is a characteristic trait of the organism but only one factor of a set of criteria that must be considered to support efficient formation of biofilms. The most important factors affecting the microbial adhesion are illustrated in Fig. 2.

The following sections give a survey of current activities within the emerging field of biofilm applications for production of valuable compounds. Initially, the different configurations of applied bioreactors are introduced, followed by a

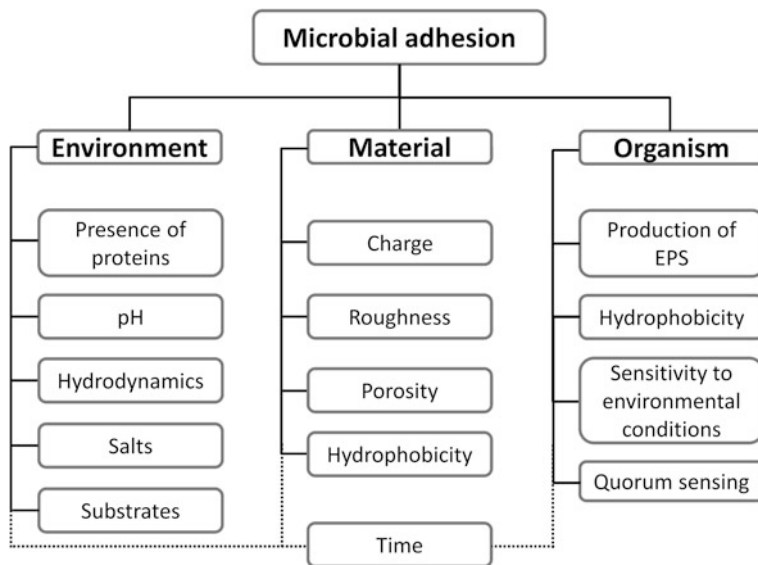


**Fig. 2** Main parameters affecting microbial adhesion on a surface/substratum

discussion about the materials applicable as biofilm supports. Several examples are presented subsequently, whereas the biofilm support, the reactor configuration, and the product formation are discussed in detail according to different classes of commodities. Finally, the potential of biofilms within industrial biotechnology is discussed bringing together the often-cited advantages of biofilms and recently published ideas of the academic realm that might push a possible transfer of such process from lab to production scale.

## 2 Biofilm Bioreactors and Applications

In principle, reactors for biofilms can be divided according to the flow pattern into different categories, including stirred-tank reactors, fixed-bed reactors, and fluidized-bed reactors. Combination and modification of these basic reactor systems broaden the range of available reactor types to improve, for example, mass transfer characteristics.

Selection of a proper reactor system is important to reflect the microbial traits and the properties of the biomass support particles or surfaces. If a transformation is carried out whereas gaseous educts or (by-)products are involved, the reactor system should support high-mass transfer of these gases. Thus, three-phase reactor systems such as a fluidized-bed or trickle-bed reactor may be used to establish an economic mass transfer. Whereas the mass transfer in stirred tank reactors is commonly high in comparison to other reactor systems, it is important to prevent

the applied biomass-surface systems from damage due to high shear stress. Moreover, application of fixed-bed reactors may result in clogging and pressure drop due to the accumulation of biomass. If an excess growth of microorganisms is expected to hamper the performance of this reactor system, the use of a fluidized-bed or airlift reactor is beneficial. In addition to these characteristics, the choice of an adequate bioreactor system must include deeper considerations of the kinetics, the nature of the substrate, operational requirements, hydrodynamics, and economics [3].

A high mass transfer is a crucial factor for proper growth and transformation behavior of a biofilm. As mentioned before, the structure of biofilms depends on several process parameters such as nutrient availability or the hydrodynamic regime, thus distinct structures occur as a result of the adjusted parameters. Mass transfer within a biofilm is achieved via convective and diffusive processes. Hence, an adequate utilization of biofilms may be hampered if the latter represents the bottleneck of the reaction and limits the transformation rate. To establish stationary conditions that are required for continuous production processes it is necessary to avoid substrate limitations that modulate the metabolic pattern of the organisms harbored in the biofilm. In particular for aerobic organisms the combination of consumption and diffusive transport of oxygen may provide anaerobic conditions. As a consequence obligate aerobic organisms get into a resting state and/or perish.

Cronenberg et al. investigated the transport of oxygen within pellets of *Penicillium chrysogenum* [10] and showed (via application of microelectrode studies) that the internal mass transport properties of pellets are highly affected by their morphological structure. They were able to prove that pellets, that occur in an early stage of a batch fermentation, feature a homogeneous and dense structure. The resulting pellets were only partly penetrated by oxygen (ca. 70  $\mu\text{m}$ ) under air-saturated conditions. A quite similar transport pattern was observed for attached growing cells. By application of microelectrodes, Hooijmans et al. have shown that the oxygen penetration depth of *E. coli* entrapped in a carrageenan matrix is approximately 100  $\mu\text{m}$  [11]. In accordance with these data, Tjihuis et al. stated that oxygen is available within the first 100–150  $\mu\text{m}$  of a biofilm and thus the data for flocculating and artificially or naturally entrapped microorganisms is on the same order of magnitude [12].

As a consequence it is recommended that biofilm thickness should not exceed a thickness of 150  $\mu\text{m}$  to avoid a limitation within oxygen-consuming processes [12]. However, this can be only a rough estimation, as the composition and structure of the biofilm matrix can be very heterogeneous. For example, channels and grooves occur, allowing an additional convective in addition to the diffusive transport, resulting in (mostly unpredictable) improved mass transfer characteristics. As a rule of thumb, most substrates (except for complex carbon or nitrogen sources) show approximately analogue transfer rates to those of oxygen (Table 3).

As mentioned in the first section, biofilm approaches can be applied for fermentative as well as biotransformation processes. If the production rate of the target compound is correlated with the biomass production as described by Gaden's type I

(i.e., the desired product is derived directly from primary metabolism), the excess generation of biomass has to be taken into account which can result in blocking of several reactor types (e.g., fixed-bed reactor). Thus, the reactor type and the substratum used for biofilm growth have to be adapted to this trait to prevent blocking. Several approaches on how this bottleneck can be tackled are discussed in the following sections. However, ethanol, a common representative of this type of kinetics, was produced by several biofilm processes as presented in Sect. 3. If one considers biomass production as one of the major drawbacks using biofilm production systems, an application of biofilms should be beneficial for biocatalytic processes following Gaden's type III kinetics, whereas the target compound is produced independently of the biomass production rate. The production rate of secondary metabolites such as bioactive compounds (e.g., penicillin) or enzymes (e.g., cellulase) is described by this type of kinetics resulting in less or no accumulation of biomass, inasmuch as the metabolites are produced under conditions of low or zero growth rate.

## ***2.1 Substrates for Biofilm Support***

The surfaces and particles applied for biofilm formation should fulfill the following criteria: the biomass support must (a) favor the adhesion of microorganisms, (b) feature a high mechanical resistance to liquid shear forces and particle collision, (c) be inexpensive, and (d) be widely available [13]. Obviously, not all desired characteristics can be fulfilled simultaneously. Aside from process engineering and economic parameters, the surface properties are of tremendous interest for adhesion and growth of the organism of interest. Thus, surface charge, hydrophobicity, porosity, roughness, particle diameter, density, shape of solid support, dimensions, and material have to be considered to obtain the required attachment and subsequent growth of the organism. To what extent these properties have an impact on cell metabolism and hence on the productivity and biotransformation capacity is still unrevealed. However, the attached growing microorganisms sometimes show a distinct morphotype pattern. Gross et al. reported that a recombinant *Pseudomonas* strain can grow with two different morphotypes in a biofilm bioreactor: smooth colonies with a plane surface, which were also found in suspended cultures, and a biofilm-specific morphotype, termed wrinkled type, featuring a higher roughness in comparison to its counterpart [14].

Because the amount of adherent growing biomass is directly linked with the provided surface within the reactor system, it is beneficial to install additional components in the reactor or to provide particle systems. Moreover the area can be further increased by application of roughened surfaces, thus more biomass will attach and may be applied for the biocatalytic process. While using particles as additional substratum inside a bioreactor in addition to roughness the dimension of the particle as well as porosity are also of great concern. Unlike mammalian cells microorganisms commonly show no constraints with regard to growth inhibition



by cell-to-cell contact thus the smaller the particles are, the higher is the provided surface. But one has to consider that the particle size should be adapted to the retention strategy; that is, process economics requires biofilm particle retention and the retention of large particles is less complex than for smaller particles. Hence, a compromise between particle size and surface area is necessary to meet the special needs of the process.

The variety of materials that can be used as biofilm supports has a broad range. Artificial construction materials or natural materials are applicable for adhesion processes and growth of microorganisms. The following two sections focus on commonly used materials for biofilm growth, with the materials classified into inorganic and organic compounds.

### 2.1.1 Inorganic Materials as Biofilm Support

Inorganic construction materials can feature a complex composition, for example, for ceramics, or a more or less simple compounding as alloys or pure elements such as metallic substrates. The application of (pure) metallic devices is quite common as implant material in medicine. Whereas microbial biofilms should be absent in this situation such contaminations take place to a small extent resulting in a negative impact on health. Titanium is often used as implant material but it is necessary to distinguish between the composition of the inner construction material and the outer layer of the implant. When the material is exposed to oxygen or oxygen-containing liquids the Ti-surface is oxidized. The resulting  $\text{TiO}_2$ -shell prevents the material from further corrosion but the surface characteristics are modified and adhesion must be evaluated for the oxidized Ti state. These examples feature the necessity of a careful observation of the true surface because almost all metallic construction materials suffer surface oxidation.

One of the main objectives of biofilm bioreactor design is to increase the specific surface within the bioreactor set-up. This can be done by using installations (e.g., baffles or other three-dimensional geometries) or particles.

If compact particles are used, one has to consider that the material's density is higher than the one of the liquid medium. Their application is therefore restricted to fixed-bed approaches. However, hollow metallic "particles" such as woven balls made from stainless steel wire gauzes can be applied as biomass support particles, which were developed by Atkinson et al. in 1979 [15]. The overall density of particle and biofilm is close to the density of the medium, hence the conglomerates can be applied in fixed-bed reactors as well as in fluidized or even airlift reactors. They stated in this early stage of using microbial films for production processes that in addition to flocculating microorganisms such particles can be filled with virtually any organism.

An improvement of surface attachment can be accomplished by chemical treatment of the applied stainless steel wires. For instance, Karsakevich et al. examined the activation of such stainless steel surfaces by treatment with titanium (IV) chloride and  $\gamma$ -aminopropyltriethoxysilane to improve cell immobilization of

*Z. mobilis* and productivity of ethanol and levan, a fructooligosaccharide [16]. Conditioning with  $\text{TiCl}_4$  allows bridging of the surface to the negatively charged bacterium and subsequently a better microbial growth and attachment of levan to the surface. Modification of the surface with  $\gamma$ -aminopropyltriethoxysilane leads to a positive charge of the wires' surface and thus to a strong electrostatic attraction of cells, whereas uncharged neutral or positively charged polysaccharides were not attached by the silanized stainless steel surface. Astonishingly, the surfaces' morphology is modified during the treatment procedure. Whereas the  $\text{TiCl}_4$  modified surface provides a topography with channels and holes, the silanized surface has a regular fine pattern as characterized by SEM studies.

In addition to titanium and stainless steel several other metals are applicable for biofilm growth but one has to balance the cost of the material and effectiveness of the attached growth pattern of a target organism. Although copper is commonly regarded as growth-inhibiting material, some studies indicate that even this metal may be used as a substratum for biofilm growth [17].

Porosity of the material is another crucial factor that determines the performance of the biofilm when used for conversion processes. The higher the porosity of the support material, the higher is the amount of biomass growing in the pores. As the biomass portion that is harbored within the channels of the material does not contribute to the reaction, it is necessary to evaluate the active fraction of the biomass. For butanol-producing *Clostridium acetobutylicum* Qureshi et al. [18, 19] have revealed that only a minor fraction of the biofilm biomass is active in terms of butanol production. They identified four different cell types in the butanol-producing biofilm: growing cells, butanol-producing cells, dead cells, and inactive cells, whereas only a minor fraction of less than 10 % of the total biomass contributed to butanol production. It is worth mentioning that dead cells and spores represented the main fraction of the biomass attached on bonechar. One may estimate that an analogue diversity of productive and nonproductive cells can also be found in other biofilm systems, thus the "true" productivities may be higher if solely the active biomass fraction is considered for calculation of the space-time yield.

However, it is important to consider the size of the pores. When the diameter of the pores is in the dimension of the biofilm-producing organisms the pores are generally blocked within short timeframes and the organisms cannot contribute to the conversion processes. But if the dimension of the pores features a diameter some orders of magnitude larger than the target organism, the pores are amenable for mass transfer even for convective transport.

Ceramic materials seem favorable because charge and pore size can be customized to the special needs of the target organism. The required manufacturing processes are well established within the field of membrane technology but have not yet been transferred to biofilm processes in a broad manner. Major drawbacks of such applications are the complexity of the production process and the corresponding costs. Furthermore, the release of positively charged ions from the carrier material (e.g.,  $\text{Al}^{3+}$ ) may hamper the performance of the biofilm organism, which has to be investigated in advance.

In addition to ceramics, glass and related materials can also be efficiently used as supports for biofilm growth. Jördening has discussed the use of glass particles and sand for application with regard to their function as support material for biofilm growth in fluidized-bed reactors [20]. To reduce the pressure drop during fluidized-bed application he used foam glass particles instead of common glass beads. Such foam glass particles provide a density similar to the liquid medium; moreover they feature a high surface area and porosity. Because foam glass is used as an isolation material by the construction industry it has a moderate price in comparison to other inorganic support materials. In comparison, the glass foam particles show an enhanced biofilm development in comparison to sand. But the author mentioned that the inoculum plays a prominent role with respect to biofilm growth. Thus, it was supposed that also a variation of growth rate up to 25 % can result from using nonsimilar inocula. An accelerated biofilm growth was observed, when already immobilized biomass was used as inoculum. Therefore the history of the inoculum has a strong impact on the following attached growth. A novel approach of foam glass particles that combines the well-known properties of glass and magnetic particles was recently patented by Süd-Chemie AG (now Clariant AG) [21]. By embedding magnetic particles within a matrix of foam glass, so-called magnetic foam glass particles result. These composite materials can be easily separated or retained in a biofilm bioreactor by application of magnetic fields.

Other cheap and widely available materials applicable as biofilm support are clay minerals. Such materials can be used as small bricks inside packed-bed reactors, a technique approved for the continuous production of butanol with *Clostridium beijerinckii* BA 101 [22].

In addition to the composition of the substratum, its morphology even influences the attachment characteristics of microorganisms. This topic is addressed in more detail in the chapter called “Novel Materials for Biofilm Reactors and Their Characterization” (cf. the chapter of Müller et al.).

## 2.1.2 Organic Materials as Biofilm Support

The variety of organic materials applicable for adhesion of microorganisms is very broad. Artificial polymeric materials can be applied as well as naturally occurring materials such as loofa sponges (see Sect. 3). Unlike inorganic materials, the polymers can be processed much more easily with regard to the special needs of the processes and are available at moderate cost. Furthermore, they can be blended or their surface modified to obtain materials with novel physicochemical properties. In comparison, materials based on organic matter commonly possess a density less than one gram per cubic centimeter. Therefore, the particles or reactor installations must be fixed to avoid detrimental sweeping.

It is assumed that the most important factors influencing the adhesion of cells or spores on organic matter are the surface morphology and hydrophobicity (surface free energy) rather than the charge of the material. Urek and Pazarlioglu have investigated the adhesion of spores of a white rot fungi (*Phanerochaete*

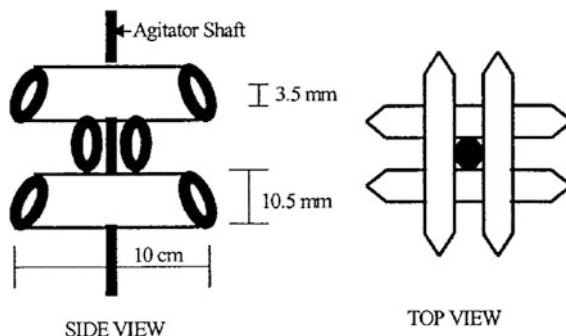
*chryso sporium*) on different materials (artificial and natural polymers as well as stainless steel) [23]. They have chosen ion-exchangers and classical adsorbers such as Amberlite IR 45, Eupergite C, Eupergite C 250 L, Purolite CT275, Purolite MN 500, polymers including PP and PP foam, and natural compounds such as cocopeat and rough bran. Furthermore, the “inorganic” material Perlit was tested. Polypropylene foam indicated the best performance and 86.4 % of spores were adsorbed by the material followed by 72.5 % of the ion-exchanger material Amberlite IR 45. Polypropylene provided as beads showed only 10.4 % adsorption of spores, but they have not characterized the roughness of the applied surface. This result is in accordance with findings from Asther et al. [24] who examined the immobilization of conidiospores and mycelium of *P. chryso sporium* on different materials. They stated that adsorption is a function of roughness and hydrophobicity, hence PP and polyurethane provide much better adsorption characteristics than such hydrophilic carriers as stainless steel or grey. Interestingly, Jones and Briedis reported that the higher the surface energy of the material is, the higher is the amount of biomass adhered to the surface [25]. They compared the adhesion of *P. chryso sporium* on the polymers polytetrafluoroethylene (PTFE), PP, polyethylene (PE), polymethylmethacrylate (PMMA), and nylon, where nylon provides the best adsorption of biomass and no attached biomass was found on PTFE. Astonishingly, attachment of biomass was reported solely after roughening of the polymeric surfaces; that is, without modification of the surfaces’ texture no attachment of biomass was observed. A similar result was observed by Guimarães et al. [26]. They reported that the surface roughness/porosity is more important for attachment of biomass than its (surface) energy.

As mentioned before, the surface charge plays only a minor role for attachment; positively charged support materials such as anion-exchangers may support binding of the microorganism. Zhang et al. investigated the polyhydroxybutyrate biosynthesis and biofilm development of *Alcaligenes eutrophus* [27] in the presence of positively charged carriers. Because bacteria feature a negative charge under physiological conditions it is assumed that positively charged surfaces support attachment of the biomass. Best performance resulted towards the strong anion exchanger DEAE-Sephadex A-25, which possesses the highest charge capacity of the investigated microcarriers (charge capacity: 3.5 meq/g).

Polymers can be very gently modified to the special needs of the adsorption process, if the regular monomers will not provide the desired characteristics of the polymer. The co-monomers possessing the required functional groups can be used during polymerization or, on the other hand, modification of the polymer can be achieved by chemical or physical means after termination of the polymerization to increase the charge density on the surface (e.g., by plasma treatment). Moreover, the materials can be processed very easily in comparison to inorganic biomass supports concerning shape and dimension of the particle or installation.

Glass and stainless steel are considered as reference materials for the cultivation of microorganisms and production of valuable processes. But in the last decade many processes were introduced applying disposable plastic materials because the regulations for establishing them in particular pharmaceutical processes are much

**Fig. 3** Configuration of the PCS tubes on the agitator shaft [28] (reprinted with kind permission from Springer Science + Business Media)



easier to fulfill and the investment costs are less compared to “standard” procedures. One major problem is that manufacturers in principle do not publish or communicate the detailed composition of the plastic material due to intellectual properties. Furthermore, no international standards are currently published that must be met by these novel types of materials. In particular, compounds migrating from the inner plastic composite to the surface and the medium, respectively, may affect attachment of cells, growth, and productivity of the adhered biomass.

Commonly, a release of compounds is undesirable, especially within manufacturing of pharmaceuticals. However, plastic composites can be modified in terms that release of specific blended compounds is achieved supporting attached growth of biofilm-producing microorganisms. Such a material was developed at Iowa State University by Pometto and co-workers (U.S. Patent Number: 5,595,893), who were able to provide a unique plastic composite support (PCS) that showed beneficial characteristics due to stimulation of biofilm formation. They investigated a broad range of blendings of the PCS. For production of lactic acid, for example, Cotton, Pometto, and Gvozdenovic-Jeremic [28] optimized the PCS blend for *Lactobacillus*. They found that best performance results from a blend containing 50 % (wt/wt) agricultural products [35 % (wt/wt) ground soy hulls, 5 % (wt/wt) soy flour, 5 % (wt/wt) yeast extract, 5 % (wt/wt) dried bovine albumin, and mineral salts] and 50 % (wt/wt) PP. The final (basic) shape was obtained by high-temperature extrusion. The resulting PCS tubes featured a wall thickness of 3.5 mm, an outer diameter of 10.5 mm, and were cut prior to application in a bioreactor into 10-cm lengths. The tubes were fixed on an agitator shaft in a stirred-tank bioreactor and allowed lactobacillus cells to adhere, while producing lactic acid. For installation of six PCS tubes, the authors applied three rows of two parallel tubes which were bound in a grid fashion to the agitator shaft of the fermentor (1.2-L vessel, New Brunswick Bioflo 3000). The principle of installation is illustrated in Fig. 3.

Thickness of the biofilm on the PCS tubes was controlled via adjustment of the stirrer speed. In a comparison of the PCS biofilm reactor and a control reactor, where PP tubes were applied without blending, the optimal production rates were 9.0 and 5.8 g/L h by application of a dilution rate of  $0.4 \text{ h}^{-1}$  and a stirring rate of 125 rpm. The obtained yield of lactic acid was given as approximately 70 %.

The blending can also be modified, thus this type of biofilm bioreactor can be adapted for a broad range of production processes. A more comprehensive overview of such biomass support material is given in this book, *Advances of Biochemical Engineering/Biotechnology*, in the chapter by Müller et al.

## 2.2 Reactor Types for Biofilm Processes

Several reactor configurations can be applied for utilization of biofilms in biotechnological production processes. However, one of the following reactor types is commonly used for cultivation of immobilized cells or biofilms with respect to the production of value-added compounds: (a) stirred-tank reactor, (b) fixed-bed reactor, (c) rotating-disc reactor, (d) fluidized-bed reactor, (e) airlift reactor, or (f) membrane biofilm reactor (see Fig. 4).

The major advantages and disadvantages of these reactor types are summarized in Table 3.

In addition to this classical biofilm reactor set-ups, a novel reactor type enabling the cultivation of phototrophic microorganisms naturally grown on surfaces exposed to air is presented.

Reactor types such as the upflow anaerobic sludge blanket reactor and expanded granular sludge-bed reactor were used for wastewater treatment. Because this chapter addresses productive biofilms, the interested reader is referred, for example, to Qureshi et al. [19] for more information about these special reactor types.

### 2.2.1 Stirred-Tank Reactor

The stirred-tank reactor used for biotechnological applications derives from the classical reactor type used in chemical engineering. This type of reactor is well established for large-scale industrial production processes for freely suspended cells. It allows the integration of several types of analytical devices (e.g., pH, pO<sub>2</sub>, optical density, in situ microscope) and moreover the control of important process parameters such as pH and concentration of dissolved oxygen. The use of stirred-tank reactors for biofilm processes requires the integration of a corresponding material supporting the attached growth of the organism. Reactor inserts and/or particles can be used to increase the specific surface inside the reactor.

Several construction materials with modified and unmodified surfaces can be applied (see Sect. 2.1) but one has to take into account that such an integration of biofilm-supporting material has an effect on the hydrodynamics and influences, for example, the Reynolds number, power input, and mixing time. Moreover, the kind of stirrer and its local energy input must be adapted to the applied particles if such kind of substratum is used for biofilm growth. Especially the six-flat-blade disc turbine or pitched-blade turbine rather than the marine impeller (propeller) provide an input regime that may result in the breakdown of fragile biofilm-supporting materials.

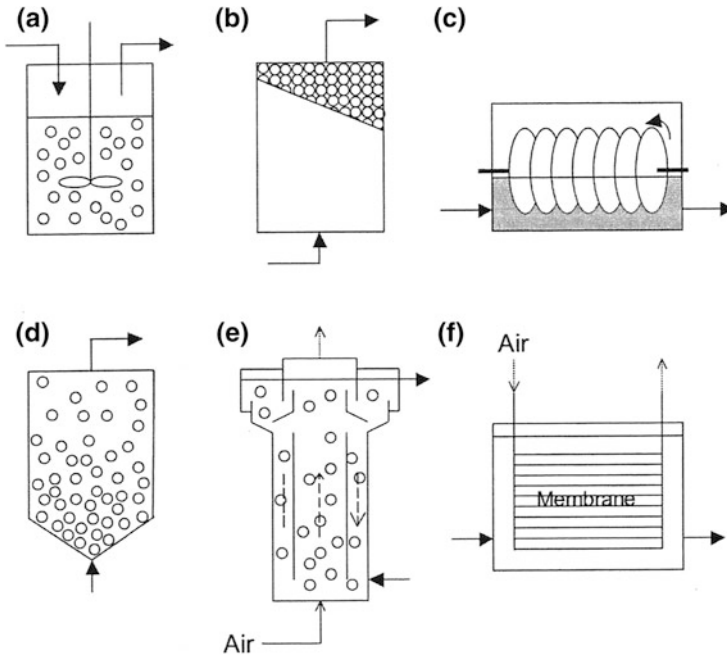


**Fig. 4** Reactor types commonly used for biofilm cultivation: **a** stirred-tank reactor, **b** fixed-bed reactor, **c** rotating-disc bioreactor, **d** fluidized-bed reactor, **e** airlift reactor, and **f** membrane biofilm reactor [13] (reprinted with permission from John Wiley and Sons)

**Table 3** Comparison of reactors types commonly applied in biofilm engineering (adapted from [29])

Reactor Type	Advantages	Disadvantages
Stirred-tank reactor	High cell density and productivity; long-term production	Shear stress of cells; high mixing power required
Fixed-bed reactor (incl. trickle-bed reactor, TBR)	High cell density and productivity; low power input requirements (TBR)	Cell fouling; gradients due to mixing problems; product recovery is difficult (TBR)
Fluidized-bed reactor	Uniform particle mixing; long-term production	High energy requirement; shear stress; long biofilm establishment time
Rotating-disc reactor	High cell density	Semi-continuous production; high risk of contamination
Membrane biofilm reactor	High cell density and productivity; easy product separation	Cell fouling; constraints in scale-up of system

Necessary for industrial application is the scale-up of the process. Scale-up of operation modes with submerged growing and producing cells is a common procedure in the industry and several criteria exist to establish the process on a larger

scale. In the case of particles used as biofilm support, an increase of reactor dimension can be accomplished by increasing the number of particles in the system, whereas such processes using fixed inserts on the reactor wall or on the stirrer shaft (e.g., the PCS approach discussed in Sect. 2.1) are restricted concerning the scalability of the approach. An appropriate scale-up is hampered because the ratio of surface to volume is decreased during scale-up.

The biofilm-harboring stirred-tank reactor can be operated in batch, fed-batch, or continuous mode. Since proper immobilization of the microorganisms requires several days, the set-up time of the reactor is very high. According to the economics of the process the prepared reactor should have a high operating time. That feature is actually fulfilled for a continuous stirred-tank reactor, whereas the fed-batch and batch processes are originally designed for short operating times. By using a repeated batch mode the operating time can be extended. Unlike the continuous mode, gradients in the reactor occur due to transient conditions.

### 2.2.2 Fixed-Bed Reactor

The fixed-bed reactor (also termed as packed-bed reactor) is presumably the most frequently applied reactor type for cultivation of immobilized cells and biofilms, respectively [3]. The solid supports within the reactor type are densely packed and colonized by the biofilm organism. Thus, this reactor type provides high interfacial areas of biomass–liquid contact. The mass transfer is a function of the volumetric flow, because the higher the flow rate, the higher is the mass transfer. Nevertheless, the flow is constrained by technical means (i.e., pressure drop) and on the other hand by resulting shear forces that damage the biofilm.

Many biocatalytic processes require an efficient gas–liquid contact and removal of carbon dioxide. As a consequence stagnant gas pockets result that may cause gas flooding and hence the performance of the bed decreases [3]. A major advantage of the fixed bed is its very high density of biomass in relation to the void volume of the packaging material. However, one should have in mind that biomass accumulation may result in clogging of the fixed bed. In such cases it might be beneficial to use a trickle-bed or fluidized-bed reactor.

The trickle-bed bioreactor (TBR) can be considered as a special type of a fixed-bed reactor. Within a TBR the liquid has a downward flow pattern over a thin film of a packed (bio)catalyst, wherein efficient oxygen supply as well as gas removal is accomplished. As mentioned before, acetic acid was produced successfully on a 60-m<sup>3</sup> scale [7], but the production process is not as economical as other submerged or emerse processes. A very promising approach of a trickle-bed reactor for production of ABE solvents was reported by Park et al. [30]. They immobilized *C. acetobutylicum* on a natural sponge and obtained a 10 times higher solvent productivity than that from a batch fermentation using suspended free cells. Moreover, the production rate was 2.76 times higher than that of immobilized cells in a CSTR approach.



Recently, an aerated continuous trickle-bed biofilm approach was reported and designed by Li et al., featuring a 3-L structured packing, liquid recycling, and pH control [31]. A biofilm of *Pseudomonas diminuta* was established on a stainless steel structured packing with a specific surface area of 500 m<sup>2</sup>/m and applied for the oxidation of ethylene glycol to glycolic acid within a time period of more than two months (continuous operation). They achieved a steady-state productivity of up to 1.6 g/L h at a dilution rate of 0.33 h<sup>-1</sup>. The structured packaging material improves flow dynamics and less stagnant pockets occur in the column resulting in higher catalyst efficiency and reactor performance. Furthermore, this packaging material overcomes common limitations such as flow channeling, incomplete catalyst wetting, poor mass transfer, reactor flooding, and blockage.

### 2.2.3 Fluidized-Bed Reactor

A fluidized-bed reactor provides a degree of mixing that can be considered as intermediate between the two extremes of the packed-bed reactor and a continuous stirred-tank reactor [3]. The fluidization (expansion) of the (biofilm) bed particles is achieved by liquid and/or gas. If air is used as the gaseous phase and the reactor provides a rising and rinsing compartment for the particles, the reactor set-up is commonly classified as an airlift reactor. An additional reactor type that can be subsumed within this category is a bubble column reactor. Consequently, the expansion of the bed requires an upward flow of the fluid that must exhibit a velocity high enough to allow the expansion of the bed. However, the bed particles must have a higher density than the applied fluid. According to Fukuda, fluidized-bed reactors provide good mixing, mass, and heat transfer characteristics, and show minimal pressure drop [3]. Furthermore, such reactor types provide advantages such as: (a) easy control and measurement of relevant process parameters (in particular, pH value and dissolved oxygen), (b) easy (particle) sampling during operation and (if required) replacements of active fractions, and (c) application of small particles to provide high specific surface area within the reactor without pressure drop as in packed-bed reactors. Due to the well-mixed hydrodynamic regime inside the fluidized bed a good gas-liquid contact and gas supply as well as removal is established. According to the resulting shear forces it is possible to get rid of accumulating biomass on the support particles as reported by Gjaltema et al. [32], thus biofilms can be investigated featuring a nearly constant thickness with approximately constant mass transfer rates.

In addition to these manifold advantages several difficulties may be encountered during operation of a fluidized bed. If the bioreactor is operated at high bed expansion and low stability levels, such reactors have only a narrow range of optimum operating conditions [3]. Therefore it is difficult to maintain nonfluctuating conditions. Moreover, an upscaling of a fluidized bed reactor is hampered because the effects of back-mixing on the production rate are difficult to predict. Efficient back-mixing also depends on the difference of the particle density and the

fluid density. If particles are selected featuring a density close to the value of the fluid, the efficiency of back-mixing is drastically decreased.

Because fluidized-bed reactors are well suited for fermentative processes in which a gaseous phase is generated, such a reactor type has been successfully applied, for example, for production of ethanol by immobilized *Z. mobilis* on/in glass foam particles [33]. In contrast to the common CSTR fermentation approach, the applied hydrolyzed B-starch is applicable without prior sterilization. A conversion rate of 99 % of the unsterile hydrolyzed B-starch was achieved (glucose concentration: 120 g/L), resulting in an ethanol concentration of 50 g/L and an ethanol space–time yield of 13 g/Lh, which is three times higher in comparison to the space–time yield obtained in continuous stirred-tank operation. A fluidized bed may also be promising concerning the production of hydrogen as reported, for instance, by Barros et al. [34].

Another reactor type that falls into this category is the modified spouted-bed reactor, developed by Webb, Fukuda, and Atkinson [35] for the continuous production of cellulase by *Trichoderma viride* QM 9123. Within this approach the microorganisms were immobilized in spherical, stainless steel biomass support particles with a diameter of 6 mm. The spouted-bed reactor used recycled broth to create a jet at the base of a bed of the applied particles, allowing the particles to spout and circulate. During circulation, the particles passed through a region of high shear near the jet inlet, thus a build-up of excess biomass was prevented. Moreover, steady-state conditions were enabled allowing a continuous operation. In comparison to the freely suspended cells, the productivity of the immobilized cells was more than three times higher. Hence, Webb et al. assumed that occurring diffusional limitations can be beneficial for the expression of the cellulase.

#### 2.2.4 Rotating-Disc Reactor

Basically, the rotating-disc bioreactor set-up uses discs as biofilm support. The discs are mounted on a shaft and can be turned with a defined frequency. Thus, the hydrodynamics can be adjusted independently of the residence time. If the discs are applied on a horizontal shaft and the reactor is operated partially filled, such an approach is commonly termed as rotating biological contactor or rotary biofilm contactor (e.g., [36, 37]). Due to rotation of the discs, the immobilized microorganisms alternately get in contact with the medium and with the atmosphere above the fluidic phase. The reactor can be equipped with several analytical devices to measure pH, dissolved oxygen, or extracellular product concentration, and can be used for aerobic as well as anaerobic fermentation. In principle the disc(s) can be used directly as solid support for biofilm attachment but alternatively other materials can be fixed onto the disc(s).

A major advantage of this reactor configuration in comparison to the stirred chemostat is its combination of fixed microbial films and suspended growth characteristics [38], thus the operation may be described as a dynamic trickling filter. To allow a well-mixed regime and to provide the cells with sufficient oxygen, the discs

are operated with a rotating speed of some rounds per minute. Interestingly, this approach can be used to mimic natural conditions that occur in intertidal marine habitats. By adjusting the rotational speed according to the interplay of the tides, Sarkar et al. used the rotating disc configuration to support biofilm formation of marine strains and the production of antimicrobial metabolites [39].

As mentioned before, the reactor approach provides excellent features to investigate the correlation of biofilm growth and shear stress/flow velocity of the fluid. For example, Lewandowski and Beyenal used a vertically mounted polycarbonate disc of 60 cm in diameter inside a temperature-controlled reactor vessel with a side length of 70 cm and a total height of 20 cm [40]. The plastic disc contained six radial grooves, which could be used for insertion of polycarbonate slides used as biofilm support. Because each position along the radius of the polycarbonate disc provides a different (linear) velocity, within the frame of one single experiment a broad range of flow velocities can be covered. However, it must be considered, that in contrast to other reactor types (i.e., such systems using particles) a sampling of the attached growing microorganisms within this reactor type is not possible.

### 2.2.5 Membrane Biofilm Bioreactor

An essential element of a membrane biofilm reactor is a specific membrane that acts as support for the microorganisms and on the other hand as a selective barrier allowing the transport of nutrients. Although the attachment of microorganisms and organic compounds on membranes is classified as biofouling because the performance of filtration is detrimentally affected (e.g., clogging and destruction), a systematic colonization of membranes by biofilm-producing microorganisms can be beneficial particularly if the membrane acts as a barrier to protect the cells from an excess of toxic products or substrates. Furthermore, such membranes can be used to achieve an adequate (bubble-free) oxygen supply of the microorganism.

A special type, called a membrane-aerated biofilm reactor (MABR) whereby the biomass is immobilized on membranes through which oxygen is supplied, seems very promising for treatment of wastewater (see, e.g., the review by Qureshi et al. [19]). As indicated by Syron and Casey, recent MABR studies commonly used commercially available membrane technology such as microfiltration or ultrafiltration membrane modules or applied polymeric materials such as silicone tubings [41]. Because these materials are not specifically designed to support microbial attachment and growth, there is a tremendous potential to improve the biofilm performance. Prior to application of a membrane module special concern should be addressed regarding the following criteria [41]:

- Pressure drop should be minimal
- Gas distribution should be uniform across the membrane
- Membrane must be resistant to microbial degradation
- Membrane pores should not wet under the prevailing operational conditions

A very simple set-up for a membrane biofilm bioreactor can be provided just by a silicone tubing in which the biofilm grows attached to the surface. Whereas the biofilm grows in the aqueous phase, the (toxic) substrate(s) are delivered by diffusion from the volume element that is separated by the membrane. Gross et al. have applied the engineered *Pseudomonas* sp. strain VLB120ΔC as a model biofilm organism to study the asymmetric epoxidation of styrene to (*S*)-styrene oxide in a tubular reactor (silicone tubing) [42], whereas the inhibition of the microorganism is prevented by in situ extraction of the product. In subsequent investigations Gross et al. identified oxygen as one of the main parameters influencing the biotransformation rate [14], and the productivity was linearly dependent with respect to the specific membrane area and the tube wall thickness. Because the performance of the system is hampered by an insufficient oxygen supply a so-called solid support membrane-aerated biofilm reactor (SMABR) was applied for growth and biotransformation [43]. This reactor type applies a microporous ceramic membrane for oxygen supply and growth of the organisms, whereas a silicone-based membrane was used as a reservoir for the toxic substrate/product. Due to its beneficial oxygen transfer the SMABR-approach is more scalable in contrast to the MABR system.

On the basis of the MABR results Gross et al. have recently evaluated a potential industrial application of such a system for the production of (*S*)-styrene oxide on a larger scale [44]. They proposed a cylindrical membrane fiber module packed with 84,000 PP fibers to realize a manufacturing process on a 1,000-tons-per-year scale, where 59 membrane fiber modules with a diameter of 0.9 m and a length of 2 m would be used. In comparison to a stirred-tank reactor process a higher yield on carbon (at least factor two) and a lesser amount of biomass waste (more than factor 400) were calculated for the MABR approach.

### 2.2.6 Emerse Photobioreactor

Monoseptic large-scale cultivation processes in industrial biotechnology mainly use heterotrophic approaches even if the organisms may be cultivated in a phototrophic manner. For example, the microalgal-based heterotrophic production of polyunsaturated fatty acids can be accomplished with productivities two to three orders of magnitude larger than those of phototrophic outdoor pond systems [45]. Several photobioreactor types were developed during the last decades allowing the cultivation of cyanobacteria and microalgae under axenic conditions. These reactors are exclusively designed for cultivation of cell suspensions rather than for cultivation of biofilms. Due to light penetration is negatively affected when the cells grow on the surfaces directed to the light supply; biofilms are commonly considered as a problem that has to be tackled, for example, by shear stress via supplementation of particles to the fermentation broth.

A novel bioreactor approach, termed emerse photobioreactor (ePBR), which was recently developed by the authors [46] is addressed in this section. The system enables the cultivation of phototrophic organisms naturally grown on surfaces exposed to air. Fermentation under such emerse (air-exposed) conditions opens up

the opportunity to cultivate phototrophic biofilms of terrestrial and aerophile microalgae. This emerge-living group represents a potential source of biomass and biofuels and can be used as animal feed [47]. Moreover, a broad variety of bioactive compounds is produced by these microorganisms.

In the last decade terrestrial cyanobacteria received increasing biotechnological interest because of their high production rates of extracellular polymeric substances (EPS) and production of bioactive substances (e.g., cryptophycin). The terrestrial cyanobacteria *Nostoc* and *Scytonema*, for example, produce the bioactive compounds cyanovirin-N [48, 49] and scytovirin [50] featuring inhibitory activity towards HIV. In addition, terrestrial cyanobacteria produce bioactive compounds such as cytotoxins, enzyme regulators, and low-molecular-weight substances [51]. Despite these interesting indications, the therapeutic potential as well as its mode of action has been little studied so far [51].

The narrow focus applying mainly aquatic cyanobacteria for biotechnological applications until now, is based on the fact that the leading role of terrestrial cyanobacteria, particularly in water- and nutrient-limited ecosystems, has been recognized quite recently [52]. The desiccation-tolerant cyanobacteria adapt to extreme abiotic conditions in arid and cold deserts. They are characterized by acclimation to low light intensities (e.g., [53]), low nitrogen availability (e.g., [54]), and variable water availability [55]. Many cyanobacteria are independent of local nitrogen fertilizers because they are able to fix dinitrogen from the air (diazotrophs) and therefore act as a nitrogen supplier in the ecosystem [54]. This natural physiological plasticity includes many advantages that can be beneficial in artificial fermentation systems. The metabolism of terrestrial cyanobacteria is activated, for example, by minimal amounts of liquid water (e.g., aerosols; [55, 56]). They are protected from too rapid dehydration, and thus anabiose, with an enveloping mucus shield [57, 58] consisting of hygroscopic EPS. In many species, this EPS also contains the anti-inflammatory-acting and UV-protective pigment scytonemin in addition to the main components such as alginate and catechines. Both represent valuable compounds that are increasingly produced during desiccation processes [59–61].

Other features of cyanobacteria are the flexible light-harvesting complexes of photosynthesis, which consist of highly efficient phycobilisomes. Such phycobilisomes are comprised of phycoerythrin and phycocyanin, and are used for both exploitation of low-light quantities as well as adaptation to light qualities (red light, green light) by flexible reconstruction of these pigments (chromatic adaptation; [62, 63]). Due to the direct influence of soil respiration, terrestrial cyanobacteria also tolerate high CO<sub>2</sub> concentrations. Therefore, terrestrial diazotroph cyanobacteria that have been isolated and cultured from savannah and arid deserts, may represent future production organisms with high potential for the production of value-added compounds in the context of phototrophic emerge fermentation.

The novel ePBR exhibits unique features and benefits for the fermentation of microalgal biofilms [46]. In comparison to submerge reactors the developed ePBR facilitates gas exchange, minimizes water usage, features an improved light path, and simplifies processing of biomass. The closed photobioreactor system (see Fig. 5)



**Fig. 5** Scheme of the novel photobioreactor enabling the cultivation of terrestrial cyanobacteria. The reactor is illuminated from the *top* by LEDs and light is supplemented via roughened glass rods, which are fixed by the lid of the reactor. Light distribution is achieved due to scattering at the boundary of glass/air, thus cyanobacteria growing on the glass surface are supplemented with light. Nutrients and water are provided as aerosol from the connections presented at the *upper part* of the reactor

consists of a cylindrical reaction vessel (current reactor volume: 0.5 L) with embedded optical waveguides (roughened glass rods) serving simultaneously as support material for the organisms (e.g., 1 g fresh weight per 100 cm<sup>2</sup> surface area).

Borosilicate glass rods (5 mm × 170 mm) are used to guide actinic light charged by external light-emitting diodes (LEDs). The light is scattered within the optical waveguide and emitted at the rod surface. The target organisms adhere to the surface of the glass rods and therefore they receive the scattered light. This light pathway optimizes the illumination level of microalgae because their photosynthesis is not limited by light penetration from the outside, which is often a problem in dense liquid cultures of submerged growing organisms. Moreover, the emitted light energy is directly transferred to the growth zones of the microalgae whereas the older cells are distally displaced/replaced outwards.

The bioreactor approach additionally allows a controlled and water-saving application of aerosol. The required aerosol is produced by a vaporizer that applies sterile culture medium as a fine mist to rewet the organisms. After wetting, the relative humidity is between 70 and 100 % for several hours depending on



**Fig. 6** Different stages of the development of ePBR designs. (Left) First prototype of the ePBR; (Middle) photobioreactor with connectors enabling sampling of liquids and biomass; (Right) photobioreactor in current geometry including a perforated tray for biomass retention

the dispensed amount of water. The addition of aerosol reduces the temperature inside the ePBR of approximately 0.8 °C due to evaporation. The application of the medium as an aerosol has several advantages in comparison to submerge cultivation; these include (a) the gas mass transfer is significantly improved (by reducing the diffusion barriers), (b) the use of water resources is reduced (currently 0.1 ml per cm<sup>2</sup> of surface area and day), (c) initiation of the desiccation process induces the production of certain valuable compounds, and (d) a simplified processing of biomass because it already exists in a concentrated form. In particular the traditional processing by thermal drying, flocculation, centrifugation, or filtration is time-, cost- and energy-consuming [64, 65]. In the ePBR, harvesting of desiccated microalgae might be implemented species-specifically by mechanical shearing (e.g., peeling knife), cell wash-off by increased aerosol delivery, or by dehydration-induced shedding when static heavier filaments or aggregates break off. Further advantages arise from the avoidance of permanent mixing of a suspension as well as absence of foam production and mechanical shear forces. Moreover, the reactor facilitates recovery of the medium filtered through a stainless steel mesh, pressure equalization through a sterile filter, and gas exchange measurements. Several stages of developed photobioreactors are presented in Fig. 6.

The described system is currently applicable for lab-scale processes and allows the production of compounds induced by desiccation stress. In this context the system is also a valuable tool to investigate the physiological responses, which are triggered by heat and desiccation. A scale-up of the system requires an increase of the available surface area inside the reactor. This might be accomplished by application of fiber optics instead of glass rods. However, such a scale-up process must find an optimal alignment of fiber optics that provides a supplementation of the surface-attached growing strains with nutrients. Moreover, the harvesting process must be selected according to the specific traits of the phototrophic microorganisms.

### 3 Potential of Biofilm Reactors within Biotechnological Production Processes

Biofilms are up to now not well established in industrial biotechnology with respect to the production of chemicals, including bulk as well as fine chemicals, even though feasibility of the biofilm approach has been shown for several reactions on the laboratory scale. Unlike wastewater or odor treatment, the use of biofilms for a production process requires the establishment of monospecies rather than multispecies/mixed-species biofilms because the control of the latter is more complex and to date barely understood.

As mentioned before a biofilm approach could be very reasonable with respect to economics and space–time yield. A major advantage of utilization of biofilms is the lifetime and robustness of the microorganisms. Within the next section some of the most relevant applications of biofilms concerning biocatalysis/production processes are summarized.

#### 3.1 *Applications of Biofilm Bioreactors for Production of Value-Added Bulk and Fine Chemicals*

The production of value-added products by application of biofilms was proven for several manufacturing processes for bulk as well as fine chemicals and enzymes. Some prospective applications with respect to productive biofilms—except for animal and plant cell processes, which are not covered within this review chapter—are highlighted in Table 4. The examples presented were ordered according to the applied reactor type of the respective biofilm approach. The illustrated biofilm processes were mainly examined in lab scale rather than pilot and/or industrial scale. The latter one was solely accomplished for vinegar manufacturing as mentioned earlier. Commonly, the space–time yield is given as the amount of product formed per volume of the reactor and time. This definition has to be considered as critical because it is not directly linked with the biomass nor the available surface area in the related system. In spite of this deficiency, the space–time yield is also used for biofilm bioreactors. Whenever possible, values of Table 4 were presented for continuous and batch processes with the unit g/L h. Inasmuch as the determination of biomass in a biofilm reactor set-up is much more complicated than for submerged growing cells, the amount of biomass used in a specific system is usually unstated. Even though the biomass could be determined with a certain accuracy, the active fraction of the biofilm is still unknown.

A major concern while focusing on a biofilm approach is its applicability. In addition to the process economics it has to be considered whether the production of the target compound is also feasible in a scientific manner; i.e., the production should not be hampered by fluctuating conditions in the bioreactor. First, the correlation of product formulation and biomass production should be known to



**Table 4** Examples of value-added products manufactured by application of biofilm bioreactors (adapted from [4, 29] and augmented)

Product	Organism	Substratum	Productivity	Ref.
<i>Packed-bed reactor</i>				
Ethanol	<i>Zymomonas mobilis</i> , <i>Saccharomyces cerevisiae</i>	PCS ring and disk	5.0–124 g/L h	[67, 68, 88]
Ethanol	<i>Z. mobilis</i>	Anionic exchange resin beads	377.4 g/L h	[66]
Butanol	<i>Clostridium acetobutylicum</i>	Tygon <sup>®</sup> rings	4.4 g/L h	[89]
ABE solvents (acetone, butanol, ethanol)	<i>Clostridium beijerinckii</i> BA101	Clay bricks	16.2 g/L h	[22]
ABE solvents (acetone, butanol, ethanol)	<i>C. acetobutylicum</i>	Bonechar	4.1 g/L h	[90]
Lactic acid	<i>Lactobacillus aminophilus</i> , <i>Lactobacillus casei</i> , <i>Lactobacillus delbrueckii</i>	PCS	13–60 g/L h	[91–93]
Succinic acid	<i>Actinobacillus succinogenes</i>	PCS	2.08 g/L h	[70, 71]
Propionic acid	<i>Propionibacterium acidi-propionici</i>	Spiral wound fibrous matrix	1.62 g/L h	[72]
Dihydroxyacetone	<i>Gluconobacter oxydans</i>	Silicone-covered Ralu rings	2.8 g/L h	[94]
1,3-propanediol	<i>Pantoea agglomerans</i>	Polyurethane foam	3.6 g/L h	[95]
Benzaldehyde	<i>Z. mobilis</i>	Glass beads	0.88 g/L h	[96]
Poly(3-hydroxybutyrate)	<i>Alcaligenes eutrophus</i>	DEAE-Sephadex A-25 beads	0.034–0.038 g/L h	[27]
Pediocin	<i>Pediococcus acidilactici</i> PO2	Spiral wound fibrous matrix	$1.0 \times 10^7$ AU/L h	[76]
Nisin	<i>Lactococcus lactis</i>	Spiral wound fibrous matrix	$1.0 \times 10^7$ AU/L h	[80]
<i>Bubble column and analogues</i>				
Citric acid	<i>Aspergillus niger</i>	Polyurethane foam	0.135 g/L h	[97]

(continued)

**Table 4** (continued)

Product	Organism	Substratum	Productivity	Ref.
Cellulase (spouted bed fermenter)	<i>Trichoderma viride</i>	Stainless steel	31.5 FPA U/L h (filter paper activity)	[35]
Cephalosporin C	<i>Cephalosporium acremonium</i>	Sintered glass particles	$7.111 \times 10^{-3}$ g/L h	[83]
<i>Rotating disc reactor</i>				
Citric acid	<i>A. niger</i>	Polyurethane foam	0.896 g/L h	[69]
Fumaric acid	<i>Rhizopus oryzae</i>	Plastic discs	3.78 g/L h	[37]
Lignin peroxidase	<i>Phanerochaete chrysosporium</i>	Several plastic discs	0.46 U/L h	[25]
<i>Stirred-tank reactor</i>				
Lignin peroxidase	<i>P. chrysosporium</i>	Nylon web cubes	5.6 U/L h	[75]
Pullulan	<i>Aureobasidium pullulans</i>	PCS tubes on agitator shaft	1.33 g/L h	[98]
Bacterial cellulose	<i>Acetobacter xylinum</i>	PCS tubes on agitator shaft	$5.9 \times 10^{-2}$ g/L h	[99]
Polyhydroxyalkanoates	<i>Bacillus</i> sp.	PCS tubes on agitator shaft	0.195 g/L h	[100]
Nisin	<i>L. lactis</i>	PCS tubes on agitator shaft	$5.4 \times 10^5$ U/L h	[101]
Lignin peroxidase (LiP)/Manganese peroxidase (MnP)	<i>P. chrysosporium</i>	PCS tubes on agitator shaft	0.35 U/L h (LiP) 0.88 U/L h (MnP)	[74]
<i>Trickle-bed reactor</i>				
Acetic acid	Acetic acid bacteria	Beechwood shavings	1.7 g/L h	[7]
Glycolic acid	<i>Pseudomonas diminuta</i>	Structured stainless steel packaging	1.6 g/L h	[31]
Hydrogen	<i>Caldicellulosiruptor saccharo-lyticus</i>	Polyurethane foam	0.044 g/L h	[85]
Hydrogen	<i>C. acetobutylicum</i>	Glass beads	220 mL/L h (0.02 g/L h)	[102]
<i>Fluidized-bed reactor</i>				
Ethanol	<i>Z. mobilis</i>	Macroporous glass beads	13 g/L h	[33]

(continued)

**Table 4** (continued)

Product	Organism	Substratum	Productivity	Ref.
Hydrogen	Anaerobic sludge	Polystyrene	0.085 g/L h	[34]
Hydrogen	Anaerobic sludge	Expanded clay	0.11 g/L h	[34]
<i>Other reactor types</i>				
(S)-styrene oxide (membrane aerated biofilm reactor)	<i>Pseudomonas</i> sp.	Ceramic membrane	1.2 g/L h	[43]
(S)-styrene oxide (tubular membrane reactor)	<i>Pseudomonas</i> sp.	Silicone membrane	0.67 g/L h	[42]
1-octanol	Recombinant <i>Pseudomonas putida</i>	Silicone membrane	0.054 g/L h	[44]
Manganese peroxidase (membrane gradostat biofilm reactor)	<i>P. chrysosporium</i>	Polysulfone membrane	1.3 U/L h	[103]
Halogenated Trp- derivates (stationary)	Recombinant <i>E. coli</i>	Glass slides	$2.35 \times 10^{-3}$ – $9.39 \times 10^{-3}$ g/ L h	[104]
Manganese peroxidase (stationary)	<i>P. chrysosporium</i>	Polystyrene foam	2.9 U/L h	[23]
Gibberellic acid (shaking flask)	<i>Fusarium moniliforme</i>	Loofa sponge	$13 \times 10^{-3}$ g/L h	[105]
Extracellular polymeric substances	<i>Nostoc muscorum</i>	Roughened glass rods	0.303 g/m <sup>2</sup> h	Unpublished data

select the optimal reactor type. If the production can be described by Gaden type I, the productivity is better the higher the growth rate is. This type of production results in massive biomass accumulation and thus blocking of the reactor type must be prevented when operation is accomplished in a continuous mode. Hence, fluidized-bed or analogue reactor types are optimally suited for such processes. It can be concluded that the biofilm production mode is most beneficial for anaerobic processes, whereas productivity and growth rate are not related. Such processes avoid possible limitations due to transport of oxygen as well as mass transfer problems and blocking of the reactor due to accumulation of biomass.

Another aspect is the location of the product because the biofilm approach is perfectly suited if the product is released from the biofilm and can be captured afterwards from the supernatant or fermentation broth, respectively. However, processes are also described, whereby the product is enriched by the biofilm-harboring organisms as described, for example, by Zhang et al. for accumulation of polyhydroxybutyrate [27]. If the target compounds are located intracellular a corresponding “milking” process must be established to operate the reactor in a continuous mode. Otherwise the process might become inefficient with respect to

process economics. If the EPS or compounds from the matrix are the targets of the process, there is of course no alternative to producing these compounds (semi-) batchwise. But a particular interest should be addressed to establish a continuous or semi-continuous process due to the fact that biofilms require a certain time period to be constructed.

Some of the examples presented are highlighted in the following sections, where the products are classified into solvents, organic acids, enzymes, bioactive compounds, and other products.

### 3.1.1 Solvent Production

Several examples of solvent production by biofilms were investigated within the last decades. The investigations were mainly driven by seeking alternative production systems for manufacturing ethanol as well as butanol and acetone. As indicated in Table 4, the production of these commodities was investigated by application of packed-bed and fluidized reactors using several kinds of support. The highest space–time yield of 377.4 g/L h was reported for a packed-bed approach by Krug and Daugulis, who immobilized *Z. mobilis* on anionic exchange resin beads [66]. In comparison Kunduru and Pometto obtained a value of 124 g/L h [67, 68], which is even approximately 10 times higher than the space–time yield reported by Weuster-Botz, Aivasidis, and Wandrey for immobilized *Z. mobilis* (13 g/L h) on macroporous glass beads [33]. However, these values must be evaluated carefully when compared with standard cultivation techniques because the applied biomass may be much higher than in the reference assay, particularly if only the void volume of the packed-bed reactor is considered. Therefore, it is necessary to calculate the productivity with respect to the whole reactor volume because this value reflects the installation costs of the required plant.

### 3.1.2 Organic Acid Production

A broad variety of organic acids is currently produced by means of stirred-tank reactor approaches applying suspended cells. Because the production is often inhibited by the relevant organic acid if a threshold concentration is exceeded, the application of biofilms might be favorable according to their higher robustness towards unphysiological environmental conditions. Many organic acids can be produced by cultivation of fungi; in particular, citric acid or fumaric acids are very prominent examples for biotechnologically manufactured compounds. But bacteria, such as *Actinobacillus* sp., can also be used to produce valuable organic acids including succinic acid. The reported productivities of citric acid [69], succinic acid [70, 71], and propionic acid [72], as well as acetic acid [7] and glycolic acid [31] were in the range of approximately 1–2 g/L h, and thus quite similar, whereas the reported productivity of fumaric acid was estimated to be 3.78 g/L h [37]. Interestingly, the productivities were obtained with different reactor types and

biofilm support materials (see Table 4). Potential routes for the synthesis of commodities might use the organic acids fumaric and succinic acid in the near future. Both acids were mentioned within the report “Top Value Added Chemicals from Biomass,” published by the US Department of Energy in 2004 [73], and identified (in addition to other microbial metabolites) as potential building blocks for manufacturing value-added chemicals from biomass resources.

### 3.1.3 Enzyme Production

Several approaches for the production of enzymes by biofilms are reported in the literature (see Table 4). Whereas the matrix should support the retention of the enzyme under natural conditions, a biotechnological production process has to maximize as well the enzyme liberation from the matrix and the production by the microorganisms growing attached to the support material. In nature, the retention of enzymes such as glycosidases or proteases supports the supply of nutrients for a broad variety of microorganisms, hence, the matrix is sometimes termed as “stomach” of the biofilm community. As well as the nutrient supply, the retention of catalases or  $\beta$ -lactamases, for example, prevent the biofilm organisms from growth and metabolic inhibition. An efficient manufacturing process must first provide a good expression of the target enzyme. Since biofilms are highly suited for long-term (continuous) processes, the production of extracellular enzymes is reasonable rather than production of intracellular enzymes. As indicated in Table 4, research was for example focused on the production of lignin peroxidase and manganese peroxidase, enzymes responsible for lignin degradation. The application of a biofilm approach for the supply of the required enzymes might be of interest because a high productivity was reported for immobilized *P. chrysosporium* [74]. The productivities for lignin peroxidase were in a narrow range for different reactor types: Jones and Briedis reported a productivity of 0.46 U/L h (*P. chrysosporium* grown on plastic discs in a rotating disc bioreactor) [25], whereas Khiyami, Pometto, and Kennedy found a productivity of 0.35 U/L h (*P. chrysosporium* grown on PCS tubes on an agitator shaft) [74]. An impressive productivity of 5.6 U/L h was reported by Linko [75] who established a *P. chrysosporium* biofilm on nylon web cubes that were used in a stirred-tank bioreactor.

Cellulases are well established in biotechnology for degradation of cellulose into its subunit glucose, which can afterwards be used as a carbon source for biotechnological production of valuable compounds. A sophisticated approach for the production of cellulase by *T. viride* was developed by Webb, Fukuda, and Atkinson [35] who applied a modified bubble column termed a “spouted-bed fermenter.” The cells were grown on hollow stainless steel wire balls and blocking of the reactor was prevented by a jet stream that provided a certain shear force to liberate excess biomass from the supporting material. The volumetric productivity of the system (31.5 FPA U/L h) was 53 % greater in comparison to the batch system.

### 3.1.4 Production of Bioactive Compounds

Microbial secondary metabolites featuring bioactive properties such as antimicrobial, antitumoral, anti-inflammatory, or antiviral properties are desirable candidates for pharmaceutical applications. The production of these compounds is commonly related to external stimuli such as phosphate limitation or regulated by quorum sensing, i.e., effects which also occur in biofilms. In particular, the stimulus can be represented by an inducing bacterium that is co-cultivated in the biofilm. Due to the highly complex fermentation of multispecies biofilms, the reported applications exploited single-species biofilms for production of the bioactive compounds (see Table 4). Cho, Yousef, and Yang used a spiral wound fibrous matrix for cultivation of *Pediococcus acidilactici* to produce pediocin [76], a plasmid-coded peptide belonging to the class of bacteriocins, featuring a molecular mass of approximately 4.6 kDa [77, 78]. The compound is of relevance due to its inhibition of *Listeria monocytogenes*, a widespread food-transmitted pathogen [77, 79]. The process was operated continuously for 3 months without clogging, degeneration, or contamination problems, indicating long-term stability of the packed-bed bioreactor, whereby a maximum bacteriocin productivity of  $1.0 \times 10^7$  AU/L d at a dilution rate of  $1.58 \text{ day}^{-1}$  and pH 4.5 was observed. By using an analogue support for the microorganisms, Xia et al. reported a space–time yield of  $1.0 \times 10^7$  AU/L d for the production of the bacteriocin nisin by *Lactococcus lactis* [80]. Application of *L. lactis* immobilized on PCS tubes on an agitator shaft of a stirred-tank reactor may support the productivity as indicated by Pongtharangkul and Demirci, who reported a space–time yield of 5.4 AU/L h [81].

The production of  $\beta$ -lactam antibiotics such as Cephalosporin C is well known and its chemical and biotechnological modification has been established for several decades. The resulting final concentration obtained in fed-batch mode operation is approximately 30 g/L with a corresponding productivity of 0.191 g/L h [82]. However, a continuous process applying a biofilm set-up might support good productivity due to the higher robustness of the microorganisms. A biofilm approach for the production of Cephalosporin C was investigated by Srivastava and Kundu [83]. They utilized sintered glass particles as biofilm support material in a bubble column set-up and reported a productivity of  $7.111 \times 10^{-3}$  g/L h. Compared to the value of the fed-batch process the obtained productivity is approximately two orders of magnitude lower.

In particular within the field of marine biotechnology many strains were identified that produce a certain antimicrobial secondary metabolite solely, when the organisms are cultivated in a biofilm; i.e., the exposition of bacteria and/or fungi towards a surface is required for production of the target metabolite. Some relevant examples are described in more detail in the chapter by Mitra et al. in this edition of *Advances of Biochemical Engineering/Biotechnology*.

### 3.1.5 Miscellaneous

Robustness of biofilms is a main argument for the application of biofilm reactor systems to produce chemicals that are classified as toxic for the producing strain(s). One fine chemical that was investigated over several years by the working group of K. Buehler and A. Schmid from the University of Dortmund is styrene oxide. This compound can be synthesized by *Pseudomonas* sp. biofilm from styrene. They investigated several set-ups for optimizing the productivity of the biofilm system and utilized ceramic and silicone membranes as support for the microorganism. An efficient mass transfer of the product as well as substrate through the membrane protects the attached growing *Pseudomonas* biofilm from inhibition. However, to date, the biotechnological synthesis of styrene oxide is less efficient and economically feasible compared to chemical synthesis. The productivity of the system immobilized on the silicone material was evaluated to 0.67 g/L h [42], whereas the corresponding activity obtained by utilization of the inorganic material was estimated to 1.2 g/L h [43]. This considerable increase in productivity is mainly attributed to the modified set-up: the ceramic material allows an aeration of the biofilm. Due to aeration the oxidation of the organic substrate is facilitated.

Another interesting approach is the use of phototrophic biofilms to produce hydrogen. Whereas microalgae and cyanobacteria produce oxygen- and energy-rich compounds due to metabolization of carbon dioxide and water when illuminated with light of appropriate wavelengths, these organisms are able to produce H<sub>2</sub> under anaerobic conditions. For instance, Zhang et al. described a novel groove-type photobioreactor for hydrogen production by immobilized *Rhodospseudomonas palustris* CQK 01. In comparison to a commonly used flat-panel photobioreactor, a significant increase of hydrogen production rate of 75 % was observed [84] and the corresponding value was estimated to 3.816 mmol<sub>Hydrogen</sub>/m<sup>2</sup> h. They assume that the higher production rate is attributed to the enriched immobilized biomass inside the reactor system. Alternatively, hydrogen can be produced by fermentation of sugars, applicable as supplements in complex media or resulting from hydrolysis of complex carbons, whereas the theoretical productivity is 4 mol<sub>Hydrogen</sub>/mol<sub>glucose</sub>. Zhang et al. applied a mesophilic unsaturated flow (trickle-bed) reactor for H<sub>2</sub>-production via fermentation of glucose [85]. The reactor consisted of a column packed with glass beads and was inoculated with a pure culture of *C. acetobutylicum*. By supplementing a defined medium containing glucose, a specific H<sub>2</sub>-production rate from 680 to 1,270 mL/g<sub>glucose</sub> per liter of reactor (total volume) was obtained. The yield of H<sub>2</sub> was indicated as 15–27 %, in comparison to the above-mentioned theoretical limit. Main by-products in the liquid effluent were acetate and butyrate. After a process time of 60–72 h the reactor became clogged with biomass, hence a manual cleaning of the system was necessary. The authors indicated that it is desired to apply this reactor technology for H<sub>2</sub> recovery from pre-treatment of high carbohydrate-containing wastewaters. Van Groenesteijn et al. operated on a 400-L scale and used a TBR for the production of hydrogen with the thermophile *Caldicellulosiruptor saccharolyticus* under non-axenic conditions [86]. They yielded 2.8 mol H<sub>2</sub> per mole hexose converted,

whereby the reactor was fed with a complex medium with sucrose as the main substrate. The reactor was continuously flushed with nitrogen gas, and operated at 73 °C. A volumetric productivity of 22 mmol H<sub>2</sub>/L<sub>filterbed</sub> h was reported. Methane production was negligible and the main by-products in the liquid phase were acetic acid and lactic acid.

### ***3.2 Prospective Applications of Biofilms in Biotechnological Production Processes***

In the previous sections the state of the art of products accessible by biofilm approaches was described. Here, a brief overview of potential (industrial) applications of biofilms is given.

A prospective application might be the construction of self-regulating biofilms, where the targets (e.g., proteins or bioactive compounds) are produced after induction via microbial communication. Thus, the cells are growing, while producing the communication molecules, and after reaching a defined threshold concentration the production or biotransformation process is (automatically) switched on by their own. Furthermore, exploitation of quorum-sensing circuits could be used to control the biomass within a bioreactor system. Here, the population density may be regulated, due to induction/expression of a toxic compound after cell density has reached a defined threshold concentration. Via tuning of the sensitivity of the communication circuit a constant cell density could be maintained in the biofilm bioreactor. Hence, blocking might be prevented by the biological system itself. This principle is not restricted to biofilms, hence cultivation of suspended microorganisms may also benefit by exploitation of the relevant quorum-sensing circuits. More information about the potential utilization of self-inducing systems within different biotechnological processes was recently highlighted by Choudhary and Schmidt-Dannert and can be found elsewhere [87].

Common bioprocesses are done under axenic conditions, in which a single species is cultivated to produce the desired compound. Herewith the manufacturing guidelines are much more easily fulfilled in comparison to bioreactions where two or more species are cultivated together for production of the target. But co-cultivation may be beneficial in particular for the recombinant production of proteins. Thus, each single species produces a fragment and, after combination of the different fragments, the relevant protein is obtained. According to the reduction of the metabolic stress of each single-used organism, the productivity may be higher than the expression of the complete system by one species. This approach may be very powerful in combination with the prospective self-inducing systems mentioned above.

Proper growth and productivity of microorganisms are restricted to the availability and supply of water. However, many organisms, such as the diverse group of terrestrial cyanobacteria, have adapted to arid conditions. Hence they can grow with



a minimum of water, and they protect themselves from desiccation by production of an EPS matrix (e.g., [58]). As mentioned in Sect. 2.2.6, these microorganisms can be grown in an aerosol atmosphere and after reduction of the water supply an enhanced production of EPS can be observed. Because some cyanobacteria co-produce bioactive metabolites during generation of the matrix, the EPS can be considered as a valuable source for recovery of several novel secondary metabolites featuring, for example, anti-inflammatory or antiviral activity. The application of biofilms for cultivation of organisms in a gaseous phase is not restricted to phototrophic organisms, which must be optimally supplied with carbon dioxide. In fact such a cultivation mode may be used in principle for several production processes, where a gaseous phase contains the substrate(s).

The productivity and production pattern (including the variation of the product spectrum) of microorganisms is affected by the presence of surfaces. But to date it is still unclear if the productivity can be tuned due to exposition of the organisms towards surfaces exhibiting different structural motifs. Within the Collaborative Research Center funded by the German Research Foundation (Collaborative Research Centre 926: “Microscale Morphology of Component Surfaces”) the relationship between surface characteristics (morphology) and production pattern is one currently investigated task. One major aim of this project is to establish novel components for biofilm reactors that may act as biofilm support materials stimulating adhesion as well as productivity of the attached growing microorganisms.

## 4 Summary and Outlook

Microorganisms growing in biofilms have proven their potential for several production processes concerning bulk and fine chemicals on a lab scale. Whereas large-scale processes are reported for multispecies biofilms in wastewater and sewage treatment, the number of full-scale applications in terms of productive biofilms is quite low. One major difficulty of transferring the biofilm from the lab to a larger scale is that the construction of the biofilm depends on many factors; for example, the biofilm properties commonly vary between two experiments. However, compared to standard cultivation techniques the application of biofilms for manufacturing value-added compounds is still in its infancy. It can be expected that some of the examples mentioned within this review may become transferred from the lab to a pilot plant. According to their robustness and long-term stability biofilms can be assumed to be very prospective in processes with fluctuating input streams. A major problem during operation of biorefineries are input streams whose composition is dependent on many environmental parameters, such as season of harvesting of the raw materials as well as storage and pretreatment. The utilization of biofilms may help to tackle these bottlenecks of classical fermentation technology. Moreover, the availability of novel biofilm support materials may complement the number of parameters to control a production process. Therefore, the

research on carrier geometries and materials applied for establishing reproducible biofilm processes must be extended to achieve these goals within the near future.

**Acknowledgments** We wish to thank the German Research Foundation (DFG) for funding under LA 1426/9-1, UL 170/7-1, and SFB 926/1-2013.

## References

1. Warnock JN, Al-Rubeai M (2006) Bioreactor systems for the production of biopharmaceuticals from animal cells. *Biotechnol Appl Biochem* 45:1–12. doi:[10.1042/ba2005023](https://doi.org/10.1042/ba2005023)
2. Harding MW, Marques LLR, Howard RJ et al (2009) Can filamentous fungi form biofilms? *Trends Microbiol* 17(11):475–480. doi:[10.1016/j.tim.2009.08.007](https://doi.org/10.1016/j.tim.2009.08.007)
3. Fukuda H (1995) Immobilized microorganism bioreactors. In: Asenjo JA, Merchuk JC (eds) *Bioreactor system design*. Marcel Dekker Inc, New York, pp 339–375
4. Gross R, Schmid A, Buehler K (2012) Catalytic biofilms: a powerful concept for future bioprocesses. In: Lear G, Lewis GD (eds) *Microbial biofilms*. Caister Academic Press, Norfolk, pp 193–222
5. Kobayashi M, Shimizu S (2000) Nitrile hydrolases. *Curr Opin Chem Biol* 4(1):95–102. doi:[10.1016/s1367-5931\(99\)00058-7](https://doi.org/10.1016/s1367-5931(99)00058-7)
6. Murphy CD (2012) The microbial cell factory. *Org Biomol Chem* 10(10):1949–1957. doi:[10.1039/c2ob06903b](https://doi.org/10.1039/c2ob06903b)
7. Crueger W, Crueger A, Brock TD (1990) *Biotechnology. A textbook of industrial microbiology*, 2nd edn. Sinauer Associates, Sunderland
8. Kersters K, Lisdiyanti P, Komagata K et al (2006) The family Acetobacteraceae: the genera *Acetobacter*, *Acidomonas*, *Asaia*, *Gluconacetobacter*, *Gluconobacter*, and *Kozakia*. In: Dworkin M (ed) *Prokaryotes*, vol 5. Springer Science + Business Media, New York, pp 163–200
9. Li XZ, Hauer B, Rosche B (2007) Single-species microbial biofilm screening for industrial applications. *Appl Microbiol Biotechnol* 76(6):1255–1262. doi:[10.1007/s00253-007-1108-4](https://doi.org/10.1007/s00253-007-1108-4)
10. Cronenberg CCH, Ottengraf SPP, Vandenheuvel JC et al (1994) Influence of age and structure of penicillium chrysogenum pellets on the internal concentration profiles. *Bioprocess Eng* 10(5–6):209–216. doi:[10.1007/bf00369531](https://doi.org/10.1007/bf00369531)
11. Hooijmans CM, Briasco CA, Huang J et al (1990) Measurement of oxygen concentration gradients in gel-immobilized recombinant *Escherichia coli*. *Appl Microbiol Biotechnol* 33(6):611–618
12. Tjihuis L, van Loosdrecht MCM, Heijnen JJ (1994) Formation and growth of heterotrophic aerobic biofilms on small suspended particles in airlift reactors. *Biotechnol Bioeng* 44(5):595–608. doi:[10.1002/bit.260440506](https://doi.org/10.1002/bit.260440506)
13. Demirci A, Pongtharangkul T, Pometto AL (2007) Application of biofilm reactors for production of value-added products by microbial fermentation. In: Blaschek HP, Wang HH, Agle ME (eds) *Biofilms in the food environment*. Blackwell Publishing Ltd., Oxford, pp 167–189
14. Gross R, Lang K, Buehler K et al (2010) Characterization of a biofilm membrane reactor and its prospects for fine chemical synthesis. *Biotechnol Bioeng* 105(4):705–717. doi:[10.1002/bit.22584](https://doi.org/10.1002/bit.22584)
15. Atkinson B, Black GM, Lewis PJS et al (1979) Biological particles of given size, shape, and density for use in biological reactors. *Biotechnol Bioeng* 21(2):193–200. doi:[10.1002/bit.260210206](https://doi.org/10.1002/bit.260210206)

16. Karsakevich A, Ventina E, Vina I et al (1998) The effect of chemical treatment of stainless steel wire surfaces on *Zymomonas mobilis* cell attachment and product synthesis. *Acta Biotechnol* 18(3):255–265. doi:[10.1002/abio.370180310](https://doi.org/10.1002/abio.370180310)
17. Schwartz T, Hoffmann S, Obst U (2003) Formation of natural biofilms during chlorine dioxide and u.v. disinfection in a public drinking water distribution system. *J Appl Microbiol* 95(3):591–601. doi:[10.1046/j.1365-2672.2003.02019.x](https://doi.org/10.1046/j.1365-2672.2003.02019.x)
18. Qureshi N, Paterson AHJ, Maddox IS (1988) Model for continuous production of solvents from whey permeate in a packed-bed reactor using cells of *Clostridium acetobutylicum* immobilized by adsorption onto bonechar. *Appl Microbiol Biotechnol* 29(4):323–328
19. Qureshi N, Annous BA, Ezeji TC et al (2005) Biofilm reactors for industrial bioconversion processes: employing potential of enhanced reaction rates. *Microb Cell Fact* 4:21. doi:[10.1186/1475-2859-4-24](https://doi.org/10.1186/1475-2859-4-24)
20. Jördening HJ (1992) Anaerobic biofilms in fluidized bed reactors. In: Melo LF, Bott TR, Fletcher M et al (eds) *Biofilms—science and technology*. Kluwer Academic Publishers, Dordrecht, pp 435–442
21. Sohling U, Ruf F, Neitmann E, Linke B (2010) Magnetische Glaspartikel zum Einsatz in Biogasanlagen, Fermentations- und Separationsprozessen(DE102010034083A1)
22. Lienhardt J, Schripsema J, Qureshi N et al (2002) Butanol production by *Clostridium beijerinckii* BA101 in an immobilized cell biofilm reactor—increase in sugar utilization. *Appl Biochem Biotech* 98:591–598. doi:[10.1385/abab:98-100:1-9:591](https://doi.org/10.1385/abab:98-100:1-9:591)
23. Urek RO, Pazarlioglu NK (2004) A novel carrier for *Phanerochaete chrysosporium* immobilization. *Artif Cell Blood Sub* 32(4):563–574. doi:[10.1081/lab-200039618](https://doi.org/10.1081/lab-200039618)
24. Asther M, Bellonfontaine MN, Capdevila C et al (1990) A thermodynamic model to predict *Phanerochaete chrysosporium* INA-12 adhesion to various solid carriers in relation to lignin peroxidase production. *Biotechnol Bioeng* 35(5):477–482. doi:[10.1002/bit.260350505](https://doi.org/10.1002/bit.260350505)
25. Jones SC, Briedis DM (1992) Adhesion and lignin peroxidase production by the white-rot fungus *Phanerochaete chrysosporium* in a rotating biological contactor. *J Biotechnol* 24(3):277–290. doi:[10.1016/0168-1656\(92\)90037-a](https://doi.org/10.1016/0168-1656(92)90037-a)
26. Guimarães C, Matos C, Azeredo J et al (2002) The importance of the morphology and hydrophobicity of different carriers on the immobilization and sugar refinery effluent degradation activity of *Phanerochaete chrysosporium*. *Biotechnol Lett* 24(10):795–800. doi:[10.1023/a:1015580322450](https://doi.org/10.1023/a:1015580322450)
27. Zhang SP, Norrlov O, Wawrzynczyk J et al (2004) Poly(3-hydroxybutyrate) biosynthesis in the biofilm of *Alcaligenes eutrophus*, using glucose enzymatically released from pulp fiber sludge. *Appl Environ Microb* 70(11):6776–6782. doi:[10.1128/aem.70.11.6776-6782.2004](https://doi.org/10.1128/aem.70.11.6776-6782.2004)
28. Cotton JC, Pometto AL, Gvozdenovic-Jeremic J (2001) Continuous lactic acid fermentation using a plastic composite support biofilm reactor. *Appl Microbiol Biotechnol* 57(5–6):626–630
29. Cheng KC, Demirci A, Catchmark JM (2010) Advances in biofilm reactors for production of value-added products. *Appl Microbiol Biotechnol* 87(2):445–456. doi:[10.1007/s00253-010-2622-3](https://doi.org/10.1007/s00253-010-2622-3)
30. Park CH, Okos MR, Wankat PC (1989) Acetone-butanol-ethanol (ABE) fermentation in an immobilized cell trickle bed reactor. *Biotechnol Bioeng* 34(1):18–29. doi:[10.1002/bit.260340104](https://doi.org/10.1002/bit.260340104)
31. Li XZ, Hauer B, Rosche B (2013) Catalytic biofilms on structured packing for the production of glycolic acid. *J Microbiol Biotechnol* 23(2):195–204. doi:[10.4014/jmb.1207.07057](https://doi.org/10.4014/jmb.1207.07057)
32. Gjaltema A, Vinke JL, van Loosdrecht MCM et al (1997) Abrasion of suspended biofilm pellets in airlift reactors: Importance of shape, structure, and particle concentrations. *Biotechnol Bioeng* 53(1):88–99. doi:[10.1002/\(sici\)1097-0290\(19970105\)53:1<88:aid-bit12>3.0.co;2-5](https://doi.org/10.1002/(sici)1097-0290(19970105)53:1<88:aid-bit12>3.0.co;2-5)
33. Weusterbotz D, Aivasidis A, Wandrey C (1993) Continuous ethanol production by *Zymomonas mobilis* in a fluidized-bed reactor. Part II: Process development for the fermentation of hydrolysed B-starch without sterilization. *Appl Microbiol Biotechnol* 39(6):685–690

34. Barros AR, de Amorim ELC, Reis CM et al (2010) Biohydrogen production in anaerobic fluidized bed reactors: effect of support material and hydraulic retention time. *Int J Hydrogen Energy* 35(8):3379–3388. doi:[10.1016/j.ijhydene.2010.01.108](https://doi.org/10.1016/j.ijhydene.2010.01.108)
35. Webb C, Fukuda H, Atkinson B (1986) The production of cellulase in a spouted bed fermenter using cells immobilized in biomass support particles. *Biotechnol Bioeng* 28(1):41–50. doi:[10.1002/bit.260280107](https://doi.org/10.1002/bit.260280107)
36. Converti A, de Faveri D, Perego P et al (2006) Investigation on the transient conditions of a rotating biological contactor for bioethanol production. *Chem Biochem Eng Q* 20(4):401–406
37. Cao NJ, Du JX, Chen CS et al (1997) Production of fumaric acid by immobilized *Rhizopus* using rotary biofilm contactor. *Appl Biochem Biotech* 63–5:387–394. doi:[10.1007/bf02920440](https://doi.org/10.1007/bf02920440)
38. Delborghi M, Converti A, Parisi F et al (1985) Continuous alcohol fermentation in an immobilized cell rotating-disk reactor. *Biotechnol Bioeng* 27(6):761–768. doi:[10.1002/bit.260270602](https://doi.org/10.1002/bit.260270602)
39. Sarkar S, Saha M, Roy D et al (2008) Enhanced production of antimicrobial compounds by three salt-tolerant actinobacterial strains isolated from the Sundarbans in a niche-mimic bioreactor. *Mar Biotechnol* 10(5):518–526. doi:[10.1007/s10126-008-9090-0](https://doi.org/10.1007/s10126-008-9090-0)
40. Lewandowski Z, Beyenal H (2007) Fundamentals of biofilm research. CRC Press Inc., Boca Raton
41. Syron E, Casey E (2008) Membrane-aerated biofilms for high rate biotreatment: performance appraisal, engineering principles, scale-up, and development requirements. *Environ Sci Technol* 42(6):1833–1844. doi:[10.1021/es0719428](https://doi.org/10.1021/es0719428)
42. Gross R, Hauer B, Otto K et al (2007) Microbial biofilms: New catalysts for maximizing productivity of long-term biotransformations. *Biotechnol Bioeng* 98(6):1123–1134. doi:[10.1002/bit.21547](https://doi.org/10.1002/bit.21547)
43. Halan B, Schmid A, Buchler K (2010) Maximizing the productivity of catalytic biofilms on solid supports in membrane aerated reactors. *Biotechnol Bioeng* 106(4):516–527. doi:[10.1002/bit.22732](https://doi.org/10.1002/bit.22732)
44. Gross R, Buehler K, Schmid A (2013) Engineered catalytic biofilms for continuous large scale production of n-octanol and (S)-styrene oxide. *Biotechnol Bioeng* 110(2):424–436. doi:[10.1002/bit.24629](https://doi.org/10.1002/bit.24629)
45. Barclay WR, Meager KM, Abril JR (1994) Heterotrophic production of long-chain omega-3-fatty-acids utilizing algae and algae-like microorganisms. *J Appl Phycol* 6(2):123–129. doi:[10.1007/bf02186066](https://doi.org/10.1007/bf02186066)
46. Kuhne S, Lakatos M, Foltz S et al (2013) Characterization of terrestrial cyanobacteria to increase process efficiency in low energy consuming production processes. *Sustain Chem Proc* 1(1):6. doi:[10.1186/2043-7129-1-6](https://doi.org/10.1186/2043-7129-1-6)
47. Mata TM, Martins AA, Caetano NS (2010) Microalgae for biodiesel production and other applications: a review. *Renew Sustain Energy Rev* 14(1):217–232
48. Boyd MR, Gustafson KR, McMahon JB et al (1997) Discovery of cyanovirin-N, a novel human immunodeficiency virus-inactivating protein that binds viral surface envelope glycoprotein gp120: potential applications to microbicide development. *Antimicrob Agents Chemother* 41(7):1521–1530
49. Bewley CA, Gustafson KR, Boyd MR et al (1998) Solution structure of cyanovirin-N, a potent HIV-inactivating protein. *Nat Struct Biol* 5(7):571–578
50. Bokesch HR, O’Keefe BR, McKee TC et al (2003) A potent novel anti-HIV protein from the cultured cyanobacterium *Scytonema varium*. *Biochemistry* 42(9):2578–2584
51. Sivonen K, Börner T (2008) Bioactive compounds produced by cyanobacteria. In: Herrero A, Flores EGF (eds) *The cyanobacteria: molecular biology, genomics, and evolution*. Caister Academic Press, Norfolk, pp 159–197
52. Belnap J, Lange OL (2001) Biological soil crusts: structure, function, and management. *Ecological studies*. Springer, Berlin

53. Lakatos M, Bilger W, Büdel B (2001) Carotenoid composition of terrestrial cyanobacteria: response to natural light conditions in habitats in Venezuela. *Eur J Phycol* 36:367–375
54. Dojani S, Lakatos M, Rascher U et al (2007) Nitrogen input by cyanobacterial biofilms of an inselberg into a tropical rainforest in French Guiana. *Flora* 202(7):521–529
55. Rascher U, Lakatos M, Büdel B et al (2003) Photosynthetic field capacity of cyanobacteria of a tropical inselberg of the Guiana Highlands. *Eur J Phycol* 38(3):247–256
56. Lange O, Bilger W, Rimke S et al (1989) Chlorophyll fluorescence of lichens containing green and blue green algae during hydration by water vapor uptake and by addition of liquid water. *Bot Acta* 102:306–313
57. Helm RF, Huang Z, Edwards D et al (2000) Structural characterization of the released polysaccharide of desiccation-tolerant *Nostoc commune* DRH-1. *J Bacteriol* 182(4):974–982
58. Shaw E, Hill DR, Brittain N et al (2003) Unusual water flux in the extracellular polysaccharide of the cyanobacterium *Nostoc commune*. *Appl Environ Microb* 69(9):5679–5684
59. Potts M (1999) Mechanisms of desiccation tolerance in cyanobacteria. *Eur J Phycol* 34(4):319–328
60. Fleming ED, Castenholz RW (2007) Effects of periodic desiccation on the synthesis of the UV-screening compound, scytonemin, in cyanobacteria. *Environ Microbiol* 9(6):1448–1455
61. Pereira S, Zille A, Micheletti E et al (2009) Complexity of cyanobacterial exopolysaccharides: composition, structures, inducing factors and putative genes involved in their biosynthesis and assembly. *FEMS Microbiol Rev* 33(5):917–941
62. de Marsac NT (1977) Occurrence and nature of chromatic adaptation in cyanobacteria. *J Bacteriol* 130(1):82–91
63. Kehoe DM, Gutu A (2006) Responding to color: the regulation of complementary chromatic adaptation. *Annu Rev Plant Biol* 57:127–150
64. Malcata FX (2011) Microalgae and biofuels: a promising partnership? *Trends Biotechnol* 29(11):542–549
65. Norsker N, Barbosa MJ, Vermuë MH et al (2011) Microalgal production—a close look at the economics. *Biotechnol Adv* 29(1):24–27
66. Krug TA, Daugulis AJ (1983) Ethanol-production using *Zymomonas mobilis* immobilized on an ion-exchange resin. *Biotechnol Lett* 5(3):159–164. doi:10.1007/bf00131895
67. Kunduru MR, Pometto AL (1996) Continuous ethanol production by *Zymomonas mobilis* and *Saccharomyces cerevisiae* in biofilm reactors. *J Ind Microbiol* 16(4):249–256. doi:10.1007/bf01570029
68. Kunduru MR, Pometto AL (1996) Evaluation of plastic composite-supports for enhanced ethanol production in biofilm reactors. *J Ind Microbiol* 16(4):241–248. doi:10.1007/bf01570028
69. Wang JL (2000) Production of citric acid by immobilized *Aspergillus niger* using a rotating biological contactor (RBC). *Bioresour Technol* 75(3):245–247
70. Urbance SE, Pometto AL, DiSpirito AA et al. (2003) Medium evaluation and plastic composite support ingredient selection for biofilm formation and succinic acid production by *Actinobacillus succinogenes*. *Food Biotechnol* 17(1). doi: 10.1081/fbt-120019984
71. Urbance SE, Pometto AL, DiSpirito AA et al. (2004) Evaluation of succinic acid continuous and repeat-batch biofilm fermentation by *Actinobacillus succinogenes* using plastic composite support bioreactors. *Appl Microbiol Biotechnol* 65(6). doi: 10.1007/s00253-004-1634-2
72. Lewis VP, Yang ST (1992) Continuous propionic-acid fermentation by immobilized *Propionibacterium acidipropionici* in a novel packed-bed bioreactor. *Biotechnol Bioeng* 40(4):465–474. doi:10.1002/bit.260400404
73. U.S. Department of Energy (2004) Top value added chemicals from biomass. Results of screening for potential candidates from sugars and synthetic gas, vol 1, Washington
74. Khiyami MA, Pometto AL, Kennedy WJ (2006) Ligninolytic enzyme production by *Phanerochaete chrysosporium* in plastic composite support biofilm stirred tank bioreactors. *J Agr Food Chem* 54(5). doi: 10.1021/jf0514241

75. Linko S (1988) Production and characterization of extracellular lignin peroxidase from immobilized *Phanerochaete chrysosporium* in a 10-l bioreactor. *Enzyme Microb Technol* 10(7):410–417. doi:[10.1016/0141-0229\(88\)90035-X](https://doi.org/10.1016/0141-0229(88)90035-X)
76. Cho HY, Yousef AE, Yang ST (1996) Continuous production of pediocin by immobilized *Pediococcus acidilactici* P02 in a packed-bed bioreactor. *Appl Microbiol Biotechnol* 45(5):589–594
77. Hoover DG, Walsh PM, Kolaetis KM et al. (1988) A bacteriocin produced by *Pediococcus* species associated with a 5.5-megadalton plasmid. *J Food Prot* 51(1):29–31
78. Lozano JCN, Meyer JN, Sletten K et al (1992) Purification and amino acid sequence of bacteriocin produced by *Pediococcus acidilactici*. *J Gen Microbiol* 138:1985–1990
79. Liao CC, Yousef AE, Richter ER et al (1993) *Pediococcus acidilactici* P02 bacteriocin production in whey permeate and inhibition of *Listeria monocytogenes* in foods. *J Food Sci* 58(2):430–434. doi:[10.1111/j.1365-2621.1993.tb04291.x](https://doi.org/10.1111/j.1365-2621.1993.tb04291.x)
80. Xia L, Chung YK, Yang ST et al (2005) Continuous nisin production in laboratory media and whey permeate by immobilized *Lactococcus lactis*. *Process Biochem* 40(1):13–24. doi:[10.1016/j.procbio.2003.11.032](https://doi.org/10.1016/j.procbio.2003.11.032)
81. Pongtharangkul T, Demirci A (2006) Evaluation of culture medium for nisin production in a repeated-batch biofilm reactor. *Biotechnol Progr* 22(1). doi: [10.1021/bp050295q](https://doi.org/10.1021/bp050295q)
82. Schügerl K (2005) Process development in biotechnology—a re-evaluation. *Eng Life Sci* 5(1):15–28. doi:[10.1002/elsc.200402166](https://doi.org/10.1002/elsc.200402166)
83. Srivastava P, Kundu S (1999) Studies on cephalosporin-C production in an air lift reactor using different growth modes of *Cephalosporium acremonium*. *Process Biochem* 34(4):329–333. doi:[10.1016/s0032-9592\(98\)00059-4](https://doi.org/10.1016/s0032-9592(98)00059-4)
84. Zhang CA, Zhu X, Liao QA et al (2010) Performance of a groove-type photobioreactor for hydrogen production by immobilized photosynthetic bacteria. *Int J Hydrogen Energy* 35(11):5284–5292. doi:[10.1016/j.ijhydene.2010.03.085](https://doi.org/10.1016/j.ijhydene.2010.03.085)
85. Zhang HS, Bruns MA, Logan BE (2006) Biological hydrogen production by *Clostridium acetobutylicum* in an unsaturated flow reactor. *Water Res* 40(4):728–734. doi:[10.1016/j.watres.2005.11.041](https://doi.org/10.1016/j.watres.2005.11.041)
86. van Groenestijn JW, Geelhoed JS, Goorissen HP et al (2009) Performance and population analysis of a non-sterile trickle bed reactor inoculated with *Caldicellulosiruptor saccharolyticus*, a thermophilic hydrogen producer. *Biotechnol Bioeng* 102(5):1361–1367. doi:[10.1002/bit.22185](https://doi.org/10.1002/bit.22185)
87. Choudhary S, Schmidt-Dannert C (2010) Applications of quorum sensing in biotechnology. *Appl Microbiol Biotechnol* 86(5):1267–1279. doi:[10.1007/s00253-010-2521-7](https://doi.org/10.1007/s00253-010-2521-7)
88. Demirci A, Pometto AL, Ho, K. L. G. (1997) Ethanol production by *Saccharomyces cerevisiae* in biofilm reactors. *J Ind Microbiol Biotechnol* 19(4). doi: [10.1038/sj.jim.2900464](https://doi.org/10.1038/sj.jim.2900464)
89. Napoli F, Olivieri G, Russo ME et al (2010) Butanol production by *Clostridium acetobutylicum* in a continuous packed bed reactor. *J Ind Microbiol Biotechnol* 37(6):603–608. doi:[10.1007/s10295-010-0707-8](https://doi.org/10.1007/s10295-010-0707-8)
90. Qureshi N, Maddox IS (1987) Continuous solvent production from whey permeate using cells of *Clostridium acetobutylicum* immobilized by adsorption onto bonechar. *Enzyme Microb Technol* 9(11):668–671. doi:[10.1016/0141-0229\(87\)90125-6](https://doi.org/10.1016/0141-0229(87)90125-6)
91. Demirci A, Pometto AL, Johnson KE (1993) Evaluation of biofilm reactor solid support for mixed-culture lactic-acid production. *Appl Microbiol Biotechnol* 38(6):728–733
92. Demirci A, Pometto AL, Johnson KE (1993) Lactic-acid production in a mixed-culture biofilm reactor. *Appl Environ Microbiol* 59(1):203–207
93. Demirci A, Pometto AL (1995) Repeated-batch fermentation in biofilm reactors with plastic-composite supports for lactic-acid production. *Appl Microbiol Biotechnol* 43(4):585–589
94. Hekmat D, Bauer R, Fricke J (2003) Optimization of the microbial synthesis of dihydroxyacetone from glycerol with *Gluconobacter oxydans*. *Bioprocess Biosyst Eng* 26(2):109–116. doi:[10.1007/s00449-003-0338-9](https://doi.org/10.1007/s00449-003-0338-9)

95. Casali S, Gungormusler M, Bertin L et al (2012) Development of a biofilm technology for the production of 1,3-propanediol (1,3-PDO) from crude glycerol. *Biochem Eng J* 64:84–90. doi:[10.1016/j.bej.2011.11.012](https://doi.org/10.1016/j.bej.2011.11.012)
96. Li XZ, Webb JS, Kjelleberg S et al (2006) Enhanced benzaldehyde tolerance in *Zymomonas mobilis* biofilms and the potential of biofilm applications in fine-chemical production. *Appl Environ Microbiol* 72(2):1639–1644. doi:[10.1128/a-em.72.2.1639-1644.2006](https://doi.org/10.1128/a-em.72.2.1639-1644.2006)
97. Lee Y, Lee C, Chang H (1989) Citric acid production by *Aspergillus niger* immobilized on polyurethane foam. *Appl Microbiol Biotechnol* 30(2):141–143. doi:[10.1007/BF00264001](https://doi.org/10.1007/BF00264001)
98. Cheng K, Demirci A, Catchmark JM (2011) Continuous pullulan fermentation in a biofilm reactor. *Appl Microbiol Biotechnol* 90(3):921–927. doi:[10.1007/s00253-011-3151-4](https://doi.org/10.1007/s00253-011-3151-4)
99. Cheng K, Catchmark JM, Demirci A (2009) Enhanced production of bacterial cellulose by using a biofilm reactor and its material property analysis. *J Biol Eng* 3:12. doi:[10.1186/1754-1611-3-12](https://doi.org/10.1186/1754-1611-3-12)
100. Khiyami MA, Al-Fadual SM, Bahklia AH (2011) Polyhydroxyalkanoates production via *Bacillus* plastic composite support (PCS) biofilm and date palm syrup. *J Med Plants Res* 5(14)
101. Pongtharangkul T, Demirci A (2006) Effects of fed-batch fermentation and pH profiles on nisin production in suspended-cell and biofilm reactors. *Appl Microbiol Biotechnol* 73(1):73–79. doi:[10.1007/s00253-006-0459-6](https://doi.org/10.1007/s00253-006-0459-6)
102. Zhang HS, Bruns MA, Logan BE (2006) Biological hydrogen production by *Clostridium acetobutylicum* in an unsaturated flow reactor. *Water Res* 40(4):728–734. doi:[10.1016/j.watres.2005.11.041](https://doi.org/10.1016/j.watres.2005.11.041)
103. Govender S, Pillay VL, Odhav B (2010) Nutrient manipulation as a basis for enzyme production in a gradostat bioreactor. *Enzyme Microbiol Technol* 46(7):603–609. doi:[10.1016/j.enzmictec.2010.03.007](https://doi.org/10.1016/j.enzmictec.2010.03.007)
104. Tsofigkas AN, Winn M, Bowen J et al (2011) Engineering Biofilms for Biocatalysis. *ChemBioChem* 12(9):1391–1395. doi:[10.1002/cbic.201100200](https://doi.org/10.1002/cbic.201100200)
105. Meleigy SA, Khalaf MA (2009) Biosynthesis of gibberellic acid from milk permeate in repeated batch operation by a mutant *Fusarium moniliforme* cells immobilized on loofa sponge. *Bioresour Technol* 100(1):374–379. doi:[10.1016/j.biortech.2008.06.024](https://doi.org/10.1016/j.biortech.2008.06.024)

# Ecological Roles and Biotechnological Applications of Marine and Intertidal Microbial Biofilms

Sayani Mitra, Barindra Sana and Joydeep Mukherjee

**Abstract** This review is a retrospective of ecological effects of bioactivities produced by biofilms of surface-dwelling marine/intertidal microbes as well as of the industrial and environmental biotechnologies developed exploiting the knowledge of biofilm formation. Some examples of significant interest pertaining to the ecological aspects of biofilm-forming species belonging to the *Roseobacter* clade include autochthonous bacteria from turbot larvae-rearing units with potential application as a probiotic as well as production of tropodithietic acid and indigoidine. Species of the *Pseudoalteromonas* genus are important examples of successful surface colonizers through elaboration of the AlpP protein and antimicrobial agents possessing broad-spectrum antagonistic activity against medical and environmental isolates. Further examples of significance comprise antiprotozoan activity of *Pseudoalteromonas tunicata* elicited by violacein, inhibition of fungal colonization, antifouling activities, inhibition of algal spore germination, and 2-*n*-pentyl-4-quinolinol production. Nitrous oxide, an important greenhouse gas, emanates from surface-attached microbial activity of marine animals. Marine and intertidal biofilms have been applied in the biotechnological production of violacein, phenylannolones, and exopolysaccharides from marine and tropical intertidal environments. More examples of importance encompass production of protease, cellulase, and xylanase, melanin, and riboflavin. Antifouling activity of *Bacillus* sp. and application of anammox bacterial biofilms in bioremediation are described. Marine biofilms have been used as anodes and cathodes in microbial fuel cells. Some of the reaction vessels for biofilm cultivation reviewed are roller bottle, rotating disc bioreactor, polymethylmethacrylate conico-cylindrical flask, fixed bed reactor, artificial microbial mats, packed-bed bioreactors, and the Tanaka photobioreactor.

---

S. Mitra · J. Mukherjee (✉)

School of Environmental Studies, Jadavpur University, Kolkata 700032, India

e-mail: joydeep\_envstu@school.jdvu.ac.in

B. Sana

Division of Bioengineering, School of Chemical and Biomedical Engineering,  
Nanyang Technological University, Singapore 637457, Singapore



**Keywords** Bioactivity · Biofilm · Bioreactor · Intertidal · Marine · *Pseudoalteromonas* · *Roseobacter*

## Contents

1	Introduction.....	164
2	Ecological Perspectives.....	165
2.1	Biofilm Formation and Bioactivities of the Roseobacter Clade.....	165
2.2	Biofilm Formation and Bioactivity of the Pseudoalteromonas Genus.....	169
2.3	Nitrous-Oxide (N <sub>2</sub> O): Emitting Biofilms.....	174
2.4	Antimicrobial and Auxin-Producing Biofilms.....	175
3	Industrial and Environmental Bioprocesses.....	176
3.1	Production of Antifouling and Biocontrol Agents.....	177
3.2	Production of Antimicrobial and Cytotoxic Compounds.....	179
3.3	Production of Exopolysaccharides.....	184
3.4	Production of Enzymes.....	185
3.5	Production of Melanin.....	188
3.6	Production of Riboflavin.....	188
3.7	Biofilm-Based Bioremediation Processes.....	189
3.8	Biofilms in Microbial Fuel Cells.....	195
3.9	Aquaculture Feedstock Production.....	196
4	Conclusions.....	199
	References.....	200

## 1 Introduction

Surface colonization is a universal phenomenon in marine systems. Microorganisms frequently live as biofilm communities which are consortia of cells having high density, contained in an extracellular matrix, and possessing microcolony structures or other multicellular arrangements [1]. The intertidal zone, occupying the upper margin of the world's coastline, covers 1,600,000 km and comprises rocky shores, sandy beaches, mudflats, estuaries, salt marshes, mangrove forests, coral reefs, and manmade civil structures. This region is an important coastal habitat in terms of biological productivity and economic value [2]. Intertidal microbial communities often exist as biofilms. Biofilms form protective micro-environments in the changing environments of intertidal regions and support a variety of microbial processes [3]. Complex and highly differentiated surface microbial communities arise due to close spatial proximity of microbial cells which produces specific intercellular communications. A highly competitive environment due to space and nutrient limitation has forced the surface-dwelling microbes to develop adaptive responses and antagonistic strategies to prevent potential competitors occupying their habitat. During surface colonization of eukaryotes, the function and composition of surface microbial consortia are

significantly influenced by chemical communication and interactions between the microbes and their eukaryotic hosts. Therefore, multiple factors define the properties and composition of a microbial surface community. The worldwide demand for developing novel bioactives has projected the unique, interactive, and highly diverse environment of marine and intertidal surfaces as a potential space for biotechnological innovations [1].

Microbial ecology and biotechnology could be innately linked to each other: microbial ecology providing the scientific basis for the processes aimed to attain the realistic goals of biotechnology and biotechnological processes affording fascinating ecosystems for microbial ecologists to investigate and evolve their concepts and methodologies. One biological system in which there is a direct association between the knowledge of the lifestyle of the marine organisms and biotechnological applications therefrom is the biofilm. This two-way learning process has proved successful in developing new methods for the prevention of marine biofouling. This review is a retrospective of first, the investigations focused on marine microbes living on surfaces and their bioactivities that have made them successful colonizers, and second, the biotechnologies (industrial and environmental) developed exploiting the knowledge of efficacious biofilm formation.

## 2 Ecological Perspectives

Microbial biofilms can be quite uneven in distribution in species as well as in chemical composition. Monospecific biofilms can have complex as well as positive or negative influences on marine flora and fauna attributed mainly to the production of antibiotic compounds and stimulatory chemical signals. Chemical compounds produced by microorganisms can alter biofilm structure by disrupting or enhancing the growth of existing biofilms. They can induce or inhibit eukaryotic larval settlement on living and nonliving surfaces [4]. In this section, some examples of these complex relationships have been provided from the *Roseobacter* clade and the genus *Pseudoalteromonas*. Nitrous-oxide—emitting marine biofilms that can have profound effects on global warming form a separate subsection.

### 2.1 *Biofilm Formation and Bioactivities of the Roseobacter Clade*

Bacteria belonging to the *Roseobacter* clade are very efficient colonizers and both attachment as well as biofilm formation has been associated with the ability of members of the clade to grow in a “multicellular rosette shape” [5, 6]. In this subsection some of the recent investigations on biofilm formation and the production of bioactive compounds by different species of the *Roseobacter* clade have been reviewed from the standpoint of microbial ecology.

Bruhn et al. demonstrated that the culture supernatant of *Roseobacter* 27-4 was inhibitory to the turbot egg yolk sac larval pathogens *Vibrio anguillarum* and *Vibrio splendidus* [5]. Known antibacterial compounds, thiotropocin or its strongly related precursor tropodithietic acid, were identified as the active principles. A thick biofilm characterized by “multicellular star-shaped aggregated cells” formed at the air–liquid interface when *Roseobacter* 27-4 was cultivated under static growth conditions. Antibacterial activity was associated with the appearance of a brownish pigment. Although aerated conditions increased cell yield 10-fold, cultures were nonpigmented, grew as single cells, and no antibacterial activity was observed. The star shape was critical for the organism to amass into a thick biofilm. Detection of 3-hydroxy-decanoyl homoserine lactone in cultures of *Roseobacter* 27-4 indicated quorum control of antibacterial production. Thus, attachment and biofilm-forming characteristics may be pivotal for survival in the marine environment. *Roseobacter* strain 27-4 was also obtained from aquaculture tank walls where the identical subtype remained over one year [7, 8]. Potential use of *Roseobacter* 27-4 as a probiotic culture should ensure that it is cultivated in stagnant or adhered states.

Bruhn et al. developed a real-time PCR method that allowed direct quantification of bacteria on a surface. Cell densities were determined by plate counting and by real-time PCR. “Cycle threshold value ( $C_T$ )” was the cycle at which fluorescence achieved an identified threshold. It corresponded to the cycle at which a statistically significant enhancement in fluorescence was first observed. Bruhn et al. noted that the number of cycles required for the amplification-associated fluorescence to attain a specific threshold level of detection (the  $C_T$  value) was inversely related to the amount of nucleic acid present in the sample [9]. The quantity of nucleic acid in the sample was proportional to the number of cells in CFU/ml. Therefore, the lowest CFU/ml on agar plates having the lowest amount of nucleic acid gave the highest  $C_T$  value and vice versa. Values of  $C_T$  and CFU/ml were compared by linear regression and resulted in a linear correlation coefficient ( $R^2$ ) of 0.991. The lowest  $C_T$  value obtained by the minimum treatment without sodium dodecyl sulfate indicated the presence of the highest number of attached cells on the surface [9]. The authors concluded that by applying species-specific primers, this method should be useful in studying microbial surface colonization as well as in quantitative evaluation of novel antifouling surfaces or newly described cleaning and disinfection methods for removing attached bacteria.

Bruhn et al. further attempted to determine whether production of antibacterial compounds and biofilm formation were common phenotypes found in strains of the *Roseobacter* clade associated with the dinoflagellate, *Pfiesteria piscicida*, and whether such activity occurred under defined growth conditions (static or shaken cultures) and was associated with a specific rosette morphotype [10]. *Silicibacter* sp. TM1040 and *Phaeobacter* (formerly *Roseobacter*) strain 27-4 produced the highest amounts of antibacterial substances and their sterile filtered supernatants were lethal to many non-*Roseobacter* marine bacteria. On the other hand, *Roseobacter* strains were inhibited only when exposed to concentrated compounds, thus implying the role of these compounds in annihilating competitors.

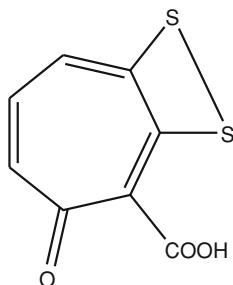


**Fig. 1** Tropodithietic acid (3-oxo-8,9-dithiabicyclo[5.2.0]nona-1,4,6-triene-2-carboxylic acid), the active compound possessing antibacterial activity of *Phaeobacter* strain 27-4

*Silicibacter* sp. TM1040 cells attached among themselves forming rosettes and produced antibacterial compounds when cultivated in a liquid medium under static conditions. A spontaneous *Phaeobacter* 27-4 mutant incapable of forming rosettes also could neither develop into a biofilm nor produce antibacterial compounds, suggesting the importance of rosette formation. In 8 of 14 *Roseobacter* clade strains examined, rosette formation was noted and was very high under static growth in 5 of these strains. Strains able to form rosettes were 13–30 times more efficient in attaching to glass compared to strains where rosette formation was not observed by Bruhn et al. [10].

The active compound of *Phaeobacter* strain 27-4 possessing antibacterial activity (Fig. 1) was tropodithietic acid (TDA) [5, 11]. *Silicibacter* sp. strain TM1040 also yielded an antibacterial compound and production in both strains was correlated with the elaboration of a brown pigment. TDA contains two sulfur atoms, which is of interest because bacteria of the *Roseobacter* clade can metabolize dimethylsulfoniopropionate (DMSP) produced by algae and dinoflagellates [12] which is linked to sulfur cycling in the ocean. DMSP was utilized through the demethylation pathway in *Silicibacter* sp. strain TM1040 and sulfur from DMSP may be employed in the synthesis of TDA [13]. The ability to synthesize TDA, a compound having an unusual seven-member aromatic tropolone ring backbone was demonstrated in several *Roseobacter* genera including *Ruegeria* and *Phaeobacter* species and is an effective model for *Roseobacter* secondary metabolite production [14, 15]. D'Alvise et al. [16] enquired if concentrations of bis-(3'-5')-cyclic dimeric guanosinmonophosphate (c-di-GMP) inside *Ruegeria mobilis* cells could be correlated with transitions between biofilm and planktonic modes of growth of this bacterium. In bacteria this compound generally functions as a second messenger regulating biofilm formation [17]. Through genome sequencing, plasmid-directed manipulation of genes, chromatography, and mass spectrophotometric studies, D'Alvise et al. concluded that biofilm formation in *R. mobilis* and associated phenotypic characteristics, in particular, TDA production, were c-di-GMP controlled [16].

Porsby et al. demonstrated that *Roseobacters* displaying inhibitory activity against *Vibrio anguillarum* colonized a Danish turbot larval farm [18]. The production

unit consisted of a fish tank, water cleaning system, and tank with copepod cultures. A bag containing the algal cultures also formed a part of the production unit; however, the significant difference was that the bag did not have a surface for attachment of cells that the other three components had. A total of 43 samples collected from the Danish turbot larval farm were screened and 100 isolates were found to have antagonistic activity against *V. anguillarum*. There were 54 isolates that showed antagonism in both spot and well diffusion assays, 51 of which were identified as members of the *Roseobacter* clade. The remaining 46 isolates showed inhibitory activity in spot assay only and 38 of them were acknowledged as *Vibrio* spp. Through phylogenetic analyses it was shown that *Phaeobacter inhibens* and *Phaeobacter gallaeciensis*-like strains were encountered in fish tanks, water cleaning systems, and tanks with copepod cultures of the production site, whereas *Ruegeria mobilis* or *Ruegeria pelagia* were present in algal cultures kept in bags. *Ruegeria* species were naturally occurring in the water from the Danish fiord and not present as a contaminant or inoculated in the bags containing the algal culture. *Phaeobacter* sp. demonstrated greater inhibitory activity against 17 microbes of the larval unit than *Ruegeria* sp. When cultivated under shaking and static conditions, *Phaeobacter* sp. produced TDA and a brown pigment and inhibited *Vibrio anguillarum*. *Ruegeria* sp., however, exhibited these three properties only under a static condition similar to the studies [5, 10]. *Phaeobacter* sp. reported in this study would be more suitable for practical application as a fish probiotic organism than the *Phaeobacter* strain 27-4 [5, 10] as few regions of an aerated fish tank would have static fluid conditions [18]. The subtypes of *Roseobacter* isolates of the production site (*Pheobacter*) differed from the isolates of the bags with algal cultures (*Ruegeria*) which established the fact that there was a tendency to grow and inhabit specific niches by particular subtypes or they may have been established randomly and continued to grow at that site [18].

*Roseobacters* are generally recognized to synthesize a multitude of secondary metabolites [5, 19–22]. However, genomic investigations by Newton et al. [23] showed that most sequenced *Roseobacters* lacked the TDA biosynthesis pathway usually considered as the *Roseobacter* secondary metabolite production model pathway [14, 15]. Against this background, Cude et al. [24] reported for the first time, synthesis of the blue pigment indigoidine (Fig. 2) by *Phaeobacter* sp. strain Y41 through a nonribosomal peptide synthase (NRPS)-based biosynthetic pathway coded by a sequence of linked genes, *igiBCDFE*. Cude et al. correlated indigoidine production by Y41 to growth inhibition of *Vibrio fischeri*, a hitherto unknown bioactivity of indigoidine [24]. This property provided Y41 a competitive advantage over *V. fischeri* during surface colonization. When cells were grown planktonically, production of indigoidine was, however, ineffectual. Furthermore, pleiotropic effects of the pigment were demonstrated through indigoidine offering protection to *Phaeobacter* sp. strain Y41 from reactive oxygen species as well as contributing to swimming motility and surface colonization. Phenotypic observations were supported by gene expression studies, in particular, upregulation of *igiD* when Y41 grew as biofilms compared to planktonic cultures.

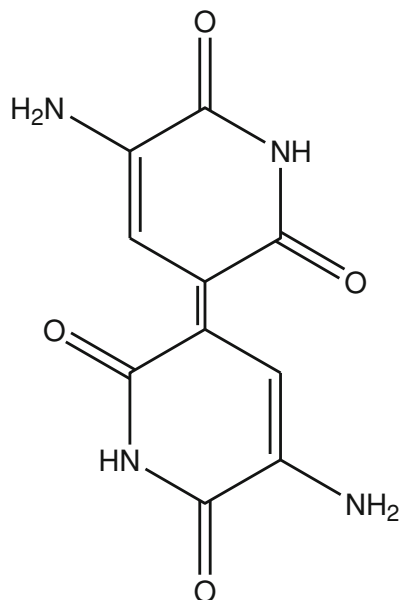


**Fig. 2** The blue pigment indigoidine [(5E)-3-amino-5-(5-amino-2,6-dioxypyridin-3-ylidene)pyridine-2,6-dione] produced by Roseobacter *Phaeobacter* sp. strain Y41

## 2.2 Biofilm Formation and Bioactivity of the *Pseudoalteromonas* Genus

Species of the genus *Pseudoalteromonas* are generally found associated with marine eukaryotes and display antibacterial, agarolytic, and algicidal activities. Several *Pseudoalteromonas* isolates specifically deter the settlement of common marine fouling organisms. Production of a variety of compounds lethal against many competitor organisms is a distinctive characteristic of this genus. Thus, *Pseudoalteromonas* cells are advantaged in their contest for nutrients and space and colonization of surfaces, and are protected against predators grazing at surfaces [25].

The most widely investigated species in the genus *Pseudoalteromonas* is the green-pigmented Gram-negative gamma-proteobacterium *P. tunicata*. Surfaces of the marine plant *Ulva lactuca* are colonized by this bacterium and it produces at least five novel inhibitory compounds [26]. A 190-kDa multisubunit antibacterial protein named AlpP was produced by a marine bacterium D2 (*P. tunicata*) that was isolated from the surface of the ascidian larvae, *Ciona intestinalis*. The protein was effective against Gram-negative and Gram-positive bacteria occurring in a variety of environments. AlpP protein was shown to be released during the stationary growth phase of D2. The protein contained at least two subunits (60 and 80 kDa), which were linked together by noncovalent bonds [27]. Rao et al. noted that expression of iron uptake and AlpP in *P. tunicata* was controlled by a ToxR-like

regulon [26]. AlpP was autoinhibitory to *P. tunicata* itself, therefore its ecological role was questionable. Rao et al. contemplated that during biofilm growth of *P. tunicata*, AlpP might provide a competitive edge over competitors [26].

Rao et al. further investigated whether *P. tunicata* was a superior competitor in comparison to other bacteria isolated from *U. lactuca* [26]. In pure culture and within 72 h, all marine isolates developed into biofilms containing microcolonies. *P. tunicata* in mixed-species biofilm with the competitor, *Pseudoalteromonas gracilis*, coexisted with *P. gracilis* until the competitor was insensitive to AlpP. Microcolony formation may improve an organism's capacity to compete against *P. tunicata* and its persistence [26]. *Roseobacter gallaeciensis*, however, demonstrated potent inhibitory activity against *P. tunicata*, outcompeted it and produced a biofilm. The AlpP (minus) mutant of *P. tunicata* was less competitive when placed into pre-established biofilms, signifying that AlpP played a role during competitive biofilm formation [26].

Barja et al. [28] reported that *Alteromonas* species (later reclassified as *Pseudoalteromonas*) isolated from seaweed produced low-molecular-weight (molecular weights less than 2 kDa) thermolabile inhibitors whereas strains isolated from seawater produced high-molecular-weight antibiotics such as a glycoprotein (molecular weight 90 kDa) purified from strain P-31. These compounds presented broad-spectrum antagonistic activity against medical and environmental isolates and their role in the prevention of surface-colonizing competitors was implicated [28].

It may be anticipated that chemical defenses in biofilms would offer vital protection against predators. Planktonic populations would be expected to depend on defense mechanisms such as cell morphology or escape and chemical defenses would be less important [29]. Matz et al. compared the occurrence and effectiveness of chemical defenses in biofilms versus planktonic populations of marine bacteria [29]. By examining growth and survival of two common bacterivorous nanoflagellates (*Cafeteria roenbergensis* and *Rhynchomonas nasuta*), Matz et al. demonstrated that chemically mediated defense against protozoan predators was common among marine bacterial biofilms. The authors further showed that the purple pigment violacein (Fig. 3), an L-tryptophan—derived alkaloid consisting of three structural units, 5-hydroxyindole, 2-pyrrolidone, and oxindole was responsible for the antiprotozoal activity of *Pseudoalteromonas tunicata* biofilm [29]. Antiprotozoal activity was also elicited by violacein derivative deoxyviolacein that was produced at a 3-fold lower concentration compared to violacein. As discussed by Matz et al. [29], cellular extracts of the  $\beta$ -proteobacterium *Chromobacterium violaceum* were the first described source of violacein [30]. An 8-kb region coding a presumed biosynthetic gene cluster comprising five open reading frames in the *P. tunicata* genome showed high predicted amino acid sequence similarity to the violacein operon *vioABCDE* of *C. violaceum* [31, 32].

Franks et al. tested the ability of *P. tunicata* to inhibit fungi [33]. During surface colonization of the green alga *Ulva australis*, *P. tunicata* was afforded a competitive advantage over the marine yeast *Rhodospiridium sphaerocarpum* through production of an antifungal compound. This yellow-pigmented broadspectrum

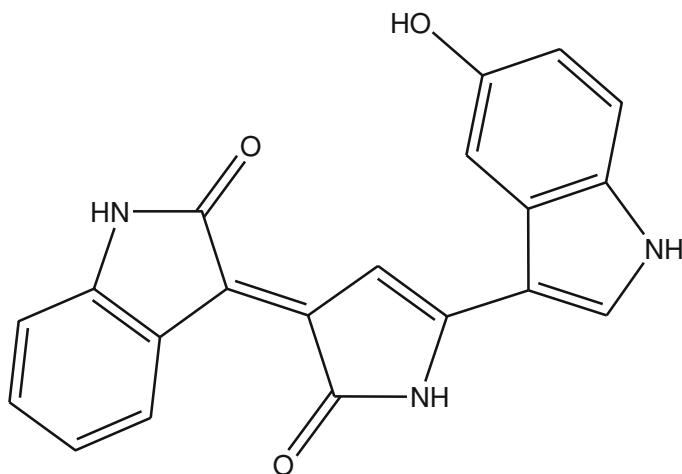


**Fig. 3** Defensive metabolite violacein (5-(5-hydroxy-3-indolyl)-3-(3-oxindolylidene)-2-oxopyrroline), the purple pigment eliciting antiprotozoal activity of *Pseudoalteromonas tunicata*

inhibitory compound (YP1) disrupted an already established fungal biofilm by reducing the number of surface-attached yeast cells. Franks et al. [33] further reported that a long-chain fatty acid-coenzyme A ligase was implicated in its production. YP1 produced by *P. tunicata* possesses a 2, 2-bipyrrole ring system with an unsaturated 12-carbon alkyl chain. It is a member of the tambjamine class of compounds and was the first reported natural tambjamine with an unsaturated alkyl chain. YP1 was previously isolated from eukaryotes in the marine environment and was reported to exhibit antimicrobial activities. It may be considered that activation of long-chain fatty acids was essential for the elaboration of an active antifungal metabolite. The yeast test strains were of industrial, agricultural, and medical importance and their growth inhibition by *P. tunicata* opens possibilities for their biotechnological applications.

To determine the level of antifouling activities and the production of bioactive compounds within the genus *Pseudoalteromonas*, 10 *Pseudoalteromonas* species derived mostly from various host organisms were examined in a number of biofouling assays [34]. The growth of the initial fouling organisms (bacteria and fungi) on marine surfaces was assayed in the presence of the 10 *Pseudoalteromonas* species. Further assays included the settlement of invertebrate larvae (*Hydroides elegans* and *Balanus amphitrite*) and settlement of *Ulva lactuca* and *Polysiphonia sp.* spores. *P. tunicata* inhibited all target fouling organisms whereas *Pseudoalteromonas haloplanktis* and *Pseudoalteromonas nigrifaciens* demonstrated feeble activity in the bioassays.

Production of bioactive compounds was correlated with the expression of pigment. The antibacterial compound produced by *P. tunicata* was a high molecular mass protein (190 kDa in size) consisting of two subunits and the effect was bactericidal, not bacteriostatic. *Pseudoalteromonas luteoviolecea*, *P. tunicata*, and



*Pseudoalteromonas aurantia* were able to inhibit most of the *Pseudoalteromonas* species as well as other marine epiphytic bacteria and nonmarine strains [34]. The strong antagonistic activity displayed by the three species may provide a competitive edge in the colonization of habitats in comparison to the other *Pseudoalteromonas* species. Six out of the ten species of *Pseudoalteromonas* encouraged the attachment of *H. elegans* larvae. Three species partially inhibited larval settlement, and *P. tunicata* showed complete inhibition of the larval surface attachment. The antilarval compound obtained from *P. tunicata* was less than 500 Da in size, heat stable, and polar. Four *Pseudoalteromonas* species strongly inhibited the settlement of *B. amphitrite* larvae and none of the species stimulated larval settlement. In a study by Egan et al., 56 marine isolates were tested for their ability to prevent spore settlement of *U. lactuca* [35]. Inhibitory activity was demonstrated by biofilms of 13 isolates and 3 of these isolates, including *P. tunicata*, completely hindered spore settlement. Biofilms of *Pseudoalteromonas* species were more effective against the settlement of *Polysiphonia* spores compared to *U. lactuca* spores as demonstrated by Holmström et al. [34]. Bacteria showing activity against the settlement of *U. lactuca* spores were generally active against *Polysiphonia sp.* spores as well. This suggested that analogous antialgal component(s) from different bacterial species targeted more than one alga [34]. It is generally presumed that bacteria possessing antibacterial activity also have the ability to produce antifouling compounds. However, it is not known if these properties are related and if an exploration for antibacterial activity can be considered a surrogate for searching antifouling activity [36]. Bernbom et al. [36] reported the highest antifouling activity in the biofilms of *Pseudoalteromonas piscicida*, *Pseudoalteromonas tunicata*, and *Pseudoalteromonas ulvae*. *P. piscicida* killed the test strain *Pseudoalteromonas* S91 in suspension cultures, whereas *P. tunicata*, *P. ulvae*, and *P. aliena* were not bactericidal against S91 but prevented its adhesion. Thus, the authors concluded that antibacterial activity was not a substitute for the antifouling effect. The alpP gene, which is responsible for antifouling, was present only in *P. tunicata*, therefore the authors speculated that there may be other molecules or mechanisms through which the other *Pseudoalteromonas* strains displayed antifouling activity. Bernbom et al. [36] further reported that during their one-year screening program for bioactive bacteria at 11 Danish coastal locations they found the numbers as well as the natures of bacteria showing bioactivity to differ with respect to season and niche.

A survey of surface-dwelling antibiotic-producing bacteria from seaweed and subsequent study of their antimicrobial potential against *Staphylococcus*, *Alcaligenes*, *Pseudomonas*, *Vibrio*, *Pasteurella*, and *Achromobacter* were carried out by Lemos et al. [37]. From five species of green and brown marine algae, 224 bacterial strains were isolated and screened for antibiotic production. Antimicrobial activity was displayed by 38 strains and *Enteromorpha intestinalis* was the superior source of producer strains. All epiphytic bacteria possessing antibiotic activity were classified in the *Pseudomonas*–*Alteromonas* group. Antagonism was demonstrated among the isolates: one producer strain inhibiting growth of other producers and other nonactive strains isolated from seaweed. Preliminary characterization of the antimicrobial substances showed that they were low-molecular-weight compounds,

thermolabile, anionic, and resistant to proteolytic enzymes. Furthermore, Lemos et al. showed that the antibiotic substances remained strongly bound in the periplasmic space after excretion [37]. Ecologically, fast discharge of antibiotic substances by producer epiphytic bacteria would not confer any competitive benefit to them as the inhibitors would be instantly washed away by the surrounding seawater. In contrast, if antibiotics remained bound to cells, they would be excreted gradually and continually to the immediate environment, thus inhibiting colonization by competitors on the algal surface.

Bacterium–bacterium interactions occur at micrometer spatial scales and antagonism is an interaction in such microenvironments. Long et al. developed a model system on the antibiotic-producing *Alteromonas* isolate (SWAT5) obtained from a marine particle and its dominant antibiotic, 2-*n*-pentyl-4-quinolinol (PQ) to investigate the significance of this antimicrobial in antibiosis and carbon cycling on particles [38]. Production of PQ by SWAT5 was observed only on surfaces and when the isolate was cultivated in polysaccharide matrices. PQ diffused within the matrices but not into the proximate seawater. Lemos et al. concluded that SWAT5 possibly created a localized zone of high antimicrobial concentration on particles suspended or sinking through seawater similar to the previous inference [37]. Bacterial respiration of exterminated bacteria was most sensitive to PQ, whereas a higher concentration of PQ was required to inhibit DNA and protein synthesis as well as bacterial motility. The structure of the bacterial community that colonized and developed in the model particle system was influenced by PQ. Long et al. noted that the particle-attached bacterium, such as SWAT5 may reduce the “biochemical influence” that competing bacteria may show enzymatically on a particle’s organic matter [38]. In the pelagic ocean, antibiosis may also play a role in distribution of bacterial species at the microscale level [39].

Results of the investigation on antibiotic production by *Pseudoalteromonas rubra* (previously *Alteromonas rubra*, isolated from the Mediterranean waters off Nice, France) indicated that maximum antimicrobial activities were observed on hydrophilic surfaces, and the number of attached cells was higher on hydrophobic surfaces [40]. Ivanova et al. demonstrated that the degree of substratum hydrophobicity influenced the production of antibacterial metabolites [41]. The highest antimicrobial activity was observed on hydrophilic surfaces notwithstanding the abundance of attached *Pseudoalteromonas* cells on hydrophobic surfaces. In response to environmental variables and stimuli present outside the cell, the elaboration of antimicrobial activity may be increased or decreased. Holmström and Kjelleberg [25] supported the conclusions of Ivanova et al. [41].

Before beginning the next subsection, it would be interesting to note the dissimilarities in colonization strategies demonstrated by the epiphytic bacteria of the *Roseobacter* clade and *Pseudoalteromonas* genus. Biofilm-forming marine bacteria *Pseudoalteromonas tunicata* and *Roseobacter gallaeciensis* are often found associated with the *Ulva australis* surface. They are believed to protect the host plant against common fouling organisms by producing inhibitory compounds. Rao et al. [42] investigated the factors influencing the surface attachment and colonization of *U. australis* by *P. tunicata* and *R. gallaeciensis*. Rao et al. further studied the

competitive interactions occurring between the two bacteria and other isolates of *U. australis* during biofilm formation on the plant surface. Although *R. gallaeciensis* was able to colonize *U. australis* under all conditions tested, colonization by *P. tunicata* was specifically enhanced by high cell densities, dark inoculation, interactions with a natural seawater community, and presence of cellobiose. It may be noted that cellulose is the main surface polymer of *U. australis*. The epiphytic habitation of *R. gallaeciensis* was attributed to its selective utilization of a number of carbon sources unavailable to competing strains as well as to the production of antibacterial compounds and signaling molecules. When a pre-established biofilm was challenged with *P. tunicata*, it resulted in the cohabitation of competitors partially due to the defensive activity of microcolonies that resisted invasion. Metabolically active cells at the outer edge of the microcolony died whereas cells in the deeper regions of the biofilm were protected from the antibacterial activity as a result of the diffusion gradient in microcolonies. Coexistence of competing strains was also due to limited nutrients on the *U. australis* surface that led them to occupy distinct niches on the plant. *R. gallaeciensis*, on the other hand, was not hindered by low-nutrient conditions and was able to attack and annihilate competing strains, indicating that its antibacterial substance was able to spread through microcolonies.

### 2.3 Nitrous-Oxide ( $N_2O$ ): Emitting Biofilms

Following carbon dioxide and methane, nitrous oxide ( $N_2O$ ) is the third most important greenhouse gas. In their article, Heisterkamp et al. [43] noted that the atmospheric concentration of  $N_2O$  is swiftly increasing, contributing appreciably to global warming as observed by the Intergovernmental Panel on Climate Change [44] and to the depletion of the stratospheric ozone layer as noted by Ravishankara et al. [45]. Heisterkamp et al. [43] commented that fertilized soils and coastal areas that are characterized by high input and turnover rates of inorganic nitrogen are considered as principal sites of  $N_2O$  emission [46]. Heisterkamp et al. [43] further observed that in coastal sediments and rock biofilms, due to high riverine input of nitrogen coupled with microbe-mediated nitrogen conversions,  $N_2O$  production is further increased [47]. Heisterkamp et al. [43] noted that nitrous oxide is also emitted by earthworms and freshwater invertebrates [48], and a dense population of filter- and deposit-feeding invertebrates [49] with exposure to high nitrate concentrations [50] that make coastal marine sediments active regions of  $N_2O$  emission. In their study, Heisterkamp et al. [43] investigated  $N_2O$  emission capacities of marine invertebrate species found in the coastal sediments of the North Sea and Baltic Sea and of the aquacultured shrimp *Litopenaeus vannamei*. Animal-associated  $N_2O$  production was strongly related to body weight, habitat, and exoskeletal biofilms. Heisterkamp et al. [43] reported that  $N_2O$  emission by the snail *Hinia reticulata* with an intact exoskeletal biofilm was approximately 3.5 times more than by a snail without the biofilm. Thus,  $N_2O$  production associated with marine invertebrates was not always due to gut denitrification, but may

originate from microbial activity on the external surfaces of the animal. The microbial pathway for biofilm-associated  $N_2O$  production was not identified. Heisterkamp et al. [43] remarked that oxygen availability inside the biofilm would determine if nitrification or denitrification or both would contribute to the production of  $N_2O$  [51]. Ammonium from animal excretion or nitrate from the water column, or both could be the sources of  $N_2O$  production in the exoskeletal biofilm. Furthermore, nitrification and denitrification would probably be coupled if an oxic–anoxic transition zone prevailed in the biofilm [52].

The next study by this group showed that 18–94 % of the total animal-associated  $N_2O$  emission arose from shell biofilms of *Mytilus edulis*, *Littorina littorea*, and *Hinia reticulata* possessing different lifestyles [53]. Nitrification and denitrification contributed equally to  $N_2O$  emission from shell biofilms and both processes occurred in biofilms as a result of heterogeneous oxygen distribution.  $N_2O$  production in shell biofilms of the three mollusc species were supported by ammonium, nitrite, and nitrate. The animals provided a nutrient-enriched microenvironment, in particular ammonium excretion, that stimulated growth and sustained  $N_2O$  production of the shell biofilm. Heisterkamp et al. [53] demonstrated that when *H. reticulata* was still living inside the shell, biofilm on the shell surface exhibited the highest  $N_2O$  emission rates.  $N_2O$  production originated from the shell biofilm of *M. edulis* whereas  $N_2O$  production by gut denitrification was negligible although *M. edulis* is known to be a very proficient filter-feeder that ingests large numbers of bacteria and is capable of high  $N_2O$  production in its gut [48]. Heisterkamp et al. [53] reasoned that most of the ingested bacteria may be digested by the high gut lysozyme activity of *M. edulis* and  $N_2O$  would not be produced due to inhibition of denitrification.

Svenningsen et al. [54], using the freshwater bivalve *Dreissena polymorpha* (zebra mussel) as the model organism, quantified the biofilm-derived  $N_2O$  production and the mechanism(s) thereof. Svenningsen et al. [54] reported that the shell biofilm contributed approximately 25 % to the total  $N_2O$  emission from this species. The mussel gut is oxygen depleted, so denitrification would be induced by denitrifiers whereas ammonia oxidation would be repressed by ammonia oxidizers in the gut. As mussel biofilms were relatively thin and presumably fully oxic,  $N_2O$  would therefore be produced mainly by nitrification, and denitrification would be repressed. However, high *nir* gene (coding for nitrite reductase) abundance implied that denitrification might contribute to  $N_2O$  production if anoxic microsites developed within the biofilm.

## 2.4 Antimicrobial and Auxin-Producing Biofilms

Wilson et al. tested whether antimicrobial activity of biofilm cultures is directed towards competing bacteria found in those biofilms [55]. Fourteen of the 105 marine isolates collected from marine invertebrate, algae, and gravel surfaces were found to possess antimicrobial activity when cultivated as biofilms. The strength and spectrum of activity were greater when isolates were grown as biofilms compared to cultivation as shaken cultures. Supernatants of biofilm cultures from

11 of the 13 isolates demonstrated activity in organic phases of varying polarity signifying the presence of multiple antibiotic molecules of different polarities. Six isolates showed activity against *Shewanella* sp. in hexane, dichloromethane, and ethyl acetate extracts and five isolates displayed activity against *Shewanella* sp. in the aqueous phase. Wilson et al. [55] thus concluded that biofilm-forming marine bacteria were active against competing bacteria in biofilms.

Two species of gliding bacteria were isolated from a marine biofilm and identified as members of the genus *Cytophaga* [56]. Colony expansion of one isolate (RB1058) was inhibited by the other (RB1057) through production of an extracellular inhibitor that prevented adhesion of RB1058 to substrata and its gliding activity. Burchard and Sorongon [56] characterized the inhibitor as a glycoprotein with 60-kDa apparent molecular mass. The metabolic cost of synthesis and export of a 60-kDa glycoprotein by RB1057 would be substantial and thus its biosynthesis should be of high ecological significance. The high-molecular-weight substance would diffuse relatively slowly through the biofilm's channels and would therefore more likely be retained in the proximity of the producing bacteria than a low-molecular-weight secondary metabolite. Similar mechanisms for antimicrobial substances to be ecologically effective were demonstrated in *Pseudoalteromonas* [37, 38].

Kerker et al. [57] noted that the natural auxin produced by plants, algae, mosses, and lichens is indole-3-acetic acid (IAA). Soil rhizosphere bacteria associated with plants are known to produce IAA. Physiological effects of IAA on plants and its role in plant-microbe interaction has been studied by Patten and Glick [58]. However, few studies have been carried out on IAA-producing bacteria found in association with aquatic biofilms and their contribution towards growth of biofilms [57]. Kerker et al. reported rapid growth of biofilm mats formed in salt-terns of the Indian west coast during the monsoon. The heterogeneous population of the biofilm comprised mainly green algae, blue green algae, Euglenophyceae, and diatoms. Four types of green algae (viz. *Pediastrum duplex*, *Oedogonium* sp., *Cladophora* sp., and *Spirogyra exiles*), three blue green algae (*Phormidium* sp. (*corium*), *Phormidium* sp. (*ambigeum*), and *Oscillatoria* sp.), and one type of *Euglenophyceae* (i.e., *Phacus* sp.) were reported. The diatoms comprised *Pleurosigma* sp. and *Navicula* sp. Among the 125 bacteria recovered from biofilms, 16 produced IAA whereas four isolates therefrom, in the presence of tryptophan, consistently produced high amounts of IAA. The IAA-producing bacteria were *Aeromonas aquariorum*, *Pseudomonas alcaliphila*, *Vibrio diazotrophicus*, and *Pseudomonas pachastrellae*. IAA produced by biofilm-associated bacteria functions as a chemical messenger between microorganisms [59].

### 3 Industrial and Environmental Bioprocesses

It is generally observed that surfaces of inanimate structures (buildings, ships) immersed in the sea swiftly become covered by a microbial biofilm. This is followed by colonization by larger organisms leading to macrofouling of the surfaces.

The majority of marine organisms, although covered with a thin film of epibiotic bacteria, are not fouled by macroorganisms. These epibionts impart protection to the host organism by releasing compounds that prevent macroorganisms from contaminating the surface. Interestingly, these epibionts may also have industrial and medical applications such as the production of antimicrobial or antifouling compounds [60]. Furthermore, a shift in the mode of culture from suspension to surface culture affects the type and quantity of compounds produced. Armstrong et al. noted that surface-grown bacteria released bioactive compounds with higher activity against target strains in comparison to those obtained from the same strain cultivated in the planktonic mode [60]. Thus, surface-dwelling bacteria of seaweed may produce greater amounts of compounds protecting the seaweed exterior from further fouling. The enhanced expression of biosynthetic genes is responsible for bioactive compound production, in a manner similar to increased extracellular polysaccharide gene expression which is also necessary for bacterial surface colonization. Wilson et al. [55], citing the literature [1, 60, 61], noted that the molecules produced by successful bacterial surface colonizers that prevent attachment, growth, and survival of competing organisms hold antifouling or antimicrobial properties. Colonization of competing organisms is hindered by antifouling molecules, whereas antimicrobial action results in the death of competing bacteria. Thus, ecological considerations directed the exploration of biotechnological applications of biofilm-forming microbes for antifouling and antimicrobial activities, with which this section begins. Applications of marine and intertidal biofilms in production of antimicrobial and cytotoxic compounds, exopolysaccharides, enzymes, melanin, riboflavin, and aquaculture feedstock as well as in bioremediation and microbial fuel cells are also described in the following section.

### ***3.1 Production of Antifouling and Biocontrol Agents***

Ortega-Morales et al. [62] observed that biofouling is the reason for massive damage to oceanic infrastructures such as ship hulls and offshore platforms, contributing to financial losses [63]. Undesirable environmental effects of applying broadspectrum biocides such as tributyl tin (TBT)—containing paints on marine structures as well as unacceptable performance of antifouling coatings have stimulated the search for natural, environmentally friendly products to tackle biofouling [62, 63]. The International Maritime Organisation (IMO) agreed at its London Assembly in November 1999 that TBT would be phased out between 2003 and 2008. According to Ortega-Morales et al. [62], although marine-algae—derived natural compounds have been projected as novel antifoulants [64], it was demonstrated that certain epibiotic bacteria living in relationship with higher organisms (including algae) yield inhibitory extracellular compounds that inhibit colonization of common fouling organisms and are thus helpful to host survival [42]. Thus, within a microorganism–macroorganism association, chemical

protection is provided to the host by the epibiotic biofilm without innate chemical defense afforded by the host [62].

Ortega-Morales et al. screened biofilm bacteria able to produce novel natural antifoulants [62]. Marine biofilm bacteria were isolated from the surfaces of turtle grass leaves and limestone fragments. The nine isolates were cultivated in planktonic condition in shake flasks containing yeast extract broth. The bacterial biomasses as well as the fermentation broths were subjected to solvent extraction to obtain the antifouling compounds. The common fouling bacterium, *Halomonas marina*, and a crustacean, *Artemia salina*, were applied as test organisms to assay antifouling activity of extracts of nine representative strains isolated from various surfaces. Antimicrobial as well as toxic activities were detected in most of the organic extracts. Molecular phylogeny revealed that the isolates were relatives of *Bacillus mojavensis* and *Bacillus firmus*. Bioactive lipopeptides surfactin A, mycosubtilin, and bacillomycin D were identified as the active factors. As stated by Ortega-Morales et al. [62], *B. mojavensis* was originally found in the soil of the Mojave Desert, United States [65], and also reported to be an endophyte [66]. Therefore, Ortega-Morales et al. [62] speculated that this bacterium might have been washed off into the coasts by terrestrial run-off. Halotolerance and exopolymer synthesis pointed towards an intertidal habitat of *Bacillus mojavensis*.

Bernbom et al. [67] examined the antifouling potential of different *Pseudoalteromonas* species in a system that simulated the natural marine environment. The bacteria were further included into ship paints and their prospective antifouling property was verified in a field situation. The authors [67] reported that *P. piscicida* strains B39bio and A38q-4a and *P. tunicata* strain J38a-5a survived as biofilms for 53 days in sterile seawater, although a 2.5-log reduction in CFU numbers over time was observed. On the other hand, *P. tunicata* strains existed for only 7 days and none of the strains were detectable after 53 days. The authors [67] further noted that after 7 days, the counts of culturable bacteria attaching to the *Pseudoalteromonas*-precoated surfaces were higher compared to the control surfaces. In spite of this, after 53 days, seven of eight *Pseudoalteromonas* strains under study had lowered bacterial adhesive capacity compared to the control. *P. piscicida*, *P. antarctica*, and *P. ulvae* were detected on the surface as was found initially, and *P. tunicata* was undetectable. *P. tunicata* strain J36q-4a prevented the attachment of the test strain (S91) significantly, although the other three *P. tunicata* strains had minute antifouling effect against S91. The authors [67] concluded that subject to the model organisms selected, marine bacteria may either deter or draw other bacteria. Next, the authors included suspensions of *P. piscicida* and *P. tunicata* into ship paints applied on plates at a test site in Jyllinge Harbor, Denmark. No disparities were noted between control and treated plates during the first 4 months. However, after 5–6 months fouling was observed on the control plates but not on the plates coated with the *Pseudoalteromonas*-based paint. It was concluded that antifouling effects were difficult to ascertain through laboratory studies only. For better assessment of the prospective antifouling capacity of novel agents or organisms, a blend of laboratory and field-based studies was recommended [67].

Holmström et al. [68] screened 40 marine bacterial isolates against laboratory-reared barnacle larvae (*Balanus amphitrite*) and ascidian larvae (*C. intestinalis*) to find bacteria with antifouling properties. A facultative, anaerobic, Gram-negative bacterium (D2, mentioned previously) was isolated from the surface of *C. intestinalis*. Biofilm was the source of the larvicidal activity and stationary-phase biofilms possessed higher activity than developing biofilms. The biologically active factor was a heat stable, <500 Da, polar, neutral, nonprotein compound contained or bound to carbohydrate moieties.

Antagonistic activity of marine biofilm bacteria against terrestrial fungal plant pathogens was studied by Ortega-Morales et al. [69]. *Colletotrichum gloeosporioides* ATCC 42374 was inhibited by close relatives of *Bacillus mojavensis* and *Bacillus firmus*. The active bacterial isolates were further challenged against *C. gloeosporioides*, *Colletotrichum fragariae*, and *Fusarium oxysporum* in different bacterial growth phases and cultivated in varying fungal nutritional conditions. Susceptibility of the pathogens was dependent on fungal nutrition and time of bacterial colonization. *Bacillus* sp. MC3B-22 proved to be a better antifungal agent than the commercially available biocontrol strain *Bacillus subtilis* G03, which indicated its biotechnological potential, specifically, prevention of fungal colonization on mango leaves. Epiphytic biofilms of *Thalassia testudinum*, a marine sea grass, was the source of the most active isolate whereas the rest were isolated from epilithic biofilms of the intertidal habitat. *B. subtilis* MC3B-22 was antagonistic to *C. gloeosporioides* independent of the colonization time (early, simultaneous, and late). Ortega-Morales et al. [69] also established that the principal polymeric material forming surface attachment structures is an extracellular heteropolysaccharide previously known to be a metabolite of *B. subtilis* MC3B-22. The authors concluded that terrestrial plant pathogens could be inhibited by biofilm bacteria isolated from the fluctuating physical and chemical environments of intertidal regions.

### 3.2 Production of Antimicrobial and Cytotoxic Compounds

Marine bacteria growing on algal surfaces and derived from intertidal regions of Japan, were investigated as potential sources of novel bioactive compounds [70]. Kanagasabhapathy et al. [70] reported that several strains were active against pathogenic as well as fouling bacteria. Molecular phylogenetic analysis identified the epibiotic bacteria as members of the *Bacillus* genus similar to the results of Ortega-Morales et al. [62]. Surface attachment was a significant factor affecting the metabolism of marine epibiotic bacteria. Vandevivere and Kirchmann found that addition of sand to shake flask cultures stimulated exopolymer synthesis by some surface-attached bacteria and that attached cells produced higher amounts of exopolymer than planktonic cells [71]. Yan et al. [72] observed that shaken flask cultivation did not provide the correct conditions of antimicrobial production by surface-growing bacteria. The authors opined that the common laboratory method



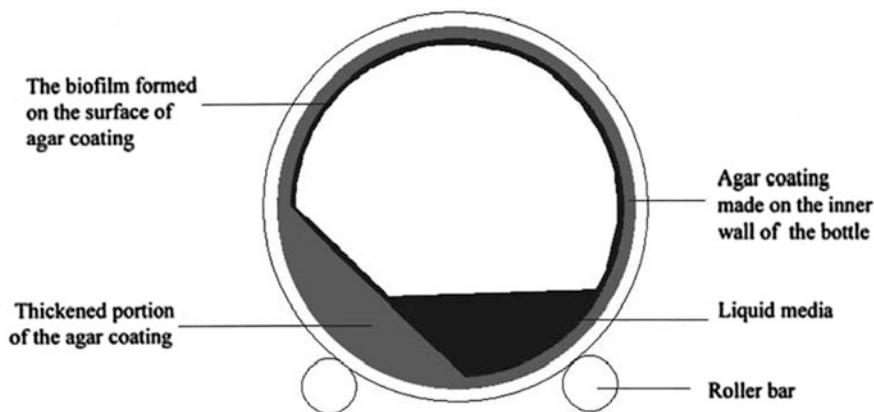


**Fig. 4** Roller-bottle cross-section as described by Yan et al. [72] for cultivation of marine epiphytic bacteria. Reprinted with permission from Springer

of agitated suspension cultures rendered artificial growth conditions to the organism contrary to the natural environment from where the bacteria are sourced. Thus, seemingly inactive surface isolates may be induced to produce bioactive compounds through novel cultivation strategies by simulating the natural habitats of microorganisms in “niche-mimicking” bioreactors. To this end, Yan et al. modeled the epibiotic growth conditions in a “modified roller bottle” culture method [72]. Two epibiotic marine strains (preliminarily identified as *Bacillus* species) isolated from the surface of marine alga *Palmaria palmata* were grown as a biofilm and shown to produce antimicrobial substances (Fig. 4). The antibiotic spectrum varied when the isolates were cultivated in the biofilm and suspension modes. Yan et al. assumed that sustained production of the antimicrobial compounds was linked to periodic exposure of the biofilm to the liquid medium and air.

Yan et al. [73] designed one more novel reactor, the “air–membrane surface” (AMS) bioreactor for attached growth of bacteria as a biofilm in contact with air. A surface-growing bacterium (*Bacillus licheniformis* EI-34-6) demonstrated antimicrobial activity (identified as bacitracin) in the AMS reactor but not in shake flask cultures. Surface-grown cells produced an unidentified red pigment not detected in planktonically grown cells. *Bacillus subtilis* strain DSM10<sup>T</sup>, applied in cross-species induction experiments, and *Bacillus pumilus* strain EI-25-8, another epibiotic isolate, were cultivated in the AMS reactor. Interestingly, spent media obtained from beneath the membrane of the reactor after growing these two strains, could stimulate production of antimicrobial compounds and a red pigment in suspension cultures of *B. licheniformis* isolate EI-34-6, but was not observed with shake flask culture spent media of DSM10<sup>T</sup> and EI-25-8. Yan et al. [73] conjectured that compounds inducing bacitracin and red pigment production diffused into the medium below the membrane and some of the compounds were retained in the biofilm which facilitated accumulation of inducer compounds. Accretion of inducer compounds in shake flask cultures was unlikely. Yan et al.

further established that ferric iron, glycerol, and air–membrane interfacial biofilm growth were essential for production of bacitracin and red pigment by EI-34-6, although the antimicrobial compound itself was not an inducer. Yan et al. [73] surmised that the physical environment of the AMS bioreactor was crucial for production of inducer compounds, which promoted bacitracin and red pigment synthesis. The physical environment was no longer required once the inducer compounds attained a threshold level.

Yan et al. [73] stated that the biofilm state is the preferred growth mode of surface-dwelling bacteria in natural environments. Yan et al. maintain that heterogeneous growth conditions may be expected in a biofilm [74] and microcolonies within the biofilm can have pH gradients [75]. Yan et al. [73] further attest that uneven bacterial starvation may occur due to constraints in substrate transport into the biofilm [76, 77], phenomena not observed in suspension cultures. Consequentially, biofilm bacterial metabolism is very dissimilar from that of suspension culture [78]. Cell density-dependent signaling and gene expression mechanisms may be presumed within biofilms as cell densities on the order of  $10^{12}$  CFU/cm<sup>3</sup> are frequently reached. Following the accepted model of bacterial quorum sensing, Yan et al. [73] reasoned that an increase in concentration of signal molecules above a threshold limit stimulated a change in gene expression that led to an altered phenotype [37, 79].

Yang et al. [80] investigated the effect of agitation on the production of the antimicrobial violacein by *Pseudoalteromonas luteoviolacea*, a surface-residing marine bacterium isolated from the marine sponge *Acanthella cavernosa*. Static growth conditions elicited the highest amounts of violacein whereas production decreased with increasing agitation speed. It was also noted [80] that cells formed clusters under stagnant conditions and higher agitation progressively separated clusters into single cells, suggesting that bacterial aggregation may be essential for violacein production by *P. luteoviolacea*. Yang et al. concluded that bacterial films formed under static conditions of the culture broth had higher cell densities on surfaces that might have triggered gene expression of certain inducers, as suggested by Boettcher and Ruby [81] in a related fashion to that expressed during extracellular polysaccharide production once bacteria attach to a surface [82]. The conclusion of this study is similar to that of Yan et al. [72, 73] where changes in the mode of culture, from suspension to biofilm affected the nature and amount of compounds produced by biofilm-forming bacteria.

*Nannocystis exedens*, a gliding bacterium belonging to the  $\delta$ -Proteobacteria class and isolated from the intertidal region of Crete, produced phenylnannolones as secondary metabolites [83]. Phenylnannolone A possessed an unusual chemical structure comprising an ethyl-substituted polyene chain linked to a pyrone moiety on one side and to a phenyl ring on the other. The compound had promising anticancer activity. Biofilm-based bioprocesses on this intertidal-dwelling organism would be of interest given the exciting advancements made in biofilm cultivations described earlier [62, 70, 72, 73].

As mentioned by Sarkar et al. [84], marine actinomycetes may be supposed to have features different from terrestrial actinomycetes as the marine habitat is completely dissimilar to the terrestrial environment. Novel chemical entities have

emerged as a result of extensive screening based on culture-dependent, culture-independent cultivation methods combined with the application of bioinformatics. The culture-dependent approach of bioprospecting is based upon microbe isolation from various geographic locations using taxon-selective isolation media and sediment pretreatments, preliminary characterization, and dereplication of isolates to avoid redundancy in screening. The culture-independent bioprospecting strategy has relied on extraction of total bacterial or actinobacterial DNA from the environment, cloning into surrogate hosts, identification of gene or gene cluster, sequencing, dereplication, and community profiling with single-strand conformation polymorphism, denaturing gradient gel electrophoresis or terminal restriction fragment length polymorphism, expression of the target gene or gene cluster, and characterization of the desired activity. The bioinformatics-based strategy that can be applied to explore novel compounds having actinobacterial properties are taxonomy as a road map to genes and the discovery of three-dimensional taxonomic space. According to Sarkar et al. [84] establishment of new marine genera, *Salinospora* and *Marinophilus*, which are taxonomically distinctive members of marine actinomycetes and the discovery of novel secondary metabolites therefrom, have given new directions to marine natural product research [85–88]. Indian investigators have identified the Bay of Bengal as a potential source of marine-derived bacterial bioactive compounds [84]. Mukherjee and coworkers isolated several microbes with novel bioactivities [89 and related references therein] from the *Sundarbans*, the world's largest tidal mangrove forest, off the Bay of Bengal. Sarkar et al. [84] also noted that in the research domain of marine bacterial antibiotic production, bioreactor engineering and design of bioprocesses have been neglected. Although a plethora of novel compounds are being reported, most cultivations were performed in shake flasks leading to poor understanding of mechanisms underlying antibiotic production processes, thus impeding prospects of commercial scale-up [90].

Inspired by the researches of Yan et al. [72, 73] and Yang et al. [80], a novel reactor system, the “rotating disk bioreactor” (RDBR), was applied by Sarkar et al. [84] to simulate the niche environment of three halotolerant estuarine actinobacteria isolated from the *Sundarbans*. Designed on the concept of a rotary biological contactor (RBC), generally used in wastewater treatment (Fig. 5), the RDBR supports the growth of surface-attached biofilms. The shaft of the RDBR on which 10 discs are coaxially mounted was rotated at an ultra-low speed of one revolution per day, 1,440 times lower than the 1.0-rpm speed used by Yan et al. [72]. When the shaft is rotated with a half-filled tank with a liquid medium, any given point on the discs would be exposed to air and submerged in the medium alternatively for 12 h. The reactor thus mimicked the intertidal environment of the location from where the actinobacteria were collected. Actinomycin D was produced within a shorter time in the RDBR compared to the time required in a conventional stirred-tank bioreactor (STBR). Similar results were noted for the other two strains and Sarkar et al. [84] reasoned that surface attachment of the microbes and biofilm formation were pivotal factors for the enhanced production of antimicrobials by the intertidal actinobacteria.

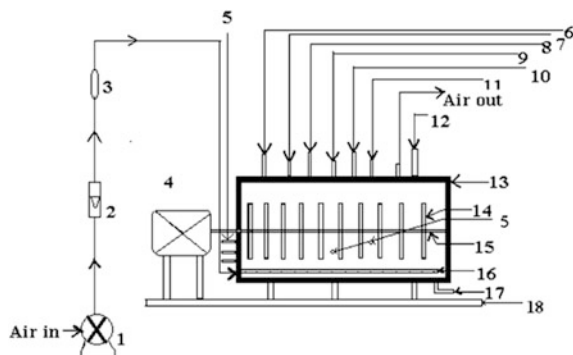


**Fig. 5** Schematic of the ultralow-speed rotating disk bioreactor as described in Sarkar et al. [92]: 1 air pump, 2 rotameter, 3 air filter, 4 electrical motor and reducing gear train, 5 sampling port, 6 temperature sensor, 7 antifoam port, 8 inoculation and medium addition port, 9 acid port, 10 pH sensor, 11 alkali port, 12 DO sensor, 13 reactor vessel, 14 rotating coaxial disks, 15 shaft, 16 sparger, 17 drain, 18 base plate. Reprinted with permission from Springer

In furtherance of this work, Sarkar et al. [91] introduced the parameters' "peak activity attainment rate" (PAAR) defined as the ratio of the "peak antibiotic activity" (PAA) and the time taken to attain this peak value, to determine the effect of environmental/operating parameters on actinomycin-D production by the biofilm-forming estuarine isolate *Streptomyces* sp. MS 310 in small-scale shake flask cultures, as well as in the RDBR. The most favorable pH and temperature for antibiotic production were ascertained through designed experiments in shake flasks. Subsequently, RDBR operating conditions were investigated employing a statistical experimental design where aeration and disk submergence were considered at three levels maintaining the rotational speed at 1.0 rev/day. The highest aeration rate in the niche-mimic condition was found to be most suitable for antibiotic production as PAA and PAAR simultaneously attained their highest values. Sarkar et al. further attributed the high actinomycin-D production by *Streptomyces* sp. MS 310 in the RDBR to biofilm formation owing to the substantial surface area (per unit volume of culture) of their reaction vessel [91].

In another study, Sarkar et al. [92] further examined the application of the RDBR for the cultivation of *Streptomyces sundarbansensis* [93], an actinomycete producing 2-allyloxyphenol, by first investigating the effect of nutrition and cultivation conditions on biofilm formation vis-à-vis antimicrobial production in small-scale experiments. Sarkar et al. [92] used the data thus obtained to examine the effect of medium pH, degree of disc submergence, and aeration rate in the RDBR on biofilm formation and antimicrobial activity of *S. sundarbansensis*. The maximum antimicrobial activity in the RDBR was attained under true intertidal conditions, 12 h periods of immersion and emersion. In the ideal niche-mimic condition, biofilm density was highest at the maximal aeration rate, where planktonic growth was also maximum and dissolved oxygen was rapidly utilized. Sarkar et al. [92] reckoned that high cell concentration during planktonic growth

allowed more cells to be recruited for biofilm formation, following which low oxygen tension reduced biofilm growth permitting the film to strengthen and attain a higher density [94]. The RDBR has been noted as the first model reactor system for in vitro process simulation of the intertidal/estuarine environment [95].

### 3.3 Production of Exopolysaccharides

Wave action, temperature and desiccation stresses, ultraviolet exposure, and nutrient depletion create a highly variable or “poikilotrophic” environment [96] in intertidal rocky shores. Ortega-Morales et al. [97] observed that an ecological strategy of microbial biofilms to cope with this harsh environment is through the production of profuse amounts of highly hygroscopic extracellular polymeric substances (EPS), the production of which is induced by desiccation [98]. The physicochemical properties of EPS of intertidal biofilms accelerate the generation of severe geochemical gradients, offering protection to the microbial cells, thus providing incredible pliancy to the biofilm during periods of stress [3, 99]. This ecological function makes EPS molecules potentially valuable as gelling, stabilizing, emulsifying, chelating, thickening, and film-making agents, which would be of significant importance in chemical and food industries as well as environmental bioremediation. Two EPS-producing biofilm bacteria from a rocky intertidal shore of the southern Gulf of Mexico were studied [97]. The major compound of the EPS synthesized by *Microbacterium* sp. MC3B-10 was a glycoprotein, whereas the polymer produced by *Bacillus* sp. MC6B-22 was an anionic polysaccharide. The biopolymer produced by *Microbacterium* sp. MC3B-10 was nonionic, had high emulsifying activity and stability at elevated temperature, and salinity. These properties may be practical in bioremediation applications. The chemical composition of polymer MC6B-22 suggested its potential utilization in tissue regeneration [2, 97].

The polychaete *Alvinella pompejana* isolated from a hydrothermal vent in the East Pacific Rise housed a heterotrophic and mesophilic marine bacterium on its surface. The bacterium was assigned to the genus *Alteromonas* and produced large amounts of an acidic polysaccharide in batch cultures during the stationary phase of growth [100]. *Alteromonas macleodii*, the single member of the *Alteromonas* genus, was isolated from a hydrothermal vent in north Fiji and was found to produce a polysaccharide having unusual high molecular weight in batch cultures. The viscosity of this exopolysaccharide is similar to that of xanthan, another bacterial polysaccharide of commercial interest, thus proving its biotechnological potential [101]. A novel bacterium, *Paracoccus zeaxanthinifaciens* subsp. *payriae* isolated from a microbial mat, “kopara” in French Polynesia produced water-soluble high-sulfate—containing exopolysaccharides. Potential cosmetic applications were envisaged [102]. Guézennec et al. [103] projected further applications of EPS-producing microbes of the kopara microbial mats in detergent, textile, adhesives, paper, paint, food, beverage, and pharmaceutical industries, specifically

in cancer therapies and drug delivery systems. The EPS can be gainfully employed for metal recovery in oil, mining industry, and industrial waste. Cell culture media can also be formulated using the EPS. Microbe-derived exopolysaccharides are used for the preparation of polysaccharide gels that are constituents of microbial cell culture media. Generally, agar, which has a high melting point of about 60–97 °C and a low solidifying point of about 32–40 °C is very useful in the preparation of a microbial culture medium. Nowadays, other compounds such as gellan or gelrite have drawn the attention of researchers as well as the industry as a substitute for agar. Gellan can be integrated into microbial culture media that allow better growth of microorganisms compared to agar-containing media. Moreover, thermophiles get a growth benefit due to the high temperature stability of gelrite [104].

Particulate material obtained from seawater and ice from the Antarctica southern ocean yielded two psychrophilic *Pseudoalteromonas* species from sea-ice microbial populations. The bacteria produced highly anionic extracellular polymers containing neutral sugars and uronic acids with sulphates [105]. Extracellular polymeric substances were purified from *Oceanobacillus iheyensis* BK6, isolated from a marine natural biofilm from a coastal region of India, the first report on the occurrence of EPS in the genus *Oceanobacillus* [106]. Antibiofilm activity of the EPS against pathogenic *Staphylococcus aureus* was observed by Kavita et al. [106]. The physicochemical properties of the polymer make it suitable for pharmaceutical and industrial applications.

### 3.4 Production of Enzymes

Identification and characterization of biofilm-forming bacteria through culture-based methods was performed by Iijima et al. [107]. Among three genera studied, *Pseudoalteromonas*, *Vibrio*, and *Halomonas*, the first was found to form active biofilms. To compare the protease activity under biofilm-based as well as planktonic cultivation the isolated bacteria were grown at standing and shaking conditions, respectively. Expression analysis of the biofilm metalloprotease I (*bmpI*) gene of *Pseudoalteromonas* sp. SB-B1 by reverse transcriptase PCR at different cultivation conditions revealed that biofilm-based cultivation stimulated *bmpI* gene expression which was responsible for enhanced protease activity. Application of the beneficial properties in fish farming was also considered. It was believed that *Pseudoalteromonas* bacteria of the biofilm community partially contributed to the elimination of excess proteins from fish farm sediment sludge. Foods and feces of fish liberate copious amounts of organic matter that result in oxygen depletion by aerobes, sulfide and methane production by anaerobes, and occurrence of pathogens [108]. Therefore, *Pseudoalteromonas* strains isolated from fish farms probably utilized *bmpI*-induced protease through biofilm formation and contributed towards removal of excess nutrients.

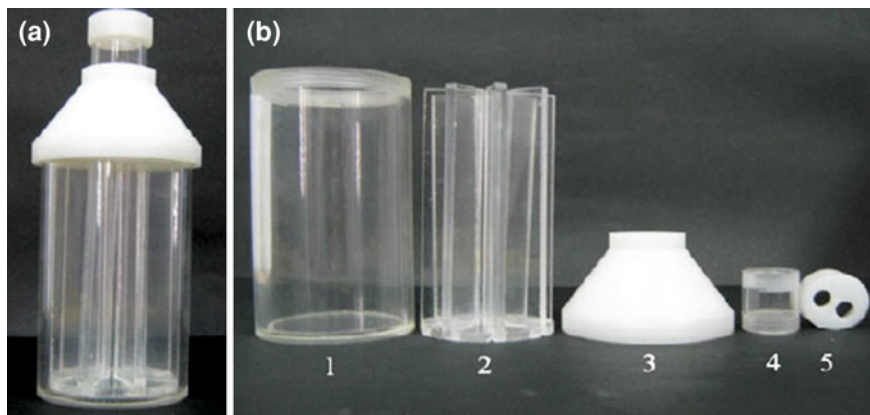


**Fig. 6** **a** Conico-cylindrical flask (CCF) described in Sarkar et al. [109] and US patent application number US2012/0295293A1 and **b** components of the CCF: 1 lower cylindrical portion, 2 inner arrangement, 3 upper funnel portion, 4 neck for joining top lid, 5 top lid for provision for aeration. Reprinted with permission from Springer

Sarkar et al. [109] designed a novel shaking flask the “conico-cylindrical flask” (CCF; Fig. 6), that promoted biofilm formation, had provision for assessment of aeration requirements, allowed the use of diverse internal surface materials, and could be easily placed in a typical rotary shaker for regular small-scale studies (US patent application number US2012/0295293A1, published November 22, 2012). This flask was applied for protease production by a biofilm-forming bacterium, an intertidal gamma-Proteobacterium (DGII) isolated from the *Sundarbans*, India. Protease activity during cultivation in the CCF with a hydrophilic (glass) surface was compared to that with a hydrophobic (PMMA) surface. The CCF with hydrophobic (PMMA) surface contained an “inner arrangement” comprising eight equidistantly arranged rectangular bars in a radial fashion on a circular disk. Because of the higher surface area, the “inner arrangement” of the vessel promoted formation of microbial biofilm on its hydrophobic surface. The second vessel, CCF with the hydrophilic (glass) surface contained 16 autoclaved glass slides that were affixed to both sides of the “inner arrangement” of PMMA-CCF with a nontoxic glue. The comparative study of protease production was done with the above-mentioned PMMA-CCF, GS-CCF, and a standard 500-ml Erlenmeyer flask (EF). The CCF allowed 30 % higher protease production and 20 % higher biomass accumulation in comparison to the standard Erlenmeyer flask. The CCF with a hydrophobic surface generated higher protease yields as well as biomass compared to the CCF with a hydrophilic surface. Sarkar et al. [109] concluded that cell growth and protease production were favored in the vessel configuration and design that supported higher cell attachment and ensuing biofilm formation. The conclusions of this study were similar to those of Yan et al. [72].

Mitra et al. [110] commented in their article on biofilm-based enzyme production by fungi that enzyme production and polyaromatic hydrocarbon oxidation

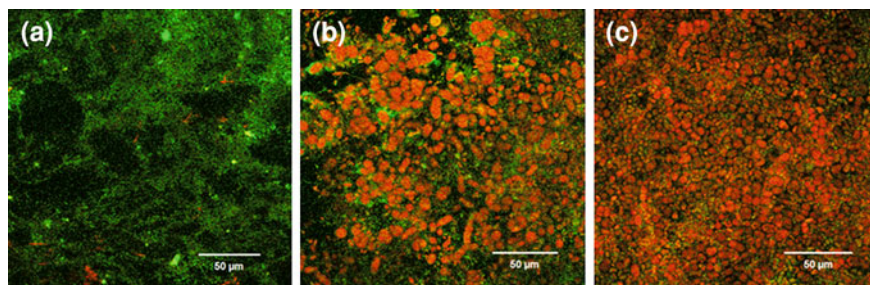


**Fig. 7** Typical confocal laser scanning micrograph of *C. crispatum* biofilm on PMMA surface as described in Mitra et al. [110]. Exopolysaccharides (EPS) are stained green and whole cells are stained red. **a** Attachment of EPS on PMMA surface **b** recruitment of cells, and **c** development of mature biofilm. Reprinted with permission from Springer

were potential biotechnological applications of filamentous fungi found in intertidal estuarine regions [111, 112]. Mitra et al. [110] highlighted the proposal of a new fermentation category named “surface-adhesion fermentation” (SAF) by Gutierrez-Correa and Villena [113]. The CCF was employed to test the hypothesis if surface attachment of intertidal fungi could increase bioactive metabolite production. Cellulase production by *Chaetomium crispatum* (obtained from estuarine sediments of the Weser River, Germany) was compared in a CCF with hydrophobic surface (PMMA–CCF), CCF with hydrophilic glass surface (GS–CCF), and a standard unbaffled Erlenmeyer flask (EF) [110]. Growth of *C. crispatum* as well as endo- $\beta$ -1,4-glucanase and FPase (filter paper degradation) activities increased 3.5- and 2.6-fold, respectively, in the PMMA–CCF compared to the other vessels. Additionally, Mitra et al. [110] studied biofilm development with a confocal laser scanning microscope (CLSM) over 6 days through two-channel fluorescence detection of EPS and whole cells. Results demonstrated 100 % increase of biovolume (an estimation of biofilm biomass), 25 % increase of thickness, and 62.5 % increase of both substratum coverage as well as the total spreading of *C. crispatum* biofilm on the hydrophobic surface (Fig. 7).

Fungal biofilm formation is initiated by active attachment to a surface by adhesive substances secreted by germinating spores and active germlings. Subsequently, microcolony formation occurs by apical elongation and hyphal branching. Hyphal ramification ensues across surfaces and a monolayer forms. Firm attachment of the growing colony to the substrate is ensured through production of a polymeric extracellular matrix [114]. Two basic processes, adhesion and successive differential gene expression, characterize fungi as regular biofilm-forming organisms. Upon attachment, fungi acquire new and discrete phenotypes diverse from those of free living conditions [113, 115]. Elements describing filamentous fungal biofilms along with a basic model depicting the different stages of biofilm development were proposed [114]. Through the investigation of Mitra et al. [110], successful satisfaction of the three proposed criteria [114] was demonstrated: first, intricate growth of the fungus by cellular or hyphal aggregation on



a surface; second, cells inlaid in an extracellular self-released polymeric matrix; and third, modified gene expression causing increased or decreased enzyme production. Biofilm architectural parameters of *C. albicans*, such as biovolume, mean thickness, roughness coefficient, and surface area/volume ratio were obtained through CLSM image analyses and calculated by COMSTAT mathematical modeling [116, 117]. Multichannel analysis as performed by Mitra et al. [110] using the PHLIP image analysis software [118] was more informative compared to single-channel analysis (e.g., COMSTAT) as this method could distinguish various biofilm components.

### 3.5 Production of Melanin

Melanin has significant relevance in the progress of organic conducting polymers (2000 Nobel Prize in Chemistry). It has applications in sunscreen cosmetics as an UV absorber, paint emulsion stabilizer, and antioxidant in coatings [40]. The CCF mentioned above was further applied for melanin production by *Shewanella colwelliana* (isolated from estuarine oyster water of Lewes, United States, previously known as *Alteromonas colwelliana*) [40]. A comparative study of melanin production in three different vessels (1) PMMA–CCF having a hydrophobic surface (2) GS–CCF having a hydrophilic surface, and (3) a standard Erlenmeyer flask (EF) was performed [40]. Compared to the other vessels, melanin production in the hydrophobic PMMA–CCF was higher by at most 33.5 % and growth of *S. colwelliana* was higher by at most 309.2 %. Reactor surface area, surface hydrophobicity, and planktonic cell growth, as well as biofilm formation were positively linked to melanin synthesis. Mitra et al. [40] noted a dual effect of enhanced surface area and hydrophobicity of the PMMA–CCF to be accountable for increased melanin activity in the hydrophobic vessel. The PMMA–CCF that supported attached growth, the inherent natural mode of growth of *S. collwelliana*, was more suitable for cell growth and melanin production. Mitra et al. [40] reasoned that biofilm cells (as higher biofilm biomass was attained in the PMMA–CCF) or positive cooperation among planktonic cells (as a higher concentration of quorum sensing molecules was observed) could be the cause for increased production. Acyl homoserine lactone molecules have been reported as quorum sensing molecules in *Shewanella* species as noted by Tait et al. [119].

### 3.6 Production of Riboflavin

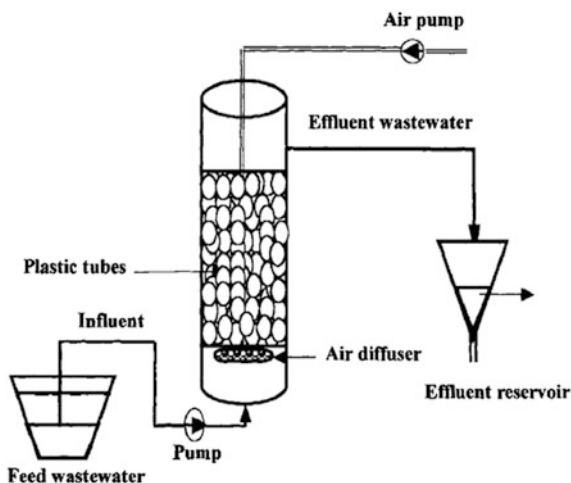
Chemical riboflavin (vitamin B<sub>2</sub>) production is eventually being replaced by microbial processes. The largest chemical company in the world, BASF (German: *Badische Anilin- und Soda-Fabrik*, English: Baden Aniline and Soda Factory) has installed a plant in South Korea that produces riboflavin using *Ashbya gossypii*.

Current approaches to improve industrial productivity in *Candida famata*, a naturally occurring overproducer of riboflavin, include selection of antimetabolite-resistant mutants, enhancing medium iron concentration, and adding biosynthetic precursors [120]. It may be conjectured that surface attachment and biofilm formation by the intertidally derived *C. famata*, isolated from the estuarine waters of Rio de Janeiro, Brazil, can enhance vitamin production. The CCF was again used by Mitra et al. [121] to compare riboflavin production between CCFs with hydrophobic or hydrophilic surfaces and Erlenmeyer flasks. Mitra et al. reported a 22-fold increase in riboflavin production in the hydrophilic GS-CCF and a 4-fold increase both in the EF and PMMA-CCF when *C. famata* was grown as “biofilm-induced” cultures in comparison to the traditional suspension culture [121]. Planktonic growth was suppressed in cultivations showing higher biofilm formation and vitamin production was related to biofilm formation. Similar to the previous CLSM study by Mitra et al. [110], early development of a mature stable biofilm on glass in contrast to a PMMA surface was demonstrated. Mitra et al. [121] concluded that the genetically modified *C. famata* strains recently developed by Dmytruk et al. [122] may be explored for further enhancement of production by switching to the biofilm cultivation mode as it is known that all species of *Candida* are able to form biofilms [123]. Primary cell separation processes may be eliminated in biofilm cultivation thus lowering downstream processing costs.

### **3.7 Biofilm-Based Bioremediation Processes**

Integration of a denitrifying step to the nitrification process leads to conversion of nitrate to nitrogen gas, thus allowing complete removal of polluting nitrogen in discharge water of recirculating aquaculture systems [124]. Van Rijn et al. remarked that the anaerobic ammonium oxidation (anammox) process can be successfully applied in this situation [125]. Under anaerobic conditions, ammonia is oxidized in the presence of nitrite in the anammox process which is performed by autotrophic bacteria belonging to the order Planctomycetales [126]. This process offers two advantages. First, in comparison to heterotrophic denitrification, complete autotrophic nitrogen removal occurs with no requirement of an organic electron source. Second, as ammonia oxidation demands less oxygen than that consumed by the conventional nitrification-denitrification process, the anammox process is economically attractive [127] as noted by Tal et al. [124]. Occurrence and functioning of anammox bacteria in aerobic and anaerobic fixed-film biofilters as well as anaerobic waste sludge sections of a marine recirculating aquaculture system were examined for the first time by Tal et al. [124]. Through community DNA analysis, Planctomycetales were found to be of ubiquitous occurrence and the anaerobic denitrifying biofilters contained one clone showing high levels of sequence identity to known anammox bacteria. Results were confirmed by fluorescence in situ hybridization studies.

**Fig. 8** Schematic diagram of the fixed-bed reactor described in Gharsallah et al. [130] and used for biological treatment of saline wastewaters. Reprinted with permission from Wiley

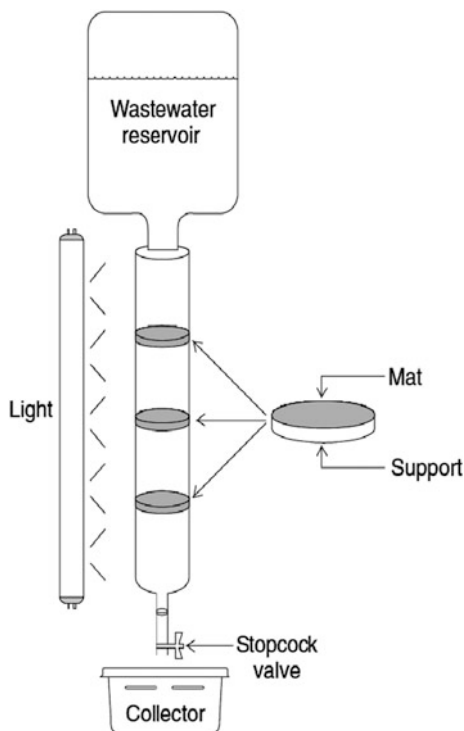


Xenobiotic compounds derived from wastewater generated by engine rooms of ships, “bilge water,” and by washing oil tanks, “slops” persist and accumulate in the marine ecosystem. The wastewater generated on the order of millions of tons per year is a major worldwide disposal problem. For the treatment of slops, Mancini et al. [128] appraised the applicability of a biological process with acclimatized microorganisms. Fitch et al. specifically considered the bioregeneration of the exhaust “granular activated carbons” [129] discharged with slops and a biofilm membrane bioreactor for secondary treatment of light-pretreated slops. Positive results were obtained by Fitch et al. [129].

High concentrations of organic compounds and salinity typified wastewater released by a factory processing marine products. Lysis of the organisms in the saline environment limited biological treatment of this wastewater in conventional systems. Gharsallah et al. [130] adapted a specific flora from a fish-processing industry by gradually increasing the salt concentration and accomplished the treatment process in a continuous fixed biofilm reactor (Fig. 8). Experiments were performed with different organic loading rates (OLR) and maximal removal efficiencies were attained at low OLR [130]. During the adaptation phase, microflora of the biofilm comprised small flocs and dispersed Gram-negative bacteria. After approximately 50 days, protozoa happened to be the predominant species, whereas under steady-state conditions, the microbial community was made up of rotifers, different ciliates, and some nematodes.

A novel method of bioremediation using microbial mats was proposed as a pragmatic, cost-effective, and environmentally acceptable treatment option appropriate for high biodiversity areas, such as coastal marine environments [131]. Consisting of vertically differentiated, interdependent layers of multiple microbial communities, microbial mats are physiologically diverse and are capable of performing heterotrophic, chemotrophic, and phototrophic metabolism [132] as mentioned by Zamora-Castro et al. [131]. The nature of the environment and

**Fig. 9** Conceptual drawing of a photobioreactor packed with constructed microbial mats as described in Zamora-Castro et al. [131]. Reprinted with permission from Springer



characteristics of the waste discharge determine the choice of support material for the construction of microbial mats [133]. Microbial mats were developed on low-density polyester for ex situ bioremediation of  $\text{NH}_4^+$ -N (ammonium nitrogen),  $\text{NO}_2^-$ -N (nitrite nitrogen),  $\text{NO}_3^-$ -N (nitrate nitrogen) and  $\text{PO}_4^{3-}$ -P (orthophosphate) [131]. Wastewater from a municipal treatment plant releasing into the beach of Todos Santos Bay, Mexico was successfully treated using this system (Fig. 9). Bacteria, microalgae, and cyanobacteria grew as self-forming and self-sustaining communities on a polyester support consuming various N and P substrates in the wastewater. Cyanobacterial genera such as *Chroococcus* sp., *Lyngbya* sp., bacteria of the subclass Proteobacteria, and the eukaryote *Nitzschia* sp. were dominant species of the microbial mat.

Low ambient temperature prevails for the major part of the year in the northern hemisphere. As it is not practical to heat the water for allowing mesophilic microbes to be active, cold-adapted microorganisms may be effective in microbial treatment processes in cold climates. The effectiveness of a suspended carrier biofilm process in attaining denitrification at low temperatures was investigated by Welander and Mattiasson [134]. Interestingly, the denitrification rate showed poor dependence on medium temperature, thus establishing a useful alternative for low-temperature denitrification.

Labelle et al. [135] noted that there is limited knowledge of biofilm processes mediating treatment of saline wastewater, especially denitrification of high

sulfate-containing aquarium and aquaculture seawater in closed circuit systems. High sulfate content in seawater obscures denitrification in biofilm processes by encouraging growth of sulfate-reducing bacteria in the anaerobic deep layer of the biofilm and residual nitrate should be made available to deter this process [134] as explained by Labelle et al. [135]. The carbon source necessary for denitrification is utilized by unwanted sulfate reduction which in turn generates sulfides that prevent the transformation of nitrous oxide to nitrogen. Labelle et al. [135] remarked that agitation methods applied in some moving-bed biofilm reactors (MBBR) were not acceptable as large dead mixing zones developed with resultant excessive biomass growth thus promoting sulfate reduction [136]. To circumvent this problem, Labelle et al. [135] designed a pilot-scale submerged MBBR at the Montreal Biodome, Canada and eventually scaled up to a commercial MBBR. Using methanol as a carbon source at various C/N ratios, seawater denitrification in a 3.25-million-liter closed-circuit mesocosm was investigated. The MBBR was partially filled with “positively buoyant” spherical polyethylene carriers representing 35 % of the total surface area. To deoxygenate the seawater prior to denitrification, pretreatment was done in a recirculated fixed bed. The carriers were maintained submerged by a conical grid and circulated through the downflow jet of an eductor (Fig. 10). Denitrification stoichiometric values corresponded to methanol consumption and sulfate reduction was not observed. Labelle et al. further noted that the C/N ratio was correlated to rates of denitrification and concentration of effluent residual dissolved organic carbon. Carrier fouling could be avoided by the downflow jet current of the denitrification unit. Low biofilm thickness was maintained during maximal denitrification activity [135].

In an attempt to maintain nitrate concentration within acceptable limits, the Montreal Biodome established a methanol-fed denitrification reactor to treat 3-million-liter seawater [137]. A denitrifying biofilm on the fluidized bed of plastic carriers was formed through colonization by naturally occurring microorganisms from seawater effluent in this completely mixed reactor. Through 16S rRNA gene sequencing the culturable isolates were established as members of alpha-Proteobacteria. The nonculturable ones were related to the *Methylophaga* members of the Piscirickettsia family (gamma-Proteobacteria) and other bacterial nitrifiers [138]. In their next study, Auclair et al. further detected functional genes coding for different denitrification reductases of the bacterial denitrifiers and their expression [139]. Quantitative PCR was applied to determine the concentrations of the different nitrate reductase gene sequences (*narG*, *napA*, *nirS*, and *nirK*) to ascertain the presence of denitrifiers and nitrate-reducing bacteria in the biofilm [139]. Sequences were found to be identical to the corresponding genes found in *Hyphomicrobium* sp. NL23 and *Methylophaga* sp. JAM1. Auclair et al. also demonstrated the predominance of *Methylophaga* sp. JAM1 and *Hyphomicrobium* sp. NL23 among the denitrifiers of the biofilm and indicated that the latter could use the nitrite generated by the former [139].

Biological fixed-film processes are advantageous for total ammonia nitrogen (TAN) removal in recirculated water systems (RAS) because of ease of operation, enhanced process stability to shock loads, and no possibility of bacterial wash off

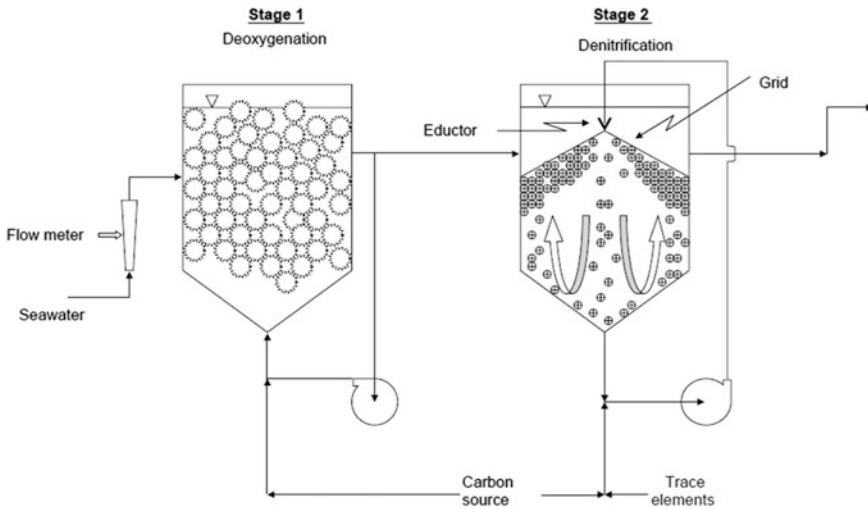


**Fig. 10** Schematic diagram of the experimental setup as described in Labelle et al. [135]. A packed-bed biofilter containing 63-mm random plastic carriers occupying 80 % of total filter volume is the first-stage pretreatment deoxygenation unit. Denitrification unit comprising a submerged MBBR designed to reduce media fouling and dead mixing zones is the second stage. Reprinted with permission from Elsevier

as reviewed by Fitch et al. [129] and noted by Rejish Kumar et al. [140]. However, despite the advantages, immobilized nitrifiers in RAS have demonstrated poor performance and require long start-up times [140]. To overcome these limitations a specialized nitrifying packed-bed bioreactor (PBBR) immobilized with ammonia-oxidizing and nitrite-oxidizing bacteria was developed. This reactor required a short start-up time and could be easily integrated into existing hatchery designs to operate under closed recirculating mode [141]. Microbial community analysis by fluorescent in situ hybridization (FISH) detected the presence of nitrifiers of the genera *Nitrosococcus*, *Nitrobacter*, and *Nitrospira* [142]. Nitrification in the PBBR integrated into a marine *Penaeus monodon* maturation system was analyzed for 70 days [140]. Instant nitrification was observed and TAN as well as  $\text{NO}_2\text{-N}$  removal were significant. FISH analysis of the biofilms showed presence of beta-ammonia oxidizers, *Nitrospira* species, halophilic *Nitrosomonas* species, and *Nitrospira* species. Rejish Kumar et al. [140] observed that the biofilm was dominated by autotrophic nitrifiers when the reactor system was operated with saturated oxygen and low concentrations of TAN and further stated that nitrifying biofilms could be excellently established on plastic bead carrier material (Fig. 11).

Although a large number of investigations have been done on bacterial biofilm-mediated bioremediation processes, fungal biofilm processes, in contrast, have not received much attention. Mitra et al. [143] studied the influence of surface attachment of *Cunninghamella elegans* and niche intertidal conditions simulated in a bioreactor on the biotransformation of fluoranthene by this filamentous fungus.

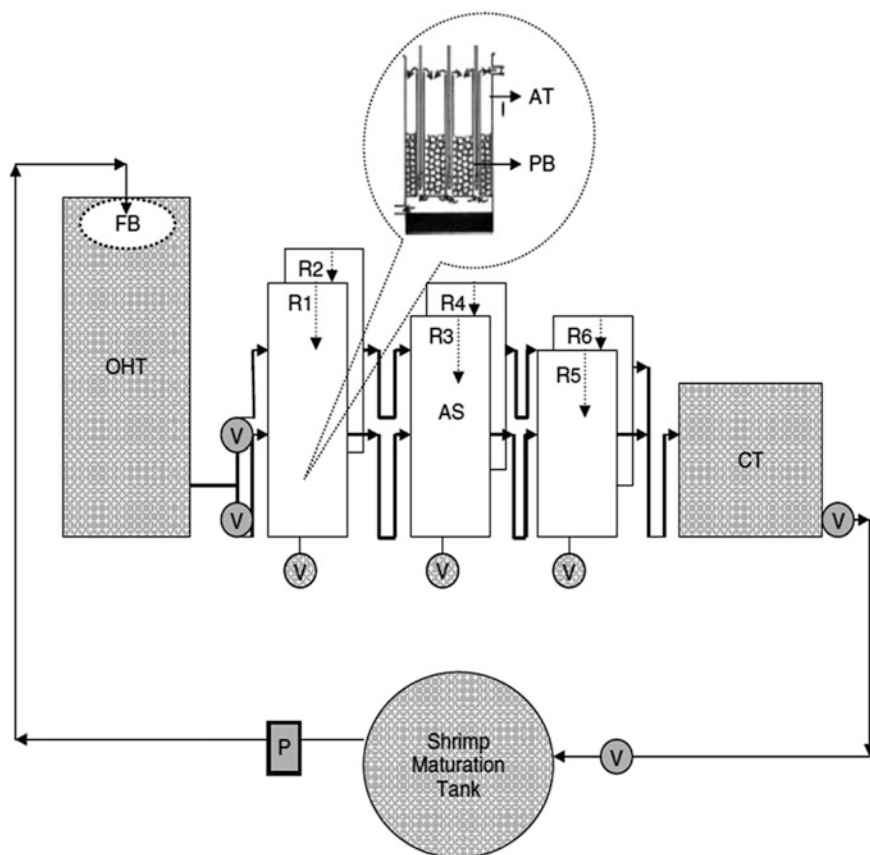


**Fig. 11** Packed-bed bioreactor connected to a shrimp maturation system as described in Kumar et al. [140]. *AS* aeration supply, *AT* aeration tube, *CT* collecting tank, *FB* filter bags, *OHT* overhead tank, *PB* polystyrene beads, *P* pump, *R1*–*R6* reactors, *V* valves. Reprinted with permission from Wiley

To this end, Mitra et al. [143] applied the CCF described earlier [40, 109, 110, 121] to compare fluoranthene biotransformation between biofilm and planktonic cultures as well as between hydrophobic and hydrophilic surfaces of biofilm attachment. Biofilm cultures showed more enhanced growth as well as fluoranthene transformation than did planktonic cultures with concomitant cytochrome P450 gene expression. Stable biofilm developed on the hydrophobic surface in comparison to the hydrophilic surface, with greater colocalization of fluoranthene in the extracellular polymeric substances as observed through three-channel confocal laser scanning microscopy. The RDBR used previously [84, 91, 92] was employed to provide six-hourly submergence and aerial exposure, thus mimicking the semidiurnal intertidal conditions from where *C. elegans* was obtained. Compared to a process not simulating the niche environmental conditions, growth, fluoranthene transformation, and cytochrome P450 gene expression were higher in

the process mimicking the intertidal conditions. Investigators concluded that in both small and large systems, biofilm formation was higher than planktonic cultures with a corresponding higher concentration of biofilm exopolysaccharides. This condition permitted enhanced movement of fluoranthene inside the biofilm with a resultant elevated gene expression.

### 3.8 *Biofilms in Microbial Fuel Cells*

About 20 years ago, microbial fuel cells employing immobilized *Proteus vulgaris* cells were used to generate continuous electric current. Improved mass-transfer kinetics resulting from the proximity of the immobilized bacteria to the electrode surface allowed increased efficiency compared to suspended cells [144]. The electrochemically active (EA) microorganisms termed “electricigens” are able to form biofilms on the electrode surface and oxidize organic compounds to CO<sub>2</sub> with simultaneous direct transfer of electrons to the electrode in measurable quantities [145]. Using acetate as the substrate, electrochemically active biofilms were developed on graphite anodes under constant polarization versus saturated calomel reference (SCE) [146]. Different microbial samples, from natural biofilm formed on a floating bridge (located in the Atlantic coastal port of La Tremblade, France) surface, marine sediments collected directly under the floating bridge, and beach sand were used to inoculate the cells. Erable et al. [146] obtained higher current densities with the biofilm inoculum compared to the other samples. Bacteria related to *Bacteroidetes*, *Halomonas*, and *Marinobacterium* were recovered from the EA biofilm, and species related to *Mesoflavibacter* were prevalent on sediment biofilm. The coulombic efficiency of acetate consumption was improved by progressively adapting the anode to acetate utilization by serial additions of the substrate. After 8 days of biofilm formation, a maximal current density of 7.9 A/m<sup>2</sup> was attained with 10 mM acetate, the highest value as claimed by Erable et al. [146]. The authors further observed that microorganisms gradually colonized the anode surface with the progressive increase in anodic current. Microbial surface growth as well as current production was stimulated by acetate addition. Current density decreased rapidly after reaching the maximum value, possibly due to acetate exhaustion. On the other hand, control experiments with seawater without biofilm inoculum did not yield any current, irrespective of acetate addition [146].

The efficiency of the cathodic reduction process in microbial fuel cells is low [147] as noted by Erable et al. [148]. Although platinum can improve the efficiency, its application is limited by high cost and anodic poisoning. Therefore, microbial cathodes have potential as a cheap and sustainable alternative to platinum. Erable et al. [148] remarked that oxygen reduction on stainless steels has been observed to be catalyzed by biofilms formed in natural seawater [149], opening up a possibility for cheap microbial cathodes for fuel cells. Erable et al. [148] further commented that current densities up to 1.89 A/m<sup>2</sup> were achieved with a biofilm-covered cathode in 2005 [150] and implementation of marine

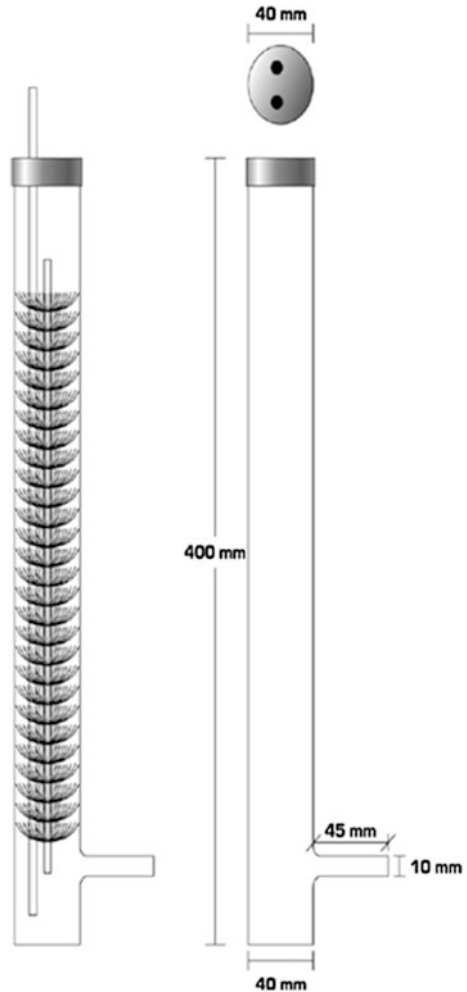


microbial cathodes in MFCs in a sea environment were later sought [151, 152]. However, the necessity of exposure of stainless steel under constant polarization for several days in large volumes of seawater with continuous renewal [153] posed a hindrance in developing efficient seawater biofilms [148]. Erable et al. attempted to develop electrochemically active (EA) biofilms in closed electrochemical vessels that could be conveniently handled [148]. A mechanistic understanding of biocatalysis was offered by identifying EA seawater biofilm-forming microbial strains and the electrochemical efficiency of each isolate was ascertained. Wild EA biofilms were developed by immersing stainless steel in open sea water with monitoring of the current generated. The film was then removed by scraping, resuspended in seawater, and applied as inoculum in closed 0.5 L electrochemical reactors. A 20-fold improvement in the current density was attained by continuously feeding an open reactor with filtered seawater. Erable et al. [148] reasoned that seawater filtration prevented indigenous common strains from competing with the EA strains. Among the biofilm formers, *Winogradskyella poriferorum* and *Acinetobacter johnsonii* yielded modest current densities and the importance of synergistic effects occurring in the biofilm was pointed out [148].

### 3.9 Aquaculture Feedstock Production

Avendaño-Hererra and Riquelme [154] explained that primary colonization of surfaces by bacteria precedes the maturation of a mixed biofilm formed of diatoms and other microorganisms [155]. The authors [154] further discussed that production of extracellular polysaccharides which function at cellular and intercellular levels enables the formation of strong irreversible bonds with the surface [156] and succession of macroorganisms follows colonization by microorganisms [157]. The bacteria of the biofilm can have stimulatory or inhibitory effects on the late-colonizing microalgae, thus influencing the microalgal population [158] as cited in [154]. Larval settlement is of vital importance in the artificial production of *Argopecten purpuratus* (Peruvian scallop). The possibility of improving postlarval settlement of *A. purpuratus* using a substrate, “cultch”, pretreated with native diatom biofilm was investigated. Avendaño-Hererra et al. [159] showed an increase of spatfall and production of larger settlement were attained by the addition of diatom biofilms. An innovative microalgal culture system was used for the production of *Navicula veneta* (diatom) biofilm by addition of bacteria [154]. NC1 (*Halomonas* sp.) was found to be the best growing strain utilizing the extracellular products of *N. veneta* in small-scale studies conducted in Petri plates. In the Tanaka photobioreactor (Fig. 12), the diatom produced the highest yields when cocultivated with NC1 (*Halomonas* sp.) in six replicate cultures running in three cycles lasting 7 days each. Chlorophyll *a* concentration (indicator of diatom growth) and bacterial cell mass were positively correlated. The Tanaka photobioreactor can be gainfully exploited for the mass production of diatom–bacteria mixed biofilms. The biofilms can find application in the settlement of mass cultures of marine

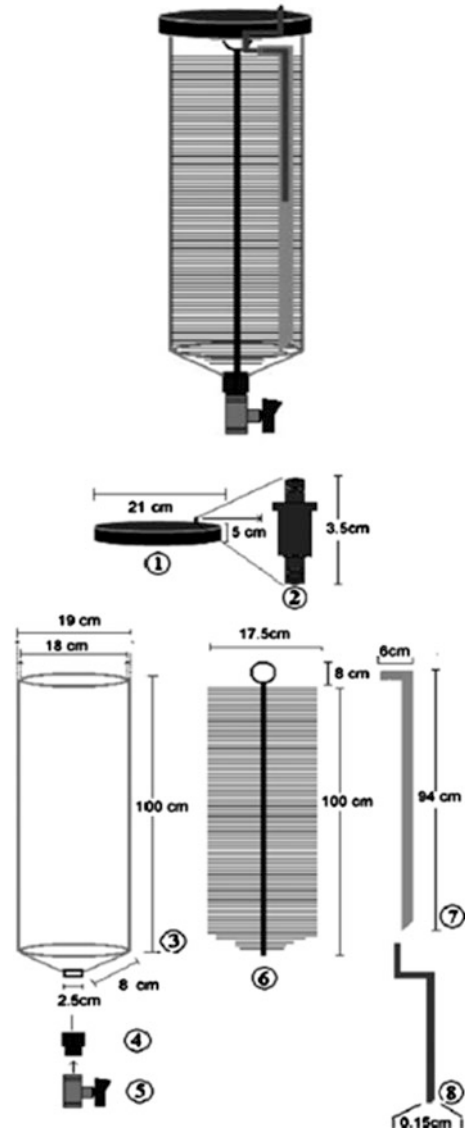
**Fig. 12** Schematic of the Tanaka photobioreactor as described in Avendaño-Herrera and Riquelme [154]. Top of the reactor allows introduction of starting inoculum, air, and bristles, and culture is harvested through the side-arm effluent tube. Reprinted with permission from Elsevier



invertebrates of commercial importance as well as aquaculture food production. Avendaño-Herrera and Riquelme [154] further remarked that the biofilm could be used to provide nutrition for abalone or scallop juvenile stages and/or to colonize the larvae settlement substrata, thus reducing the process time [160].

Similar to the observations of Yan et al. [72] and Yan et al. [73], Silva-Aciaries and Riquelme [161] noted that traditionally used suspension microalgal culture systems were not suitable for benthic diatoms that have characteristic surface-attached lifestyles. Larval settlement and metamorphosis of *Pinctada maxima* (pearl oyster) in response to both natural (bacterial biofilms) and artificial inducers ( $K^+$ ,  $Ca^{2+}$ , and  $NH_4^+$  and seven types of neuroactive compounds such as 3-isobutyl-1-methylxanthine,  $\gamma$ -aminobutyric acid, choline chloride, acetylcholine chloride, serotonin hydrochloride, 3-(3,4-dihydroxyphenyl)-L-tyrosine and dopamine) were investigated by Zhao et al. [162]. Natural bacterial biofilms supported

**Fig. 13** Diagram of the bristles photobioreactor (PBB) as described in Silva-Aciars and Riquelme [161]. A general view of the PBB: 1 top of the tube with a PVC cap, 2 air inlet PVC connector, 3 clear acrylic tube, 4 base coupling, 5 ball valve, 6 PVC bristles in a “bottle brush” with a metal axis coated by plastic, 7 PVC “bubbling column,” and 8 plastic compressed airline. Reprinted with permission from Elsevier



larval settlement. Zhao et al. [162] noted that some pharmacological agents acted as potent artificial inducers of *P. maxima* larval settlement. These ecological observations, however, were not transformed into large-scale production of algal biofilms [161]. Mass culture of six benthic diatom species in a bristles photobioreactor (PBB; Fig. 13) were undertaken by Silva-Aciars and Riquelme [161]. The reactor holds polyvinyl chloride bristles providing a surface for attachment of adhesive diatoms and constant water movement was afforded by an airlift system [161]. Performance of this reactor was compared with that attained by cultivating

the diatom species in a bubble column photobioreactor without support bristles (PBC), while maintaining a turbulent hydrodynamic regime through a strong current of air bubbles. The PBB proved to be a superior reactor for adhesive diatoms *Amphora* sp., *Amphora* sp. 2, *Navicula* sp., and *Nitzschia ovalis*. The PBC system, on the other hand, was more suitable for the lesser adhesive diatoms *Nitzschia* sp. and *Cylindrotheca closterium* which grew better in suspension mode. Higher bacterial counts were obtained in the systems having maximum microalgal populations. The positive correlation between the bacterial concentration and the number of microalgae in photobioreactors is mutually beneficial. Diatoms are recognized for secretion of organic compounds with high amounts of carbohydrates [163] that supply nutrients to heterotrophs [164]. Several studies suggest that during the bacterial–microalgal interactions, various bacterial species secrete organic compounds which support the microalgal growth [154, 158]. These organic compounds may be converted to carbon dioxide by the bacteria that is utilized for photosynthesis by the phototrophic microalgae [165].

At least seven mechanisms of attachment in solitary or colonial arrangement have been described for diatoms [166] as cited in [161]. Diatoms grow in two-dimensional or multiple three-dimensional layers governed by their motility and adhesive force. The high degree of adhesion and slow movement that typifies “type B” growth was observed on the PVC bristles but not in the water column microalgae. Diatoms that yielded higher concentrations and biomass in the PBC systems, and developed satisfactorily in the water column forming biofilm microaggregates, had “type A” growth distinguished by weak substrate adhesion and fast movement [166].

## 4 Conclusions

This chapter reviews the research done on the ecological perspectives of marine and intertidal surface-attached microbes and their bioactivities as well as the industrial and environmental bioprocesses dependent on biofilm formation. Biofilm formation and bioactivities of the *Roseobacter* clade and the *Pseudoalteromonas* genus are described in detail. Nitrous-oxide (N<sub>2</sub>O)—emitting biofilms, antimicrobial- and auxin-producing biofilms are also illustrated. The chapter discusses biofilm-mediated production of antifouling, antimicrobial, and cytotoxic compounds, exopolysaccharides, enzymes, melanin, riboflavin, and aquaculture feedstock. Bioremediation processes and operation of microbial fuel cells through application of marine and intertidal surface-attached microbes are important components of the chapter. From a biotechnological perspective, the production of bioactive compounds for competition and defense by surface-associated marine and intertidal microorganisms represent an unmatched pool for the discovery of new molecules, with medical, industrial, and environmental applications.

Through the nexus of ecology and engineering it is important to comprehend the fundamental characteristics concerning the behavior of cells in a biofilm such as cell physiology and mobility of established biofilms. Development and progression

of biofilms can be controlled to make them productive through understanding of biofilm growth mechanisms against an ecological background. With an improved knowledge of these physicochemical properties of biofilms, further optimization of process conditions and design of reactors based on fundamental information can be visualized. The prospects of multispecies marine/intertidal biofilms in bioprocess development need to be researched. A potentially interesting field of research would be to understand the role of multiple species catalyzing a series of reactions in a cascade. Comprehension of the basis of interspecies dependencies of microbial communities requires further fundamental research [167, 168].

Future research should be directed to target new areas for the use of marine/intertidal biofilms in productive catalysis. Possibilities exist for applications of biofilms in biotransformations involving solvents or other daunting reactants as biofilms display increased resistance to toxic substrates and products. Biofilms might prove useful for the production of low-value bulk chemicals because they can provide the required catalyst concentration (biomass) to achieve an efficient transformation of the substrate. Another emerging area of research is the prospective use of extracellular enzymes produced by biofilms, such as hydrolases for use in biofuel production. Christenson and Sims noted all microalgal cultivations for biofuel production involve substantial challenges of biomass harvesting that can account for up to 30 % of total costs [169]. Because of the high centrifugation costs associated with harvesting suspended microalgae, there is interest in using surface-attached algal biofilm systems that are naturally concentrated and more readily harvestable. Another promising sector for biofilm applications is the pharmaceutical industry. Biofilm reactors can support continuous processing of enzyme cascades within whole cells that may be used to synthesize complex pharmaceuticals, for example, those containing multiple chiral centers [170].

## References

1. Egan S, Thomas T, Kjelleberg S (2008) *Curr Opin Microbiol* 11:219
2. Ortega-Morales BO, Chan-Bacab MJ, De la Rosa-García SDC, Camacho-Chab JC (2010) *Curr Opin Biotechnol* 21:346
3. Decho AW (2000) *Cont Shelf Res* 20:1257
4. Bowman JP (2007) *Mar Drugs* 5:220
5. Bruhn JB, Nielsen KF, Hjelm M, Hansen M, Bresciani J, Schulz S, Gram L (2005) *Appl Environ Microbiol* 71:7263
6. Ruger HJ, Hofle MG (1992) *Int J Syst Bacteriol* 42:133
7. Hjelm M, Bergh Ø, Riaza A, Nielsen J, Melchiorsen J, Jensen S, Duncan H, Ahrens P, Birkbeck H, Gram L (2004) *Syst Appl Microbiol* 27:360
8. Hjelm M, Riaza A, Formoso F, Melchiorsen J, Gram L (2004) *Appl Environ Microbiol* 70:7288
9. Bruhn JB, Haagenen JAJ, Bagge-Ravn D, Gram L (2006) *Appl Environ Microbiol* 72:3011
10. Bruhn JB, Gram L, Belas R (2007) *Appl Environ Microbiol* 73:442
11. Brinkhoff T, Bach G, Heidorn T, Liang L, Schlingloff A, Simon M (2004) *Appl Environ Microbiol* 70:2560
12. Moran MA, González JM, Kiene RP (2003) *Geomicrobiol J* 20:375

13. Miller TR, Belas R (2004) *Appl Environ Microbiol* 70:3383
14. D'Alvise PW, Melchiorson J, Porsby CH, Nielsen KF, Gram L (2010) *Appl Environ Microbiol* 76:2366
15. Geng H, Bruhn JB, Nielsen KF, Gram L, Belas R (2008) *Appl Environ Microbiol* 74:1535
16. D'Alvise PW, Magdenoska O, Melchiorson J, Nielsen KF, Gram L (2013) *Environ Microbiol* (in press)
17. Smith KD, Shanahan CA, Moore EL, Simon AC, Strobel SA (2011) *Proc Natl Acad Sci USA* 108:7757
18. Porsby CH, Nielsen KF, Gram L (2008) *Appl Environ Microbiol* 74:7356
19. Brinkhoff T, Giebel HA, Simon M (2008) *Arch Microbiol* 189:531
20. Buchan A, González JM, Moran MA (2005) *Appl Environ Microbiol* 71:5665
21. Lafay B, Ruimy R, De Trautenberg CR, Breittmayer V, Gauthier MJ, Christen R (1995) *Int J Syst Bacteriol* 45:290
22. Wagner-Döbler I, Biebl H (2006) *Annu Rev Microbiol* 60:255
23. Newton RJ, Griffin LE, Bowles KM, Meile C, Gifford S, Givens CE, Howard EC, King E, Oakley CA, Reisch CR, Rinta-Kanto JM, Sharma S, Sun SL, Varaljay V, Vila-Costa M, Westrich JR, Moran MA (2010) *ISME J* 4:784
24. Cude WN, Mooney J, Tavanaei AA, Hadden MK, Frank AM, Gulvik CA, May AL, Buchan A (2012) *Appl Environ Microbiol* 78:4771
25. Holmström C, Kjelleberg S (1999) *FEMS Microbiol Ecol* 30:285
26. Rao D, Webb JS, Kjelleberg S (2005) *Appl Environ Microbiol* 71:1729
27. James SG, Holmström C, Kjelleberg S (1996) *Appl Environ Microbiol* 62:2783
28. Barja JL, Lemos ML, Toranzo AE (1989) *Antimicrob Agents Chemother* 33:1674
29. Matz C, Webb JS, Schupp PJ, Phang SY, Penesyan A, Egan S, Steinberg P, Kjelleberg S (2008) *PLoS ONE* 3:e2744
30. Riveros R, Haun M, Campos V, Duran N (1988) *Arq Biol Technol* 31:475
31. August PR, Grossman TH, Minor C, Draper MP, MacNeil IA, Pemberton JM, Call KM, Holt D, Osburne MS (2000) *J Mol Microbiol Biotechnol* 2:513
32. Sánchez C, Braña AF, Méndez C, Salas JA (2006) *ChemBioChem* 7:1231
33. Franks A, Egan S, Holmström C, James S, Lappin-Scott H, Kjelleberg S (2006) *Appl Environ Microbiol* 72:6079
34. Holmström C, Egan S, Franks A, McCloy S, Kjelleberg S (2002) *FEMS Microbiol Ecol* 41:47
35. Egan S, James S, Holmström C, Kjelleberg S (2001) *FEMS Microbiol Ecol* 35:67
36. Bernborg N, Ng YY, Kjelleberg S, Harder T, Gram L (2011) *Appl Environ Microbiol* 77:8557
37. Lemos ML, Toranzo AE, Barja JL (1985) *Microb Ecol* 11:149
38. Long RA, Qureshi A, Faulkner DJ, Azam F (2003) *Appl Environ Microbiol* 69:568
39. Long RA, Azam F (2001) *Aquat Microb Ecol* 26:103
40. Mitra S, Sarkar S, Gachhui R, Mukherjee J (2011) *Appl Microbiol Biotechnol* 90:321
41. Ivanova EP, Nicolau DV, Yumoto N, Taguchi T, Okamoto K, Tatsu Y, Yoshikawa S (1998) *Mar Biol* 130:545
42. Rao D, Webb JS, Kjelleberg S (2006) *Appl Environ Microbiol* 72:5547
43. Heisterkamp IM, Schramm A, De Beer D, Stief P (2010) *Mar Ecol Prog Ser* 415:1
44. IPCC (Intergovernmental Panel on Climate Change) (2007) *Climate change 2007, the physical science basis—summary for policy makers*. Cambridge University Press, Cambridge
45. Ravishankara AR, Daniel JS, Portmann RW (2009) *Science* 326:123
46. Bange HW (2006) *Atmos Environ* 40:198
47. Magalhães CM, Wiebe WJ, Joye SB, Bordalo AA (2005) *Estuaries* 28:592
48. Stief P, Poulsen M, Nielsen LP, Brix H, Schramm A (2009) *Proc Natl Acad Sci USA* 106:4296
49. Philippart CJM, Beukema JJ, Cadée GC, Dekker R, Goedhart PW, Van Iperen JM, Leopold MF, Herman PMJ (2007) *Ecosystems* 10:95

50. Van Beusekom JEE, Weigelt-Krenz S, Martens P (2008) *Helgol Mar Res* 62:49
51. Meyer RL, Allen DE, Schmidt S (2008) *Mar Chem* 110:68
52. Jenkins MC, Kemp WM (1984) *Limnol Oceanogr* 29:609
53. Heisterkamp IM, Schramm A, Larsen LH, Svenningsen NB, Lavik G, De Beer D, Stief P (2013) *Environ Microbiol* 15:1943
54. Svenningsen NB, Heisterkamp IM, Sigby-Clausen M, Larsen LH, Nielsen LP, Stief P, Schramm A (2012) *Appl Environ Microbiol* 78:4505
55. Wilson GS, Raftos DA, Nair SV (2011) *Microbiol Res* 166:437
56. Burchard RP, Sorongon ML (1998) *Appl Environ Microbiol* 64:4079
57. Kerkar S, Raiker L, Tiwari A, Mayilraj S, Dastager S (2012) *Biologia* 67:454
58. Patten CL, Glick BR (2002) *Appl Environ Microbiol* 68:3795
59. Kogure K, Simidu U, Taga N (1979) *J Exp Mar Biol Ecol* 36:201
60. Armstrong E, Yan L, Boyd KG, Wright PC, Burgess JG (2001) *Hydrobiologia* 461:37
61. Tait K, Sutherland IW (2002) *J Appl Microbiol* 93:345
62. Ortega-Morales BO, Chan-Bacab MJ, Miranda-Tello E, Fardeau ML, Carrero JC, Stein T (2008) *J Ind Microbiol Biotechnol* 35:9
63. Callow ME, Callow JA (2002) *Biologist* 49:10
64. Steinberg PD, De Nys R, Kjelleberg S (2001) Marine chemical ecology. In: McClintock JB, Baker BJ (ed). CRC, Florida, pp 355–388
65. Roberts MS, Nakamura LK, Cohan FM (1994) *Int J Syst Bacteriol* 44:256
66. Bacon CW, Hinton DM (2002) *Biol Control* 23:274
67. Bernbom N, Ng YY, Olsen SM, Gram L (2013) *Appl Environ Microbiol* 79:6885
68. Holmström C, Rittschof D, Kjelleberg S (1992) *Appl Environ Microbiol* 58:2111
69. Ortega-Morales BO, Ortega-Morales FN, Lara-Reyna J, De La Rosa-García SC, Martínez-Hernández A, Montero-M J (2009) *Mar Biotechnol* 11:375
70. Kanagasabhapathy M, Sasaki H, Haldar S, Yamasaki S, Nagata S (2006) *Ann Microbiol* 56:167
71. Vandevivere P, Kirchman DL (1993) *Appl Environ Microbiol* 59:3280
72. Yan L, Boyd KG, Burgess JG (2002) *Mar Biotechnol* 4:356
73. Yan L, Boyd KG, Adams DR, Burgess JG (2003) *Appl Environ Microbiol* 69:3719
74. Wimpenny J, Manz W, Szewzyk U (2000) *FEMS Microbiol Rev* 24:661
75. Vroom JM, De Grauw KJ, Gerritsen HC, Bradshaw DJ, Marsh PD, Watson GK, Birmingham JJ, Allison C (1999) *Appl Environ Microbiol* 65:3502
76. Beuling EE, Van Den Heuvel JC, Ottengraf SP (2000) *Biotechnol Bioeng* 67:53
77. James GA, Korber DR, Caldwell DE, Costerton JW (1995) *J Bacteriol* 177:907
78. Evans LV (2000) *Biofilms: recent advances in their study and control*. Harwood Academic, Marston, Amsterdam, The Netherlands
79. Boyd KG, Adams DR, Burgess JG (1999) *Biofouling* 14:227
80. Yang LH, Xiong H, Lee OO, Qi SH, Qian PY (2007) *Lett Appl Microbiol* 44:625
81. Boettcher KJ, Ruby EG (1995) *J Bacteriol* 177:1053
82. Davies DG, Chakrabarty AM, Geesey GG (1993) *Appl Environ Microbiol* 59:1181
83. Ohlendorf B, Leyers S, Krick A, Kehraus S, Wiese M, König GM (2008) *ChemBioChem* 9:2997
84. Sarkar S, Saha M, Roy D, Jaisankar P, Das S, Gauri Roy L, Gachhui R, Sen T, Mukherjee J (2008) *Mar Biotechnol* 10:518
85. Fiedler HP, Bruntner C, Bull AT, Ward AC, Goodfellow M, Potterat O, Puder C, Mihm G (2005) *Antonie Van Leeuwenhoek* 87:37
86. Jensen PR, Mincer TJ, Williams PG, Fenical W (2005) *Antonie Van Leeuwenhoek* 87:43
87. Bull AT, Stach JEM, Ward AC, Goodfellow M (2005) *Antonie Van Leeuwenhoek* 87:65
88. Imada C (2005) *Antonie Van Leeuwenhoek* 87:59
89. Mitra A, Santra SC, Mukherjee J (2008) *Appl Microbiol Biotechnol* 80:685
90. Marwick JD, Wright PC, Burgess JG (1999) *Mar Biotechnol* 1:495
91. Sarkar S, Mukherjee J, Roy D (2009) *Biotechnol Bioprocess Eng* 14:775
92. Sarkar S, Roy D, Mukherjee J (2010) *Bioprocess Biosyst Eng* 33:207

93. Arumugam M, Mitra A, Pramanik A, Saha M, Gachhui R, Mukherjee J (2011) *Int J Syst Evol Microbiol* 61:2664
94. Ahimou F, Semmens MJ, Haugstad G, Novak PJ (2007) *Appl Environ Microbiol* 73:2905
95. Zhang Y, Arends JBA, Van de Wiele T, Boon N (2011) *Biotechnol Adv* 29:312
96. Kirkwood AE, Buchheim JA, Buchheim MA, Henley WJ (2008) *Microb Ecol* 55:453
97. Ortega-Morales BO, Santiago-García JL, Chan-Bacab MJ, Moppert X, Miranda-Tello E, Fardeau ML, Carrero JC, Bartolo-Pérez P, Valadéz-González A, Guezennec J (2007) *J Appl Microbiol* 102:254
98. Ortega-Morales BO, López-Cortés A, Hernández-Duque G, Crassous P, Guezennec J (2001) *Methods Enzymol* 336:331
99. Mancuso Nichols CA, Guezennec J, Bowman JP (2005) *Mar Biotechnol* 7:253
100. Vincent P, Pignet P, Talmont F, Bozzi L, Fournet B, Guezennec J, Jeanthon C, Prieur D (1994) *Appl Environ Microbiol* 60:4134
101. Raguenes G, Pignet P, Gauthier G, Arènes A, Christen R, Rougeaux H, Barbier G, Guezennec J (1996) *Appl Environ Microbiol* 62:67
102. Raguenes G, Moppert X, Richert L, Ratiskol J, Payri C, Costa B, Guezennec J (2004) *Curr Microbiol* 49:145
103. Guézennec J, Moppert X, Raguénès G, Richert L, Costa B, Simon-Colin C (2011) *Process Biochem* 46:16
104. Sutherland IW (1996) Extracellular polysaccharides. In: Rehm HJ, Reed G (eds) *Biotechnology: products of primary metabolism*. Verlag Chemie, Weinheim, Germany, pp 613–657
105. Mancuso Nichols CA, Garon S, Bowman JP, Raguénès G, Guézennec J (2004) *J Appl Microbiol* 96:1057
106. Kavita K, Singh VK, Mishra A, Jha B (2014) *Carbohydr Polym* 101:29
107. Iijima S, Washio K, Okahara R, Morikawa M (2009) *Microb Biotechnol* 2:361
108. Verschuere L, Rombaut G, Sorgeloos P, Verstraete W (2000) *Microbiol Mol Biol Rev* 64:655
109. Sarkar S, Roy D, Mukherjee J (2011) *Bioresour Technol* 102:1849
110. Mitra S, Banerjee P, Gachhui R, Mukherjee J (2011) *Bioprocess Biosyst Eng* 34:1087
111. Niture SK, Pant A (2007) *World J Microbiol Biotechnol* 23:1169
112. Da Silva M, Cerniglia CE, Pothuluri JV, Canhos VP, Esposito E (2003) *World J Microbiol Biotechnol* 19:399
113. Gutiérrez-Correa M, Villena GK (2003) *Rev Peru Biol* 10:113
114. Harding MW, Marques LLR, Howard RJ, Olson ME (2009) *Trends Microbiol* 17:475
115. Wimpenny J, Manz W, Szewzyk U (2000) *FEMS Microbiol Rev* 24:661
116. Heydorn A, Nielsen AT, Hentzer M, Sternberg C, Givskov M, Ersbøll BK, Molin S (2000) *Microbiology* 146:2395
117. Da Silva WJ, Seneviratne J, Samaranyake LP, Del Bel Cury AA (2010) *J Biomed Mater Res B Appl Biomater* 94:149
118. Mueller LN, De Brouwer JFC, Almeida JS, Stal LJ, Xavier JB (2006) *BMC Ecol* 6:1
119. Tait K, Williamson H, Atkinson S, Williams P, Cámara M, Joint I (2009) *Environ Microbiol* 11:1792
120. Stahmann KP, Revuelta JL, Seulberger H (2000) *Appl Microbiol Biotechnol* 53:509
121. Mitra S, Thawrani D, Banerjee P, Gachhui R, Mukherjee J (2012) *Appl Biochem Biotechnol* 166:1991
122. Dmytruk KV, Yatsyshyn VY, Sybirna NO, Fedorovych DV, Sibirny AA (2011) *Metab Eng* 13:82
123. Malm A, Chudzik B, Piersiak T, Gawron A (2010) *Ann Agric Environ Med* 17:115
124. Tal Y, Watts JEM, Schreier HJ (2006) *Appl Environ Microbiol* 72:2896
125. Van Rijn J, Tal Y, Schreier HJ (2006) *Aquac Eng* 34:364
126. Terada A, Zhou S, Hosomi M (2011) *Clean Technol Envir* 13:759
127. Jetten MSM, Wagner M, Fuerst J, Van Loosdrecht M, Kuenen G, Strous M (2001) *Curr Opin Biotechnol* 12:283



128. Mancini G, Cappello S, Yakimov MM, Polizzi A, Torregrossa M (2012) *Chem Eng Transac* 27:37
129. Fitch MW, Pearson N, Richards G, Burken JG (1998) *Water Environ Res* 70:495
130. Gharsallah N, Khannous L, Souissi N, Nasri M (2002) *J Chem Technol Biotechnol* 77:865
131. Zamora-Castro J, Paniagua-Michel J, Lezama-Cervantes C (2008) *Mar Biotechnol* 10:181
132. Stolz JF (2000) Structure of microbial mats and biofilms. In: Riding RE, Awramik SM (eds) *Microbial sediments*. Springer, Heidelberg, pp 1–8
133. Ebeling JM, Rishel KL, Sibrell PL (2005) *Aquac Eng* 33:235
134. Welander U, Mattiasson B (2003) *Water Res* 37:2394
135. Labelle MA, Juteau P, Jolicoeur M, Villemur R, Parent S, Comeau Y (2005) *Water Res* 39:3409
136. Tal Y, Watts JEM, Schreier SB, Sowers KR, Schreier HJ (2003) *Aquaculture* 215:187
137. Parent S, Morin A (2000) *Water Res* 34:1846
138. Labbé N, Juteau P, Parent S, Villemur R (2003) *Microb Ecol* 46:12
139. Auclair J, Parent S, Villemur R (2012) *Microb Ecol* 63:726
140. Kumar VJR, Joseph V, Vijai R, Philip R, Singh ISB (2011) *J Chem Technol Biotechnol* 86:790
141. Kumar VJR, Achuthan C, Manju NJ, Philip R, Singh ISB (2009) *J Ind Microbiol Biotechnol* 36:355
142. Kumar VJR, Joseph V, Philip R, Singh ISB (2010) *Water Sci Technol* 61:797
143. Mitra S, Pramanik A, Banerjee S, Haldar S, Gachhui R, Mukherjee J (2013) *Appl Environ Microbiol* 79:7922
144. Allen RM, Bennetto HP (1993) *Appl Biochem Biotechnol* 39–40:27
145. Lovley DR (2006) *Nat Rev Microbiol* 4:497
146. Erable B, Roncato MA, Achouak W, Bergel A (2009) *Environ Sci Technol* 43:3194
147. Rismani-Yazdi H, Carver SM, Christy AD, Tuovinen OH (2008) *J Power Sources* 180:683
148. Erable B, Vandecandelaere I, Faimali M, Delia ML, Etcheverry L, Vandamme P, Bergel A (2010) *Bioelectrochemistry* 78:51
149. Scotto V, Cintio RD, Marcerano G (1985) *Corros Sci* 25:185
150. Bergel A, Féron D, Mollica A (2005) *Electrochem Commun* 7:900
151. Dumas C, Mollica A, Féron D, Basséguy R, Etcheverry L, Bergel A (2007) *Electrochim Acta* 53:468
152. Dumas C, Mollica A, Féron D, Basséguy R, Etcheverry L, Bergel A (2008) *Bioresour Technol* 99:8887
153. Faimali M, Chelossi E, Garaventa F, Corrà C, Greco G, Mollica A (2008) *Electrochim Acta* 54:148
154. Avendaño-Herrera RE, Riquelme CE (2007) *Aquac Eng* 36:97
155. Allison DG, Gilbert P (1992) *Sci Prog* 76:305
156. Wetherbee R, Lind JL, Burke J, Quatrano RS (1998) *J Phycol* 34:9
157. Wahl M (1989) *Mar Ecol Prog Ser* 58:175
158. Avendaño RE, Riquelme CE (1999) *Aquac Res* 30:893
159. Avendaño-Herrera R, Riquelme C, Silva F, Avendañod M, Irgang R (2003) *J Shellfish Res* 22:393
160. Lebeau T, Robert JM (2003) *Appl Microbiol Biotechnol* 60:612
161. Silva-Aciaras FR, Riquelme CE (2008) *Aquac Eng* 38:26
162. Zhao B, Zhang S, Qian PY (2003) *Aquaculture* 220:883
163. Myklestad SM (1995) *Sci Total Environ* 165:155
164. Lancelot C (1983) *Mar Ecol Prog Ser* 12:115
165. Pisman TI, Galayda YV, Loginova NS (2005) *Adv Space Res* 35:1579
166. Kawamura T (1996) The role of benthic diatoms in the early life stages of the Japanese abalone (*Haliotis discus hannai*). In: Watanabe Y, Yamashita Y, Oozeki Y (eds) *Survival strategies in early life stages of marine resources*. A. A Balkema, Rotterdam, The Netherlands, pp 355–367
167. Cheng KC, Demirci A, Catchmark JM (2010) *Appl Microbiol Biotechnol* 87:445

168. Halan B, Buehler K, Schmid A (2012) *Trends Biotechnol* 30:453
169. Christenson LB, Sims RC (2012) *Biotechnol Bioeng* 109:1674
170. Rosche B, Li XZ, Hauer B, Schmid A, Buehler K (2009) *Trends Biotechnol* 27:636

# Novel Materials for Biofilm Reactors and their Characterization

**C. Müller-Renno, S. Buhl, N. Davoudi, J. C. Aurich, S. Ripperger, R. Ulber, K. Muffler and Ch. Ziegler**

**Abstract** The application of adherently growing microorganisms for biotechnological production processes is established, but it is still a niche technology with only a small economic impact. However, novel approaches are under development for new types of biofilm reactors. In this context, increasingly more microstructured metal surfaces are being investigated, and they show positive effects on the bacterial growth and the biofilm establishment. However, for comparison of the data, the different surface materials have to correspond in their different characteristics, such as wettability and chemical composition. Also, new materials, such as plastic composite supports, were developed. To understand the interaction between these new materials and the biofilm-producing microorganisms, different surface science methods have to be applied to reveal a detailed knowledge of the surface characteristics. In conclusion, microstructured surfaces show a high potential for enhanced biofilm growth, probably accompanied by an enhanced productivity of the microorganisms.

**Keywords** Biofilm reactor · Interaction · Interface · Reactor materials · Surface science methods

---

C. Müller-Renno (✉) · N. Davoudi · Ch. Ziegler

Department of Physics and Research Center OPTIMAS, University of Kaiserslautern,  
67663 Kaiserslautern, Germany  
e-mail: cmueller@physik.uni-kl.de

S. Buhl · S. Ripperger

Department of Mechanical and Process Engineering, University of Kaiserslautern,  
67663 Kaiserslautern, Germany

J. C. Aurich

Institute of Manufacturing Engineering and Production Management,  
University of Kaiserslautern, 67663 Kaiserslautern, Germany

R. Ulber · K. Muffler

Institute of Bioprocess Engineering, University of Kaiserslautern,  
67663 Kaiserslautern, Germany

## Contents

1	Introduction.....	208
2	Surfaces with Nano- and Microstructures .....	210
2.1	Examples of Surface Modifications .....	211
3	Characterization of the Surfaces.....	213
3.1	Characterization of the Surfaces: Topography .....	213
3.2	Characterization of the Surfaces: Physicochemical Properties (Surface Charge and Wettability) .....	216
3.3	Characterization of the Surfaces: Chemical Composition .....	218
4	Interaction with Biological Molecules/Organisms .....	219
5	Biological Modification of the Surface.....	226
6	Plastic Composite Supports.....	227
7	Conclusions.....	230
	References.....	231

## 1 Introduction

Biofilm reactors usually use surfaces such as steel, glass, polymers, and even beechen splints, which have a technological statistical roughness or structure. New ideas follow a concept of a modification of the structure on the nano- or micro-scale. Especially for animal cells but also for bacterial cells, effects in the interaction of the cell with surface structures in the size range of the cell are observed [1]. The goal is a cultivation of bacterial biofilms on these structures and to use biofilm as productive medium.

On the one hand, the novel materials should stably bind the bacteria to establish a biofilm; on the other hand, the detachment from the surface should be easy to reuse in the reactors. Thus, the development of novel materials for biofilm reactors requires a better understanding of cell–surface interactions under the influence of different parameters, such as the structure of the material.

Basically, any support used for biofilms must fulfill the following criteria: it should (a) favor adhesion of microorganisms, (b) feature a high mechanical resistance to liquid shear forces and particle collision, (c) be inexpensive, and (d) be widely available [2]. The adhesion is principally a function of surface charge, hydrophobicity, porosity, roughness, particle diameter, density, and time. To optimize the productivity of the system, the specific surface area inside the reactor system must be maximized, which is accomplished by variation of the dimension and shape of the support material. It will be shown in this chapter that such variations may either come from structuring the surface of more classical metal surfaces or by using new plastic composite supports. It can be assumed that further material systems will be introduced in the coming years.

The literature concerning interaction of biomolecules/organisms with surfaces shows that the chemical and physical surface properties are of high importance for

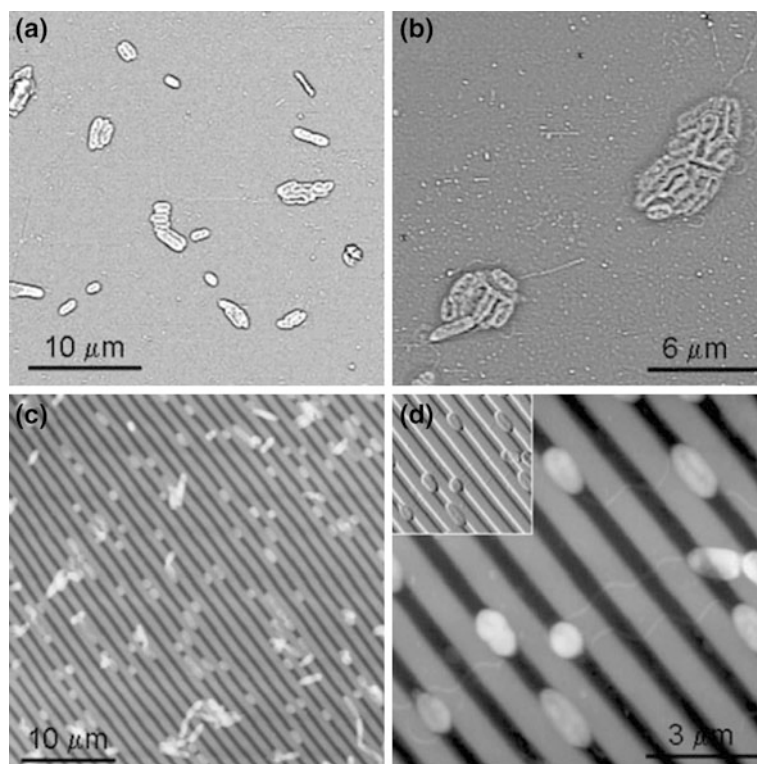


**Fig. 1** Scanning force microscopy images of bacteria on smooth (*top*) and structured (*bottom*) gold surfaces. The bacteria prefer to lie in line with the trenches, which are in the size range of the bacterial cell diameter. Reprinted with permission from [4]

the observed results. Thus, the knowledge of surface properties is crucial for the successful development of new materials, even in biotechnological areas. In addition to the physical and chemical properties, the structure of the surface seems to play a key role in the initial self-assembly of biological entities, such as bacterial cells [3, 4]. As an example, some self-assembled bacteria on a gold surface without and with regular trenches can be seen in Fig. 1. The bacteria seem to prefer the colonization of the trenches; in addition, the cells respond in similar ways to the same topography (see Fig. 1, from [4]). In addition, Diaz et al. investigated the influence of the chemistry of the surface on the bacterial adsorption (not shown here). They found that the topography prevails over the chemistry [5]. Figure 2 shows an additional example for the influence of structured and unstructured surfaces on the bacterial colonization. In this case, rods were produced and the bacteria accumulate in between the rods [6]. In general, it can be observed that the bacteria adsorb in both cases in line with the long side of the structures (see Figs. 1 and 2).

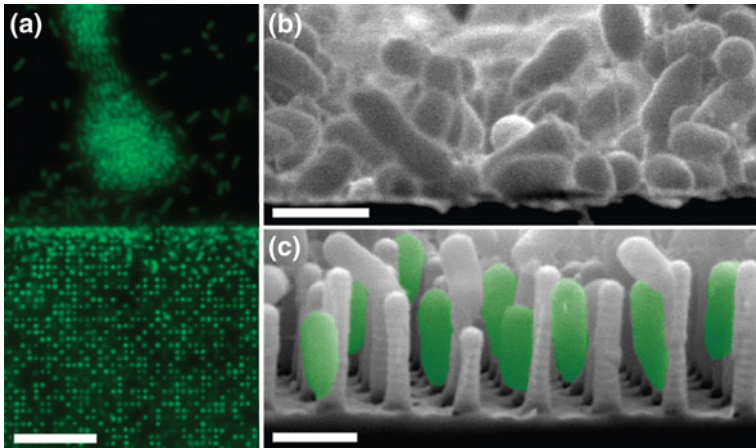


**Fig. 2** *P. aeruginosa* on structured and unstructured regions of the surface. (a) Fluorescence images show the differences on flat surfaces (*top*) compared to structured surfaces (*bottom*). (b, c) Cross-sectional scanning electron microscopy images on flat (*top*) and structured (*bottom*) samples. Reprinted with permission from [6]

The presented data show the importance and the effect of nano- and microstructures on the bacterial colonization of a sample and thus on biofilm formation. As mentioned, the chemical and physical properties of the surface play an important role. A key question is to understand the involved processes of bacterial cell surface interaction and its dependency on physical and chemical properties as well as the nanostructures on the surface to engineer customized novel materials for bioreactors. Here, we present methods for developing novel material surfaces by microstructuring, which is achieved by mechanical and physical means without changing the chemical composition of the surface. We discuss the properties of the different surfaces and present methods to characterize these novel materials concerning their physicochemical properties and their interactions with bacterial cells.

In addition to structured materials, plastic composite supports as novel polymeric composite materials are able to support the growth and the productivity of attached microorganisms. More about the properties and characteristics for biofilm reactors can be found later in this chapter.

## 2 Surfaces with Nano- and Microstructures

Microstructures can be created by many different methods (dip pen, e-beam, lift off, photolithography, etc.) [1]. Details about these methods can be found in the literature (e.g. [7]). The biggest problem by the use of these methods is a change of the surface chemistry (e.g. the chemical differences between the structures after a

photolithographic process) and thus the different behavior in the interaction with biological molecules. This makes it difficult to distinguish between the effect of the microstructure and that of the changed chemistry. Especially in the case of bio-reactors, steel and metals are potential materials that cannot be structured easily. The best experimental setup to investigate the influence of the structure is to have chemically identical surfaces. In our own studies, the attention lies on convex structures created by particles on the surface and concave structures (trenches) produced in a milling process, which have a similar surface composition to investigate the influence of the curvature on the cell interaction in detail. This seems to be interesting because for eukaryotic cells that adhered on top of a convex structure, it was assumed that the cell stretching enhances the cell attachment but the background of the effect is unknown yet [8].

## *2.1 Examples of Surface Modifications*

Convex structures with the same surface composition as titanium can be created by using titanium dioxide particles, for example, because titanium metal is always covered by titania. The results presented here were obtained by particles that are applied in a suspension made of 0.033 % by weight  $\text{TiO}_2$  (Degussa P25) and a continuous fraction consisting of distilled water and 10 % by weight hydrochloric acid (0.1 mol/l). Initial measurements gave the best results when  $100 \mu\text{l}/\text{cm}^2$  of this suspension were applied on a titanium surface and dried in an oven for 60 min at  $70^\circ\text{C}$ .

The particles can be immobilized by using a pulsed laser treatment. Therefore, the power density is adjusted by defocusing in order to receive an intensity of  $1.55 \cdot 10^{11} \text{ W}/\text{m}^2$  with a duration of 17 ns. This amount of energy causes the very top of the surface and a small part of the particle to melt.

The laser beam scans the surface line by line with an off-set ( $20 \mu\text{m}$ ) that is much smaller than the diameter of the beam ( $553.9 \mu\text{m}$ ). The pulse frequency (33 kHz) of the laser is adjusted to the speed of scanning (10 mm/s) in a way that the distance between two closely spaced center points of the laser beam is also much smaller than the diameter of the beam. These parameters ensure a continuous treatment of the whole surface. Particles treated this way have a sufficient adhesion to stand an ultrasonic cleaning procedure (Fig. 3). Several ultrasonic treatments do not cause a significant change to the results of a single treatment.

Particle modification of the surface to obtain micro- or nanostructures has the advantage of the flexibility of the particle surface chemistry and the very easy and cheap production process, in which structures down to the tenths of nanometer range can be produced.

A good way to manufacture concave structures is micromilling. Although milling usually generates structures in the range from millimeters to decimeters, current research has minimized tools and machines, so that by now structure sizes of  $10\text{--}50 \mu\text{m}$  have become feasible. The structures depicted in Fig. 4 were produced by

**Fig. 3** Scanning electron micrograph of TiO<sub>2</sub> particles on a titanium surface after ultrasonic treatment

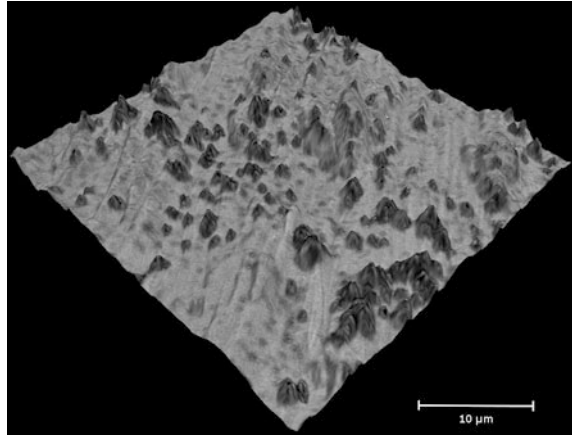
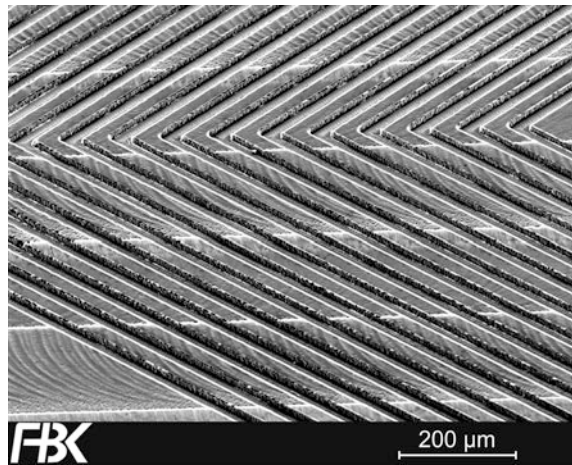


**Fig. 4** Scanning electron micrograph of a micromilled structure



micromilling. The rotating milling tool is moved along the surface with a certain depth of cut (typically between 1–20 μm) and infeed (around 5 mm/minute). The main advantages of micromilling when manufacturing microstructures are the high achievable aspect ratio, the flexibility in terms of tool and thus structure geometry, the large variety of materials that can be milled, and its applicability to low-volume production. Actually, such structures are not commercially available; in particular, the very small structure sizes need a lot of knowledge in the mechanical processing of the sample.

To investigate and later to forecast and optimize the interaction of bacterial cells with the surfaces for productive biofilms, a detailed characterization of the surfaces and investigation of their interaction with the bacterial cells is necessary. In the following section, several methods to characterize the surfaces and to investigate the biological interaction are described together with our own results.



### 3 Characterization of the Surfaces

A variety of methods are applicable and necessary to characterize surfaces on the micro- and nanoscale. Especially in the case of conductive surface materials, more methods are usable than on nonconductive surfaces. In the following sections, the possible methods and some obtained results are described, which can be distinguished between topographical measurements, methods that give the chemical composition, and general measurements of chemical or physical properties. The described methods will be scanning electron microscopy (SEM), scanning force microscopy (SFM), static contact angle measurements, zetapotential, and X-ray photoelectron spectroscopy (XPS), to name here a few. Especially the wettability (determined by the static contact angle) and the charge of the surface (determined by zetapotential) are essential to interpret the measured adhesion forces and the interaction between the bacteria and the surfaces. These properties are known to have a big influence and they can be taken into account to change and govern the interaction. In addition, it is necessary to guarantee absolute comparable surface properties concerning the chemical composition, which allows the comparison of the obtained data under the influence of different structured surfaces.

#### 3.1 *Characterization of the Surfaces: Topography*

The topography of a bioreactor material and thus the structure on the micro- or nanoscale is an outstanding factor that influences the interaction with bacteria and thus the biofilm formation. In this section, the topography analysis of the different surfaces with convex and concave structures as well as unstructured titanium is exemplified by the use of different methods. In addition, the stability of the particle structured surfaces is of enormous importance.

SFM, which was invented by Binnig, Quate, and Gerber in 1986 [9], is a useful tool to image a sample with a nanometer resolution. It can be used to visualize and analyze the micro- and nanostructures in detail in all three dimensions. SFM can be used in different modes, whose applicability depends on the research question. Hard samples, such as steel or titanium, can be easily imaged in the contact mode, whereas softer or sensitive samples can be imaged in dynamic mode. In contact mode, the sharp tip of a cantilever is in repulsive contact with the sample and the deflection of the cantilever is translated into a topographic image. In dynamic mode, the cantilever oscillates while the change of the amplitude during the oscillation is translated into the topographic information. The detailed working principles can be found elsewhere [7, 9]. Figure 5 shows images of untreated, particle-treated, and milled titanium. The images show dimension data in all three spatial directions. Therefore, the interesting dimensions of the surfaces can be measured, visualized, and compared. It can be seen that the preparation of concave and convex structures was successful.

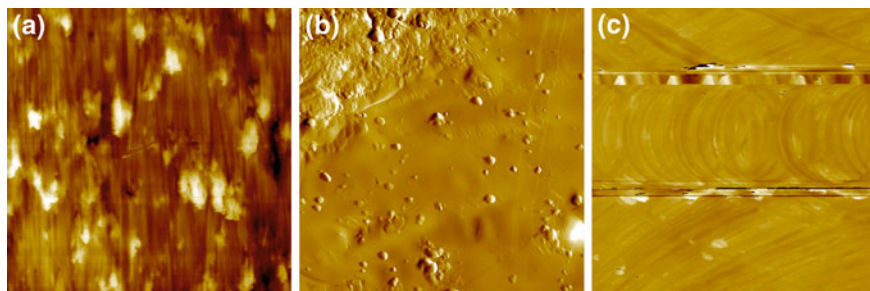


**Fig. 5** Scanning force microscopy images taken in contact mode of the different titanium structures: **a** 100- $\mu\text{m}$  height image of unstructured titanium with a z-range of 1.7  $\mu\text{m}$ . **b** 10  $\mu\text{m}$  (for better contrast) with particles on titanium and with a z-range of 513 nm in the corresponding height image. **c** 100- $\mu\text{m}$  image of micromilled titanium with a z-range of 8  $\mu\text{m}$

In the case of convex structures, titanium dioxide particles were immobilized on titanium dioxide by a laser melting process, like the one described above. This setup allows a nanostructure with the same surface chemistry over the whole surface (see XPS spectra in the following section). However, the particles have to adhere with such a force that they are not washed away (e.g. in a bioreactor). They have to stick harder than the bacteria particle interaction is. A good method to control the adherence of the particles, to characterize the tolerable shear forces, and to guarantee a stable coupling, even in the bioreactor, is the use of the lateral force microscope (LFM). In principle, there is no difference between the SFM and LFM. The LFM works also in contact mode; beside the SFM data, the lateral force data is recorded and visualized. In the LFM experiment, the hard cantilever is pushed with a defined force ( $F_z$ ) to the solid surface and is laterally moved over it. Thus, different lateral forces ( $F_L$ ) as a function of  $F_z$  are applied to the sample (the applied dwell force to the cantilever in  $z$  direction ( $F_z$ ) can be easily correlated with the applied shear forces ( $F_L$ ) by using the parallelogram of forces) and the obtained images with increasing  $F_L$  acting on the particle reveal the loss of the particles. The lateral force signal increases as long as the particle is connected; after loosening the particle, the lateral force signal stays at zero. Thus, the highest dwell force  $F_z$  that did not eliminate particles is representative for the maximum of the tolerable shear force.

The first LFM experiments were performed to characterize the strength of the bond between the particles and the surface. In these first experiments, we found that an increasing laser intensity correlates with an increased normal and thus lateral force to detach the particles, determined by lateral force microscopy (LFM). Figures 6 and 7 show vertical deflection images (SFM images for visualization) of the particles on the titanium taken during the LFM scan with a scanning force microscope. The particles in the two figures are melted with different power densities of the laser; thus, different applied forces were measured for lateral detachment of the particles. In each figure, the applied force increases from left to right. The lower power density of the laser needs a dwell force  $F_z$  of 400 nN,

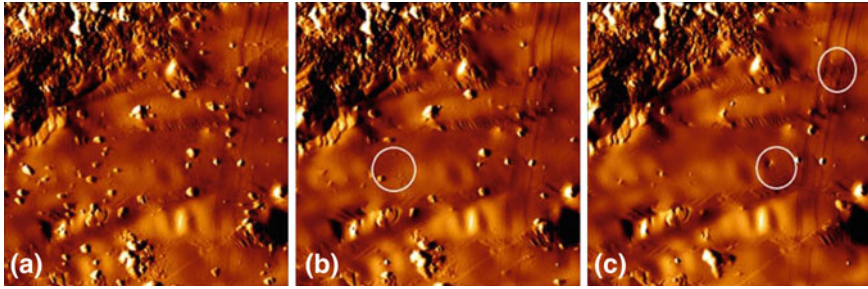


**Fig. 6** Scanning force microscopy deflection images,  $10 \times 10 \mu\text{m}^2$ : Increment of the dwell forces in  $z$ -direction from 200 nN (a), 400 nN (b) and finally to 800 nN (c) on the particles that are fixed to the surface with the lower power of the laser. The *white circles* indicate selected regions in which particles vanish between the subsequent images

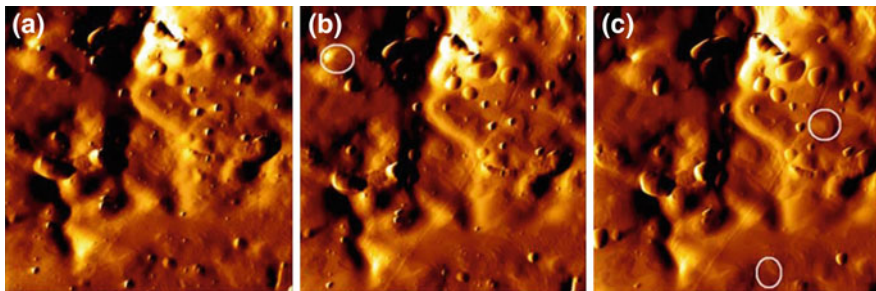


**Fig. 7** Scanning force microscopy deflection images,  $10 \times 10 \mu\text{m}^2$ : Increment of the dwell forces in  $z$ -direction from 214 nN (a), 769 nN (b) and finally to 2,500 nN (c) on the particles that are fixed to the surface with the higher power of the laser. The *white circles* indicate selected regions in which particles vanish between the subsequent images

whereas the higher power of the laser needs a force  $F_Z$  of 769 nN to loosen particles. By imaging and comparing the same region again and again, the areas that lost particles can be identified. At these positions, the lateral force signal suddenly stays zero when the particle is lost (not shown). Some regions with missed particles are marked with a white circle.

We can summarize that the higher the laser power, the more stable the particles are fixed. For the bacterial attachment and adhesion measurements, it is important to have particles that are more adhesive to the surface than the interaction between the bacteria and the particle. It is hard to generalize adhesion forces for bacteria surface interactions, but for a couple of *Escherichia coli* and some mineral surfaces, adhesion forces in the range of 20 nN were observed [10]. Thus, the particles would adhere strong enough to use them for a biofilm reactor.

However, the SFM allows imaging of only a small part (maximum  $100 \mu\text{m}$  scan size) of the sample. Therefore, additional measurements have to be done to control the quality of the structuring over larger surface parts. Another well-known

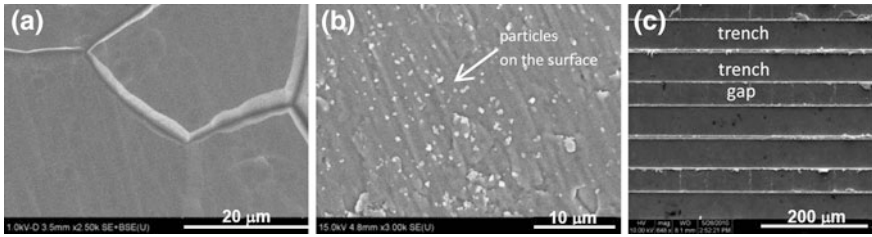


**Fig. 8** Scanning electron microscopy images of (a) unstructured titanium, (b) particle structured titanium, and (c) micromilled titanium. In the left, image cracks between the crystal boundaries visible due to the roll thread process can be seen. Especially in the right image burrs on the edge of the trenches can be seen

method to image surfaces or substrates is the scanning electron microscope (SEM). High-resolution images as well as images with smaller resolution can be obtained. Figure 8 shows some exemplary images of unstructured, micromilled, and particle-structured titanium. For the micromilled surfaces, the regularity of the surface structure can be easily seen. Concerning the particle structured titanium, the regularity of the particle distribution is acceptable for the used structuring method.

### 3.2 Characterization of the Surfaces: Physicochemical Properties (Surface Charge and Wettability)

The physico-chemical properties of a bioreactor are an outstanding factor that influences the interaction with bacteria and thus the biofilm formation. Important properties are the wettability as well as the surface charge. In this section, the properties of the different surfaces with convex and concave structures as well as unstructured titanium will be presented as an example by the use of different methods, such as static contact angle, zetapotential, and XPS. The static contact angle is a value to determine the wettability of a surface material and to distinguish between hydrophilic and hydrophobic characteristics. The value is determined by putting a water droplet onto the surface and measuring the angle between the solid surface and the tangent on the droplet (Fig. 9).

In a superhydrophilic surface, the droplet flattens and the angle is near zero. In a hydrophobic surface, the droplet takes a spherical shape to minimize the contact area with the solid (Fig. 10). The distinction between hydrophilic and hydrophobic surfaces follows different definitions. The classic definition by Young puts the border at  $90^\circ$  contact angle [11]. Lower angles are correlated with a hydrophilic surface. Especially for the case of biological molecules, Vogler et al. and Berg et al. assume an upper limit of  $65^\circ$  for a hydrophilic surface because the water network at the surface differs, which is especially important for biological interactions [12–14].

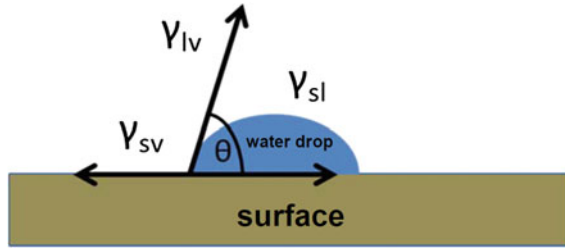


**Fig. 9** A water droplet on the surface together with the involved surface tensions ( $\gamma_{lv}$  liquid–vapor,  $\gamma_{sv}$  solid–vapor,  $\gamma_{sl}$  solid–liquid) which influence the contact angle  $\theta$

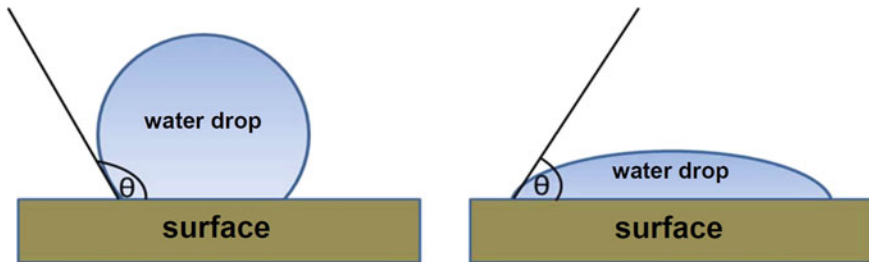


**Fig. 10** A droplet on a hydrophobic surface (*left*) and a hydrophilic surface (*right*)

An additional important point is the difference in wettability caused by surface topography. One well-known example is the lotus effect. The microstructures or nanostructures on the sample increases the contact area with air and thus the contact angle is increased [15–17]. Two different models describe the influence of micro- and nanostructures on the wettability: Wenzel and Cassie-Baxter [18, 19]. Wenzel predicts that the fluid fills the structures completely, whereas Cassie-Baxter assumes that the droplet sits on top of the structures, which are filled with air. The structure size determines which model describes the situation. The model of Cassie-Baxter explains the lotus effect. Thus, for productive biofilms, the structure size is highly significant to wet the trenches in the sample to enable bacterial growth in the grooves.

The influence of the surface wettability on the interaction with biological molecules is well known [20–23]. In particular, hydrophobic surfaces are known to enhance the interaction through the so-called hydrophobic effect, in which large molecular folding processes can occur. Hydrophobic surfaces thus often lead to protein denaturation. As a rule of thumb, hydrophobicity (of the material surfaces) was identified by many researchers as a remarkable process parameter supporting the adhesion of cells (e.g. [24, 25]). However, contrary observations are reported, in which hydrophilic bacteria were efficiently attached by hydrophilic surfaces rather than hydrophobic ones (e.g. [26]). Besides the direct interference of the surface hydrophobicity and the hydrophobicity of the microorganism, other effects

may superimpose such physical parameters and affect attachment and growth of the organism.

Protein adhesion does not only depend on the wettability but also on the surface charge. Mueller et al. and Hartvig et al. investigated this influence and found tremendous influence by electrostatic forces [20, 27]. The surface charge can be estimated by the zeta potential, which describes the charge at the fluid solid interface and is an indicator for the surface chemistry and for adsorption processes on solid surfaces. The reasons for a surface charge are different: Functional groups on surfaces show different protonation states at different pH values. On chemically inert surfaces, such as polytetrafluoroethylene, the dissociation of water molecules at different pH values is the reason for a charge at the surface. Thus, the surface charge is an essential factor in the biomolecule interaction to understand the influence of electrostatic interactions. As a function of pH, the measurement delivers the isoelectric point of the sample. At the pH value of the isoelectric point (IEP), the net charge of the surface is zero. pH values higher than the IEP show a negative charge on the surface, whereas pH values lower than the IEP show a positive charge. For commercially pure titanium, values in the range between pH 4.5 and 5 are found for the IEP, whereas unstructured titanium shows an IEP at pH 4.60 and structured titanium (50- $\mu\text{m}$  trench, 250- $\mu\text{m}$  gap between the trenches) at pH 4.57. Thus, no influence can be seen and the chemistry of the surface can be assumed to be similar.

### ***3.3 Characterization of the Surfaces: Chemical Composition***

As mentioned in the introduction and also discussed in the literature [3, 4], the chemical composition of a surface influences biological and bacterial interactions. The influence of micro- and nanostructures on the interaction with biomolecules can be investigated if the chemical and physical properties of the samples are well comparable and the topography is the only variable that is modified. A method to determine the chemical composition is XPS. Photo-electrons are emitted from a sample after bombardment with a beam of x-rays. The obtained spectra allow the determination of the elemental composition and the element's oxidation state of material surfaces. In the case of micromilled and particle structured surfaces compared to native titanium (unstructured), only small differences in the chemical composition were measured (Fig. 11). In particular, the micromilled sample shows some more contaminations, which can be seen in the increased carbon peak.

Another method to investigate the chemical composition of a surface is time-of-flight secondary ion mass spectrometry (SIMS). The specimen is bombarded with a focused primary ion beam, which ejects secondary ions from the surface. The mass/charge ratios of these ions are measured with a mass spectrometer to determine the molecular composition of the surface to a depth of 1–2 nm, the technique is very sensitive. With the use of standards, SIMS can be a quantitation method.

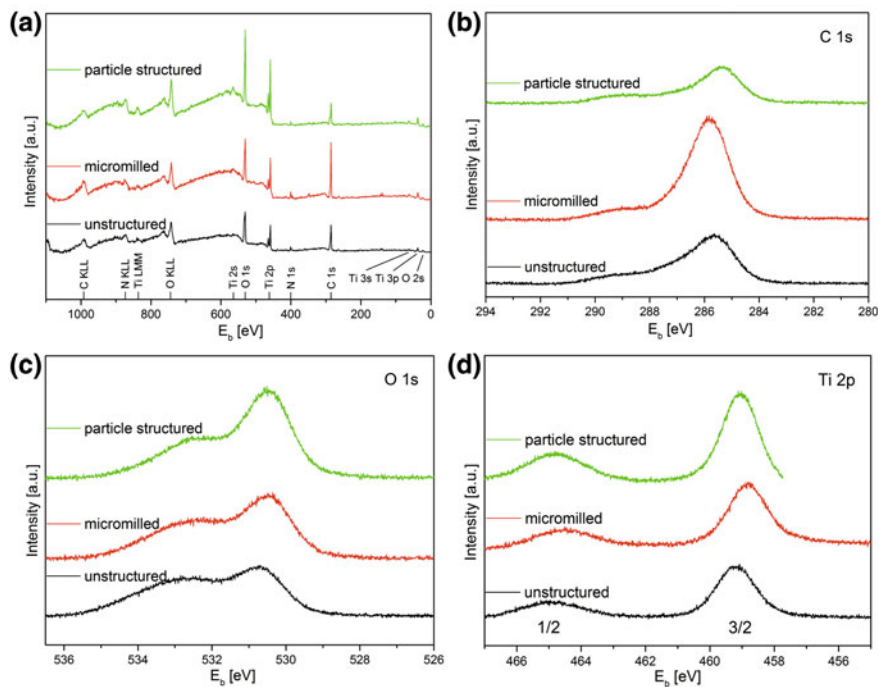


**Fig. 11** X-ray photoelectron spectroscopy survey of Mg  $K_{\alpha}$  photoelectron spectra of unstructured titanium, micromilled titanium, and particle structured titanium (a), carbon peak showing hydrocarbons and carbonates as contamination (b), oxygen peak with oxide peak (from  $\text{TiO}_2$ ) and hydroxide (c), and Ti peak showing only  $\text{TiO}_2$  within the information depth of around 10 nm (d)

## 4 Interaction with Biological Molecules/Organisms

So far, only a few studies have concentrated on the influence of structured surfaces on bacterial adhesion and biofilm formation. Thus, the involved processes are not understood in detail. However, the behavior of bacteria on structured surfaces is essential for the design of novel materials and to find a correlation between surface morphology, surface properties, and biological response. In general, it is hard to generalize results obtained during investigations of solely a few types of bacteria because different results can be found for gram-positive and gram-negative bacteria, for example. Thus, it is important to measure the interaction of biological molecules or organisms with structured surfaces on the micro- or nanoscale. In this section, the methods to measure the interactions between bacteria and surfaces and some general results are discussed.

The interaction of cells with surfaces can be studied either directly by imaging the process, indirectly by analyzing the functions generated in cells upon adsorption, or by measuring the adhesion forces between one single cell and the

surface. The main focus is on SFM and scanning force spectroscopy, accompanied by SEM and fluorescence microscopy. The scanning force microscope (SFM) makes it possible to image bacterial cells and biofilms on the structured surface with a nanometer resolution. A general overview on the application of SFM on bacterial cells can be found in Ref. [28]. The measurement can be done in air as well as in a medium such as water or buffer; thus, the SFM can deliver results that are representative of the natural environment (or in the case of a bioreactor, the technical environment).

Besides the well-known contact and intermittent mode of the SFM, new developments allow more detailed insights into the cell–surface interaction or the properties of the adhered cell. Quantitative mapping modes, for example, use force–distance curves to analyze and visualize physical properties of the sample. It is possible to image the elastic modulus as well as the adhesion dispersion of the cantilever on the sample, to name only a few [29, 30], and to investigate the influence of structures on the surface to these properties of the cell. The theoretical background of force–distance curves can be found in Ref. [31] and some exemplary images can be seen in Ref. [28].

The most important point that has to be considered is the preparation of the sample. It is essential to immobilize or to fix the cells on the sample, especially in the case of a biofilm to be imaged in a liquid phase. However, a pretreatment of the surface comes not into consideration if the influence of a structure should be investigated, because the pretreatment can influence the bacterial colonization of the sample. Our own measurements indicate that the subsequent crosslinking of amino groups in a grown biofilm by using glutaraldehyde (crosslinking of the bacteria) delivered applicable measurement conditions, but formalin, paraformaldehyde, or methanol/acetone (1:1) can also be used [32].

In contrast to the usual SFM modes, quantitative mapping modes can be used without any fixation or treatment of the sample. They apply no lateral force to the samples due to their operating principle, which works on the basis of force–distance curves. Figure 12 shows an example for bacteria adsorbed to an unstructured titanium surface and imaged by SFM afterwards. The image shows the height, elasticity, and adhesion of the sample. It can be seen that the bacteria are much softer than the surrounding areas. Within the collaborative research center SFB 926, *Paracoccus seriniphilus* was chosen as the model organism and is shown in the following figures.

Another application of force–distance curve based imaging modes is the use of functionalized cantilevers for molecular recognition measurements. The cantilevers can be functionalized with a variety of different molecules, such as antibodies, and the specific recognition events between the functionalization, and the receptors on the cell can be measured and visualized as an increased adhesion force [30, 33, 34]. The use of hydrophobically or hydrophilically functionalized tips allows the determination between hydrophobic and hydrophilic cell parts [35]. Different research groups published a variety of useful strategies of cantilever functionalization techniques, but additional approaches can also be found in other



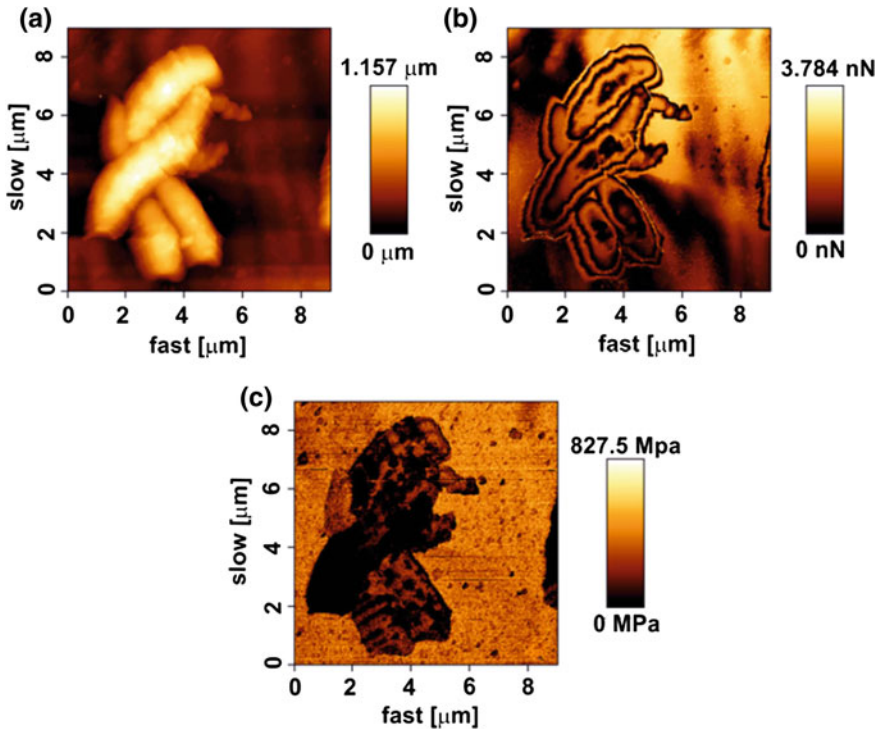


**Fig. 12** Physical properties of *Paracoccus seriniphilus* on titanium taken with scanning force microscopy in QI<sup>TM</sup> mode. Topography (a), adhesion (b), and elasticity (c). The elasticity image shows the differences in softness between the cells and the surrounding area. The adhesion differs as a function of the position on the bacteria. Reprinted with permission from [28]

papers [34, 36, 37]. Some additional recommended references for the application of the SFM on cells are Refs. [38–40].

Besides morphology imaging or interaction measurements between tip and sample, the SFM can also be used to determine the interaction between a cell and a solid support or a biofilm. Force–distance curves are taken with a tip, on which one or several cells are immobilized. In the case of a single cell, the mode is called single- cell force spectroscopy (SCFS). This mode is described in detail in Refs. [33, 41]. Adhesion forces of single or multiple cells up to the piconewton regime can be measured. The cell can be fixed on the cantilever by different possibilities:

- Electrostatic coupling
- Covalent coupling.

The functionalized cantilever is brought into contact with the cell of interest using an optical microscope with which the cell and the cantilever can be observed. The cantilever is gently pushed to the cell for a time range of a few

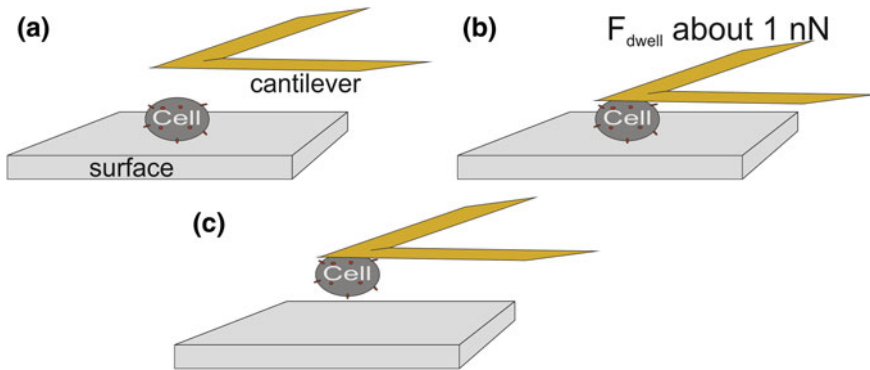


**Fig. 13** Preparation of the cell probe (a). The functionalized cantilever is positioned above a single cell and brought into contact with it with a gentle dwell force (about 1 nN) for several minutes (b). The cantilever together with the cell is withdrawn from the surface and force–distance curves for adhesion measurements can be performed (c). Reprinted with permission from [28]

minutes to establish the coupling of the cell. For example, on unstructured titanium, the cell surface binding is already finished within about 1 min. Afterwards, the cantilever is retracted and typical force–distance curves to determine the adhesion force of the cell can be performed as a function of different parameters, such as the size of the surface structures. Figure 13 shows the binding process systematically and Fig. 14 shows an exemplary measurement.

The importance of the chosen cantilever geometry has to be highlighted. The cantilever geometry influences the results by the correlation between the number of interacting bacteria and the measured force. Tipless cantilevers as well as cantilevers with a sphere, a sharp pyramidal tip, or plateau tips can be used; tipless cantilever are typically used, however. For all described cantilever types, a correction of the measured forces by the number of interacting cells may be necessary because more than one bacterium can be bound to the contact area. Beside the cantilever geometry, the glue or the chemical functionalization to bind the bacteria is essential. On the one hand, the bacteria must be attached to the cantilever by a force that is higher than the force between cell and surface. On the other hand, the cell should stay alive and the properties of the cell should not be changed. Different binding protocols, including covalent binding as well as electrostatic interactions for the cells, can be found elsewhere [42–47]. In the case of bacteria, concanavalin A can be used for establishing covalent bonds. Some important points which have to be considered performing SCFS and a type of handout can be found in Ref. [28].

Finally, the adhesion forces of the cells can be measured as a function of different parameters such as the contact time between cell and surface or the surface structures on the nano- or microscale. Within some seconds or minutes, the adhesion force increases by increasing the contact times followed by a steady state. The slope of the increase as well as the absolute value in the steady state depends

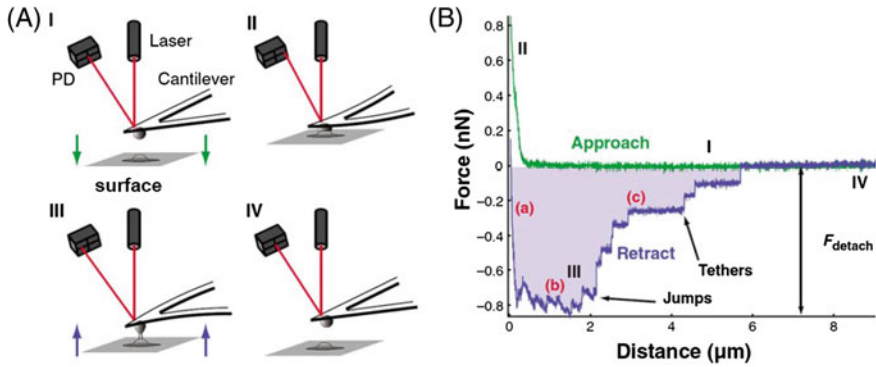
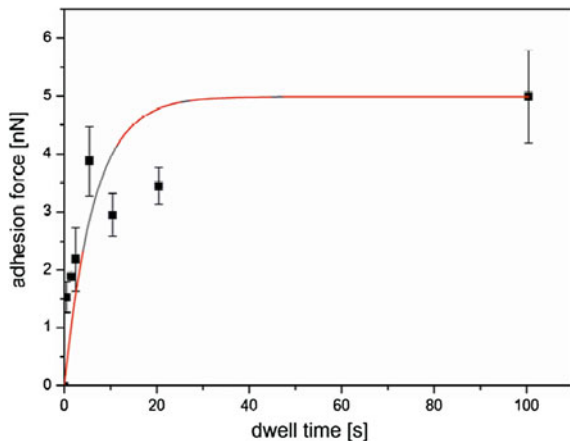


**Fig. 14** Outline of the typical single cell force spectroscopy experiment (A) together with a typical force–distance curve (B). The cell is pushed to the surface for a defined time-period with a user-specified dwell force (A, I and II). After that, the cell is retracted from the surface (A, III and IV), and the force–distance curve (B) that contains the cell adhesion information is recorded.  $F_{detach}$  denotes the maximum adhesion force and is composed of different cell-surface detachments ((a) to (c)). In addition, the area between the approach and retract gives the work of cell detachment. Reproduced with permission of Journal of Cell Science [41]

**Fig. 15** Mean adhesion force of a single *Paracoccus seriniphilus* cell as a function of contact time on unstructured titanium as reference. The typical increase of the adhesion force with a steady state afterwards can clearly be seen



on the cell type properties and the surface [48]. Such a behavior was also found for the marine bacterium *P. seriniphilus* (Fig. 15). During the first seconds of contact, the adhesion bonds have to be established and the first contact with the surface can be optimized.

The measurements on structured titanium are still ongoing. In general, the literature does not describe a lot of adhesion force measurements of bacteria on structured surfaces. In most cases, qualitative methods, such as imaging by SFM or optical microscopy, are used to determine differences in the cell–surface interaction. Verran et al. describes some investigations on differently grooved titanium [49]. The samples were prepared by the use of physical vapor deposition of

titanium on a prestructured sample with differently sized grooves. Thus, the samples are also chemically comparable. However, instead of typical force–distance curves, lateral detachment forces by scanning with different perpendicular dwell forces were measured.

Analogous to the measurements shown above, to determine the lateral detachment force of the titanium particles after laser treatment, the applied perpendicular force can be correlated with different lateral shear forces. Thus, the forces measured by Verran et al. give a trend for the correlation between the structure size and the bacterial adhesion to the surface. They observed different behavior on grooved titanium (width about 600 nm and 1  $\mu\text{m}$ , depth about 200 nm) for two different bacteria types (*E. coli* and *Staphylococcus sciuri*). No lateral force was needed to detach *E. coli*; only rinsing with water was necessary. However, *S. sciuri* shows a different removal behavior varying with the underlying topography. The highest force had to be applied on structures comparable to the cell size (about 1  $\mu\text{m}$ ) and the least for the smaller geometries. Some additional results for shear forces to detach different bacteria types can be found in Ref. [50].

The use of SCFS combined with other methods will clarify whether the increase of adhesion force is a result of the increased contact area between the cell and the surface due to the groove or whether the adhesion force of the bacterium is actually affected. In addition, the individual behavior of the different bacteria has to be pointed out. As a function of the experimental parameters, different force ranges were measured by Verran et al. [49]. Due to the huge variety of different bacteria, it is not possible to generalize the results because the microorganisms differ, for example, in structure, membrane composition, and protein composition. However, sometimes it may be possible to declare a trend for one group of bacteria, such as gram-positive bacteria.

Besides SFM, SEM is also used to analyze biofilms grown on surfaces. Especially in the last decade, the possibilities for investigating nonconductive samples advanced. However, SEM usually works in a vacuum, and its influence on a biological sample is not yet clear. Thus, the results have to be considered carefully. Better results could be obtained by using an environmental scanning electron microscope (ESEM). Figure 16 shows some SEM images of a few-days-old biofilm of *P. seriniphilus* on unstructured titanium. The bacteria seem to be collapsed, probably due to the vacuum, but it can also be seen that some single bacteria formed a chain within the biofilm.

SEM is also an indirect method; thus, only the number of adherent bacteria can be determined. However, the number of adherent bacteria can also be analyzed by the use of normal optical/fluorescence microscopy, but with much lower resolution. The use of optical and fluorescence microscopy is described in more detail below.

Optical microscopy approaches are mostly used for studying the number, orientation, and physiological state of bacteria that are in contact with surfaces. It is important to observe the bacteria in aqueous media to avoid alteration of physiology. Indeed, drying the samples can change the bacterial orientation and the cell shape, and they can die. Fluorescence staining gives more insight into the

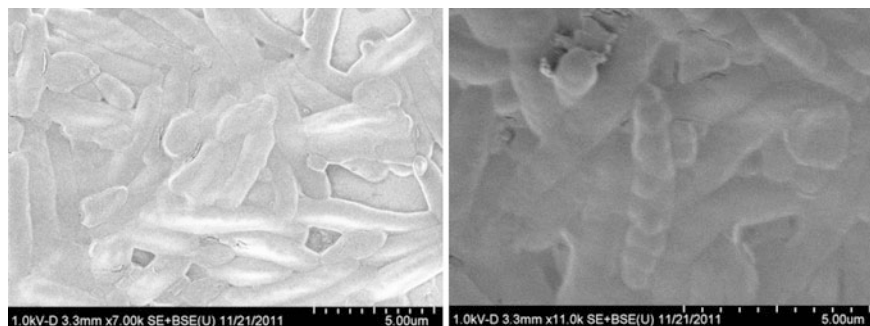


**Fig. 16** Scanning electron microscopy images of a few-days-old biofilm of *Paracoccus seriniphilus* on titanium cultivated in minimal medium

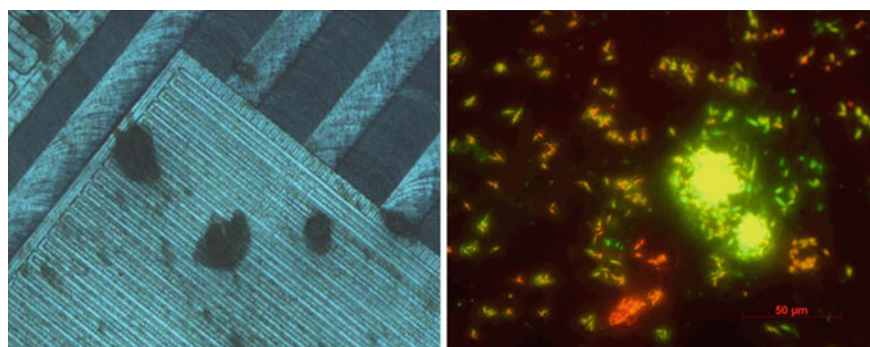


**Fig. 17** Optical microscopy (*left*) of *Paracoccus seriniphilus* in micromilled structures in titanium. The black spots show bacterial biofilm. Fluorescence microscopy (*right*) after live dead staining of a *Paracoccus seriniphilus* biofilm on unstructured titanium

biofilm properties. Biologists have developed antibodies and fluorescence dyes, which allow one to detect the present molecules or to distinguish between living and dead bacteria. Figure 17 (*left*) shows an optical image of *P. seriniphilus* biofilms on a structured titanium sample and a fluorescence live dead staining on unstructured titanium. Both samples were incubated in a shaking flask with a predetermined shaking speed over several days.

Scheuermann et al. showed that the orientation of the grooves relative to the bacterial flow direction in a dynamic experimental approach influences the bacterial surface colonization [51]. They observed significant differences in the number of attached bacteria to the downstream and upstream parts of the tops of the grooves, probably because of the different initial contacts between the bacteria and the surface due to the different flows at the structures. Therefore, an influence of the orientation of grooves perpendicular or in line with the flow is conceivable, just like the influence of dynamic and static experimental approaches. The key finding was that grooves perpendicular to the flow direction resulted in a

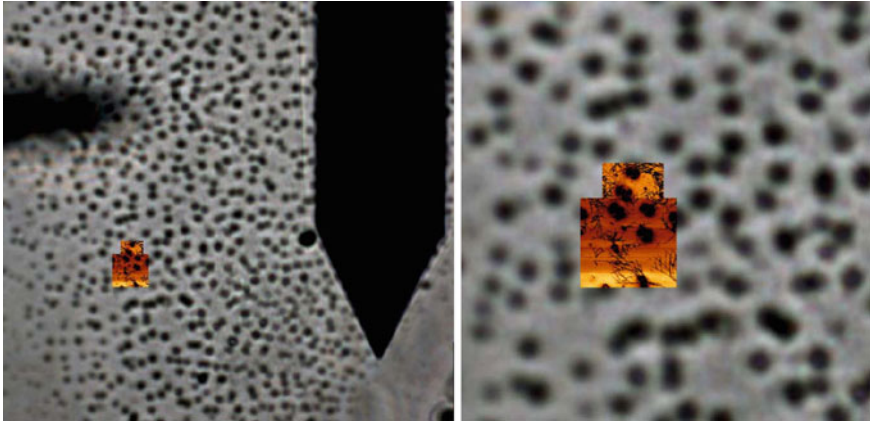


**Fig. 18** The combination of optical microscopy and scanning force microscopy (SFM) on an inverted optical microscope allows one to choose the area of interest for SFM imaging in the optical image. Later, the SFM images can be presented space-resolved in the optical image. Here, *Paracoccus seriniphilus* bacteria (adhesion images taken in QI<sup>TM</sup> mode) fixed on aminopropyl-trimethoxysilane on a glass coverslip are shown. Even some filamentous structures between the bacteria can be seen. An overlay of fluorescence and SFM images can be done in the same way. Reprinted with permission from [28]

preferential attachment of the bacteria to the downstream edges. Xu et al. observed a reduction in bacterial adhesion (*Staphylococci*) and biofilm formation on a surface structured on the submicron scale by determination of the adsorbed cell numbers with optical microscopy [52].

An expansion of the method can be achieved by a combination with SFM. It is possible to calibrate the optical microscope and the SFM against each other. In the optical image, interesting areas can be chosen and subsequently be imaged with the SFM with nanometer resolution. For example, living and dead bacteria can be imaged to determine differences in their elastic behavior. Even fluorescence microscopy can be combined in a special way with the SFM to investigate non-transparent samples. Figure 18 shows a combination of common optical microscopy with the described quantitative mapping mode on an inverted optical microscopy. Due to the previous combined calibration of the systems, the SFM images can be overlaid with the optical images. Other exemplary images can also be found in Ref. [53]. Further information concerning the future applications of the SFM in biology can be found in Ref. [54].

## 5 Biological Modification of the Surface

Within the biofilm formation, it is also interesting to investigate the interaction between a preadsorbed biofilm or cell and further adsorbing bacteria. Especially in the investigation under dynamic conditions, shear forces acting on the adsorbing

bacteria can be interesting and thus be influenced by underlying structures on the surface. Currently, the optimal tool for such measurements is the scanning force microscope. Although all the imaging techniques fail by distinguishing the preadsorbed and the subsequently adsorbed bacteria, single cell force spectroscopy allows the direct measurement of involved forces perpendicular to the surface. A preadsorbed layer of biomolecules or organisms on top of the substratum usually reduces the adhesion forces for further adsorptions, which was investigated with the example of bovine serum albumin as passivating layer [55]. Using the already described method to bind a single cell to the cantilever, the adhesion forces of a cell on the established biofilm or even on the regions covered with extracellular polymeric substances can be measured. More details about the measurement procedure for the example of eukaryotic cells can be found elsewhere (e.g. [56]). It is also possible to image the biofilm by using fluorescence microscopy, as described above; to navigate within the optical image to interesting points, such as a dead or a living cell or the extrapolymeric substances; and to perform SCFS measurements at the regions of interest. Thus, it is possible to navigate directly to a groove or a trench in the underlying surface and to compare the influence of the structure on the adhesion forces of further cell or biofilm layers.

Another possibility on an established biofilm is to use a modified cantilever (see the section on single cell force spectroscopy) to select and pick a cell from the biofilm. Afterwards, the adhesion force of this cell can be compared with cells grown in suspension in the shaking flasks. Herewith the influence of the biofilm community and the different growing parameters can be characterized.

For the described research questions and the applications discussed in these last paragraphs, no specific results or data can be found in the literature yet. Thus, a lot of work and statistics have to be done to get an overview. In addition, it has to be mentioned again that the variety of bacterial species, their properties, and the associated problems have to be characterized to generalize or to forecast their interaction with a surface. However, perhaps a trend can be seen for one group of bacteria (e.g., gram-negative and gram-positive bacteria).

## 6 Plastic Composite Supports

As discussed before, attachment of microorganisms is a function of the surface as well as the physical process parameters. In this section, novel polymeric composite materials are discussed, which are able to support additionally the growth and productivity of attached microorganisms.

Besides the direct interference of the surface hydrophobicity and the hydrophobicity of the microorganism as described above, other effects may superimpose such physical parameters and affect attachment and growth of the organism. In this context, Ho et al. reported that leaching of nutrients may compensate for the hydrophobic nature of solid plastic supports, resulting in an increased biofilm on more hydrophobic support materials [57]. Leaching occurs from any plastic

material and may affect the biological systems that are exposed to the artificial material. In particular, leaching is a tremendous problem within the application of single-use (disposable) bioreactor systems for production of pharmaceuticals, because the migrating compounds may stimulate or inhibit the productivity of the applied cells or reduce the product quality. Therefore, an accumulation of such unwanted migrating compounds must be prevented.

Although leaching is a challenging task within the pharmaceutical field, it can be turned into a beneficial process for the cultivation of biofilms. If the released compounds can be used by the adherently growing microorganisms as nutrient source, growth is stimulated. An interesting approach was developed at Iowa State University (U.S. Patent Number: 5,595,893). They established the so-called plastic composite support (PCS), which is an extrusion product of the polymer polypropylene and agricultural products. The PCS material is based on agricultural products, such as oat hulls, soybean hulls, yeast extract, soybean flour, dried bovine erythrocytes, bovine albumin, and/or mineral salts and was applied initially as chips supporting an improved lactic acid production by pure and mixed culture continuous fermentation [58]. Within repeated-batch fermentation processes, biofilms of pure and mixed-cultures on such chips were successfully applied for more than two months of lactic acid production [59]. The use of chips may result in medium channeling and clumping of cells, thus mixing, pH control, and productivity are (negatively) affected. Therefore, the plastic composite manufacturing process was modified to obtain a continuous material featuring a tube-shaped geometry, which provided a central large hole and allowed the convective transport of nutrients [57]. After the mixing of polypropylene and the additional agricultural compounds, they were extruded for example with a twin crew co-rotating Brabender PL2000 extruder at a rate of 11 rpm (barrel temperature: 200 °C, die temperature: 167 °C) to form a continuous tube, whereas the tubes feature a wall thickness of 3.5 mm and an outer diameter of 10.5 mm [2]. A subsequent modification of the material is realized by cutting of the tubes, whereas longer tubes of approximately 10 cm in length can be used as biofilm support material on an agitator shaft; smaller pieces can be used as rings or disks in a shaking flask or as packing material in fixed-bed bioreactors.

The blending of polypropylene can be customized to the relevant strain; thus, adhesion and growth are maximized. The most important variables that can be addressed via alteration of the PCS composition are the hydrophobicity and surface roughness/porosity. However, only the effects of the ingredients on the hydrophobicity have been quantified. The findings were in accordance with the conclusions of van Loosdrecht et al., who have shown that hydrophobic bacteria adhered more readily to hydrophobic surfaces than hydrophilic bacteria [60]. A comparison of commonly applied PCS blendings and its effects on the hydrophobicity are presented in Table 1. The contact angles of the PCS and polypropylene discs ranged from 88–112°; thus, all supports feature a hydrophobic character. Moreover, interfering effects of the ingredients were observed. For instance, Ho et al. reported an interfering effect of yeast extract and bovine dried red blood cells, whereas the hydrophilic nature of the yeast extract is masked by



**Table 1** Effects of different plastic composite support blendings on the hydrophobic/hydrophilic characteristics of the composite material (according to [26])

PCS ingredient	Effect on contact angle
Hull (soybean)	↓
Hull (oat)	↑
Soybean flour	↓
Yeast extract	↓
Dried bovine red blood cells	↑
Dried bovine albumin	↑
Mineral salts	↓

the hydrophobic characteristics of the blood cells. Addition of mineral salts may overcome the hydrophobic effect resulting from the blood cells [26].

As mentioned, the hydrophobic and hydrophilic effects may be overcome by nutrient release. In this case, the adhesion of the selected microbial strain cannot be predicted by only considering the contact angles of the strain and the support. Yeast extract features a high leaching rate; therefore it is not suitable for long-term fermentation processes if used as a single blending. However, compounds such as dried bovine red blood cells, dried bovine albumin, and soybean flour provide a gradual release of nitrogenous compounds from the PCS. Thus, Ho et al. concluded that PCS with soybean hulls, yeast extract, soybean flour, dried bovine albumin, and/or dried bovine red blood cells are well-suited to perform a slow release of nutrients from the carrier material [58].

Another major aspect (besides hydrophobicity and nutrient release) that accounts for cell adhesion is surface morphology. By blending the PCS with hulls, a network of grooves, ridges, and pits is provided. This morphology provides a higher surface area than the nonblended material; furthermore, the generated network shelters the attached microorganisms from hydraulic shear forces [26].

Blending of the PCS with compounds that explicitly stimulate attachment of microbial strains, growth, and productivity such as signaling molecules (i.e. molecules supporting cell–cell-communication) may push the PCS approach and facilitate novel production procedures. To the best of our knowledge, no relevant modified composite support blended with the corresponding signal molecules is currently available. For instance, an integration of acylated homoserine lactones could be used to improve the performance of gram-negative strains, whereas blending of the PCS with oligopeptides may be beneficial concerning the cultivation of gram-positive microorganisms. However, it could be necessary that the manufacturing process of the composite support has to be adapted to avoid degradation of the signaling molecules.

The so-called PCS materials use polypropylene as a matrix compound (commonly 50 % [wt/wt]), but in principle other polymers could be also used as the plastic component of the PCS. Polypropylene features a high contact angle of  $83^\circ \pm 2.5^\circ$  (water) [24]; thus, attachment of cells is supported according to the concept of hydrophobicity as mentioned above. However, less hydrophobic matrix compounds, such as polyethylene, polyurethane, polyvinyl chloride, or polymethyl methacrylate, may provide a material with decreased hydrophobicity. Because the

release of nutrients from the composite material must also be taken into account, these materials may exhibit a more sophisticated release pattern, which might be beneficial for cultivation of several microbial strains.

Because surface roughness can play a dominant role (e.g. [61]) within the attachment of cells, it is necessary to evaluate composite or pure plastic materials with almost similar roughness parameters. However, if the roughness of the plastic material should be modified, some methods are available to change the surface characteristics. Mechanical treatments (e.g. grinding, sand blasting, milling) and optical procedures (e.g. laser ablation) can be applied to increase the surface roughness within a post-manufacturing step. If the plastic material is processed as a foam, the roughness can be gently increased up to the desired grade during the manufacturing process. Some examples of the manufacturing processes of valuable compounds are presented by Muffler et al. within this issue of *Advances in Biochemical Engineering/Biotechnology*. Furthermore, other materials that were successfully applied as biofilm support, such as charged organic adsorber materials or inorganic compounds made from glass, steel, or ceramics, were introduced.

## 7 Conclusions

The presented examples show the importance of the surface or material in a bioreactor and the potential of structured metals and plastic composite surfaces for productive biofilms. It was shown that the presented structuring methods produce chemical and physicochemical comparable surfaces to investigate the influence of the structure type and size on the biofilm growth, the bacterial interaction, and thus the productivity of the biofilm. By structuring metal surfaces, the bacterial adsorption and adhesion can be largely enhanced, especially against shear forces, which are of great importance in a dynamic system like a bioreactor. The reason is that the commonly used methods for the structuring of surfaces are accompanied with a chemical alteration of the surface. It is therefore required to generate more data with chemically comparable surfaces and moreover the combination of different analyzing methods must be further developed. More data under the influence of the structure type and size can be collected now to see the detailed influence and to find the advantageous structure type and size for biofilm reactors. Furthermore, plastic composite surfaces are able to support the growth and the productivity of attached microorganisms. Thus, it could be a benefit to combine plastic composite surfaces with the methods used for microstructuring to enhance the biofilm growth.

In summary, the new structures will allow a customized cultivation of biofilms. Thus, an alternate product spectrum of the biofilm might be obtained—a feature that may lead to novel production processes in biotechnology.

**Acknowledgments** We acknowledge the financial support from the Deutsche Forschungsgemeinschaft (SFB926).

## References

1. Anselme K et al (2010) The interaction of cells and bacteria with surfaces structured at the nanometer scale. *Acta Biomater* 6:3824–3846
2. Demirci A et al (2007) Application of biofilm reactors for production of value-added products by microbial fermentation. *Biofilms in the food environment*. Blackwell Publishing Ltd, Oxford, pp 167–189
3. Bazaka K et al (2011) Do Bacteria Differentiate Between Degrees of Nanoscale Surface Roughness? *Biotechnol J* 6(9):1103–1114
4. Diaz C et al (2008) Influence of Surface Sub-Micropattern on the Adhesion of Pioneer Bacteria on Metals. *Artif Organ* 32(4):292–298
5. Diaz C et al (2010) Organization of *Pseudomans fluorescens* on Chemically Different Nano/Microstructured Surfaces. *Appl Mater Interfaces* 2(9):2530–2539
6. Hochbaum AI et al (2010) Bacteria pattern spontaneously on periodic nanostructure arrays. *Nano Lett* 10:3717–3721
7. Bhushan B (2010) *Springer Handbook of Nanotechnology*, 3rd edn. Springer, Heidelberg
8. Anselme K et al (2010) Cell/Material interfaces: influence of surface chemistry and surface topography on cell adhesion. *J Adhes Sci Technol* 24:831–852
9. Binnig G et al (1986) Atomic force microscope. *Phys Rev Lett* 56(9):930–933
10. Lower SK et al (2000) Measuring interfacial and adhesion forces between bacteria and mineral surfaces with biological force microscopy. *Geochim Cosmochim Acta* 64(18):3133–3139
11. Young T (1805) An essay on the cohesion of fluids. *Philos Trans R Soc Lond* 95:65–87
12. Vogler EA (1998) Structure and reactivity of water at biomaterial surfaces. *Adv Colloid Interface Sci* 74:69–117
13. Vogler EA (1999) Water and the acute biological response to surfaces. *J Biomater Sci Polym Ed* 10:1015–1045
14. Berg JM et al (1994) Three-component Langmuir-Blodgett film with a controllable degree of polarity. *Langmuir* 10:1225–1234
15. Marmur A et al (2004) The lotus effect: superhydrophobicity and metastability. *Langmuir* 20:3517–3519
16. Cheng YT et al (2005) Is the lotus leaf superhydrophobic? *Appl Phys Lett* 86:144101
17. Martines E et al (2005) Superhydrophobicity and superhydrophilicity of regular nanopatterns. *Nano Lett* 5(10):2097–2103
18. Wenzel RN (1936) Resistance of solid surfaces to wetting by water. *Ind Eng Chem* 28:988–994
19. Cassie ABD et al (1944) Wettability of porous surfaces. *Trans Faraday Soc* 40:546–551
20. Müller C et al (2010) Initial bioadhesion on dental materials as a function of contact time, pH, surface wettability and isoelectric point. *Langmuir* 26(6):4136–4141
21. Finlay JA et al (2010) Barnacle settlement and the adhesion of protein and diatom microfouling to xerogel films with varying surface energy and water wettability. *Biofouling: J Bioadhesion Biofilm Res* 26(6):657–666
22. Dúfrene YF (2003) Recent progress in the application of atomic force microscopy imaging and force spectroscopy to microbiology. *Curr Opin Microbiol* 6(3):317–323
23. Mazumder S et al (2010) Role of hydrophobicity in bacterial adherence to carbon nanostructures and biofilm formation. *Biofouling: J Bioadhesion Biofilm Res* 26(3):333–339
24. Teixeira P et al (1999) Influence of surface characteristics on the adhesion of *Alcaligenes Denitrificans* to polymeric substrates. *J Adhes Sci Technol* 13(11):1287–1294
25. Pereira MA et al (2000) Influence of physico-chemical properties of porous microcarriers on the adhesion of an anaerobic consortium. *J Ind Microbiol Biotechnol* 24(3):181–186
26. Ho KLG et al (1997) Ingredient selection for plastic composite supports for L-(+)-lactic acid biofilm fermentation by *Lactobacillus Casei* Subsp. *Rhamnosus*. *Appl Environ Microbiol* 63(7):2516–2523

27. Hartvig RA et al (2011) Protein adsorption at charged surfaces: the role of electrostatic interactions and interfacial charge regulation. *Langmuir* 27(6):2634–2643
28. Müller C et al (2013) The Scanning Force Microscope in Bacterial Cell Investigations. *Phys Status Solidi A* 210(5):846–852
29. Touhami A et al (2003) Nanoscale mapping of the elasticity of microbial cells by atomic force microscopy. *Langmuir* 19:4539–4543
30. Webb HK et al (2011) Physico-chemical characterization of cells using atomic force microscopy—current research and methodologies. *J Microbiol Methods* 86(2):131–139
31. Cappella B et al (1997) Force–Distance curves by AFM. *IEEE Eng Med Biol* 16(2):58–65
32. Chao Y et al (2011) Optimization of fixation methods for observation of bacterial cell morphology and surface ultrastructures by atomic force microscopy. *Appl Microbiol Biotechnol* 92:381–392
33. Stroth C et al (2004) Single molecule recognition imaging microscopy. *PNAS* 101(34):12503–12507
34. Dupres V et al (2007) Probing molecular recognition sites on biosurfaces using AFM. *Biomaterials* 28:2393–2402
35. Dorobantu LS et al (2008) Atomic force microscopy measurement of heterogeneity in bacterial surface hydrophobicity. *Langmuir* 24:4944–4951
36. Ebner A et al (2005) Localization of single Avidin–Biotin interactions using simultaneous topography and molecular recognition imaging. *Chem Phys Chem* 6(5):897–900
37. Ebner A et al (2007) A new simple method for linking of antibodies to atomic force microscopy tips. *Bioconjug Chem* 18(4):1176–1184
38. Dufrene YF et al (2002) Atomic force microscopy, a powerful tool in microbiology. *J Bacteriol* 184(19):5205–5213
39. Dufrene YF (2011) *Life at the nanoscale—atomic force microscopy of live cells*, pan stanford publishing, Singapore
40. Hinterdorfer P et al (2006) Detection and localization of single molecular recognition events using atomic force microscopy. *Nat Methods* 3:347–355
41. Helenius J et al (2008) Single cell force spectroscopy. *J Cell Sci* 121:1785–1791
42. Lee H et al (2009) Facile conjugation of biomolecules onto surfaces via mussel adhesive protein inspired coatings. *Adv Mater* 21:431–434
43. Kang S et al (2009) Bioinspired single bacterial cell force spectroscopy. *Langmuir* 25(2009):9656–9659
44. Lower SK et al (2001) Bacterial recognition of mineral surfaces: nanoscale interactions between *Shewanella* and  $\alpha$ -FeOOH. *Science* 292:1360–1363
45. Neal AL et al (2005) Cell adhesion of *Shewanella oneidensis* to iron oxide minerals: effect of different single crystal faces. *Geochem Trans* 6:77–84
46. Wojcikiewicz EP et al (2004) Force and compliance measurements on living cells using atomic force microscopy (AFM). *Biol Proced Online* 6(1):1–9
47. Buck AW et al (2010) Bonds between fibronectin and fibronectin-binding proteins on *Staphylococcus aureus* and *Lactococcus Lactis*. *Langmuir* 26:10764–10770
48. Müller DJ et al (2011) Force nanoscopy of living cells. *Curr Biol* 21(6):R212–R216
49. Verran J et al (2010) Use of the atomic force microscope to determine the strength of bacterial attachment to grooved surface features. *J Adhes Sci Technol* 24(13–14):2271–2285
50. Boks NP et al (2008) Forces involved in bacterial adhesion to hydrophilic and hydrophobic surfaces. *Microbiology* 154:3122–3133
51. Scheuermann TR et al (1998) Effects of substratum topography on bacterial adhesion. *J Colloid Interface Sci* 208:23–33
52. Xu LC et al (2012) Submicron-textured surface reduces Staphylococcal bacterial adhesion and biofilm formation. *Acta Biomater* 8:72–81
53. Geisse NA (2009) AFM and combined optical techniques. *Mater Today* 12(7–8):40–45
54. Casuso I et al (2011) Biological AFM: where we come from—where we are—where we may go. *J Mol Recognit* 24(3):406–413

55. Rösch c. et al (2013) Influence of Protein Immobilization on Protein-Protein Interaction Measured by Scanning Force Spectroscopy. *Physica Status Solidi A* 210 (5): 945 – 951
56. Puech PH et al (2006) A new technical approach to quantify cell–cell adhesion forces by AFM. *Ultramicroscopy* 106:637–644
57. Ho KLG et al (1997) Nutrient leaching and end product accumulation in plastic composite supports for L-(+)-lactic acid biofilm fermentation. *Appl Environ Microbiol* 63(7):2524–2532
58. Demirci A et al (1993) Evaluation of biofilm reactor solid support for mixed-culture lactic-acid production. *Appl Microbiol Biotechnol* 38(6):728–733
59. Demirci A et al (1995) Repeated-batch fermentation in biofilm reactors with plastic-composite supports for lactic-acid production. *Appl Microbiol Biotechnol* 43(4):585–589
60. van Loosdrecht MCM et al (1987) The role of bacterial-cell wall hydrophobicity in adhesion. *Appl Environ Microbiol* 53(8):1893–1897
61. Asther M et al (1990) A thermodynamic model to predict phanerochaete-chrysosporium Ina-12 adhesion to various solid carriers in relation to lignin peroxidase production. *Biotechnol Bioeng* 35(5):477–482

# Microsensors and Microscale Gradients in Biofilms

Haluk Beyenal and Jerome Babauta

**Abstract** Understanding the limiting factors and mechanisms of biofilm processes requires the direct measurement of microscale gradients using the appropriate tools. Microscale measurements can provide mechanistic information that cannot be obtained from bulk-scale measurements. Among the most used and trusted tools in microscale biofilm research are microsensors. The goal of this chapter is to introduce microsensor technology along with several examples to illustrate microscale processes in biofilms that are usually absent in bulk. We define a microsensor for biofilm research as a needle-type sensor with tip diameter of a few microns and a length up to several hundred microns. Microsensors can be used noninvasively to monitor in situ biofilm processes. Both optical and electrochemical microsensors can be used for biofilm applications. Because of newly discovered biofilm processes, the design and use of microsensors require customization and carefully designed experiments. In this chapter we present several examples describing the use of microsensors (1) in environmental biofilms, (2) in medical biofilms, and (3) in biofilms for energy and bioproducts. Microsensors can be the most useful if the measured profiles are integrated into the study of overall biofilm processes.

**Keywords** Biofilm · Fiberoptic · Microelectrode · Microscale gradient · Microsensor

## Contents

1	Introduction.....	236
1.1	Definition of Microsensors for Biofilm Studies.....	236
1.2	Biofilm Processes and Microsensors .....	237
2	Microsensors.....	239
2.1	Electrochemical Microsensors: Microelectrodes .....	239

---

H. Beyenal (✉) · J. Babauta  
Gene and Linda Voiland School of Chemical Engineering and Bioengineering,  
Washington State University, PO Box 642710 Pullman, WA 99164-2710, USA  
e-mail: beyenal@wsu.edu

2.2	Optical Microsensors .....	243
3	Measurement Systems for Microsensors .....	244
3.1	Obtaining Relevant Information from Microsensors.....	245
4	Selected Applications of Microsensors .....	248
4.1	Microbial Mats.....	249
4.2	Correlating Flavin Secretion with Oxygen Concentration.....	249
4.3	Oxygen Concentration in a Termite Gut.....	251
4.4	Fluorescent Light Intensity Distribution in a Biofilm.....	252
4.5	Electrode Respiring Biofilms.....	252
5	Summary, Conclusions, Outlook .....	254
	References .....	255

## 1 Introduction

Microsensors are sensors with a tip diameter of only a few microns [1]. With such small tip diameters, they can be used to perform measurements at the microscale, on the order of microns. Thus, microsensors can be applied to measure microscale gradients in many biological processes. This chapter focuses on microscale processes in biofilms and extends the principles to several other applications. Biofilms are cells attached to a surface covered with extracellular polymeric matrix (Fig. 1) [1]. In Fig. 1a, several single cells are shown attached to a surface. The presence of a few individual cells can change the local concentrations of chemicals close to the surface. As the cell number increases (Fig. 1b) over time, extracellular polymeric substances are secreted and cover a significant portion of the surface. Eventually, the local concentrations differ quantifiably from their respective bulk concentrations, giving rise to what is simply called “concentration profiles” (Fig. 1c). Concentration profiles of specific chemicals such as oxygen and chemical gradients such as pH are referred to as oxygen profiles and pH profiles, respectively. For example, if the biofilm shown in Fig. 1 consumes oxygen, the concentration profiles can represent oxygen profiles at various growth stages. In the bulk solution, the oxygen concentration can be at saturation; however, consumption by the cells decreases the oxygen concentration towards the bottom of the biofilm. The exact shape of the oxygen profile will be difficult to predict and therefore requires direct measurement. This chapter describes the microsensor technologies that can be used to quantify concentration profiles. Measurement systems, microsensor types, measurement techniques, and data interpretation are also described.

### 1.1 Definition of Microsensors for Biofilm Studies

Not all microsensors described in the literature can be used to quantify microscale gradients in biofilm [1]. Many are planar sensors of the micron size used in analytical detection. For biofilm studies we define a microsensor as a needle-type

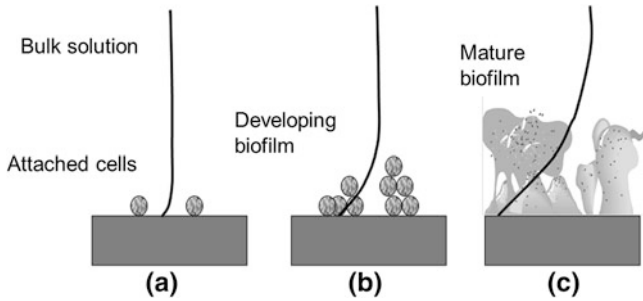


**Fig. 1** Attached cells on a surface. **a** A few cells are attached to the surface, starting biofilm and concentration profile development. **b** The cells increase in number and start to cover the surface. **c** The surface is covered by layers of cells. The continuous lines show hypothetical concentration profiles. The bulk concentrations are expected to remain constant, whereas biofilm processes close to the surface consume and decrease the concentrations of chemicals. The shape of the profile will reverse when the chemical is produced by the biofilm (increase towards the surface)

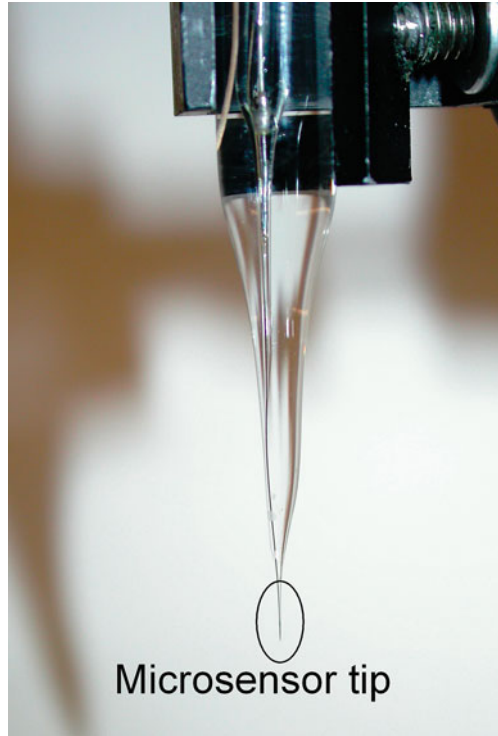
sensor with a few microns-tip diameter. An example microsensor (dissolved oxygen microsensor) is shown in Fig. 2. Details of its operation are given later. The reason why needle-type sensors are used is to enable measurements of microscale gradients without disturbing the biofilm, which is specifically the biofilm structure. Simply, planar-type microsensors cannot “fit” into a biofilm. A second requirement is that the materials used to construct the microsensor do not affect the biofilm, either negatively or positively. For example, a microsensor that leaches out a disinfectant would be particularly unusable for biofilm studies. Even those microsensors that slowly leach chlorides could potentially affect the biofilm. Another possibility is for the biofilm to utilize the material for metabolism. For example, a microsensor with exposed iron would be unusable to study microscale gradients in biofilms containing iron-oxidizing bacteria. These are all exaggerated examples as most microsensors are constructed of inert materials such as glass and the sensitive components are usually protected by membranes [1]. However, biofilm researchers interested in using microsensors should know whether the microsensor is compatible with their experimental system. For example, biofilm researchers studying extremophiles need to be aware of whether a microsensor is operable under the experimental conditions of interest (i.e., temperature, pressure, pH, salinity, etc.).

## 1.2 Biofilm Processes and Microsensors

Our research group has more than two decades of experience in using microsensors. We found that some microsensors had to be specifically constructed for particular biofilm applications; these are described in the following pages. In the more extreme cases, calibration procedures had to be modified. Because these



**Fig. 2** Photograph of a dissolved oxygen microsensor

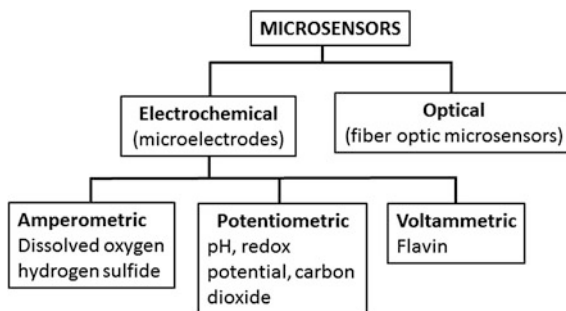


specialized steps were necessary, users must recognize the importance of identifying the biofilm processes of interest. The biofilm processes of interest need to be defined in terms of environmental conditions, chemical composition, and biofilm metabolic pathway(s) before microsensor use is discussed. Broadly, biofilms can be categorized into three groups based on their research focus:

1. Environmental biofilms
2. Medical biofilms
3. Biofilms for energy and bioproducts.

Biofilm used in wastewater treatment and subsurface biofilm can be cited as examples of environmental biofilm [2–6]. Microbial mats can also be considered a part of this group because of their apparent stratification [7–9]. However, their structure is significantly different from that of biofilm. Examples of medical biofilm include biofilm growing on wounds, medical devices, or implants that are detrimental to human health [10–14]. Biofilm for energy and bioproducts may be biofilms that produce harvestable energy via electron exchange with electrode surfaces, which are often termed electrochemically active biofilms [15, 16]. For example, an anodic biofilm respiring on the anode of a microbial fuel cell could be considered a member of this group. Still other biofilms produce bioproducts in bioreactors. The microscale processes in biofilms can vary greatly from sulfidic

**Fig. 3** Microsensor types, their subgroups, and relevant examples used in biofilms



processes to microaerophilic or aerobic processes in the presence of different buffering systems [17–22]. Knowing the microscale processes allows users to choose the right suite of microelectrodes to characterize an entire biofilm process. If chosen correctly, mass balances can be done, reaction kinetics can be quantified, and the presence of active metabolic pathways can even be discovered. Conversely, a lack of understanding of the biofilm processes studied will likely lead to costly, incomplete, and/or misinterpreted datasets.

## 2 Microsensors

The microsensors used in biofilms can be categorized by operating principle into two groups: electrochemical microsensors and optical microsensors (Fig. 3) [23]. Electrochemical microsensors are called microelectrodes, referring to their electrode origin, and optical microsensors are called fiber-optic microsensors, referring to their construction using fiber-optic cabling. However, we should note that most fiber-optic sensors used without modification do not meet the criteria for use in biofilms. Fiber-optic microsensors have also been referred to as microoptodes [24, 25]. As seen in Fig. 3, microelectrodes are categorized into two subgroups, potentiometric and amperometric microelectrodes, and voltammetric microelectrodes can be considered as a subgroup of amperometric microelectrodes [26]. Unlike microelectrodes, fiber-optic microsensors are usually not constructed differently for the different modes of light collection (i.e., absorbance, transmittance, or fluorescence) [26]. Rather, it is the peripherals of the light collection system that are changed [1, 6, 27]. Because fiber-optic microsensors have limited applicability in biofilm processes, we discuss them briefly and point readers to more detailed reviews elsewhere [25].

### 2.1 Electrochemical Microsensors: Microelectrodes

Microelectrodes use well-known electrochemical concepts to measure an electrochemical signal in the form of either a potential difference or current. These electrochemical concepts include measuring potential differences across semipermeable

membranes and mass-transport-limited current (limiting current). At the basic level, all microelectrodes consist of either a 2-electrode or a 3-electrode electrochemical cell designed in such a way as to select for the electrochemical signal of a specific analyte. The construction of an electrochemical cell at the micron scale allows better response times, lower analyte detection limits, and enhanced sensitivity to changes in analyte concentration, compared to their macroscale counterparts. One of the reasons for the enhanced abilities of microelectrodes is the hemispherical diffusion patterns that arise for micron-sized electrodes, which are a faster diffusion process than simple planar diffusion. Analyte diffusion to the microelectrode tip is faster and therefore allows for an enhanced overall performance. Several other factors add value to reducing electrode sizes to microscale dimensions and are discussed in detail in classical electrochemical texts [28]. Here we focus on the basic electrochemical identities required to select an appropriate microelectrode and use it successfully.

### 2.1.1 Potentiometric Microelectrodes

When the concentration of an analyte is detected by measuring a potential difference, the microelectrode is called a potentiometric microelectrode. The potential difference is measured between the microelectrode tip and a reference electrode. Usually an ion-selective membrane is used such that the potential difference measures the potential drop across the membrane in a practical way. The well-known example of this microelectrode type is the pH microelectrode. For an ion-selective microelectrode, when the chemical potential of the measured ion activity on the inner side of the sensor is kept constant ( $a_{\text{constant}}$ ), the Nernst equation can be simplified to describe the response of the sensor:

$$E_{\text{unknown}} = E_{\text{constant}} \pm \frac{RT}{zF} \ln \frac{a_{\text{unknown}}}{a_{\text{constant}}} \quad (1)$$

where  $a$  is the activity of the chemical potential of the measured ion on the inner side ( $a_{\text{constant}}$ ) and on the outer side ( $a_{\text{unknown}}$ ),  $z$  is the charge of the ion,  $F$  is Faraday's constant,  $E_{\text{unknown}}$  is the measured potential difference,  $E_{\text{constant}}$  is an arbitrary offset constant, and  $T$  is temperature. The sign of  $z$  is positive for a cation and negative for an anion. It is important to note that  $E_{\text{constant}}$  is an arbitrary parameter necessary to fit the data obtained from potentiometric microelectrode measurements. Although it has a physical meaning, this is not relevant to microelectrode operation and is not discussed further. Potentiometric microelectrodes are calibrated by correlating the measured potential difference with the activity of the ions in a series of calibration solutions. For example, the calibration of a pH microelectrode in a series of calibration solutions would exhibit a linear correlation when plotted on a semilog plot of measured potential difference against proton activity [1]. Of course, using the definition of pH, a simple plot of pH

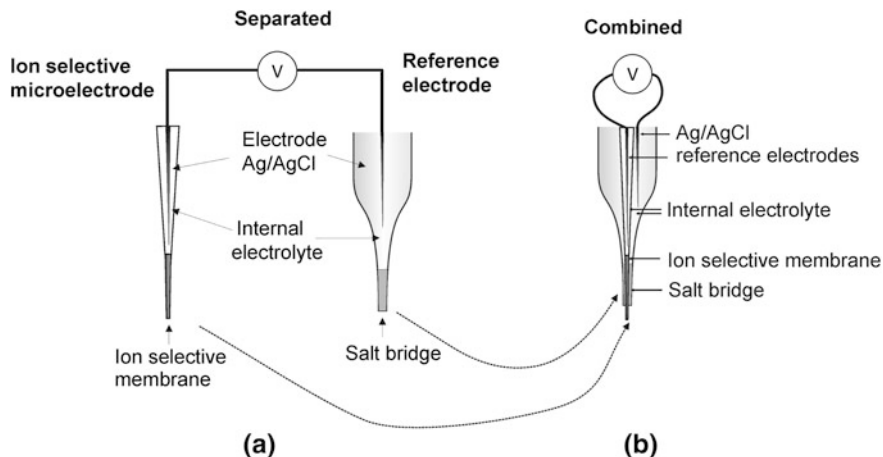


**Fig. 4** Two types of potentiometric microelectrodes. **a** The ion-selective-microelectrode and the reference electrode are separated. **b** The ion-selective-microelectrode and the reference electrode are combined

against measured potential differences in pH calibration solutions yields a linear correlation.

Figure 4 shows two methods of constructing potentiometric microelectrodes that we use in our research. Figure 4a shows the commonly used method, in which the ion-selective electrode and the reference electrode are separated. Parameter  $a_{\text{constant}}$  is defined for the internal solution inside the outer case. By placing the microelectrode and the reference electrode into solutions with known concentrations of a chemical, a calibration curve can be prepared. If the measured potential difference of an unknown solution falls within the range of measured potential differences used in the calibration curve,  $a_{\text{unknown}}$  can be calculated from the calibration curve. In cases where the distance between the electrodes needs to be minimized, the combined method of construction shown in Fig. 4b is advantageous [16, 29]. To determine whether the combined method is necessary, users must quantify the effect of the reference electrode distance from the microelectrode tip on the measured potential difference and decide whether the effect is significant.

### 2.1.2 Amperometric Microelectrodes

When the concentration of the analyte is detected by measuring a current, the microelectrode is called an amperometric microelectrode [1]. Amperometric microelectrodes detect the current from known oxidation/reduction reactions occurring on the microelectrode tip. Most amperometric microelectrodes are constructed in a 2-electrode configuration in which a known reference electrode also functions as the auxiliary electrode that completes the electrochemical cell.

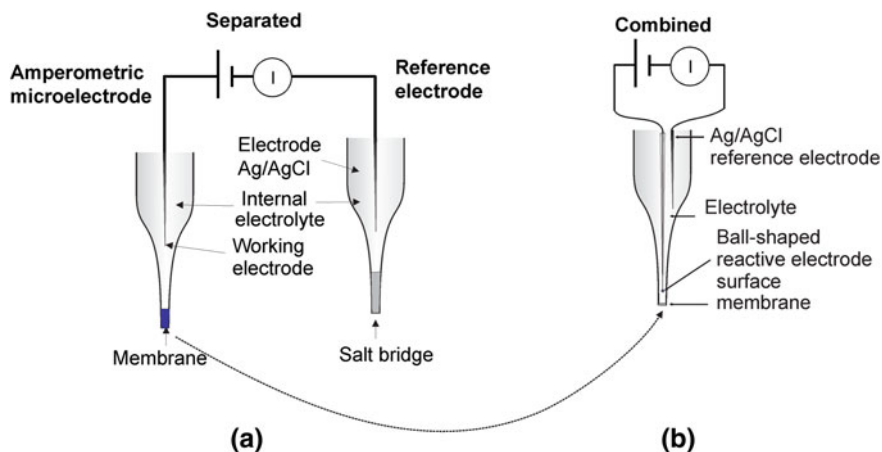


**Fig. 5** Two types of amperometric microelectrodes. **a** The microelectrode tip and the reference electrode are separated. **b** The microelectrode tip and the reference electrode are placed in the same case behind the membrane. The microelectrode tip is always separated from the bulk solution with a selective membrane, regardless of the location of the reference electrode

The amount of current passed by the microelectrode is small, insignificant compared to the capacity of the reference electrode. In practical terms, this means that the reference electrode potential remains constant during the operation of the amperometric microelectrode. We should note that macroelectrodes cannot function in this way and users should be aware of this fact. We do recommend that, over the long term, the reference electrode potential always be checked against another standard reference electrode. Amperometric microelectrodes are usually operated in potentiostatic mode, in which the microelectrode tip is polarized against the reference electrode at an applied potential that allows oxidation/reduction of the analyte. The resulting current gives the reaction rate on the electrode surface and correlates with the concentration of the analyte in the vicinity of the microelectrode tip. In the presence of interfering chemicals, a membrane that is selective for the analyte is required. It should not be sensitive to convection (i.e., stirring of a solution). The membranes used in amperometric sensors serve to separate the chemistry of the bulk solution from that of the electrolyte solution; this should not be confused with the function of potentiometric microelectrode membranes. The membrane controls the mass transfer of the analyte, and the current is given by the following equation,

$$i_L = S_b n F \frac{P_m}{\delta} \quad (2)$$

where  $i_L$  is the limiting current density,  $S_b$  is the bulk concentration of the analyte,  $n$  is the number of electrons required per mole of analyte oxidized/reduced,  $F$  is Faraday's constant,  $P_m$  is the permeability of the membrane, and  $\delta$  is the thickness of the membrane. To improve sensitivity, it is necessary to construct thinner

membranes with higher permeability for the analyte. As seen from this equation, the current is directly proportional to the bulk concentration. This is because, by definition, the limiting current implies that the surface concentration of the analyte is zero. We should note that, in practice, there is always a background current.

Figure 5 shows two example methods of constructing amperometric microelectrodes. A hydrogen peroxide microelectrode is an example of the method in which the microelectrode tip and the reference electrode are separated, whereas a dissolved oxygen microelectrode is an example of the method in which they are combined [1, 30]. As in a potentiometric microelectrode, the distance between the microelectrode tip and the reference electrode in an amperometric microelectrode can cause a decrease in performance due to the presence of solution resistance [15, 16, 29]. For solutions with low ionic conductivity, the distance must be minimized or the ionic conductivity of the solution increased.

## 2.2 Optical Microsensors

Optical microsensors are generally constructed by etching the ends of fiber-optic cables. Figure 6 shows a tip of a fiber-optic cable that is only a few microns in diameter, which is what we consider a fiber-optic microsensor. The tip detects a fluorescence signal from (1) either cells or the interstitial solution inside a biofilm, or (2) from a fluorophore immobilized on the tip of the sensor (Fig. 6). For example, a fiber-optic dissolved oxygen microsensor has ruthenium salts immobilized on the tip of the fiber [31]. A green fluorescent protein (GFP) sensor has an open tip that detects the fluorescent light from cells expressing GFP [24]. Depending on the application of the microsensor, a beam splitter, filters, and couplers can be customized. In some cases, the fiber-optic microsensor is connected directly to a spectrophotometer to detect light intensity. Quantifying light penetration of microbial mats is one example application of this configuration [25].

The Stern–Volmer equation is used to describe the lifetime of a fluorescence signal coming from a fluorophore immobilized on a fiber-optic tip [1]:

$$\frac{\tau_o}{\tau} = 1 + k_o\tau_o C_q \quad (3)$$

where  $\tau$  is the fluorescence lifetime in the presence of the quencher,  $\tau_o$  is the fluorescence lifetime in the absence of the quencher,  $k_o$  is the rate constant for the dynamic reaction of the quencher with the fluorophore, and  $C_q$  is the concentration of the quencher. Fluorescence lifetime can be written as a function of fluorescent light intensity:

$$\frac{I_o}{I} = \frac{\tau_o}{\tau} \quad (4)$$

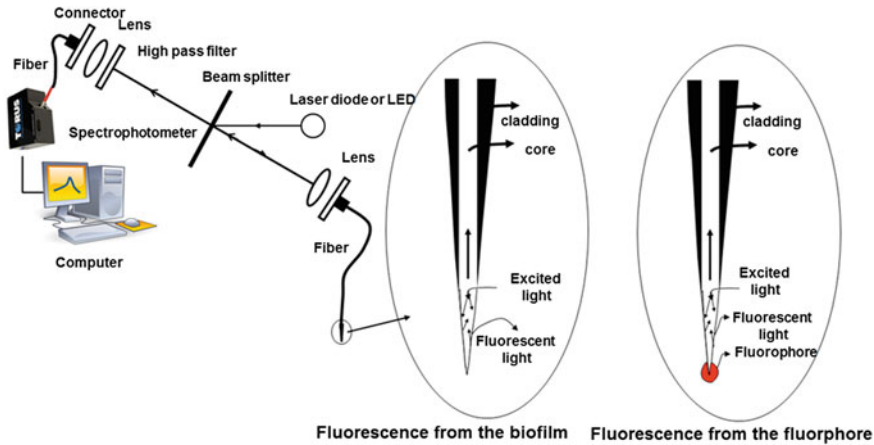


**Fig. 6** Schematic diagram of a fiber-optic system detecting fluorescence from the biofilm or from a fluorophore immobilized on the tip of the fiber-optic microsensor

where  $I$  is the fluorescent light intensity in the presence of the quencher and  $I_0$  is the fluorescent light intensity in the absence of the quencher. Simply, by measuring fluorescent light intensity, it is possible to calculate the concentration of the quencher in the vicinity of the fiber-optic tip.

### 3 Measurement Systems for Microsensors

Figure 7 shows the setup and components used for microelectrode measurements in our lab. The setup starts with a microelectrode. The microelectrode is attached to a stepper motor controlled by a stepper motor controller. In our lab, we use an ultrahigh-resolution linear actuator with submicron resolution (PI M-230.10). The stepper motor controller is connected to a computer. The relative position of the microelectrode along a set distance is controlled by computer using custom-written software (Microprofiler©). The relative position of the stepper motor determines the position of the microelectrode during measurements. Depending on the microelectrode type, an electrometer can be used to monitor potential from the microelectrode or a picoammeter can be used to monitor current in conjunction with a voltage source. The output of the electrometer/picoammeter is connected to an analog-to-digital control (ADC) board so that the potential or current can be monitored and recorded by the computer. After a microelectrode is calibrated, the potential data from the ADC board can easily be converted to concentration. In our lab, we use custom-written software to monitor and record the position of the microelectrode tip and the concentration. The output data are saved to the computer and displayed on the monitor in realtime.

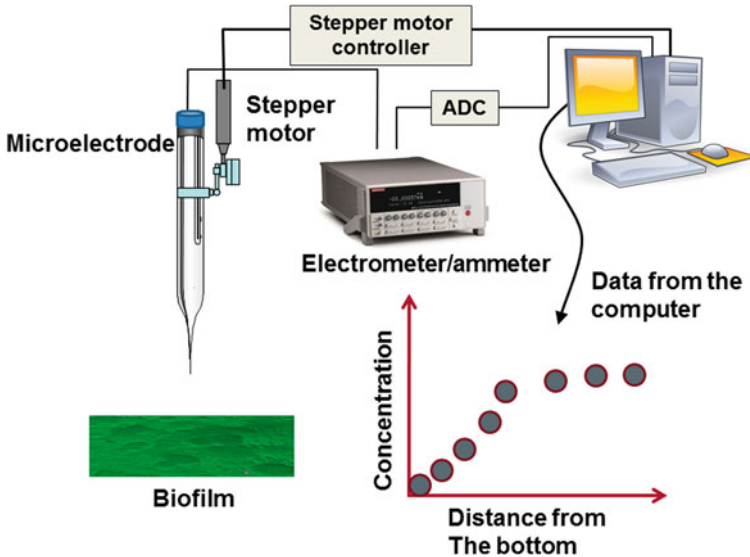


Fig. 7 Measurement setup and components used to operate microelectrodes

For optical microsensors, we use the setup shown in Fig. 6 with the fiber-optic microsensor attached to the stepper motor shown in Fig. 7. The electrometer/picoammeter is replaced by a spectrophotometer/photo-multiplying tube (PMT). Data from a spectrophotometer or PMT need to be analyzed and stored using software designed for the model used. For example, from a spectrophotometer, we can store light spectra from different depths and determine the light penetration inside a biofilm or a microbial mat. For our research we used single-mode fiber with a very small core diameter, which requires precise alignment (Fig. 6). This type of setup is not practical unless the researcher’s goal is to develop new fiber-optic sensors. Usually, a multimode cable is pulled to make a fiber-optic tip. The details of the construction process and measurement setup are described in the literature [1, 25].

### 3.1 Obtaining Relevant Information from Microsensors

For a microsensor to be useful for determining microscale gradients in a biofilm, there are several criteria that need to be met: (1) the microsensor tip diameter must be small enough not to affect biofilm structure, and (2) a second profile measured in the same location must be almost identical. If their shapes differ, this means that the microsensor tip damaged the biofilm structure, likely because the tip was too large. (3) After a measurement, the microsensor must be recalibrated successfully. As much as some of the microsensors have short lifetimes, this step is critical. Moreover, an inexperienced user can measure a profile and damage the tip during



the measurement. Even with a damaged tip, a profile can be measured. However, the profile does not represent the system studied. Therefore, recalibration of the microsensors after the measurement cannot be overlooked. From the above criteria, it can be understood that the difficulty in using microsensors in biofilms lies in the measurement techniques. Because many microelectrodes are becoming commercially available ([www.unisense.com](http://www.unisense.com)), improving our understanding of the measurement techniques and data interpretation will potentially increase the use of microsensors in biofilm research.

The tip of a microsensor is a few microns in diameter; therefore, it is very difficult to locate the tip. Often only experienced users can use microsensors in very precise measurements. Such experience comes from cases where the location of the tip can be determined by breaking the tip. The use of high-quality inverted microscopes or stereomicroscopes can be helpful in some cases. Regardless of the method of imaging, knowing the exact position of the tip is critical to interpreting microsensor data correctly that, without this knowledge, could be misleading. The position of the microelectrode tip is often referenced from a known position such as the biofilm surface, from an air/liquid interface, from a solid surface (i.e., substratum that the biofilm is grown on), or other easily observable/relevant positions. In the examples of this chapter, the  $z$ -axis is referenced from different positions inside each respective biofilm system and the name reflects these differences. Multiple location measurements is the most challenging skill needed for using microsensors in biofilms, one that must be mastered over many years of research. During this process, our students or research associates are almost guaranteed to break tips and require multiple replacements. This is one of the barriers to overcome in microsensor-related research if the microsensors are bought commercially. Therefore, our research group constructs its own microelectrodes. The construction processes for selected microsensors are detailed in our previous book [1].

Microsensors provide the capability of making both spatial and temporal measurements inside biofilms. From Fig. 1, we assumed that the relevant information for biofilm processes is generally analyzed in terms of concentration gradients with depth existing inside the biofilm. We call this type of profile “depth profiles”. However, temporal variation in concentration can also be monitored, by fixing the microsensor in a stationary position and monitoring concentration over time. We call this type of profile “stationary profiles”. Using a combination of the two types of concentration profiles allows users to obtain information on both steady-state fluxes of analytes and biofilm responses to controlled stressors.

As long as the duration of the depth profile measurement is short enough that the consumption/production of the analyte by the biofilm is invariable, depth profiles will show the variation of the analyte concentration through the biofilm. Subsequently, pseudo-steady-state or steady-state fluxes of the analyte can be estimated. As an example, Fig. 8a shows the variation of  $H_2$  concentration with distance from the bottom of a sediment biofilm where zero on the  $x$ -axis refers to the approximate biofilm surface. Careful inspection of the  $H_2$  depth profile tells us that no  $H_2$  was detected in the bulk solution hundreds of microns away from the

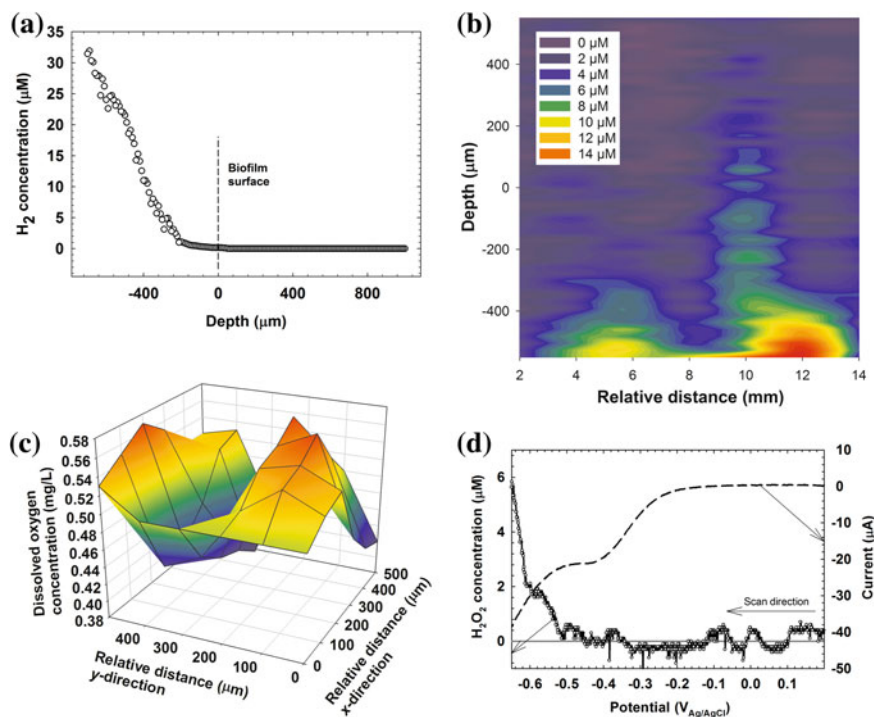


**Fig. 8** Profile types measured using microsensors: **a** A H<sub>2</sub> depth profile in a sediment biofilm, **b** A 2D map of H<sub>2</sub> distribution in the same biofilm, **c** A 3D map of oxygen distribution 40 μm from the bottom of the biofilm, and **d** A stationary profile of H<sub>2</sub>O<sub>2</sub> concentration quantified 100 μm from a metal surface. **b** is modified from Nguyen et al. [32]. **d** is modified from Istanbulu et al. [30]

biofilm surface. However, approximately 500 μm from the bottom of the biofilm, H<sub>2</sub> was detected and the H<sub>2</sub> concentration increased towards the bottom. Near the bottom of the biofilm, the H<sub>2</sub> concentration was approximately 32 μM. Several concepts about microsensor research are highlighted in this depth profile: (1) by looking at the bulk data, researchers could conclude that these biofilms were not producing H<sub>2</sub>, which is incorrect; (2) depth profiles, and microsensor data in general, are only useful when correlated with specific locations in the biofilm (e.g., biofilm surface); (3) depth profiles should span contrasting zones of analyte concentration (i.e., bulk to biofilm or top of biofilm to bottom). In the case of environmental biofilms, incomplete depth profiles or a poor understanding of the location of the microsensor tip may lead to erroneous conclusions. One depth profile alone usually provides limited information. More information can be obtained by asking additional questions, such as, “Is the profile identical at different locations in the biofilm?”

To address the question above, we can perform additional depth profiles at different relative *x* or *y*-coordinates to generate a 2D map or at different relative

$xy$ -coordinates to generate a 3D map of analyte concentration. Figure 8b shows a 2D map of  $H_2$  concentration corresponding to the biofilm shown in Fig. 8a. Figure 8b demonstrates that  $H_2$  was localized at specific sites in the biofilm, which we term “hot spots.” Hot spots can be defined as microenvironments in biofilm with relatively high or low activity and are a new concept for biofilm researchers [32]. Because the biofilm consisted of indigenous bacteria growing in their natural environment (subsurface) we expected to see some heterogeneity. Such distinct hot spots were surprising to us. Such hot spots in natural environments likely correspond to the location of active  $H_2$  producers. These interesting observations bring new ways of using microsensors on productive environmental biofilms. In a similar manner, 3D maps can provide further evidence of biofilm heterogeneity. Figure 8c shows a 3D map of dissolved oxygen concentration at a fixed distance from the bottom of a biofilm. Similar maps can be presented for varying distances from the bottom of the biofilm. If we calculate the average oxygen concentration for each distance, we can generate averaged oxygen depth profiles with standard deviations. Averaged depth profiles with standard deviations are described by Lewandowski and Beyenal and are used to describe biofilm heterogeneity and flux through biofilms [1]. They provide more representative information about depth profiles but are difficult to obtain.

Figure 8d shows temporal measurements of stationary profiles, a technique newly developed by our research group [30]. Although stationary profiles often appear similar to depth profiles, careful inspection of Fig. 8d shows that a stressor is applied in the form of a change in the applied potential at a metal surface. In this case, the microelectrode tip was placed approximately  $100\ \mu\text{m}$  from the metal electrode surface to characterize the reaction kinetics of oxygen reduction. At this depth, the applied potential was scanned linearly and the variation of both current and  $H_2O_2$  concentration were recorded over time. We confirmed that (1)  $H_2O_2$  could be detected and was therefore produced by incomplete oxygen reduction, (2) the onset of  $H_2O_2$  production was at approximately  $-0.4\ \text{V}_{\text{Ag}/\text{AgCl}}$ , and (3) the current increase was associated with  $H_2O_2$  production, which is an indicator for the process. By having this information, we can predict the approximate concentrations of  $H_2O_2$  that a biofilm is exposed to when grown on a metal surface and determine whether  $H_2O_2$  inhibits growth. This new technique has applications beyond biofilm: it could be used to determine surface reactions that cannot be determined in the bulk solution.

## 4 Selected Applications of Microsensors

Over the years we have measured a countless number of concentration profiles in biofilms. Our cumulative experience has always reflected one unchanging fact about microsensor research, that the existence of a profile by itself does not provide critical information nor assign importance. Regardless of the measurement

types described above, profiles can be useful only if they are used to address a scientific question. For this reason, the following sections highlight several examples of microsensor measurements with relevant scientific questions.

#### ***4.1 Microbial Mats***

Microbial mats are one of the earliest ecosystems on Earth. Oxygenic phototrophic microorganisms such as diatoms and cyanobacteria existing in microbial mats can capture carbon dioxide and generate energy by providing organic substrates and oxygen [33, 34]. Although microbial mats show differing characteristics when compared to biofilms, microsensors are useful tools for studying them because they are stratified, a few millimeters thick, and densely populated with a variety of microorganisms. The microorganisms in a mat coexist through chemical (oxygen, sulfide, pH, and redox potential) and physical (light) gradients shaped by the activity and interactions of the microorganisms. Most microbial mats are composed of oxygenic and anoxygenic layers [7, 8, 35–37]. The measurement of oxygen profiles in the mat can show the apparent thickness of the oxygenic layers in the mat. We expect that cyanobacteria near the top of the microbial mat can capture light energy and produce oxygen. In this case, the oxygen concentration should increase near the mat surface. By measuring oxygen depth profiles through the mat, we can verify this hypothesis.

Figure 9 shows the variation of dissolved oxygen concentration inside a microbial mat with distance. We should note that for this figure we use relative distance for the  $x$ -axis. We could not locate the bottom of the mat as it rested on a soft sediment layer. However, knowledge of the relative distance from the surface of the mat was adequate for verifying our hypothesis. The increase in oxygen concentration above that of air-saturated water at the microbial mat surface indicates oxygen production and verified our expectation. Additionally, the decreasing oxygen concentration in deeper regions of the mat demonstrates stratification as microorganisms in this layer consume oxygen. Important features of the oxygen depth profile include a smooth exponential decrease in oxygen concentration away from the mat surface, indicating simple Fickian diffusion. This is contrasted with complex uneven changes in oxygen concentration deeper inside the mat, suggesting mixed processes of diffusion and consumption.

#### ***4.2 Correlating Flavin Secretion with Oxygen Concentration***

Recently, our research group developed a microelectrode to measure flavin concentrations in biofilms. We specifically targeted the measurement of flavin concentration in *Shewanella oneidensis* MR-1 biofilms growing anaerobically on

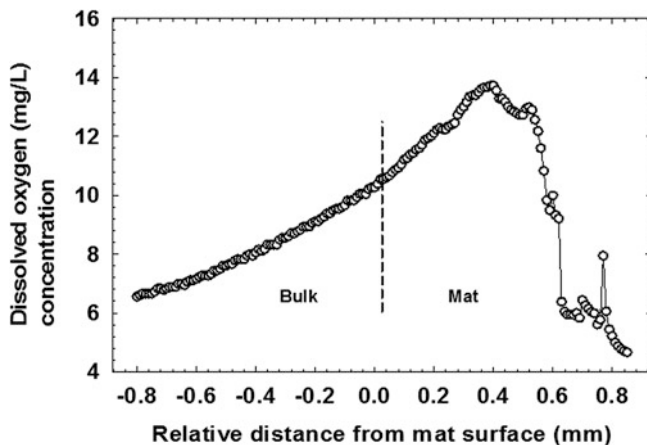


**Fig. 9** Variation of dissolved oxygen concentration with distance from the surface of a microbial mat. The increase in oxygen concentration near the surface of the microbial mat shows oxygen production. However, oxygen concentration decreased in the deeper part of the mat, demonstrating the consumption of oxygen. The *line* shows the approximate location of the interface between the bulk and the microbial mat

electrodes. *S. oneidensis* MR-1 is a facultative anaerobic bacterium that is capable of respiring on electrodes. It has been shown that *S. oneidensis* MR-1 biofilms can utilize both c-type cytochromes and secreted flavins to carry out electrode respiration [26]. Therefore, we were interested in measuring flavin concentration and expected to see a flavin concentration profile in the biofilm. However, despite many measurements we could not detect any secreted flavins inside *S. oneidensis* MR-1 biofilms. Possible reasons for this are that the flavin concentration was below our detection limit (50 nM) and that there are other mechanisms triggering flavin production. As much as *S. oneidensis* MR-1 is a facultative anaerobe, based upon previous published studies [15, 29, 38] we hypothesized that the presence of oxygen was required for flavin secretion in *S. oneidensis* MR-1 biofilms. The interaction between flavins and oxygen could be quantified by measuring oxygen and flavin depth profiles in *S. oneidensis* MR-1 biofilms.

Figure 10 shows concentration depth profiles measured in a *S. oneidensis* MR-1 biofilm. The biofilm we used was approximately 300- $\mu$ m thick. The dissolved oxygen concentration was  $\sim$ 8 mg/L in the bulk and decreased to 0 mg/L at  $\sim$ 120  $\mu$ m away from the bottom. This is a typical oxygen depth profile, found in many aerobic biofilms. When we measured the flavin depth profile in the same biofilm, the results verified our hypothesis. The flavin concentration was below our detection limit in all places except for a sudden increase in concentration near the bottom of the biofilm, where the oxygen was depleted. We speculate that flavins are produced in the anaerobic zone to act as intermediate electron acceptors in the deeper parts of the biofilm. The reduced flavins can then be transported to the aerobic zones, where they deposit the electrons to oxygen, which acts as the

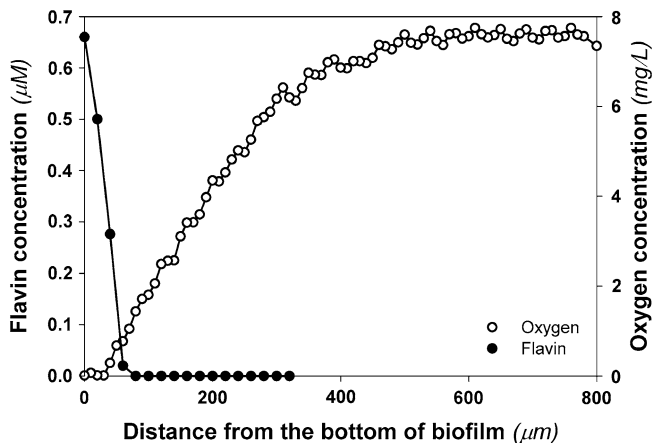


**Fig. 10** Flavin and oxygen concentration profiles in a *S. oneidensis* MR-1 biofilm. The top of the biofilm was approximately 300  $\mu\text{m}$  from the bottom (reprinted from Nguyen et al. [32])

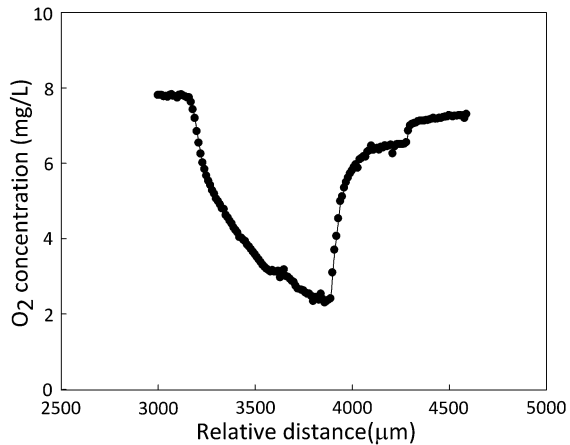
terminal electron acceptor. However, this hypothesis requires further experiments using microsensors. The example data shown in Fig. 10 show the importance of combined measurements of different analytes in biofilms and how they can be used to address a hypothesis.

### 4.3 Oxygen Concentration in a Termite Gut

Lignin modification in wood-feeding termites (WFTs) has been known for a long time. Microorganisms in the termite gut are involved in the degradation of lignin. It was believed that the termite gut was anaerobic; however, lignin degradation requires a high oxygen concentration [39, 40]. A dissolved oxygen microelectrode was used to measure oxygen profiles in termite gut to address the conflicting information.

Figure 11 shows oxygen concentration profiles in a wood-feeding termite gut [41]. The oxygen concentration profile was asymmetric, showing a decrease and an increase in oxygen concentration. Because the oxygen concentration was always above 2 mg/L we conclude that the gut of the termite was aerobic. The gut segments showed different oxygen gradients, indicating different oxygen penetration or consumption rates in these gut segments. For example, a sharp and a slow decrease were observed in the foregut and midgut, respectively. In both foreguts, there were zones of sharp oxygen concentration change.

**Fig. 11** Oxygen concentration change in a termite gut. The measurements started in the air and ended in the agar layer in which we placed the termite gut. The *hollow arrowheads* indicate the locations of gut walls, and the *solid arrowheads* indicate the points of inflection of the oxygen profiles. (modified from Ke et al. [41])



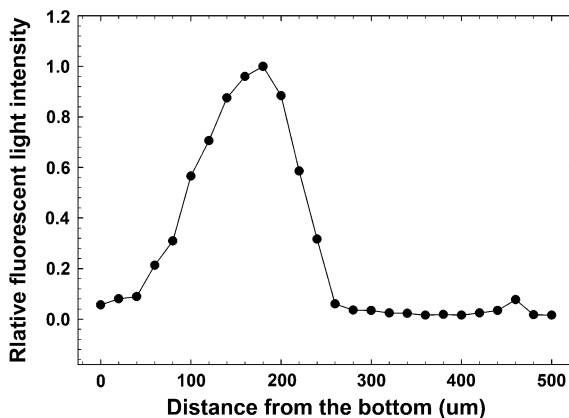
#### 4.4 Fluorescent Light Intensity Distribution in a Biofilm

Fiber-optic microsensors can be used to determine a fluorescence signal in a biofilm. An example application was described in our previous publication [24]. A biofilm of *S. aureus* expressing yellow fluorescent protein (YFP) can be used to determine relative toxic shock syndrome toxin-1 (TSST-1) expression. If the organisms produce YFP in response to their TSST-1 expression, the YFP intensity gives the relative TSST-1 concentration in the biofilm [24]. Measurement results are given in Fig. 12. The maximum fluorescent light intensity was near the middle of the biofilm. The fluorescent light intensity reached a maximum around 150  $\mu\text{m}$  from the bottom. As we stated earlier, this single profile gives limited information. In the following measurements we verified that the YFP intensities also correlated with the oxygen concentration [24]. It had been demonstrated that TSST-1 can be produced under critical concentrations of carbon dioxide and dissolved oxygen. However, these values were not known for biofilm. We obtained relative TSST-1 profiles, therefore these can be combined with oxygen and carbon dioxide profiles to find the critical conditions. These measurement results are given in detail elsewhere [24]. As we demonstrate in this example, measuring one profile by itself is not enough to explain an underlying mechanism. In most cases, combined measurements are needed to obtain useful information.

#### 4.5 Electrode Respiring Biofilms

Electrode respiration by electrochemically active biofilms results in the formation of electrochemical gradients [15, 16, 29]. The electrochemical gradients are manifested as potential drops across the biofilm/electrode interface and as ionic gradients diffusing away from the biofilm/electrode interface. Simply, electrons

**Fig. 12** Relative fluorescent light intensity profiles measured in a biofilm producing yellow fluorescent protein. Fluorescent light intensities were normalized by dividing each datum by the maximum value. The maximum intensity was near the middle of the biofilm (modified from Beyenal et al. [24])



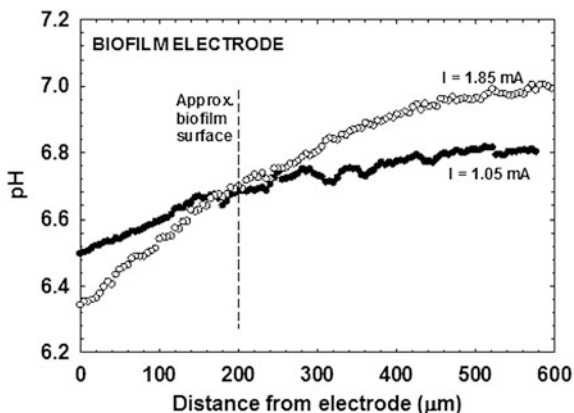
move towards the electrode surfaces whereas cations move away in the opposite direction. Additionally, the generation of proton equivalents to electrons is observed in the metabolism of the biofilm and proton secretion also results in the formation of proton gradients inside the biofilm during electrode respiration. Under increasing electron transfer rates, measured as current output of the electrode, proton gradients were expected to increase proportionally with the increase in current. To verify this effect, we used pH microelectrodes to measure pH depth profiles inside electrode-respiring *G. sulfurreducens* biofilms at increasing electron transfer rates [16].

Unlike other biofilm processes, the electrochemical gradients formed inside electrode-respiring biofilms can interfere with microelectrode operation because microelectrodes also operate using electrochemical gradients. This is a critical factor that is often overlooked when commercial microelectrodes are purchased. It is only noticeable in carefully designed calibration experiments. Additionally, we constructed new pH microelectrodes using the combined method shown in Fig. 4b to be sure that interference from external electrochemical gradients was minimized. We do not recommend the use of the method shown in Fig. 4a and reiterate the importance of knowing the critical components of the biofilm process of interest.

Figure 13 shows the pH decreasing towards the bottom of the biofilm up to the biofilm/electrode interface. The bottom was found by breaking the pH microelectrode tip on the electrode surface while the biofilm surface was imaged by microscopy. The pH depth profiles confirmed our expectation that the pH inside the biofilm would decrease with an increasing electron transfer rate. Surprisingly, contrary to what was speculated in the literature, the pH at the bottom of the biofilm did not reach completely inhibiting levels [15], even at the maximum steady-state current. Therefore, we concluded that the proton gradient inside *G. sulfurreducens* biofilms was not likely current-limiting. We should note that the experimenter relying on the first measurement could conclude there was a pH limitation after noticing changes in pH. However, further measurements,



**Fig. 13** pH Depth profiles inside *G. sulfurreducens* biofilm producing increasing current, from 1.05 mA (closed circles) to 1.85 mA (open circles). The approximate biofilm surface is indicated by the vertical dashed line (modified from Babauta et al. [16])



performed when the biofilms were generating more current, demonstrated that pH was not limiting during the first measurements. The measurement results given here reinforce our message. A single profile always gives limited information. Additional profiles can generate the more critical information needed for the process studied.

## 5 Summary, Conclusions, Outlook

Microsensors are among the most powerful, nondestructive tools for quantifying microscale chemistry and activity in biofilms. They provide information that cannot be obtained in the bulk solution. Their high resolution and in situ applicability to biofilms are vital for determining electron donor and electron acceptor limitations in biofilms as well as the flux of a chemical of interest. So far most microsensors are used for studying laboratory biofilm. However, recent use in the field in environmental biofilm demonstrates that they have great potential for investigating microscale processes in situ. For example, they can be used to discover hot spots in environmental biofilm. The use of a mapping technique can generate data critical to correlating biofilm activity distribution with overall biofilm activity. The use of new measurement techniques, such as stationary profile microelectrodes, can extend our understanding of mechanisms and critical factors in biofilm processes. We expect that microsensor research will continue to expand our knowledge of the productive biofilms cultured both in laboratories and found in the environment.

**Acknowledgments** U.S. Office of Naval Research (ONR) grant #N00014-09-1 0090, National Science Foundation (NSF) grant #0954186, and the US Department of Energy (DOE) Office of Biological and Environmental Research (BER), under the Subsurface Biogeochemical Research (SBR) Program (grant DE-FG92-08ER64560), supported our research on using microsensors. The data related to microbial mats were generated using support from the Genomic Science

Program (GSP), the Office of Biological and Environmental Research (OBER), and the US Department of Energy (DOE) and were a contribution of the Pacific Northwest National Laboratory (PNNL) Foundational Scientific Focus Area. We thank the students, postdoctoral researchers, and colleagues who were involved in microsensor research in our research group.

## References

1. Lewandowski Z and Beyenal H (2007) *Fundamentals of biofilm research*. CRC Press, Boca Raton
2. Hibiya K et al (2003) Simultaneous nitrification and denitrification by controlling vertical and horizontal microenvironment in a membrane-aerated biofilm reactor. *J Biotechnol* 100(1):23–32
3. Ito T et al (2002) Successional development of sulfate-reducing bacterial populations and their activities in a wastewater biofilm growing under microaerophilic conditions. *Appl Environ Microbiol* 68(3):1392–1402
4. Li BK, Bishop PL (2004) Micro-profiles of activated sludge floc determined using microelectrodes. *Water Res* 38(5):1248–1258
5. Okabe S et al (2002) Structure and function of nitrifying biofilms as determined by molecular techniques and the use of microelectrodes. *Water Sci Technol* 46(1–2):233–241
6. Santegoeds CM, Schramm A, de Beer D (1998) Microsensors as a tool to determine chemical microgradients and bacterial activity in wastewater biofilms and flocs. *Biodegradation* 9(3–4):159–167
7. Roeselers G et al (2007) Diversity of phototrophic bacteria in microbial mats from Arctic hot springs (Greenland). *Environ Microbiol* 9(1):26–38
8. Wieland A et al (2003) Microbial mats on the Orkney Islands revisited: microenvironment and microbial community composition. *Microb Ecol* 46(4):371–390
9. Nubel U et al (2001) Diversity and distribution in hypersaline microbial mats of bacteria related to *Chloroflexus* spp. *Appl Environ Microbiol* 67(9):4365–4371
10. Zhao G et al (2012) Time course study of delayed wound healing in a biofilm-challenged diabetic mouse model. *Wound Repair Regen* 20(3):342–352
11. Kirker KR et al (2012) Differential effects of planktonic and biofilm MRSA on human fibroblasts. *Wound Repair Regen* 20(2):253–261
12. Zhao G et al (2010) Characterization of biofilm infected wounds in diabetic mice. *J Invest Dermatol* 130:S2–S2
13. James GA et al (2008) Biofilms in chronic wounds. *Wound Repair Regen* 16(1):37–44
14. Stewart PS, Costerton JW (2001) Antibiotic resistance of bacteria in biofilms. *Lancet* 358(9276):135–138
15. Babauta J et al (2012) Electrochemically active biofilms: facts and fiction. A review. *Biofouling* 28(8):789–812
16. Babauta JT et al (2012) pH, redox potential and local biofilm potential microenvironments within *Geobacter sulfurreducens* biofilms and their roles in electron transfer. *Biotechnol Bioeng* 109(10):2651–2662
17. Glud RN et al (1994) Effects on the benthic diffusive boundary-layer imposed by Microelectrodes. *Limnol Oceanogr* 39(2):462–467
18. Kuhl M, Jorgensen BB (1992) Microsensor measurements of sulfate reduction and sulfide oxidation in compact microbial communities of aerobic biofilms. *Appl Environ Microbiol* 58(4):1164–1174
19. Ica T et al (2012) Characterization of mono- and mixed-culture campylobacter jejuni biofilms. *Appl Environ Microbiol* 78(4):1033–1038
20. Okabe S et al (2003) Effect of nitrite and nitrate on biogenic sulfide production in sewer biofilms determined by the use of microelectrodes. *Water Sci Technol* 47(11):281–288

21. Okabe S et al (1999) Microbial ecology of sulfate-reducing bacteria in wastewater biofilms analyzed by microelectrodes and fish (fluorescent in situ hybridization) technique. *Water Sci Technol* 39(7):41–47
22. Schramm A et al (2000) Microenvironments and distribution of nitrifying bacteria in a membrane-bound biofilm. *Environ Microbiol* 2(6):680–686
23. Revsbech NP (2005) Analysis of microbial communities with electrochemical microsensors and microscale biosensors. In: Leadbetter JR (ed) *Environmental microbiology*, New York, USA pp. 147–166
24. Beyenal H et al (2004) An optical microsensor to measure fluorescent light intensity in biofilms. *J Microbiol Methods* 58(3):367–374
25. Kuhl M (2005) Optical microsensors for analysis of microbial communities. In: Leadbetter JR (ed) *Environmental Microbiology*, New York, USA pp. 166–199
26. Nguyen HD et al (2012) A voltammetric flavin microelectrode for use in biofilms. *Sens Actuators B-Chem* 161(1):929–937
27. Klimant I, Holst G, Kuhl M (1997) A simple fiberoptic sensor to detect the penetration of microsensors into sediments and other biogeochemical systems. *Limnol Oceanogr* 42(7):1638–1643
28. Bard AJF, Larry R (2001) *Electrochemical methods: fundamentals and applications*. Wiley, New York
29. Babauta JT, Nguyen HD and Beyenal H (2011) Redox and pH microenvironments within *Shewanella oneidensis* MR-1 biofilms reveal an electron transfer mechanism. *Environ Sci Technol* 45(15), 6654–6660
30. Istanbulu O et al (2012) Electrochemical biofilm control: mechanism of action. *Biofouling* 28(8):769–778
31. Klimant I, Meyer V, Kuhl M (1995) Fiberoptic Oxygen Microsensors, A New Tool In Aquatic Biology. *Limnol Oceanogr* 40(6):1159–1165
32. Nguyen HD et al (2012) Microscale geochemical gradients in Hanford 300 area sediment biofilms and influence of uranium. *Water Res.* 46(1):227–234
33. Ferris MJ et al (2003) Cyanobacterial ecotypes in different optical microenvironments of a 68 degrees C hot spring mat community revealed by 16S-23S rRNA internal transcribed spacer region variation. *Appl Environ Microbiol* 69(5):2893–2898
34. Fourans A et al (2004) Characterization of functional bacterial groups in a hypersaline microbial mat community (Salins-de-Giraud, Camargue, France). *FEMS Microbiol Ecol* 51(1):55–70
35. Epping E, Kuhl M (2000) The responses of photosynthesis and oxygen consumption to short-term changes in temperature and irradiance in a cyanobacterial mat (Ebro Delta, Spain). *Environ Microbiol* 2(4):465–474
36. Fenchel T, Kuhl M (2000) Artificial cyanobacterial mats: growth, structure, and vertical zonation patterns. *Microb Ecol* 40(2):85–93
37. Pringault O et al (1999) Dynamics of anoxygenic photosynthesis in an experimental green sulphur bacteria biofilm. *Environ Microbiol* 1(4):295–305
38. Beyenal H, Babauta JT (2012) Microscale gradients and their role in electron-transfer mechanisms in biofilms. *Biochem Soc Trans* 40:1315–1318
39. Brune A, Miambe E, Brenzak JA (1995) Roles of oxygen and the intestinal microflora in the metabolism of lignin-derived phenylpropanoids and other monoaromatic compounds by termites. *Appl Environ Microbiol* 61:2688–2695
40. Ten Have R, Teunissen PJM (2001) Oxidative mechanisms involved in lignin degradation by white-rot fungi. *Chem Rev* 101(11):3397–3414
41. Ke J et al (2010) In-situ oxygen profiling and lignin modification in guts of wood-feeding termites. *Insect Sci* 17(3):277–290

# Index

## A

ABE solvents, 147  
*Acanthella cavernosa*, 181  
Acetaldehyde, 117, 127  
Acetic acid, 126, 148, 150, 154  
*Acinetobacter johnsonii*, 196  
Acridine orange, 6  
Actinomycin D, 182  
Activated sludge models (ASM), 69  
Activity measurements, 13  
Acyl homoserine lactones (AHL), 79, 100, 113, 188, 229  
Adhesion, 128  
Aggregates, 19  
Air–membrane surface (AMS) bioreactor, 180  
*Alcaligenes eutrophus*, 134  
2-Allyloxyphenol, 183  
AlpP protein, 169  
*Alteromonas macleodii*, 184  
*Alvinella pompejana*, 184  
6-Aminopenicillanic acid (6-APA), 103  
Aminopropyltriethoxysilane, 131  
Ammonia nitrogen (TAN) removal, 192  
Ammonium oxidation (anammox), 189  
Ammonium oxidizing bacteria (AOB), 61  
Anammox bacteria, 189  
Antibodies, 13, 23, 124, 220, 225  
Antifouling agents, 163, 177, 199  
Antimicrobials, 57, 78, 179–183  
Antiprotozoan activity, 163, 170  
Aquaculture feedstock, 196  
AQUASIM, 62  
Architecture, 77  
*Argopecten purpuratus* (Peruvian scallop), 196  
*Ashbya gossypii*, 188

Auxin, 175  
*Azotobacter vinelandii*, 91

## B

Bacillomycin D, 178  
*Bacillus firmus*, 178  
*Bacillus licheniformis*, 91  
*Bacillus mojavensis*, 178  
Bacterial activity, 13  
Benzaldehyde, 147  
Bioactive compounds, 152  
Bioactivity, 163  
Bioaggregates, 1, 6  
Biocatalysis, 77, 125  
Biofilm metalloprotease I, 185  
Biofilms, 1  
    artificial/synthetic, 84  
    engineering, 123  
    modeling, 53, 56  
    productive, 123  
    reactors, 56, 123, 207  
    support, substrates, 130  
    synthetic, 77  
    thickness, 129  
Biofouling, 18, 26, 68, 70, 141, 165, 171, 177  
Biofuels, 78  
Biomass-based models (BbM), 66  
Biominalization, 78  
Bioreactors, 128, 163  
Bioremediation, 189  
Biotransformation, 125  
Boundary layer, 57  
Bristles photobioreactor, 198  
Bromodeoxyuridine (BrdU), 13

Bulk chemicals, 123, 146  
 Bulk/biofilm interface, mass transfer, 57  
 Butanol, 132, 147, 150

## C

*Cafeteria roenbergensis*, 170  
*Caldicellulosiruptor saccharolyticus*, 153  
*Candida famata*, 189  
 Catalase, 82  
 Catalysis, 123  
 Cell-cell communication, engineered, 97  
 Cellular automata (CA), 64  
 Cellulases, 130, 140, 148, 151, 163, 187  
 Cephalosporin C, 148, 152  
 Ceramics, 132  
*Chaetomium crispatum*, 187  
 Cholera autoinducer 1 (CAI-1), 113  
*Chromobacterium violaceum*, 170  
*Ciona intestinalis*, 169  
 Citric acid, 147, 148, 150  
*Clostridium acetobutylicum*, 132  
*Clostridium beijerinckii*, 133  
 Concentration boundary layer (CBL), 58  
 Confocal laser scanning microscopy (CLSM),  
 1, 4, 56, 79  
*Cunninghamella elegans*, 193  
 Cyanobacteria, 8, 16, 23, 142, 191, 249  
 Cyanovirin-N, 143  
 Cytotoxic compounds, 179

## D

DEAE-Sephadex A-25, 134  
 Delta-Notch signaling pathway, 104  
 Denitrification, 189  
 Dental plaque, 78  
*Desulfitobacterium frappieri*, 83  
 Detachment, 53, 63  
 4,6-Diamidino-2-phenylindole (DAPI), 5  
 Dielectrophoresis (DEP), 88  
 Diffusion boundary layer (DBL), 57  
 Dihydroxyacetone, 147  
 Dimethylsulfoniopropionate (DMSP), 167  
 DNA, extracellular, 11

## E

Electricigens, 195  
 Electrochemically active (EA) microorganisms,  
 195  
 Electrode respiration, 252  
 Emerse photobioreactor (ePBR), 142  
 Endo- $\beta$ -1,4-glucanase, 187

Environmental scanning electron microscope  
 (ESEM), 224  
 Enzymes, 151, 185  
 Erosion, 63  
 Ethanol, 127, 130, 140, 147, 150  
 Excitation, one-photon, 1  
 two-photon, 1, 5  
 Exopolysaccharides, 184  
 Extracellular polymeric substances (EPS), 1, 8,  
 53, 79, 149, 184, 187

## F

Fiberoptics, 235  
 Filter paper degradation, 187  
 Fine chemicals, 123, 146  
 Finite element methods (FEM), 69  
 FISH-MAR, 14  
 Fixed-bed reactor (packed-bed reactor), 138  
 Flavin, 249  
 Floccs, 19  
 Fluid dynamics, 68  
 Fluid structure interactions, 53  
 Fluidized-bed reactor, 139  
 Fluoranthene, 193  
 Fluorescence, 1  
 Fluorescence dyes, 225  
 Fluorescence in situ hybridization (FISH), 8  
 Fluorescence lifetime, 243  
 Fluorochromes, 1, 6  
 Foam glass particles, 133  
 Fumaric acid, 150  
 FUN-1, 23  
 Fungi, 23

## G

Gellan, 185  
 Gelrite, 185  
 Gene circuits, 97, 104  
 GFP, 14, 104, 111, 116, 243  
 Gibberellic acid, 149  
 Glass, 133  
 Glycoconjugates, 10  
 Glyolic acid, 150  
 Granules, 24  
 Grazing, 19  
 Guanosinmonophosphate, bis-(3'-5')-cyclic  
 dimeric (c-di-GMP), 167

## H

*Halomonas marina*, 178  
 Hg(II)-sensitive species, 87

*Hinia reticulata*, 174  
Hydrogen, 148, 153  
Hydrogen peroxide, 82  
Hydrophobic effect, 217  
3-Hydroxy-decanoyl homoserine lactone, 166

**I**

Immobilization, 86, 125  
Indigoidine, 168, 169  
Individual-based models (IbM), 66  
Indole-3-acetic acid (IAA), 176  
Industrial production, 123  
Interactions, 207  
Interfaces, 207  
Intertidal microbes, 163  
Isoelectric point (IEP), 218

**K**

Kármán vortex, 69  
Kopara, microbial mats, 184

**L**

$\beta$ -Lactamases, 151  
Lactic acid, 135, 147  
*Lactococcus lactis*, 152  
Laser scanning microscopy (LSM), 4  
Lateral force microscope (LFM), 214  
Lectins, 9  
Lichens, 23  
Lignin peroxidase, 151  
*Listeria monocytogenes*, 152  
*Litopenaeus vannamei*, 174  
Lotus effect, 217  
LuxR/LuxI, 100

**M**

Manganese peroxidase, 149  
Marine microbes, 163  
Mass transfer, 53, 129  
Melanin, 163, 188  
Membrane biofilm reactor, 141  
Metabolites, 83  
Methane, 78, 154, 174, 185  
Methanogenesis, 78, 83  
Methanol, 9, 127, 192  
*Methylophaga*, 192  
Microautoradiography (MAR), 14  
Microbial fuel cells, 195  
Microbial mats, microsenors, 249  
Microbial secondary metabolites, 152

Microcontact printing patterns ( $\mu$ CP), 87  
Microelectrodes, 235, 239  
    amperometric, 241  
    potentiometric, 240  
Microenvironments, 77  
Micomilling, 211  
Microscale gradients, 235  
Microsenors, 235  
    optical, 243  
Microstructures, 210  
Modeling, 53  
Monolayers, self-assembled, 87  
Moving-bed biofilm reactors (MBBR), 192  
Multidimensional models, 53, 64  
Mycosubtilin, 178

**N**

*Nannocystis exedens*, 181  
*Navicula veneta*, 196  
Navier–Stokes equation, 53  
Neumann boundary condition, 58  
Nisin, 147, 148, 152  
Nitrification–denitrification, 189  
Nitrite oxidizing bacteria (NOB), 61  
Nitrogen removal, 189  
Nitrous oxide, 163, 165, 174  
Nucleic acids, fluorochromes, 7  
Nylon, 134

**O**

1-Octanol, 149  
Optical coherence tomography (OCT), 28  
Organic acids, 150  
Organochlorides, 83  
Oxygen, 58, 129, 175, 236  
    termites, microelectrodes, 251

**P**

*Paenobacillus curdlanolytica*, 91  
PALM/STORM/GSD, 28  
*Paracoccus seriniphilus*, 220  
*Paracoccus zeaxanthinifaciens*, 184  
Particle modification, 211  
Pattern-forming systems, 103  
Peak activity attainment rate (PAAR), 183  
Pediocin, 152  
*Pediococcus acidilactici*, 152  
*Penicillium chrysogenum*, 129  
2-*n*-Pentyl-4-quinolinol, 163, 173  
*Pfiesteria piscicida*, 166  
pH microelectrode, 240

- Phaeobacter gallaeciensis*, 168  
*Phaeobacter inhibens*, 168  
 Phages, 26  
*Phanerochaete chrysosporium*, 133  
 Phenylannolones, 163, 181  
 Photobioreactors, 142, 153, 196-199  
 Phototrophic biofilms, 19  
 Phycocyanin, 143  
 Phycoerythrin, 143  
*Pinctada maxima* (pearl oyster), 197  
 Pipelines, 78  
 Plant surfaces, 23  
 Plastic composite supports (PCS), 135, 227  
 Polyethylene (PE), 134  
 Polyhydroxyalkanoates, 148  
 Polyhydroxybutyrate, 147, 149  
 Polymethylmethacrylate (PMMA), 134  
 Polypropylene, 134, 229  
 Polytetrafluoroethylene (PTFE), 134  
 Predator-prey systems, 101  
 1,3-Propanediol, 147  
 Propionic acid, 147, 150  
 Proteases, 112, 151, 163, 185  
 Proteins, adhesion, 218  
*Pseudoalteromonas*, 163, 169  
*Pseudoalteromonas luteoviolacea*, 181  
*Pseudoalteromonas tunicata*, 163, 169  
*Pseudomonas aeruginosa*, 79  
 Pullulan, 148
- Q**  
 Quantitative mapping modes, 220  
 Quorum sensing (QS), 79, 100  
   inhibition/disruption, 112
- R**  
*Ralstonia metallidurans*, 87  
 Reaction/diffusion, mass balances, 56  
   models, 59  
 Reactors, 123, 128, 207  
   materials, 207  
 Recirculated water systems (RAS), 192  
 Resistance, 82  
 Reynolds number, 58  
 Rhamnolipid, 79  
*Rhodococcus rhodochrous*, 126  
*Rhodospiridium sphaerocarpum*, 170  
*Rhynchomonas nasuta*, 170  
 Riboflavin, 163, 188  
 River biofilms, 19  
*Roseobacter* clade, 163, 165  
*Roseobacter gallaeciensis*, 170  
 Rotating-disc bioreactor, 140, 148, 182  
*Ruegeria mobilis*, 167, 168  
*Ruegeria pelagia*, 168
- S**  
 Scanning force microscope (SFM), 220  
 Schmidt number, 58  
 Scytonemin, 143  
 Scytovirin, 143  
 Secondary ion mass spectrometry (SIMS), 218  
 Selected plane illumination microscopy (SPIM), 29  
 Self-assembly, 86  
 Self-regulating biofilms, 154  
 Sender-receiver system, 105  
 Sherwood number, 58  
*Shewanella colwelliana*, 188  
*Shewanella oneidensis*, flavin, 249  
 Simpson's paradox, 102  
 Single-cell force spectroscopy (SCFS), 221  
 Solid support membrane-aerated biofilm reactor (SMABR), 142  
 Solvents, production, 150  
*Sphingobium chlorophenicum*, 87  
 Stainless steel surfaces, 131  
 Stimulated emission depletion microscopy (STED), 28  
 Stirred-tank reactor, 136, 148  
*Streptomyces sundarbansensis*, 183  
 Structured illumination microscopy (SIM), 28  
 Styrene, 153  
 Styrene oxide, 153  
 Succinic acid, 147, 150  
 Surface science methods, 207  
 Surface-adhesion fermentation (SAF), 187  
 Surface-dwelling marine/intertidal microbes, 163  
 Surfaces, biological modification, 226  
   charge, 216  
   microstructured, 207  
   modifications, 211  
 Syntrophic degradation, 83
- T**  
*Thalassia testudinum*, 179  
 Thiotropocin, 166  
 Thymidine analogues, 13  
 Titanium, 131, 211  
 Topography, 213  
 Toxic shock syndrome toxin-1 (TSST-1), 252  
 Tributyl tin (TBT), 177  
*Trichoderma viride*, 140

Trickle-bed bioreactor (TBR), [138](#), [148](#)  
Tropodithietic acid (TDA), [166](#)

**U**

Ultrasound, [88](#)  
*Ulva lactuca*, [169](#)  
Uronic acids, [185](#)

**V**

Viability, [11](#)  
*Vibrio anguillarum*, [167](#)  
Violacein, [163](#), [171](#), [181](#)  
Viruses, [26](#)

**W**

Waddington's landscape, [103](#)  
Wanner-Gujer model, [61](#)  
Wastewater, engine rooms, [190](#)  
Wettability, [216](#)  
*Winogradskyella poriferorum*, [196](#)

**X**

X-ray photoelectron spectroscopy, [219](#)  
Xylanase, [163](#)

**Y**

Yellow fluorescent protein (YFP), [252](#)  
YP1, [171](#)